Comparative study on the nervous system of Tunicata to elucidate tunicate phylogeny and character transformations

DISSERTATION

zur Erlangung des akademischen Grades

Doctor rerum naturalium
(Dr. rer. nat.)

eingereicht an der
Lebenswissenschaftlichen Fakultät der Humboldt-Universität zu Berlin
von

M.Ed. Katrin Braun

Präsidentin der Humboldt-Universität zu Berlin:
Prof. Dr.-Ing. Dr. Sabine Kunst

Dekan der Lebenswissenschaftlichen Fakultät der Humboldt-Universität zu Berlin:
Prof. Dr. Bernhard Grimm

Gutachter
1. PD Dr. Thomas Stach
2. Prof. Dr. John A. Nyakatura
3. Prof. Dr. Lucia Manni

Tag der mündlichen Prüfung: 24. April 2019

Vergleichende Untersuchung des Nervensystems von Tunikaten zur Aufklärung phylogenetischer Verwandtschaftsbeziehungen und evolutiver Transformationen

Erklärung

Hiermit erkläre ich, dass ich die vorliegende Arbeit ohne die unzulässige Hilfe Dritter und ohne die Verwendung anderer als der angegebenen Hilfsmittel angefertigt habe. Die aus anderen Quellen direkt oder indirekt übernommenen Daten und Konzepte sind unter Angabe der Quelle gekennzeichnet. Diese Arbeit wurde keiner anderen Prüfungsbehörde vorgelegt.

Berlin, den

Katrin Braun

„Die Beschäftigung mit der Biologie der Tiere bedeutet gleichzeitig ein tieferes Verständnis des eigenen Ichs.“

Heinrich Dathe

Contents

1 Abstract

Tunicata comprises approximately 3000 exclusively marine species with very diverse habitats and life-history strategies. As one of the three major chordate taxa, the evolution of tunicates might play a key role to elucidate chordate and craniate (=vertebrate) evolution, especially since large-scale molecular phylogenetic analyses consistently indicated that Tunicata — not the more “fish-like” Cephalochordata — are probably the closest living relatives to Craniota. To inform chordate evolution from tunicate evolution, a broader understanding of character transformations within tunicates is essential, however, the interrelationships of the five main tunicate subtaxa (Appendicularia, “Thaliacea”, Aplousobranchiata, “Phlebobranchiata” and Stolidobranchiata) in previous molecular phylogenetic analyses were contradictory. Morphological phylogenetic analyses are hitherto rare and based on only a small taxon sampling or included merely a small number of phenotypic characters. With the detailed investigation and documentation of new character complexes for a representative sampling of tunicate species, the present study is specifically designed to address the aforementioned shortcomings.

Particular emphasis was hereby given to neuroanatomical characters, as the nervous system is a supposedly slowly evolving organ system and probably contains phylogenetic information as has been shown in previous studies focusing on different metazoan taxa. Studies on the tunicate central nervous system are so far limited to certain stages or taxa. The present study included the investigation of yet understudied stages, e.g., adult ascidians, and understudied species, e.g., representatives of “Thaliacea” such as *Pyrosoma atlanticum* and the oozooid and blastozooid stages of *Doliolum nationalis* and *Iasis cylindrica*. Applying modern morphological techniques like antibody-staining in combination with high-resolution confocal laser scanning microscopy (CLSM), electron microscopy (SEM and TEM), serial sectioning for light microscopy, and digital 3d reconstruction, the number of available tunicate neuroanatomical data was considerably increased. These investigations revealed, e.g., that the variation of neuroanatomical characters on an interspecific level is higher than previously assumed, that the anatomy of the brains in different life-cycle stages (oozooid and blastozooid stages) clearly differs, and that a recognizable subdivision of tunicate brains with the applied methods is not detectable.

Based on these comparative morphological investigations, novel independent characters of the central nervous system, concerning, e.g., the anatomy of the brain or the position of emerging nerves, as well as distribution patterns of neurotransmitters were coded in a data matrix for a formal cladistic analysis. Including characters that are traditionally used in tunicate taxonomy and that were re-analyzed in the present study, this effort resulted in the largest morphological data matrix for tunicates to date, containing 116 phenotypic characters coded for 49 tunicate species and five chordate outgroup species. Based on this data matrix, a cladistic analysis was

performed that yielded a new hypothesis for the internal relationships of Tunicata. Within monophyletic Tunicata, Appendicularia forms the sister taxon to the remaining tunicates supporting the hypothesis of a free-living last common ancestor of tunicates. Furthermore, the monophyly of Ascidiacea is supported, whereas the pelagic "Thaliacea" is found to be paraphyletic. An additional phylogenetic analysis combining morphological and 18S rDNA-sequence data was performed in order to evaluate the respective contribution of phenotypic and molecular characters toward the resulting phylogenetic hypothesis. A reevaluation of this dataset with a successively increased weighting of the phenotypic data showed that morphological data strongly influence the outcome of the cladistic analysis and the resulting phylogenetic hypothesis. The evolution of serotonin-like immunoreactive cells and the anatomy of the central nervous system of Tunicata is reconstructed based on the new phylogenetic hypothesis. The study revealed that several homoplasies are necessary to explain certain character state distributions. These results indicate that similarities in certain neuroanatomical characters — e.g., the numbers of nerves, the size and shape of the brain, or the shape of the dorsal tubercle — in specific tunicate species is more likely correlated with similar life-history strategies rather than retained from a common ancestor.

2 Zusammenfassung

Das Taxon Tunicata (Manteltiere) umfasst ungefähr 3000 beschriebene, ausnahmslos marine Arten, die sich durch ausgesprochen unterschiedliche Habitate und Lebensstrategien auszeichnen. Da die Tunikaten eines der drei großen Taxa innerhalb der Chordaten bilden, stellt die Evolution der Tunikaten eine Schlüsselkomponente bei der Aufklärung der Evolution der Chordaten und Cranioten (=Vertebraten) dar. Dies gilt insbesondere seit molekular-phylogenetische Untersuchungen übereinstimmend darauf hindeuten, dass Tunicata, und nicht die eher fischartigen Cephalochordata, die nächsten lebenden Verwandten der Craniota sind.

Um ausgehend von der Evolution der Tunikaten Rückschlüsse auf die Evolution der Chordaten ziehen zu können, ist ein weitreichendes Verständnis der Merkmalstransformationen innerhalb der Tunikaten unbedingt notwendig. Allerdings sind die internen Verwandtschaftsverhältnisse der fünf großen Teilgruppen der Tunikaten (Appendicularia, „Thaliacea“, Aplousobranchiata, „Phlebobranchiata“ und Stolidobranchiata) in verschiedenen molekularphylogenetischen Studien widersprüchlich. Bisher gibt es nur wenige morphologische phylogenetische Analysen und diese basieren zumeist auf der Untersuchung von nur wenigen Arten oder einer geringen Anzahl von Merkmalen. Mit einer detaillierten Untersuchung und Dokumentation neuer Merkmalskomplexe für ausgesuchte, repräsentative Vertreter der Tunikaten, ist die hier vorgestellte Studie speziell dazu entworfen diese Wissenslücken zu schließen.

Ein besonderer Schwerpunkt wurde dabei auf die Untersuchung von neuroanatomischen Merkmalen gelegt, da speziell das Nervensystem ein nur langsam evolvierendes Organsystem ist. Es kann daher zur Rekonstruktion von Verwandtschaftsverhältnissen herangezogen werden, was durch verschiedene Studien für unterschiedliche Taxa der Metazoa nachgewiesen wurde. Studien des zentralen Nervensystems der Tunikaten sind bisher auf bestimmte Stadien oder Taxa beschränkt. In die vorliegende Studie wurden auch kaum untersuchte Stadien (wie adulte Ascidien) und wenig untersuchte Arten (wie Vertreter der „Thaliacea“, zum Beispiel *Pyrosoma atlanticum* und die Oozooide und Blastozooide von *Doliolum nationalis* und *Iasis cylindrica*) einbezogen. Durch das Anwenden moderner morphologischer Methoden, wie das Färben mittels Antikörper in Kombination mit hochauflösender konfokaler Laserscanmikroskopie (CLSM), die Elektronenmikroskopie (REM und TEM), das Anfertigen von Schnittserien für die Lichtmikroskopie sowie der 3d Rekonstruktion, wurde die Menge der zur Verfügung stehenden neuroanatomischen Daten der Tunikaten wesentlich erhöht. Die vorliegenden Untersuchungen konnten zeigen, dass die Variation neuroanatomischer Merkmale im Vergleich mehrerer Arten miteinander größer ist als bisher angenommen, dass die Gehirnanatomie in verschiedenen Lebenszyklusstadien der Thaliaceen (Oozooid und Blastozooid) sich ganz klar unterscheidet, aber auch, dass eine weitere Unterteilung des Tunikatengehirns mit den hier angewendeten Methoden, insbesondere der immunhistochemischen Analyse, nicht nachweisbar ist.

Basierend auf diesen vergleichend-morphologischen Untersuchungen konnten neue unabhängige Merkmale des zentralen Nervensystems in einer Datenmatrix zusammengetragen, konzeptualisiert und kodiert werden, um diese für eine formelle kladistische Analyse zu nutzen. Diese Merkmale beziehen sich zum Beispiel auf die Anatomie des Gehirns, die Position austretender Nerven aus dem Gehirn und auch auf die Verteilungsmuster von Neurotransmittern. Traditionelle, in der Tunikatentaxonomie verwendete, Merkmale wurden ebenfalls miteinbezogen, sodass diese Bemühungen die bisher umfangreichste morphologische Datenmatrix ergaben, die 116 kodierte Merkmale für insgesamt 49 Tunikatenarten und fünf Außengruppenvertreter umfasst. Die anschließende kladistische Analyse dieser Datenmatrix führte zu einer neuen Hypothese der internen Verwandtschaftsverhältnisse der Tunicata. Innerhalb der monophyletischen Tunicata bilden die Appendicularia die Schwestergruppe der übrigen Tunikaten, was die Hypothese eines freilebenden letzten gemeinsamen Vorfahren der Tunikaten stützt. Weiterhin bekräftigt die Analyse die Monophylie der Ascidiacea, während die pelagischen „Thaliacea“ als paraphyletische Gruppe herausgestellt werden. Zusätzlich wurde eine kombinierte phylogenetische Analyse basierend auf den morphologischen Daten und 18S rDNA-Sequenzen durchgeführt, um den jeweiligen Beitrag der phänotypischen und molekularen Merkmalen zur resultierenden phylogenetischen Hypothese abzuschätzen. Eine Neubewertung des Datensatzes mit einer stufenweise stärkeren Gewichtung der phänotypischen Merkmale stellt deutlich heraus, dass die morphologischen Daten das Ergebnis der kladistischen Analyse und damit die resultierende phylogenetische Hypothese stark beeinflussen. Basierend auf der hier neu vorgestellten Hypothese zur Verwandtschaft der Tunicata, wurde die Evolution des zentralen Nervensystems sowie die Evolution von serotoninähnlichen immunreaktiven Zellen innerhalb der Tunicata rekonstruiert. Es stellte sich heraus, dass häufig mehrere Homoplasien notwendig sind, um die Verteilung bestimmter Merkmalszustände zu erklären. Diese Ergebnisse deuten darauf hin, dass Ähnlichkeiten bei bestimmten neuroanatomischen Merkmalen, wie beispielsweise die Nervenanzahl, die Größe und Form der Gehirne oder die Form der Dorsaltuberkel, in speziellen Tunikatenarten eher mit ähnlichen Lebensstrategien korrelieren, als dass diese Merkmalszustände von einem gemeinsamen Vorfahren übernommen wurden.

3 Introduction

The enigmatic animals belonging to the taxon Tunicata are little known to a broader public. Because of the simple appearance and sessile lifestyle of many of them, tunicates do not attract the attention of most people. At least in science, this view dramatically changed when large-scale molecular analyses indicated that tunicates are the closest living relatives to Craniota (=vertebrates), a group that also comprises humans (Delsuc et al. 2006, Dunn et al. 2008, 2014, Edgecombe et al. 2011). This phylogenetic upheaval resulted in many open questions, because former evolutionary scenarios of a stepwise appearance of "fish-like" characteristics in the stem lineages of vertebrates and lancelets (=cephalochordates), traditionally believed to be their closest allies, were overturned. Apart from their important phylogenetic position as a key taxon to study vertebrate evolution, tunicates also possess great ecological and economical value.

3.1 Tunicata

Tunicata are exclusively marine animals that constitute one of the three major monophyletic chordate taxa and probably date back to the Early Cambrian, approximately 540-500 million years ago (Shu et al. 2001, Chen et al. 2003). As eponymous characteristic for the group the protective covering, named tunic, is a unique feature.

3.1.1 General anatomy

Lamarck discovered and named the taxon Tunicata in 1816 because of the extraordinary durable and often leathery coating (Lamarck 1816). Until today, Tunicata are regarded as a monophyletic group with the tunic as one major apomorphy. The tunic is synthesized by cells of the epidermis and contains the polysaccharide tunicin, which is animal cellulose (Schmidt 1845). Within the animal kingdom, Tunicata are the only clade with the ability to produce cellulose (Kimura et al. 2001).

Tunicata consists of approximately 3000 species that are not only quite varied in outer appearances but also show diverse life-histories (Fig. **1A**–**F**). Adult tunicates can be sessile (Ascidiacea[1]) or planktonic (Appendicularia or "Thaliacea"[2]), they live in colonies or are solitary, and colonial tunicates usually develop through metagenesis, some even with polymorph sexual and asexual generations. Most tunicates are filter-feeders with a perforated pharynx, the branchial basket, as main organ system (see below), but some ascidians with a

[1]: Although the group Ascidiacea in most molecular phylogenetic analyses is found paraphyletic or polyphyletic, I did not put the taxon's name in quotation marks to indicate that in the present morphology-based phylogenetic analysis Ascidiacea is recovered monophyletic.

[2]: Although the group "Thaliacea" in traditional taxonomy and most molecular phylogenetic analyses is regarded as monophylum, I put the taxon's name in quotation marks to indicate that in the present phylogenetic analysis based on morphological data the group was found paraphyletic.

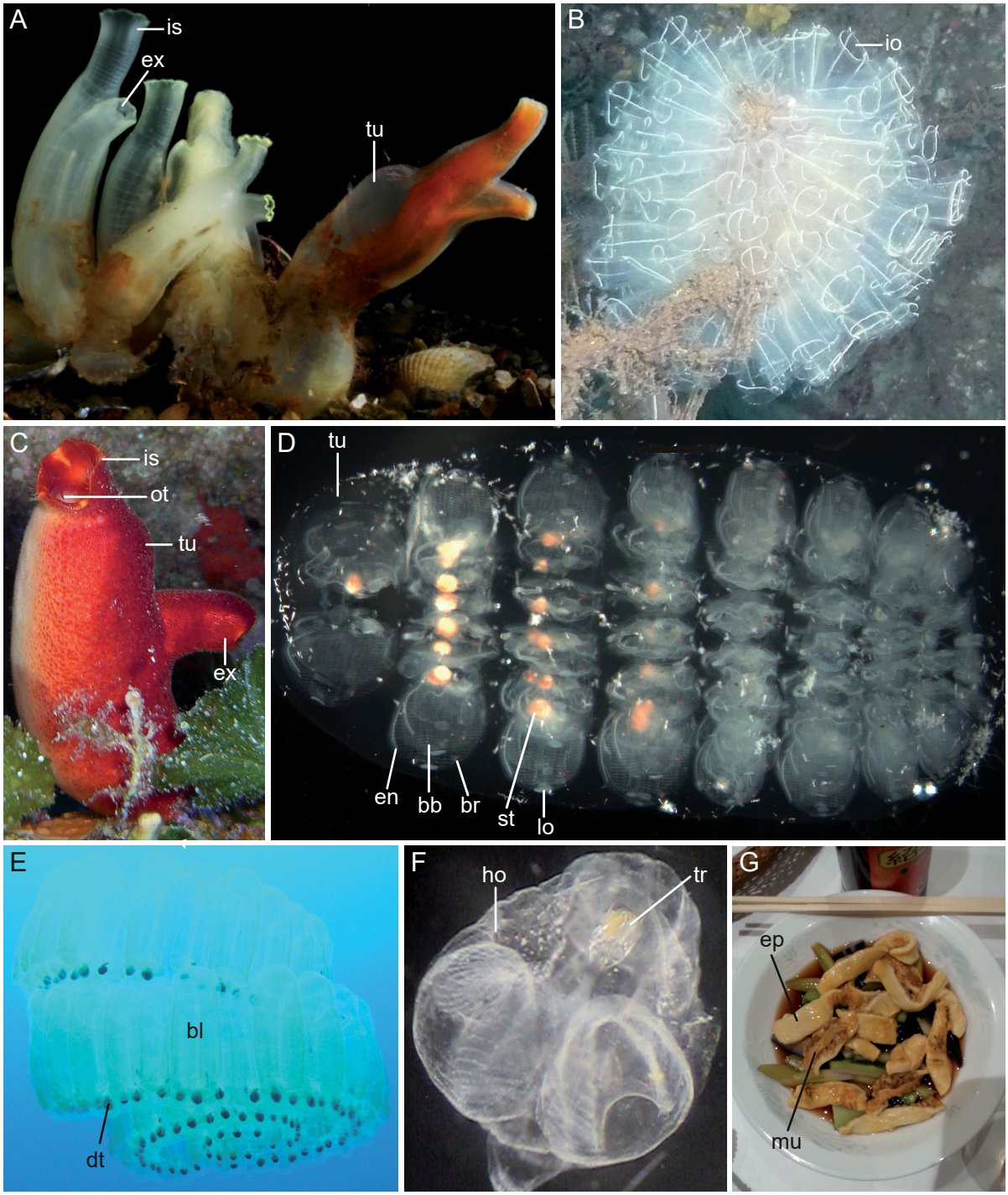

Figure 1: Representatives of the five major tunicate taxa showing the diversity in lifestyles. **A**: Five sessile adults of the solitary ascidian *Ciona intestinalis* ("Phlebobranchiata"). **B:** Colony of sessile adults of *Clavelina lepadiformis* (Aplousobranchiata). **C:** Solitary and sessile adult of *Halocynthia papillosa* (Stolidobranchiata). **D**: Planktonic colony of *Pyrosomella verticillata* (Pyrosomatida). The zooids are connected through a common almost transparent tunic (tu) and are known for their bright bioluminescence produced by light organs (lo). **E:** Chain of sexually propagating blastozooids (bl) probably of *Salpa maxima* (Salpida). **F:** *Oikopleura dioica* (Appendicularia) shown in its filter-feeding house (ho) formed by the tunic. They move through the water column and are solitary during their entire lives. **G:** Dish with the *Halocynthia roretzi* (Stolidobranchiata) in a Chinese restaurant. Images **A** and **F** provided by Priv.-Doz. Dr. Thomas Stach, images **B**, **C,** and **E** provided by Dipl. Biol. Peer Martin. bb: branchial basket, br: brain, dt: digestive tract, en: endostyle, ep: epidermis, ex: excurrent siphon, is: incurrent siphon, mu: musculature, ot: oral tentacle, st: stomach, tr: trunk

carnivorous diet are described as well (Monniot and Monniot 1990, Okuyama et al. 2002, Lambert 2005).

3.1.2 Anatomy of the branchial basket

Most postmetamorphic tunicates are sessile. Their most striking phenotypic characteristic is the branchial basket that is present in all tunicates and also in outgroup species within Chordata, i.e., Cephalochordata and Craniota. In planktonic Appendicularia and "Thaliacea", the branchial baskets are somewhat reduced, nevertheless, the branchial basket in most tunicates assumes the tasks of accumulating food and of respiration. A water stream is produced by numerous cilia within the branchial basket and water enters the animal through an incurrent siphon (also called branchial or oral siphon) or incurrent opening. A mucous net is secreted by a structure in the branchial basket, called endostyle (e.g., Orton 1913). As the endostyle also binds iodine and in lampreys develops into follicles of the thyroid gland, it is probably homologous to the thyroid gland in Craniota (e.g., Barrington and Thorpe 1965, Dunn 1974, Wright and Youson 1976). The mucous net covers the branchial basket and traps food particles while water streams through it and leaves the branchial basket through gill slits. Cilia of the branchial basket maneuver the food-laden mucous net toward the esophagus where the entire

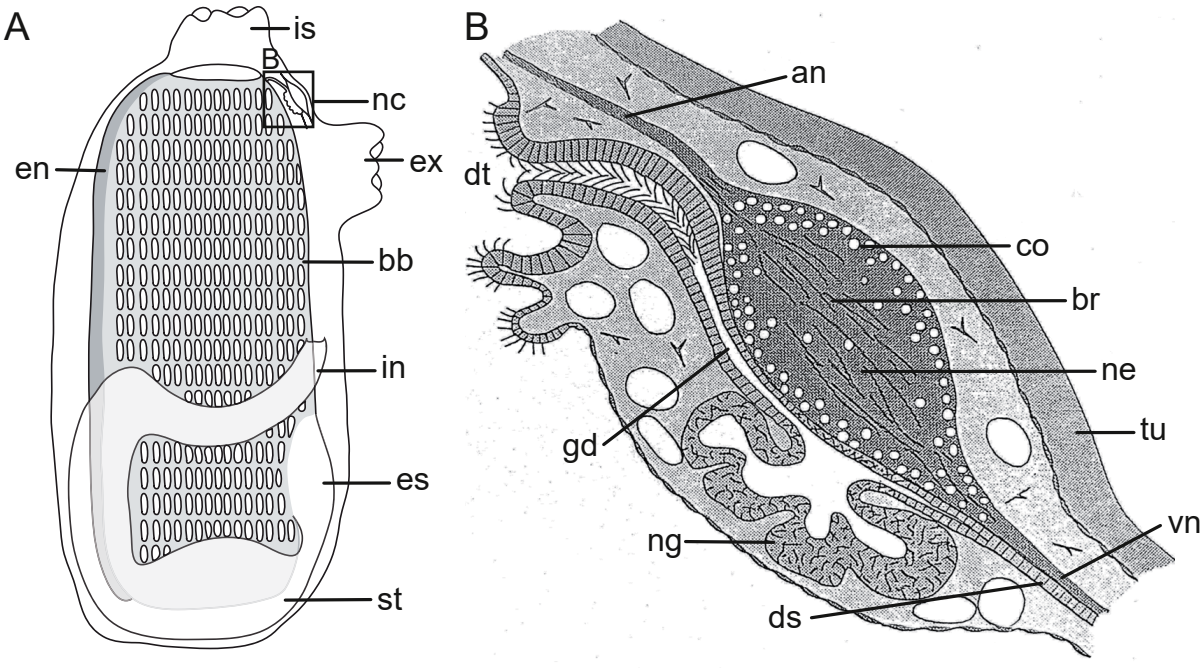

Figure 2: Schematic drawings of the internal anatomy of adult ascidians. **A**: Complete internal anatomy, view from the left side, anterior to the top. **B:** Higher magnification of the neural complex (nc) modified from Brien (1948). The brain (br) is usually associated with a neural gland (ng). Magnification of area marked with black rectangle in **A**. an: anterior nerve, bb: branchial basket, co: cortex, ds: dorsal strand, dt: dorsal tubercle, en: endostyle, es: esophagus, ex: excurrent siphon, gd: gland duct, in: intestine, is: incurrent siphon, st: stomach, tu: tunic, vn: ventral visceral nerve

food together with the net is digested. Indigestible remnants and remaining water exit the animal through the excurrent (or atrial) siphon (MacGinitie 1939, Millar 1971, see also Fig. **2A** for the internal ascidian anatomy).

3.1.3 Anatomy of Ascidiacea

Within the 3064 described tunicate species, Ascidiacea account for 2918, while Appendicularia and "Thaliacea" only consist of 68 and 78 species respectively. Ascidiacea is divided into three clades according to structures of their branchial baskets (see below): Aplousobranchiata, "Phlebobranchiata"[3], and Stolidobranchiata. Most species belong to Aplousobranchiata (1544) and Stolidobranchiata (1039), considerably less to "Phlebobranchiata" (335) (WoRMS Editorial Board 2018, http://www.marinespecies.org, accessed 2018-08-02).

Aplousobranchiata contains usually colonial ascidians (Fig. **1B**) with an alternation of sexually and asexually propagating generations with uniform morphologies, except from the possession of gonads. Typical of adult aplousobranchs is a body division into two or three body parts: thorax, abdomen, and sometimes postabdomen. The thorax mainly contains the branchial basket while stomach, intestine, heart, and gonads are situated in the abdomen. If a postabdomen is present, heart and gonads are shifted into the postabdomen. Within Aplousobranchiata, several modes of budding evolved and extensive colonies are established mostly by asexual reproduction (Huus 1956).

"Phlebobranchiata" consists of species that are usually solitary, however, some colonial species also exist (Perophoridae). They do not show any sign of body division. The well-known chordate model organism *Ciona intestinalis* is allocated to "Phlebobranchiata" (Fig. **1A**).

Colonial species also occur within Stolidobranchiata (Botryllinae, Ärnbäck 1923), although most species are solitary animals (Fig. **1C**). Just as in the colonial phlebobranch Perophoridae, the body of Botryllinae is uniform, without body division. Some Stolidobranchiata have a very thick protective tunic with a firm layer of muscles beneath the epidermis. Molgulidae feature a kidney as specialized excretion organ (Monniot 1969).

3.1.4 Anatomy of "Thaliacea"

Planktonic "Thaliacea" possess a translucent tunic and the excurrent and incurrent siphons of the animals are positioned at opposite poles. Traditionally, "Thaliacea" is constituted of the taxa Salpida, Doliolida, and Pyrosomatida (Huxley 1851). While pyrosomes stay in a colony during their entire lifespan, colonial chains of Doliolida and Salpida break up when the sexually propagating generation is fertilized. Salpida and Doliolida develop through a

[3]: The traditional ascidian group "Phlebobranchiata" is put in quotation marks because most molecular phylogenetic analyses in line with the present morphological phylogeny assume that the group is not monophyletic.

metagenetic life cycle with polymorph generations (reviewed in Bone 1998). Individuals in the asexually propagating generation are called oozooids and gives rise to a long chain of buds that are produced at a specialized ventral organ, the stolo prolifer. These buds are called blastozooids and they reproduce sexually, generally while they are still aggregated in the chain (Delage and Hérouard 1898, see also Fig. **1E**). Blastozooids are fertilized by other blastozooids, usually from the same chain. After fertilization the chain of blastozooids breaks up and fertilized blastozooids bear at least one embryo that will develop into an oozooid again (Chamisso 1819, Krohn 1846, Ihle 1956). Salpida do not develop through a larval stage. Due to metagenesis they may appear in large numbers at the coasts if ecological conditions are beneficial for them. Salps are mainly moved by water currents, but they have the ability to actively move through muscle contractions as well.

Doliolids have barrel-shaped bodies that usually measure 2 cm or less in length and are surrounded by continuous circular muscle bands (Quoy and Gaimard 1834, reviewed in Piette and Lemaire 2015). With their transparent tunic and the reduced sizes, they often escape attraction. Doliolids develop through even more complicated life cycles than salps, with six different forms described for a single species. Doliolid embryos develop into a larva or tadpole stage, as a first form. The larva develops into the second form, the solitary asexually propagating oozooid. The oozooid degenerates into the old nurse stage as a third form. Through budding at the ventral stolo prolifer of the old nurse blastozooids develop. These buds (blastozooids) are moved to the caudal peduncle, a posterior extension, and develop into three blastozooid forms according to their position. These blastozooids become trophozooids (or gastrozooids), phorozooids, and gonozooids and fulfill different tasks within the colony (Godeaux 1998). Trophozooids feed the colony, phorozooids carry and nurse gonozooids, and gonozooids become sexually mature and reproduce sexually (Neumann 1956, Godeaux 2003).

The third group of “Thaliacea” is Pyrosomatida. Muscles are nearly completely reduced in pyrosomes. The aggregated colony (Fig. **1D**) floats feebly through the water passively utilizing the stream of exhaled water from the common excurrent opening. Therefore, a colony cannot actively determine the direction of its movement. Pyrosomes have light organs where symbiotic luminescent bacteria live. Each zooid is equipped with eyes and probably able to detect the refulgence of other zooids. Today it is known that different species produce different light-patterns, but the function of the bioluminescence still remains obscure (Lambert 2005). Like in Salpida, the tadpole larva in Pyrosomatida is reduced. In other respects the life cycle of Pyrosomatida is similar with the one present in colonial ascidians (Huxley 1860, Godeaux et al. 1998).

3.1.5 Anatomy of Appendicularia

Most species belonging to Appendicularia are only few millimeters in length. Without exception, they are solitary animals that build highly elaborated filter-feeding houses from their epidermis (Fig. **1F**). These houses correspond to the tunic of other species of Tunicata (Kimura et al. 2001) and efficiently trap very small food particles. If filters of the house are blocked the animal leaves the old house and unfolds a new one (Körner 1952, Onuma et al. 2017). As usual in tunicates, Appendicularia are hermaphrodites but the model organism *Oikopleura dioica* is diecious. Appendicularia have very short lifespans of only a few days. During their whole life, the outer appearance resembles that of a tadpole larva often taken as evidence for an evolution via paedomorphosis (reviewed in Fenaux 1998, Stach 2007).

3.1.6 Ontogeny

Usually, tunicates develop indirectly through a larva that is called tadpole larva. In 1866, Kowalevsky investigated the development of the ascidian *Ciona robusta* (identified by him

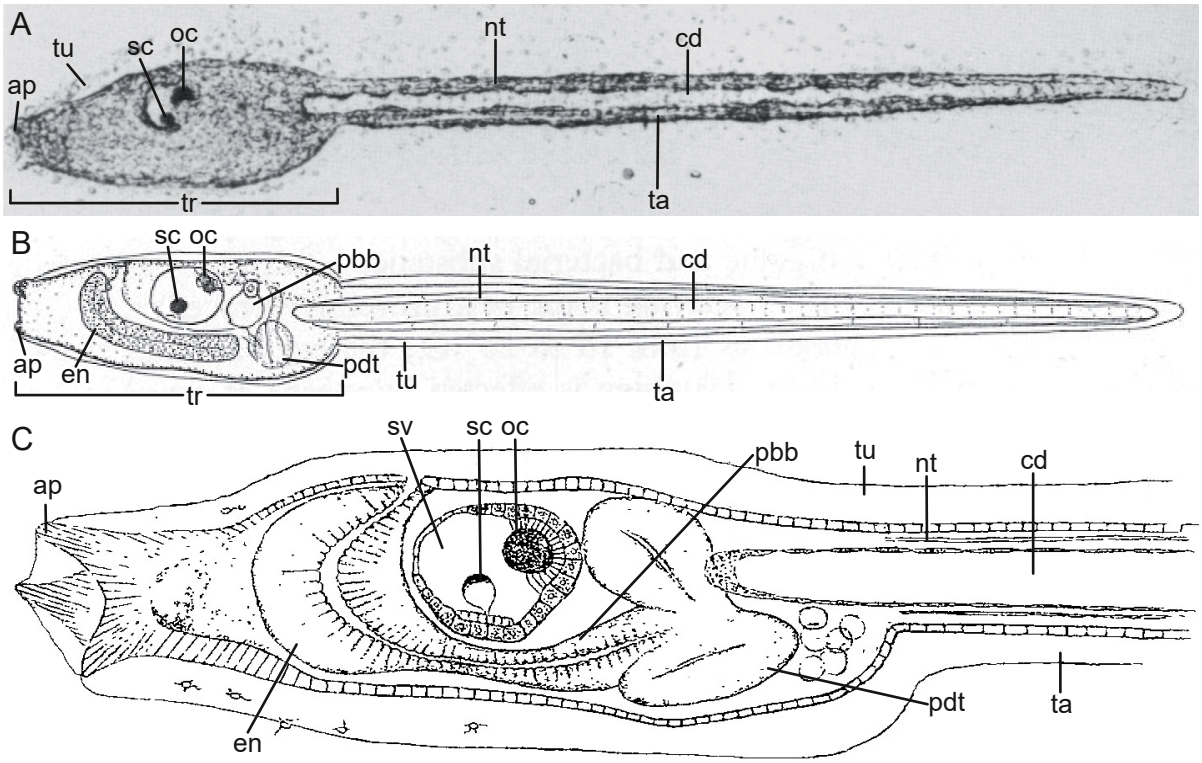

Figure 3: Morphology of the tadpole larva of *Ciona intestinalis* and *Ciona robusta*. **A:** Light micrograph of *Ciona intestinalis* by Katz (1983). The most prominent structures are the pigmented cells of the sensory vesicle (sv) and vacuolated cells in the notochord (chorda dorsalis (cd)). **B** and **C**: Schemes of the inner anatomy of ascidian tadpole larvae. **B:** Entire tadpole larva of *Ciona intestinalis* modified from Berrill (1947). **C:** Magnification of the trunk (tr) of the larva of *Ciona robusta* modified from Kowalevsky (1866, referred to as *Ascidia intestinalis*). The incurrent and excurrent openings are still blocked, the larva feeds from yolk. ap: adhesive papillae, en: endostyle, nt: neural tube, oc: larval ocellus, pbb: primordial branchial basket, pdt: primordial digestive tract, sc: larval statocyte, ta: tail, tu: tunic

as *Ascidia intestinalis*) with the significant finding that larvae possess a notochord (=Chorda dorsalis) and a neural tube both features typical of Chordata. Therefore, he reclassified the taxon Tunicata that before this investigation was thought to belong to Mollusca (Cuvier 1840), within Chordata (Kowalevsky 1866). Most lecitotrophic tadpole larvae remain planktonic for only a few hours until they find a beneficial spot to settle and then metamorphose into a filter-feeding adult. Ascidian tadpole larvae find a new place to settle with the aid of an ocellus and a statocyte (Millar 1971, see also Fig. **3** for the morphology of larvae). Additionally, they are equipped with adhesive papillae that probably also chemically test the substratum on which they settle (Torrence and Cloney 1982, Takamura 1998, Groppelli et al. 2003, Caicci et al. 2010).

3.1.7 Ecological and economical value

The high ecological significance of tunicates is a result of their filter-feeding lifestyle. Jørgensen (1952) showed that individuals of the ascidians *Molgula manhattensis* and *Ciona intestinalis* filter up to 20 liters of water per hour. As ascidians constantly filter water throughout the entire day (MacGinitie 1939), this filtration rate would result in up to 500 liters of filtered sea water per day per individual. At the same time tunicates also accumulate toxins (reviewed in Lambert 2005), which is of high ecological importance in a world with increasing human population growth and pollution of oceans caused by humans. “Thaliacea” and Appendicularia are also a major component of the zooplankton in the oceans so that many other marine animals feed on them. Moreover, “Thaliacea” have high metabolic rates of oxygen consumption and ammonium excretion, which means they probably play an important role in recycling nitrogen in the upper mixed layer of the seawater (Biggs 1977, Bone 1998). Also, Appendicularia have been found to strongly influence the marine organic carbon flux. When the animal’s filter-feeding house is clogged by food particles the house is discarded and the animal builds a new one. That way, a considerable amount of carbon and nutrients from upper sea levels sinks to the deep sea floor, supplying benthic organisms with nutrients and influencing the greenhouse effect (Alldredge 2005, Robison et al. 2005).

Some ascidians are edible and a delicacy mainly in East Asian countries, certain parts of the Mediterranean, and some countries in South America (Fig. **1G**). Because of their sessile lifestyle, several ascidian species synthesize toxins that they store in the tunic to prevent being eaten by predators like fishes and crabs. Some of these toxins turned out to be useful as pharmaceuticals for humans. One very successful pharmaceutical is ecteinascidin which is synthesized by the sessile colonial ascidian *Ecteinascidia turbinata* and used as antitumor agent (Rineheart et al. 1990). However, the dispersion of ascidians can also cause ecological problems when invasive ascidian species, as competitively dominant fouling organisms, have deleterious effects on native species or when ascidians overgrow commercially farmed oysters (Miyazaki 1938, Lambert 2005, Rodriguez and Ibarra-Obando 2008).

3.2 The central nervous system of Tunicata

3.2.1 Central nervous system of larvae

Belonging to the taxon Chordata, Tunicata also develop the central nervous systems (CNS) during a process called neurulation. After gastrulation is complete, ectodermal cells of the dorsal side of the embryo invaginate induced by the notochord (Chorda dorsalis) (Jacobson 1962, van Straaten et al. 1988, Schoenwolf and Smith 1990). Lateral parts of the invagination fuse and become the neural tube (e.g., Nicol and Meinertzhagen 1988). The Chorda dorsalis in every tunicate stage is limited to the tail, which is the reason why tunicates are sometimes called urochordates (after Balfour 1881). The larval CNS of some tunicate species is well studied. For the phlebobranch ascidian species and model organisms *Ciona intestinalis* (e.g., Imai and Meinertzhagen 2007, Ryan et al. 2018), and the closely related *Ciona robusta* (Takamura et al. 2010), the stolidobranch ascidian species *Botryllus schlosseri* (Manni et al. 1999), and the appendicularian species *Oikopleura dioica* (Cañestro et al. 2005, Søviknes et al. 2007) neuroanatomical data of the larvae are available. The larval ascidian CNS consists of a sensory vesicle, a neck region, a visceral ganglion, and a tail nerve cord. The sensory vesicle comprises a statocyte, an ocellus, and coronet cells that are presumably hydrostatic pressure receptors (Eakin and Kuda 1970). Appendicularian hatchlings possess a CNS that consists of a brain, a compact nerve trunk, a caudal ganglion, and a hollow tail nerve cord (Cañestro et al. 2005). The brain is equipped with coronet cells; ocelli and a statocyte are missing (Olsson 1975).

3.2.2 Central nervous system of adults

In adult tunicates, the CNS consists of a simple dorsal ganglion or brain (sensu Richter et al. 2010), which is located on the dorsal side, between the incurrent and excurrent siphons (Fig. **2A**). The brain is divided into an area that primarily contains nerve fibers, the central neuropil, and a superficial layer of nerve cell somata, the cortex. The adult brain anatomy has been described in some detail for selected tunicate species (Huus 1956, Olsson et al. 1990, Koyama and Kusunoki 1993, Lacalli and Holland 1998, Zaniolo et al. 2002). Although these studies already revealed a great variation in the development and shape of certain structures of the CNS, the adult tunicate CNS in recapitulating reviews is described as neural complex consisting of a cerebral ganglion (brain) and an associated enigmatic neural gland. Mainly five nerves emanate from the brain — paired anterior and posterior nerves, and an unpaired ventral visceral nerve. The neural gland is connected to the branchial basket via a ciliated duct and a funnel-shaped dorsal tubercle, and has a posterior extension, the dorsal strand (Burighel and Cloney 1997, Manni and Pennati 2016, see also Fig. **2B**). The function of the neural gland is still controversially debated (e.g., Ruppert 1990, Nozaki and Gorbman 1992, Burighel et al. 1998, Deyts et al. 2006, Joly et al. 2007, Dahlberg et al. 2009). The shape of the dorsal tubercle differs on the interspecific level and therefore is a valuable taxonomic

characteristic in the identification of species (e.g., Van Name 1945, Berrill 1950, Rocha et al. 2012) and possibly phylogenetically informative. The dorsal strand is described as a long posterior extension that runs toward the gonads. This cell cord probably contains stem cells and provides new nerve cells during regeneration processes (Koyama 2002, Dahlberg et al. 2009). The CNS of adult tunicates is studied for the phlebobranch model organisms *Ciona intestinalis* (Mackie 1995, Dahlberg et al. 2009) and *C. robusta* (Osugi et al. 2017), the stolidobranchs *Polyandrocarpa misakiensis* (Koyama and Kusunoki 1993) and *Botryllus schlosseri* (Zaniolo et al. 2002), the thaliacean *Thalia democratica* (Lacalli and Holland 1998 – oozooid stage), and the appendicularian *Oikopleura dioica* (Olsson et al. 1990).

Thaliacean brains are also constituted of a central neuropil and a surrounding cortex of neuronal cell somata (reviewed in Bone 1998). Only one electron microscopical investigation of the brain of a salp — an oozooid — exists. In that study, the neural gland and a gland duct were missing, although a dorsal tubercle is developed in the salp. Moreover, it was discovered that the brain anatomy is bilaterally symmetrical and three clusters of motoneurons were revealed (Lacalli and Holland 1998). The brains of Doliolida and Pyrosomatida are described to still be associated with neural glands. The neural gland of Doliolida is located on the ventral side of the brain, visible as a small projection (Uljanin 1884). The organ seems to be more extensive in Pyrosomatida, however, descriptions here are also brief (Neumann 1909). A connection of the neural gland with the branchial basket via the dorsal tubercle and gland duct is present in Doliolida and Pyrosomatida (Uljanin 1884, Neumann 1909), in Salpida only the dorsal tubercle is developed (Metcalf 1898). For the three thaliacean taxa a dorsal strand is not described.

The neural complex of adult appendicularians is described based on transmission electron microscopy for *Oikopleura dioica* (Holmberg 1982, 1984, Olsson et al. 1990). These studies show that adult appendicularians retain the larval CNS but additionally develop a neural gland, consisting only of a few cells, with a gland duct and dorsal tubercle on the right side of the brain (Holmberg 1982). From the brain two pairs of anterior nerves, a pair of posterior nerves and the caudal nerve cord branch off.

3.2.3 Eyes as integrated part of the brain

A more elaborate brain is described for “Thaliacea”. The brain in Pyrosomatida and Salpida also features eyes that are an integrated part of it. Lacalli and Holland (1998) even discovered additional optical neuropils in the brain of the oozooid of the salp *Thalia democratica* that connect the eye with the main part of the brain. Further anatomical studies of thaliacean eyes and brains date back to more than a century ago (e.g., Ussow 1876, Brooks 1893, Göppert 1893, Metcalf 1898, Redikorzew 1905 — for Salpida; Neumann 1909 — for Pyrosomatida). Electron microscopical investigation by Gorman et al. (1971) showed one photoreceptor cell of the eyes of *Thalia democratica* that should be classified as rhabdomeric type. In rhabdomeric photoreceptor cells the membrane for the storage of photosensitive pigments (opsins) is

provided by the apical cell surface. In ciliary photoreceptor cells the enlarged membrane is generated by the membrane of the cilium. Ciliary photoreceptor cells are present in the ocelli of ascidian tadpole larvae (Dilly 1964, Eakin and Kuda 1970, Kusakabe and Tsuda 2007). While for salps from diverse studies it was shown that the asexual oozooids in various species are equipped with a single horseshoe-shaped eye, the sexual blastozooids possess several pigment cup eyes with different arrangements of the single eyes in different species (e.g., Ussow 1876, Brooks 1893, Göppert 1893, Metcalf 1898, Redikorzew 1905). Little is known about the eye anatomy in Pyrosomatida. Only a brief description and a drawing of a sagittal and a transverse section through the eye and brain of *Pyrosomella verticillata* exist (Neumann 1909). Unfortunately, the anatomy of the complete eye cannot be reproduced from that study and no other investigations were conducted on the anatomy of the pyrosome eye, yet.

3.2.4 Distribution of serotonin

Studies on the distribution of neurotransmitters in various metazoan taxa produced insights in subdivisions of brains (e.g., Brenneis et al. 2008, Mayer et al. 2010, Krieger et al. 2012). An overview of investigations and localizations of neurotransmitters in tunicate species can be found in a review by Manni and Pennati (2016). However, these authors point out that the knowledge of distribution patterns of neurotransmitters in tunicates is fragmentary and usually limited to the chordate model organism *Ciona intestinalis*. Serotonin is a neurotransmitter that is common throughout metazoan taxa (see e.g., Schmidt-Rhaesa et al. 2015). The distribution of the neurotransmitter serotonin is described for larvae and juveniles of the solitary phlebobranch *Phallusia mammillata* (Pennati et al. 2001), for adults of the solitary phlebobranch species *Ascidiella aspersa*, *Ascidia mentula*, *Ciona intestinalis*, and *Phallusia mammillata* (Georges 1985), for adults of the colonial stolidobranch species *Botryllus schlosseri* (Tiozzo et al. 2009), for adults of the solitary stolidobranch species *Styela clava*, *Styela rustica*, and *Molgula retortiformis* (Sakharov and Salimova 1982), for the appendicularian species *Oikopleura rufescens*, and *Oikopleura fusiformis*, for the blastozooid of the doliolid species *Doliolum nationalis*, and for diverse larvae of ascidian species (Stach 2005), for the salp species *Thalia democratica* (Pennati et al. 2012), for the pyrosome species *Pyrosomella verticillata* and for the blastozooid (phorozooid) of the doliolid species *Doliolina muelleri* (Valero-Gracia et al. 2016). These studies showed serotonin-like immunoreactivity (serotonin-lir) by labeling complete specimens or dissected organs with antibodies against serotonin. Although some of the studies focused on single organs, they mainly showed that serotonin is present in ascidian endostyles, peripharyngeal bands, esophagus, and intestines, but could not show a localization of the neurotransmitter within the adult ascidian and pyrosome CNS (e.g., Georges 1985, Pennati et al. 2001, Tiozzo et al. 2009, Valero-Gracia et al. 2016). On the other hand, in Salpida and Doliolida serotonin-lir is present in the CNS, but also in the intestines, and peripharyngeal bands (Stach 2005, Pennati et al. 2012). To the exception of a few cells in

the brain of *Oikopleura rufescens*, serotonin-lir is not present in Appendicularia. Most ascidian larvae possess serotonin-lir in the CNS and digestive tract, but in some aplousobranch larvae serotonin-lir cells seem to be reduced (Pennati et al. 2001, Stach 2005).

3.3 Phylogeny

3.3.1 Tunicata

Because of their soft bodies, Tunicata at first were considered to belong to Mollusca (Linneaus 1758). Not before 1866, Tunicata were reclassified as Chordata because of Kowalevsky's famous investigation of the ontogeny of the two solitary ascidian tunicates *Phallusia mammillata* and *Ciona robusta* (referred to as *Ascidia intestinalis*), revealing that the larvae of these two "molluscan" species develop their nervous systems through neurulation, which is typical of chordate species (Kowalewsky 1866).

The classification of Tunicata was based on differences in phenotypic characters or life history strategies. Traditionally, they are divided into three major taxa: Ascidiacea, "Thaliacea" and Appendicularia (Huxley 1851). Lahille proposed a classification of Ascidiacea into three clades that is based on the morphology of the branchial baskets: Aplousobranchiata, "Phlebobranchiata", and Stolidobranchiata. Species belonging to Aplousobranchiata possess branchial baskets without folds, papillae or internal longitudinal blood vessels; "Phlebobranchiata" are ascidians with papillae and internal longitudinal blood vessels in the branchial baskets; and branchial baskets of Stolidobranchiata are folded and contain internal longitudinal blood vessels (Lahille 1886). In 1898, Perrier suggested to subdivide Ascidiacea due to the position of the gonads in relation to the branchial basket. Gonads of "Enterogona"[4] (grouping Lahille's Aplousobranchiata and "Phlebobranchiata") are located within the intestinal loop and connected with the visceral wall, while gonads of Pleurogona (considering Lahille's Stolidobranchiata) are connected with the parietal body wall (Lahille, 1886, Perrier 1898, see Fig. **4A** for an overview on traditional tunicate taxa).

With molecular techniques making enormous progress at the end of the 20th century, tunicate classifications based on phenotypic characters were challenged. Many analyses of 18S rDNA were conducted. Most of these molecular phylogenetic studies found "Phlebobranchiata" paraphyletic or polyphyletic and grouped "Thaliacea" within Ascidiacea, resulting in a paraphyletic Ascidiacea. These studies consequently supported the hypothesis that planktonic "Thaliacea" derived from a sessile ascidian-like ancestor (Wada 1998, Swalla et al. 2000, Stach and Turbeville 2002, Zeng et al. 2006, Tsagkogeorga et al. 2009, Govindarajan 2011, Delsuc et al. 2018, Kocot et al. 2018, Fig. **4B**), challenging the traditional view that "Thaliacea" represent an ancestral plesiomorphic planktonic lifestyle (e.g., Garstang 1928, Berrill 1936, Lacalli 1999). In most molecular phylogenies Appendicularia were sister taxon to the other

[4]: The group "Enterogona" is put in quotation marks because the present phylogenetic analyses and some published molecular analyses illustrate that the group is not monophyletic.

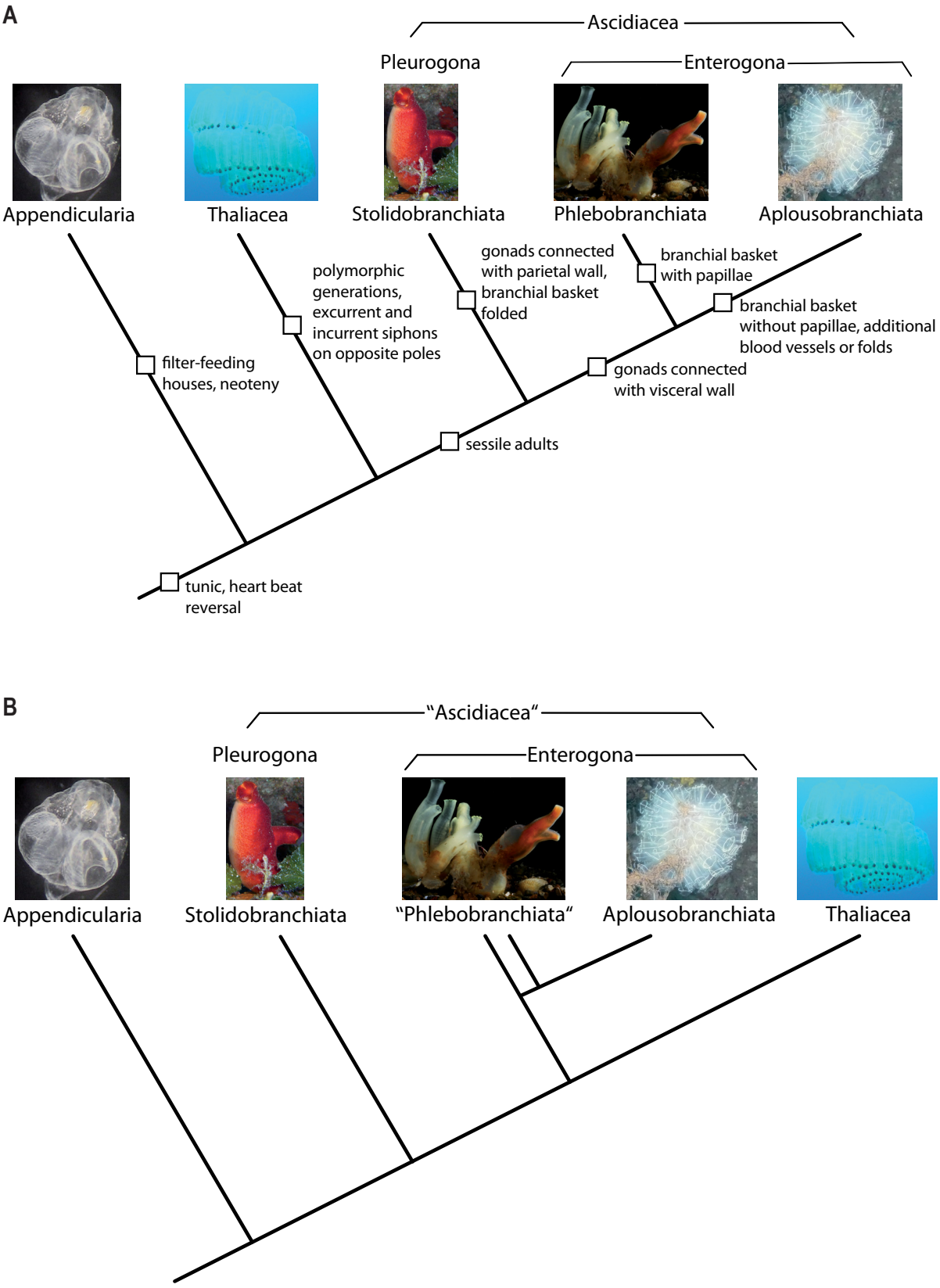

Figure 4: Two cladograms on tunicate evolution. Images of representatives of "Phlebobranchiata" and Appendicularia provided by Priv.-Doz. Dr. Thomas Stach, pictures of "Thaliacea", Stolidobranchiata, and Aplousobranchiata provided by Dipl. Biol. Peer Martin. **A:** Traditional phylogeny of Tunicata with inferred apomorphies (e.g., after Seeliger 1885). **B:** Recently published tree of tunicate evolution based on phylogenomic studies (Delsuc et al. 2018, Kocot et al. 2018).

tunicate taxa, indicating that the free-living lifestyle is plesiomorphic for Tunicata and not a derived state (e.g., Wada 1998, Govindarajan et al. 2011, Delsuc et al. 2018, Kocot et al. 2018, see above). Nevertheless, the interrelationships of the five major tunicate groups in molecular phylogenetic analyses are highly contradictory. It has been pointed out by various authors that within Tunicata, increased mutation rates (Wada 1998, Tsagkogeorga et al. 2010) and long-branch-artefacts (Swalla et al. 2000, Delsuc et al. 2008) might strongly affect the results of molecular phylogenies, and that the phylogenetic signal might not be as high as indicated by potentially misleading statistic support values in published phylogenies (Stach 2014). Phylogenies that are based on morphological data with a consequent character coding and parsimony analysis as proposed by Hennig (1982) in tunicates are limited to selected taxa (Moreno and Rocha 2008) or to comparatively few characters (Stach and Turbeville 2002, Rigon et al. 2013). Therefore, the present study was carried out to remedy these defects. Tunicate morphology contains phylogenetic information and should be used as an independent data set to understand and substantiate phylogenetic hypotheses (after Wägele, 2001). Likewise, a profound understanding of phenotypic character transformations within Tunicata is indispensable in order to reconstruct the ground pattern of the last common tunicate ancestor and to elucidate chordate evolution which still is elusive.

3.3.2 Chordata

Traditionally, Cephalochordates, with a more "fish-like" morphology and Craniota were grouped together, to the exclusion of Tunicata (Ax 2001, Stach 2008; Notochordata hypothesis, see Fig. **5A**). However, several large-scale molecular phylogenetic analyses recover Tunicata as sister group to Craniota, to the exclusion of Cephalochordata (Delsuc et al. 2006, Edgecombe et al. 2011, Dunn et al. 2014; Olfactores hypothesis, see Fig. **5B**), with weak morphological support (Stach 2008, Swalla and Smith 2008). A third possible, but rarely supported, hypothesis places Tunicata and Cephalochordata as sister taxa, to the exclusion of Craniota (Minot 1897, Masterman 1898; Atriozoa hypothesis, see Fig. **5C**).

With the Olfactores hypothesis as widely accepted nowadays, a "fish-like" ancestor must have evolved in the stem lineage of Chordata. An evolution of this putative ancestor to a sessile ascidian on the one hand, and a vertebrate "fish" on the other hand, from a morphological point of view is difficult to imagine. Especially, as non-chordate deuterostomes (Echinodermata and Hemichordata) probably derived from an ancestor with a worm-like appearance or even a sessile lifestyle (Garstang 1928, Gee 1996, Cameron et al. 2000, Swalla and Smith 2008, Stach 2014). The Olfactores hypothesis also raises the question, whether remnants of the active planktonic and "fish-like" lifestyle can be traced in the present — usually sessile — tunicates. Character transformations from a sessile (in Deuterostomia) to a free-living (in Chordata) and again sessile mode of life in Tunicata are obscure. If these transformations left any traces in the morphologies of recent species, they could be found in the most complex organ system,

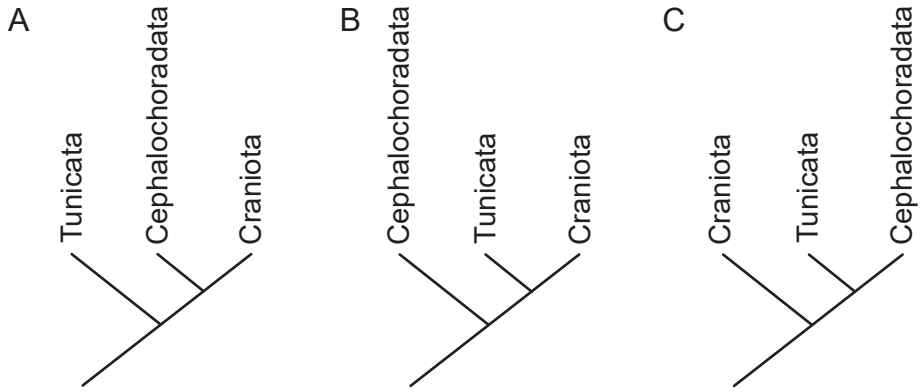

Figure 5: Three possible cladograms showing three hypotheses of chordate evolution. **A:** Notochordata hypothesis. **B:** Olfactores hypothesis. **C:** Atriozoa hypothesis.

the nervous system. Although, the nervous system is considered to change slower than other organ systems (Fritzsch et al. 1990, Gilland and Baker 2005), it can also be variable and adaptive to different lifestyles (e.g., Quiroga et al. 2015). With one of the main function of the nervous system to react to outer stimuli, usually by motor activity, the CNS controls patterns of activity. In the case of Tunicata, the CNS therefore could preserve traces of a more active lifestyle.

3.4 Aims and scope of present work

Detailed studies on the neuroanatomy of tunicates are limited to certain stages or taxa. As Tunicata might be the closest living relatives to Craniota (with a highly elaborated CNS), these studies so far mainly cover tunicate model organisms that might reflect the planktonic vertebrate lifestyle (larvae of the phlebobranch ascidian species *Ciona intestinalis* and the appendicularian species *Oikopleura dioica*). Studies on the neuroanatomy of adult ascidians or thaliaceans are largely missing, with only few exceptions. A broader-scaled comparative analysis of the morphology of the tunicate CNS with a phylogenetic framework has never been conducted. Many of the available data on the neuroarchitecture are more than 100 years old and lack sufficient documentation. Due to technical limitations of that time, for most tunicate species descriptions of the fine anatomy of the CNS are lacking, e.g., numbers and positions of nerves, subdivisions of the brain, compositions of eyes, and comparative distributions of neurotransmitters are almost completely missing (see reviews by Madin 1995, Bone 1998, Mackie and Burighel 2005, Piette and Lemaire 2015, Manni and Pennati 2016). Thus, important characters for phylogenetic analyses are missing and homology hypotheses of individual phenotypic characters regarding the tunicate nervous system are not tested.

To increase the number of available neuroanatomical data of Tunicata, my morphological study presents high-resolution confocal laser scanning microscopy and electron microscopy,

together with serial sectioning for light microscopy and digital 3d reconstructions of the tunicate neural complexes. I mainly focused on the adult tunicate CNS and the general anatomy, as this allows for coding of many independently evolved phenotypic characters. For comparative investigations on distribution patterns of neurotransmitters, antibodies against serotonin were utilized. In Tunicata, studies on the distribution of this neurotransmitter are rare, comparative studies are nearly entirely missing. For Salpida and Doliolida — taxa that comprise animals with different polymorphic life cycle stages — studies are usually limited to a single stage, although it has been shown that the morphologies of the different stages considerably differ (Chamisso 1819, Brooks 1893, van Soest 1998, Godeaux 2003).

In the present study, I collected morphological data, which were used for the coding of independent characters. We followed Sereno's suggestions for character coding and distinguished between neomorphic ("absent-present-characters") and transformational characters (characters with comparable character states including defined variables, e.g., length, shape) (Sereno 2007). Morphological characters of the nervous system were analyzed in a phylogenetic framework for Tunicata for the first time, although it was previously shown that neuroanatomical characters serve as a valuable source for phylogenetic inferences in diverse metazoan taxa (Loesel 2011, Nieuwenhuys et al. 2014, Schmidt-Rhaesa et al. 2015). A new tunicate phylogeny based on morphological data is suggested. Additionally, a second combined phylogenetic analysis was performed based on combined morphological and 18S rDNA-sequence data, in order to gauge the influence of morphological data toward the resulting phylogenetic hypothesis. The resulting morphology-based phylogeny allowed for the tracing of character transformations and for inferring ancestral character states. At the same time, my comparative investigations strongly further the amount of available morphological data for these beautiful and peculiar animals.

4 Serotonin-like immunoreactivity in Tunicata

4.1 Publication

This is a post-peer-review, pre-copyedit version of an article published in *Zoomorphology*. The final authenticated version is available online at:

http://dx.doi.org/10.1007/s00435-016-0317-8.

Comparative study of serotonin-like immunoreactivity in the branchial basket, digestive tract, and nervous system in tunicates

Authors

Katrin Braun, Humboldt-Universität zu Berlin, Institut für Biologie, katrin.braun@hu-berlin.de

Thomas Stach, Humboldt-Universität zu Berlin, Institut für Biologie, thomas.stach@hu-berlin.de

Acknowledgements

The authors would like to thank Dr. Carsten Lüter from the Museum für Naturkunde Berlin for permitting access to the Leica SPE CLSM. Funding by the Deutsche Forschungsgemeinschaft (DFG) and the Elsa-Neumann-Stipendium des Landes Berlin are gratefully acknowledged.

Abstract

As one of the three major chordate taxa the highly diverse taxon Tunicata has always played a key role in considerations of evolutionary origins of vertebrates, especially since several larger-scaled molecular phylogenetic analyses support the hypothesis that tunicates are the sister group to vertebrates. Molecular phylogenetic studies of the relationships within Tunicata are highly contradictory and cladistic analyses of morphological characters for Tunicata remained limited. In order to come to a better understanding of chordate evolution, we comparatively investigated nine different tunicate species belonging to five different higher tunicate taxa: Phlebobranchiata, Aplousobranchiata, Stolidobranchiata, Thaliacea, and Appendicularia using immunofluorescence labeling with antibodies against serotonin in conjunction with confocal laser scanning microscopy. We found that adult ascidians are comparable in regards to their respective patterns of serotonin-lir, whereas the planktonic tunicates differ in several respects. The distribution patterns of serotonin-lir suggest that serotonin-lir can behave as an independent character during evolution. While the distribution pattern of serotonin-lir agrees well with classical taxonomic groupings, phylogenetic interpretation remains inconclusive, as ad hoc hypotheses are always necessary to explain contradictory character distribution. Based on light-microscopically observed morphology, we could distinguish three different types of serotonin-lir cells, most probably functionally distinctive. These were more or less spherical serotonin-lir cells, possibly involved in the control of ciliary beating and mucus secretion, elongated serotonin-lir cells potentially involved in hormonal regulation of feeding, and serotonin-lir neurons that might be implicated in the initiation of locomotory behavior.

Keywords

Ascidians, larvaceans, salps, evolution, cell type, confocal microscopy

Introduction

Since Alexander Kowalewsky showed in his famous study on the ontogenetic development of the ascidian tunicates *Phallusia mammillata* (Cuvier, 1815) and *Ciona robusta* Hoshino and Tokioka, 1967 (referred to as *Ascidia intestinalis* by Kowalewsky), that these marine invertebrates developed similarly to chordates (Kowalewsky 1866), tunicates, and especially ascidians played a central role in all considerations of evolutionary origins of the equally chordate vertebrates (e.g., Romer 1972, Jefferies 1986, Maisey 1986). The interest in tunicates was renewed through the establishment of ascidian species as model organisms for molecular developmental studies (Dehal et al. 2002, Imai et al. 2006, Abitua et al. 2012, Diogo et al. 2015). An additional finding that generated new interest in this group of animals, was the result from several larger scale molecular phylogenetic analyses that tunicates might even be more closely related to vertebrates than had been previously assumed (Delsuc et al. 2006, Dunn et al. 2008, Edgecombe et al. 2011). While the majority of recent molecular phylogenies supports the hypothesis that tunicates are the sister group to vertebrates, the decisiveness of the data at the base of these analyses has been criticized (Stach 2014) and it is notable that morphological support for this hypothesis remained rather weak (see e.g., reviews by Swalla and Smith 2008, Stach 2008).

In order to come to a better understanding of chordate evolution, a strategy could be to reconstruct ground patterns of the taxa to be compared in detail (Stach 2015, Scholtz 2013, Richter and Wirkner 2014). The more than 2500 described species of tunicates offer the opportunity to do so, because they comprise a bewildering variety of life cycles, encompassing the sessile ascidians as well as the free-living, planktonic salps, the brightly bioluminescent pyrosomes, the doliolids with their unique polymorphism, and the larvaceans with their intricate and elaborate filtering houses (e.g., Bone 1998, Lemaire 2011). Molecular phylogenetic studies of the relationships of higher taxonomic groups within Tunicata are highly contradictory (see e.g. Stach and Turbeville 2002, Swalla et al. 2000, Stach et al 2010, Zeng et al. 2006, Tsagkogeorgas et al. 2009, Govindarajan et al 2011) perhaps reflecting an elevated mutation rate (e.g., Tsagkogeorgas et al 2009). Cladistic analyses of morphological characters for Tunicata on the other hand are available for a limited set of taxon and character samplings only (Stach and Turbeville 2002, Moreno and da Rocha 2008, Van Soest 1981).

Because nervous systems have been shown to allow phylogenetic interpretations in numerous taxa (e.g. Krieger et al. 2012; Mayer et al. 2010; Moret et al. 2004, Schmidt-Rhaesa et al. 2015), we explored this potential in tunicates by comparatively investigating nine different tunicate species belonging to five different higher tunicate taxa: Phlebobranchiata, Aplousobranchiata, Stolidobranchiata, Thaliacea, and Appendicularia using immunofluorescence labeling in conjunction with confocal laser scanning microscopy.

Material and methods

Collection localities of all specimens along with taxonomic details are listed in **Table 1**. Ascidian specimens were collected in the lower intertidal or upper subtidal. *Thalia democratica* was collected manually from the water column using snorkeling gear. Three chains of blastozooids were carefully transferred into a wide neck Kautex bottle. Specimens of *Oikopleura dioica* were provided from Sars International Centre for Marine Molecular Biology and reared at Humboldt-Universität zu Berlin through numerous generations.

Fixation

Before fixation all ascidians were anaesthetized for approximately an hour using menthol crystals. *T. democratica* and *O. dioica* were fixed directly without anaesthetization. All specimens were fixed in 4% paraformaldehyde in phosphate-buffered saline (PBS: 0.01M, pH 7.4) for at least 30 minutes to a maximum fixation time of 1 h. Samples were rinsed in PBS and stored in PBS containing 0.05% NaN_3 at 4°C for no longer than 6 months after fixation.

Immunohistochemistry

Prior to whole-mount incubation the tunic of all ascidians was removed. From three specimens of *Ciona intestinalis* the neural complex was dissected and afterwards embedded in 2% Agarose (low gelling temperature; Sigma, St. Louis, Missouri, USA) diluted in PBS. Afterwards serial transverse and longitudinal sections of 75µm thickness were cut with a Leica VT1200 S vibratome (Leica Biosystems, Nussloch, Germany) and transferred into PBS.

All specimens and sections were rinsed three times for 5 min in PBS, three times for 10 min and four times for 30 min in PBTx (PBS containing 0.5% Bovine Serum Albumine (BSA), 0.3% Triton-X-100, and 1.5% Dimethyl Sulfoxide (DMSO)). Samples were blocked with 5% Normal Goat Serum (NGS) in PBTx twice for 30 min. Incubation in primary antibodies against serotonin (5-HT (Serotonin) Rabbit; ImmunoStar, Hudson, Wisconsin, USA) and against tyrosinated-α-tubulin (Anti-Tubulin, Tyrosine antibody produced in mouse; Sigma, St. Louis, Missouri, USA) was carried out in preincubation fluid at a dilution of 1:100 (serotonin) and 1:1000 (tyrosinated-α-Tubulin) at 4°C for at least 2.5 days. Samples were rinsed three times for 10 min and again four times for 30 min in PBTx at room temperature. Preincubation was carried out twice for 30 min in 5% NGS diluted in PBTx. Animals and sections were incubated over night at room temperature in darkness in secondary antibodies Alexa Fluor® 488 goat anti-rabbit IgG (Molecular Probes, Eugene, Oregon, USA) and Cy™3 AffiniPure Goat Anti-Mouse IgG (Jackson ImmunoResearch Laboratories, Inc., Philadelphia, Pennsylvania, USA) diluted in preincubation fluid at a concentration of 1:100 each. All specimens and sections were washed in PBS three times for 10 min and labeled with 4'6-Diamidino-2-Phenylindole (DAPI) for at least 1h, and Hoechst 33342 (Sigma, St. Louis, Missouri, USA) for at least 15 min. Samples were rinsed in PBS for 10 min twice, for 30 min again, and dehydrated through an ethanol series. All specimens and sections were cleared with Murray's fluid (2 parts benzyl benzoate: 1 part benzyl alcohol) and mounted in Murray's fluid on microscope slides. Every staining experiment was performed together with two

different controls, one with primary antibodies omitted, the second with secondary antibodies omitted.

Microscopy

All specimens were examined using a Leica TCS SPE confocal laser scanning microscope (Leica Microsystems, Heidelberg, Germany). Appropriate filter settings were applied to record stacks of confocal optical sections. FIJI software (Schindelin et al. 2012) and Adobe Photoshop CS3 software were used for the analysis of images. One stack of confocal images of *O. dioica* was processed with Amira 5.4.3 software (FEI Visualization Sciences Group, Berlin, Germany) to create a three-dimensional (3D) model of the nervous system. To this end the tyrosinated-α-Tubulin channel was used to label only nerve fibers. Additionally the volume of the cilia was rendered from the same channel to show the position of inner organs.

Table 1: Information on examined specimens; adult stages were used in all species. In the salp *T. democratica* blastozooid stages were analyzed.

Species	Family	Order	Origin	# Specimens examined
Clavelina lepadiformis (Müller, 1776)	Clavelinidae	Aplousobranchiata	Helgoland, Germany	5
Diplosoma listerianum (Milne-Edwards, 1841)	Didemnidae	Aplousobranchiata	Helgoland, Germany	5
Ascidiella scabra (Müller, 1776)	Ascidiidae	Phlebobranchiata	Helgoland, Germany Kristineberg, Sweden	9
Corella parallelogramma (Müller, 1776)	Corellidae	Phlebobranchiata	Kristineberg, Sweden	8
Ciona intestinalis (Linnaeus, 1767)	Cionidae	Phlebobranchiata	Helgoland, Germany Kristineberg, Sweden	15
Perophora japonica Oka, 1927	Perophoridae	Phlebobranchiata	Helgoland, Sweden	5
Botryllus schlosseri (Pallas, 1766)	Styelidae	Stolidobranchiata	Kristineberg, Sweden	17
Oikopleura dioica Fol, 1872	Oikopleuridae	Appendicularia	Bergen, Norway	22
Thalia democratica (Forskål, 1775)	Salpidae	Thaliacea	Ibiza, Spain	5

Results

Phlebobranchiata

The solitary ascidian species *Ascidiella scabra* showed a specific pattern of serotonin-like immunoreactivity (serotonin-lir). Serotonin-lir cells are positioned along the peripharyngeal band forming a line that runs into the endostyle and retropharyngeal band ending in the esophagus (see **Fig. 1A**). In the peripharyngeal and retropharyngeal band positively labeled cells constitute several rows of irregularly arranged spherically shaped cells with a diameter of 5µm. In the endostyle these cells are elongated with a length of approximately 7µm and symmetrically arranged in two bands (**Fig. 1B-D**). Some serotonin-lir cells are approached by nerve fibers originating in a nerve that parallels the endostyle (**Fig. 1C**). Numerous serotonin-lir cells are also distributed in the epithelia of the esophagus, the stomach and intestine. These cells are spherical with a diameter of approximately 5µm or elongated with a length of approximately 8µm. No serotonin-lir neurons could be observed in the central nervous system of *A. scabra*.

In the solitary ascidian species *Corella parallelogramma* the intestine is situated on the right side of the branchial basket, contrary to most other ascidians. Serotonin-lir cells are present in *C. parallelogramma* in several rows along the peripharyngeal band extending into the endostyle and retropharyngeal band and continuing into the esophagus (**Fig. 1E**). While several rows of irregularly arranged serotonin-lir cells parallel the peripharyngeal and retropharyngeal band, two symmetric bands of serotonin-lir cells extend along the endostyle. All positively labeled cells are roughly spherical with a diameter of 4-6µm (see **Fig. 1F-H**). Only few individual serotonin-lir cells are positioned in the stomach. In all areas where serotonin-lir cells occur, neurites approaching these cells were detected. These neurites have their origin in a nerve that runs along the endostyle. In the central nervous system no serotonin-lir cells could be allocated.

Perophora japonica is a colonial ascidian species, in which individual zooids are connected through stolons. Specimens of *P. japonica* showed a distinct pattern of serotonin-lir cells along the peripharyngeal band, the endostyle and retropharyngeal band running into the esophagus (see **Fig. 1I**). In the peripharyngeal and retropharyngeal bands serotonin-lir cells are irregularly arranged in several rows. These cells have a spherical shape and measure approximately 4µm in diameter. In the endostyle two symmetric bands of positively labeled spherical cells with a diameter of approximately 4µm are present (see **Fig. 1J**). In the esophagus, stomach and intestine numerous serotonin-lir cells are scattered in the epithelium. Some of these cells are spherical measuring approximately 4µm in diameter. Other serotonin-lir cells in the esophagus, stomach and intestine are elongated with a length of up to 10µm (see **Fig. 1K**). In the endostyle and in the epithelium of the stomach neurites could be detected closely approaching serotonin-lir cells. In the central nervous system of *P. japonica* no serotonin-lir was detected.

The solitary ascidian species *Ciona intestinalis* is traditionally considered to belong to the Phlebobranchiata although the taxonomic position is debatable (Kott 1985; see also discussion).

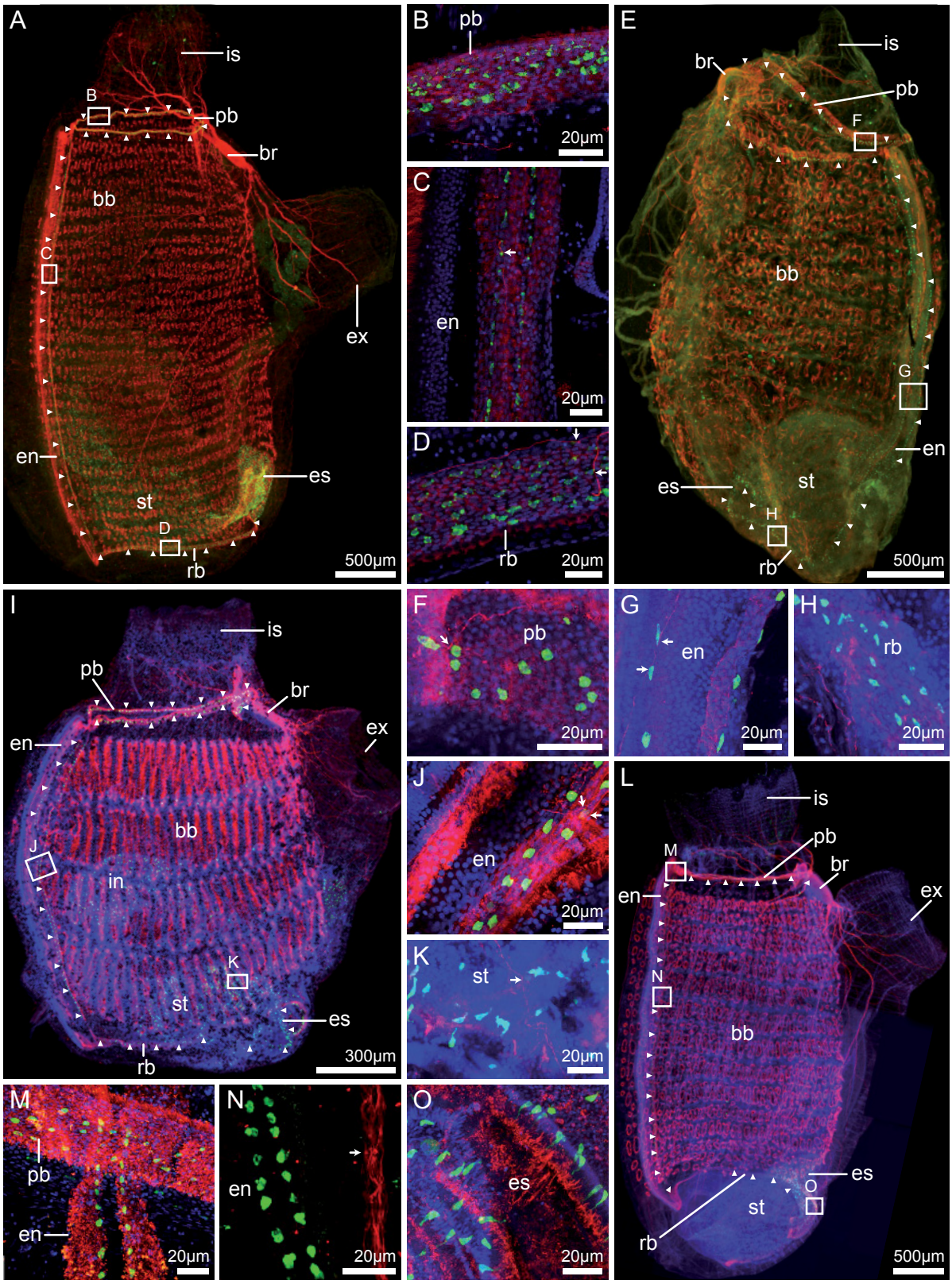

Fig. 1: Z-projections of confocal laser scanning micrographs of four phlebobranch ascidian species. Specimens are stained with antibodies against serotonin (green), tyrosinated-a-Tubulin (red), and with DAPI and Hoechst (blue). **A** Lateral view of a complete individual of *Ascidiella scabra*, the dorsal side is to the right. A band of serotonin-lir cells extends from the peripharyngeal band (pb), through the endostyle (en) and the retropharyngeal band (rb) into the esophagus (es); individual cells are marked with arrowheads. Note that in the brain (br), no serotonin-like immunoreactivity is detectable. **B-D** Details of areas marked in **A**. **B** Several irregular rows of serotonin-lir cells are present in the peripharyngeal

band. **C** In the endostyle, serotonin-lir cells form two rows that are bilaterally symmetrically extending toward the retropharyngeal band. The subendostylar nerve parallels the band and innervates serotonin-lir cells (arrow). **D** In the retropharyngeal band, serotonin-lir cells are irregularly arranged, forming several irregular rows. Arrows indicate innervation of two serotonin-lir cells. **E** Whole-mount of *Corella parallelogramma*. View from right side, ventral is to the right. The distribution pattern of serotonin-lir cells (see arrowheads) is the same as the one in *A. scabra*. **F-H** Details of areas marked in **E**. Arrows point to serotonin-lir cells in close proximity to neurites. **F** Several irregular rows of serotonin-lir cells are present in the peripharyngeal band. **G** In the endostyle, serotonin-lir cells form two rows that are bilaterally symmetrically extending toward the retropharyngeal band. **H** In the retropharyngeal band, serotonin-lir cells are irregularly arranged, forming several irregular rows. **I** Lateral view of *Perophora japonica* from left side. Almost the same distribution pattern of serotonin-lir cells (arrowheads) as in **A** and **E**. Details of areas marked with rectangles are shown in **J** and **K**. **J** Two bands of serotonin-lir cells in the endostyle are paralleled by the subendostylar nerve (arrows). **K** In the epithelium of the stomach (st), elongated and almost spherical serotonin-lir cells are located. **L** Whole-mount of *Ciona intestinalis*, view from left side, same orientation as in **A** and **I**. Serotonin-lir cells are present in the peripharyngeal bands, endostyle, and esophagus. In the retropharyngeal band, the band of serotonin-lir cells is discontinuous. Bands of serotonin-lir cells extend into the endostylar appendix and are present in the dorsal half of the retropharyngeal band. **M-O** Details of areas marked in **L**. **M** Magnification of transition zone between peripharyngeal band and endostyle. Serotonin-lir cells in peripharyngeal band form several irregular rows, whereas in the endostyle, they form two bilaterally symmetric rows. **N** Serotonin-lir cells in the endostyle are paralleled by the subendostylar nerve. **O** Some serotonin-lir cells in the epithelium of the esophagus are elongated, some are approximately spherical. *bb* branchial basket, *ex* excurrent siphon, *in* intestine, *is* incurrent siphon, and *sl* stolon

Serotonin-lir cells in C. intestinalis are arranged in a band that stretches from the peripharyngeal band into the endostyle. In the endostylar appendix the band of serotonin-lir cells ends. Serotonin-lir cells recur again in the dorsal half of the retropharyngeal band, running into the esophagus (see **Fig. 1L**). Spherical serotonin-lir cells measuring 4-5µm in diameter are irregularly arranged in diverse rows in the peripharyngeal and retropharyngeal bands (**Fig. 1M**). In the endostyle serotonin-lir cells form two symmetric bands and are with 4-5µm of similar diameter as in the peripharyngeal and retropharyngeal bands. Spherical serotonin-lir cells, again with a diameter of 4-5µm, are also present in the esophagus and stomach. Additionally, elongated serotonin-lir cells with a length of 10µm are positioned in the epithelium of the esophagus and stomach (see **Fig. 1O**). Serotonin-lir cells in the endostyle are accompanied by numerous neurites, originating in a nerve paralleling the endostyle (**Fig. 1N**). In the central nervous system of *C. intestinalis* serotonin-lir could not be demonstrated. To exclude penetration problems of the antibody into nervous tissue, sections through the neural complex of *C. intestinalis* were prepared with a vibratome and subsequently stained with anti-serotonin and anti-tyrosinated-α-Tubulin antibodies yielding the same negative result for the anti-serotonin staining.

Aplousobranchiata

Clavelina lepadiformis is a medium sized colonial ascidian species. Serotonin-lir cells in *C. lepadiformis* are positioned in the peripharyngeal bands that continue into two bands of positively labeled cells in the endostyle. These serotonin-lir cells are spherical with a diameter of approximately 4µm. At the transition from endostyle to retropharyngeal band the serotonin-lir cells end. The band-like pattern of serotonin-lir cells reappears again in the dorsal part of the retropharyngeal ciliary band terminating in the esophagus (see **Fig. 2A**). In the peripharyngeal and retropharyngeal band the positively labeled cells are spherical with a diameter of approximately 4µm. These cells are irregularly arranged in several rows. In the epithelium of the stomach and intestine of *C. lepadiformis* alongside spherical serotonin-

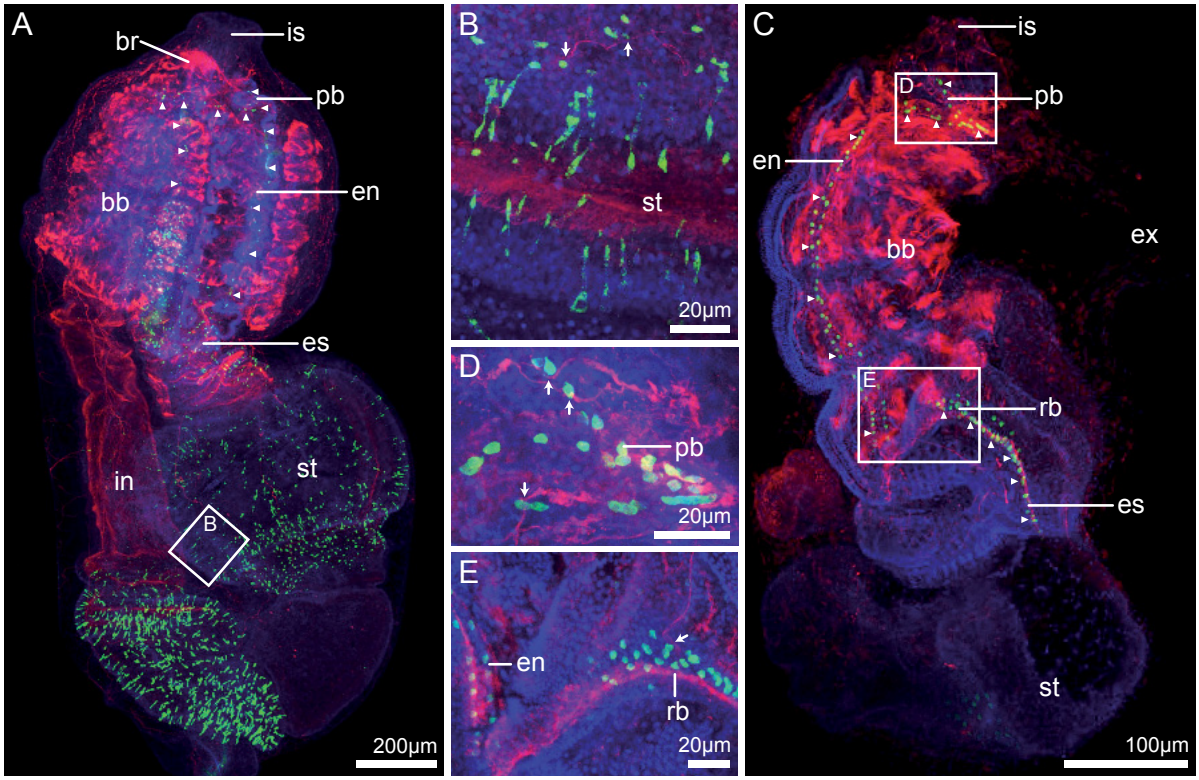

Fig. 2: Z-projections of confocal laser scanning micrographs of two aplousobranch ascidian species stained with antibodies against serotonin (green), tyrosinated-a-Tubulin (red) and with DAPI and Hoechst (blue). **A** Whole-mount of *Clavelina lepadiformis*, ventral view, right side of animal is left in the picture. Serotonin-lir cells are present in the peripharyngeal band (pb), the endostyle (en), in dorsal parts of the retropharyngeal band, and the esophagus (es) (arrowheads). In addition, conspicuous serotonin-like immunoreactivity is seen in the epithelium of the stomach (st) and the proximal part of the intestine (in). Note absence of serotonin-like immunoreactivity in the brain (br). **B** Detail of area marked in **A** showing elongated and approximately spherical serotonin-lir cells in the stomach epithelium. Arrows show neurites closely approaching two of the approximately spherical cells. **C** Whole-mount of *Diplosoma listerianum*, view from left side, ventral is to the left. Almost the same distribution pattern of serotonin-lir cells as in *C. lepadiformis*. **D, E** Details of areas marked in **C**. **D** A single row of serotonin-lir cells is located in the peripharyngeal band. Arrows show neurites closely approaching approximately spherical serotonin-lir cells. **E** Two rows of bilaterally symmetrically arranged serotonin-lir cells are present in the endostyle. Serotonin-lir cells are absent from the proximal part of the retropharyngeal band (rb). *bb* branchial basket, *ex* excurrent siphon, and *is* incurrent siphon

lir cells with a diameter of 4µm, 20µm long elongated positively labeled cells can be detected. Nerve fibers are situated close to serotonin-lir cells (see **Fig. 2B**). However, in the central nervous system of *C. lepadiformis* serotonin-lir could not be detected.

The zooids in the colonial ascidian species *Diplosoma listerianum* are small measuring less than 1mm. In *D. listerianum* a band of serotonin-lir cells runs from the peripharyngeal band into the endostyle ending at the endostylar appendix. Serotonin-lir cells are again detectable in the transition region between retropharyngeal band and esophagus. In the peripharyngeal band a single row of spherically shaped serotonin-lir cells that measure 4µm in diameter can be seen (see **Fig. 2D**). In the endostyle positively labeled spherical cells are of the same size, but form two symmetrically arranged parallel bands. From the dorsal part of the retropharyngeal band several rows of spherical serotonin-lir cells approximately 4µm in diameter are extending into the esophagus (see **Fig. 2E**). In *D. listerianum* only few spherical cells in the posterior epithelium of the stomach show a weak positive immunoreaction against serotonin. No elongated or spherical serotonin-lir cells could be observed in residual parts of the digestive tract (see **Fig. 2C)**. Nerve fibers approach the serotonin-lir cells in the peripharyngeal and retropharyngeal bands. In the central nervous system serotonin-lir neurons were not detectable.

Stolidobranchiata

In the colonial ascidian species *Botryllus schlosseri* a single row of serotonin-lir cells runs along the peripharyngeal band into the endostyle forming two symmetric bands. After passing the endostyle the two rows of positively labeled cells are reduced to a single row in the retropharyngeal band ending in the esophagus. Serotonin-lir cells in the endostyle, peripharyngeal and retropharyngeal band are roughly spherical in shape and measure 4-5µm in diameter (see **Fig. 3B**&**C**). In addition to these spherical serotonin-lir cells, 10µm long elongated positively labeled cells are present in the epithelium of the stomach and intestine (see **Fig. 3D**&**E**). Serotonin-lir cells were absent from the central nervous system of *B. schlosseri*.

Thaliacea

Salps are planktonic tunicates that occur in two different forms, the aggregate blastozooid and the solitary oozooid. In the aggregate blastozooid of *Thalia democratica* the serotonin-lir cells in the peripharyngeal band do not form a continuous band. Only cells in the dorsal half are positively labeled (see **Fig. 4A**). Serotonin-lir cells thus form several rows of irregularly arranged cells in the dorsal part of the peripharyngeal band. The cells themselves are spherical with a diameter of approximately 8-10µm. Nerve fibers are detectable approaching serotonin-lir cells in the peripharyngeal band (see **Fig. 4 C**). No serotonin-lir can be seen in the endostyle and such cells are also absent from the retropharyngeal band. However, serotonin-lir cells are present in the epithelium of the esophagus and intestine. In different regions of the esophagus the positively labeled serotonin-lir cells differ conspicuously in size and shape. While in the opening of the esophagus the dorsal epithelium contains several rows of elongated serotonin-lir cells that are 15-20µm long, the more ventrally lying epithelium includes a single row of spherical cells that measure 8-10µm in diameter in addition to elongated serotonin-lir

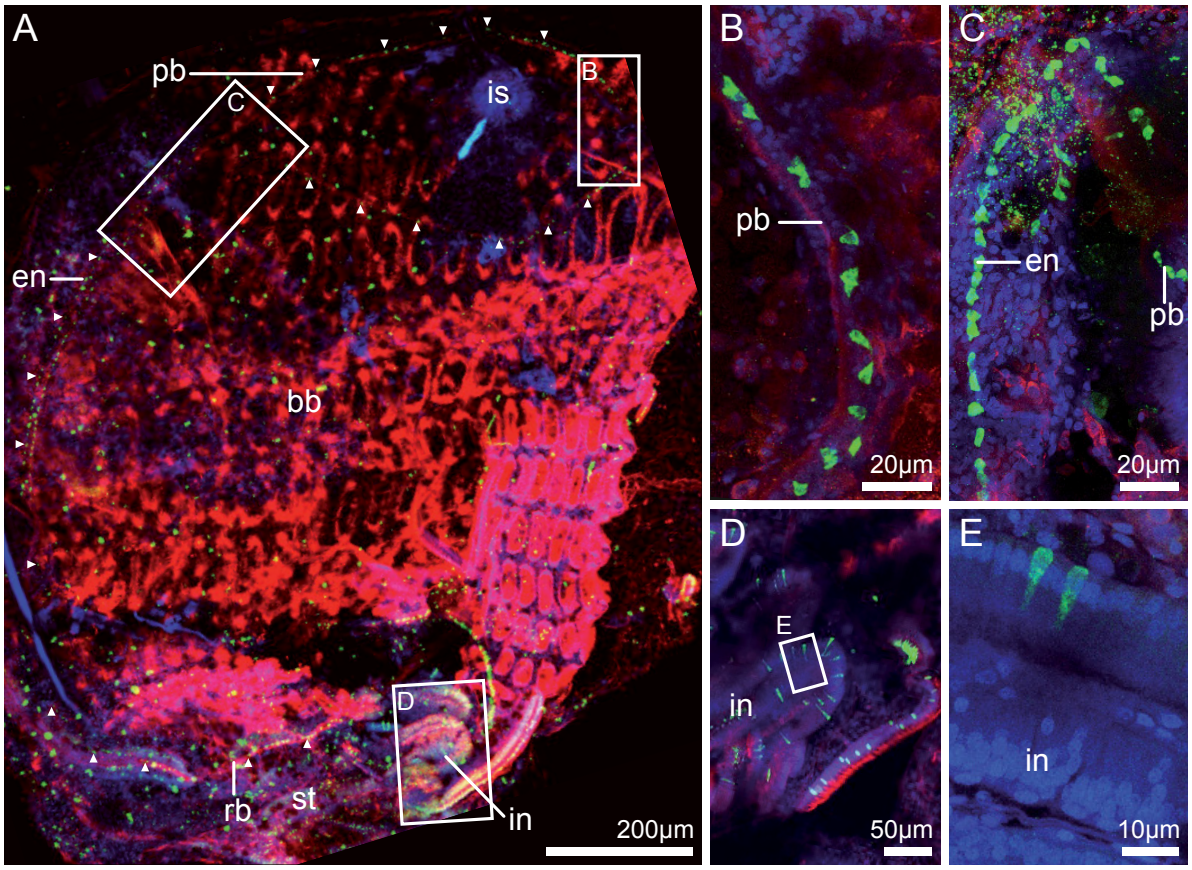

Fig. 3: Z-projections of confocal laser scanning micrographs of the stolidobranch ascidian *Botryllus schlosseri*. Localization of antibodies against serotonin (green), against tyrosinated-a-Tubulin (red), and of DAPI and Hoechst (blue). **A** Whole-mount, view from left side, ventral is to the left. Serotonin-lir cells (arrowheads) are present in the peripharyngeal band (pb), the endostyle (en), the retropharyngeal band (rb), the stomach (st), and intestine (in). **B-D** Details of areas marked in **A**. **B** A single row of serotonin-lir cells is located in the peripharyngeal band. **C** Two rows of bilaterally symmetrically arranged serotonin-lir cells are present in the endostyle. **D, E** Elongated serotonin-lir cells are present in the intestinal epithelium. *bb* branchial basket, *is* incurrent siphon

cells that measure approximately 18µm in length. At the passage to the stomach the epithelium of the esophagus contains several more rows of irregularly arranged spherical and elongated serotonin-lir cells with a diameter of approximately 10µm (spherical cells) and a length of 18-20µm (elongated cells) (**Fig. 4D&E**). All positively labeled cells are accompanied by neurites that are in close contact with some serotonin-lir cells (see **Fig. 4C-E**). In *T. democratica* serotonin-lir can also be demonstrated in the central nervous system. Serotonin-lir neurons are scattered among the posterior part of the cortex of the brain. Serotonin-lir neurites are present in the neuropile as well (see **Fig. 4B**). However, motoneurons (described by Lacalli and Holland 1998) show no serotonin-lir.

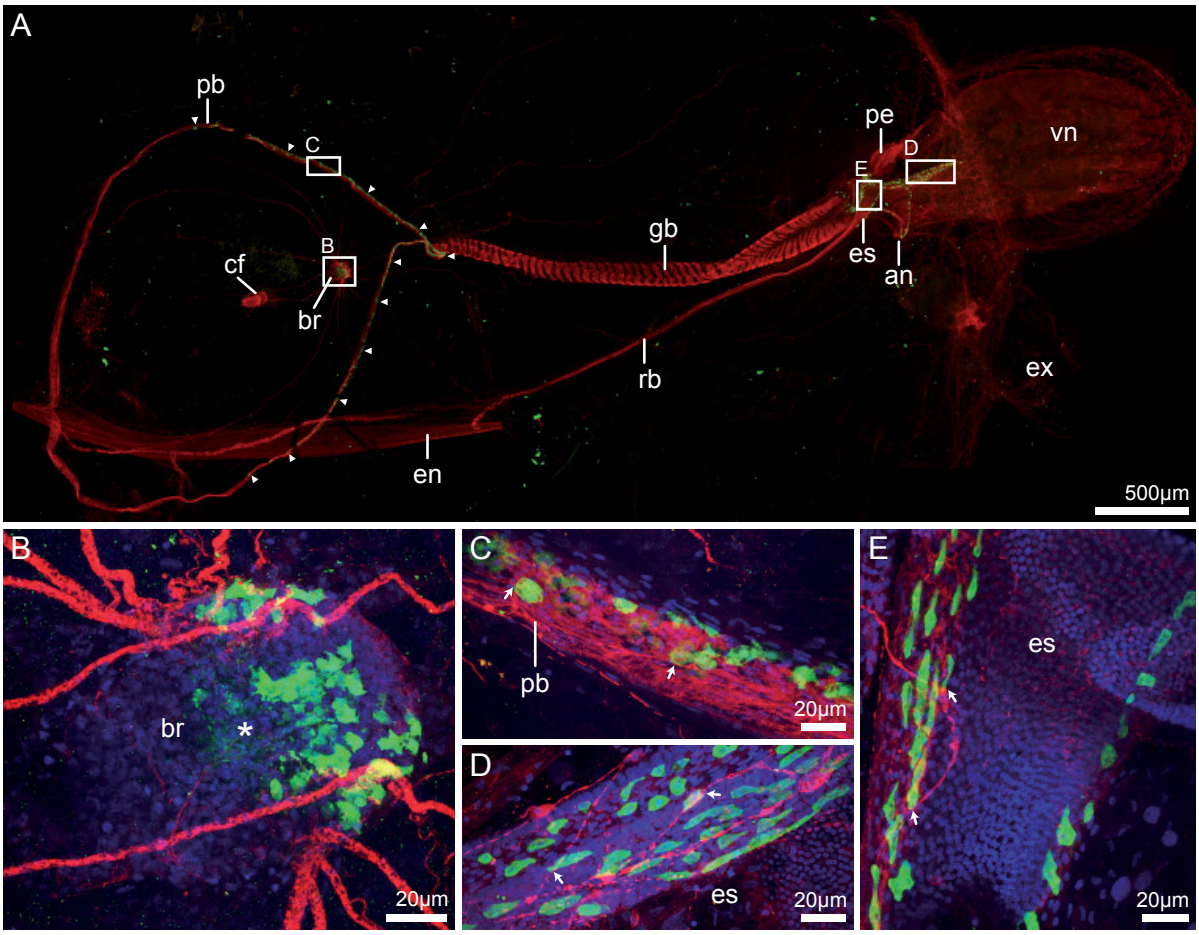

Fig. 4: Z-projections of confocal laser scanning micrographs of the salp *Thalia democratica*. Localization of antibodies against serotonin (green), against tyrosinated-a-Tubulin (red), and of DAPI and Hoechst (blue). Oblique dorsal view, anterior is to the left. **A** Whole-mount of complete individual. Serotonin-like immunoreactivity is present in the dorsal part of the peripharyngeal band (pb) (arrowheads), in the esophagus (es), the rectum, and the posterior part of the brain (br). No serotonin-lir cells are located in the endostyle (en) or retropharyngeal band (rb). **B-E** Details of areas marked in **A**. **B** Several rows of serotonin-lir cells are present in the peripharyngeal band. Serotonin-lir cells are in close proximity to neurites (arrows). **C** Several rows of serotonin-lir cells are present in the esophagus. Serotonin-lir cells are in close proximity to neurites (arrows). **D** In the anterior epithelium of the esophagus, several rows of elongated serotonin-lir cells are present, whereas in the posterior epithelium only a single row of approximately spherical serotonin-lir cells is present. **E** Higher magnification of the brain. Serotonin-like immunoreactivity is present in the fibrous neuropil (np) (asterisk) and cell bodies in the cortex (bc). *an* anus, *cf* ciliated funnel, *ex* excurrent siphon, *gb* gill bar, *pe* pericardium, and *vn* visceral nucleus

Appendicularia (Larvacea)

Oikopleura dioica is a small planktonic tunicate with a generation time of only five days. Specimens of *O. dioica* show no serotonin-lir in the peripharyngeal band, the endostyle, stomach, intestine, or nervous system (see **Fig. 5A&B**, **D&E**). Sporadically serotonin-lir was detected in the pharynx, gut and parts of the oikoplastic epithelium, specifically Fol's oikoplast cells and Eisen's oikoplast cells (see **Fig. 5A**). Position and random nature of these stainings indicate that in these cases antibodies attached to the sticky surface of oikoplast cells or ingested food particles respectively.

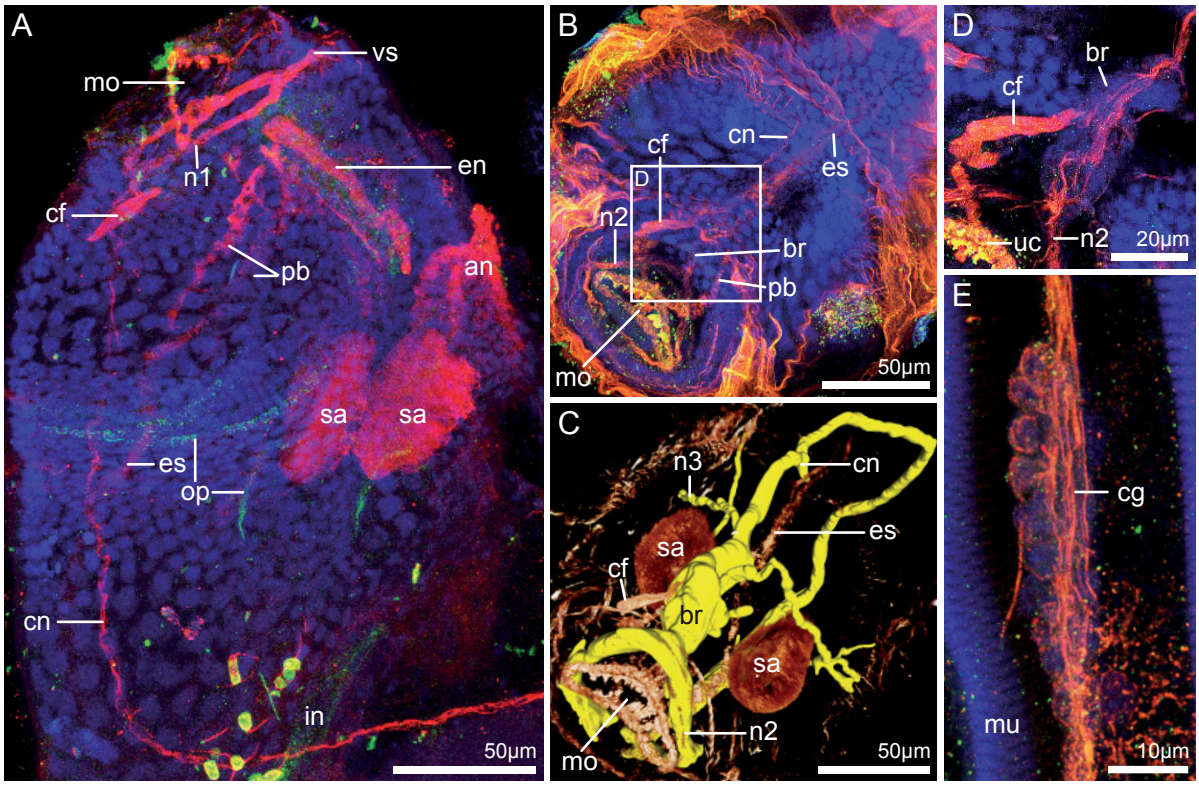

Fig. 5: Z-projections of confocal laser scanning micrographs of the appendicularian *Oikopleura dioica*. Localization of antibodies against serotonin (green), against tyrosinated-a-Tubulin (red), and of DAPI and Hoechst (blue). **A-D** Trunk (see Fig. 6). **A** Whole-mount, view from right side, dorsal is to the left, anterior up. No serotonin-lir cells are present in the peripharyngeal band (pb), the endostyle (en), the esophagus (es), the stomach, and the nervous system. **B** Oblique dorsal view of another specimen, anterior is to the lower left corner. No serotonin-lir cells are present in the nervous system or digestive tract. **C** 3D-reconstruction of nervous system (yellow) and rendered signal of tyrosinated-a-Tubulin immunostaining (red/brown) of same specimen shown in **B**. **D** Detail of area marked in **B**. No serotonin-lir cells are present in the brain (br). **E** Z-projections of confocal laser scanning micrographs of the caudal ganglion (cg) of the tail, anterior is to the top. No serotonin-like immunoreactivity is present in the caudal ganglion. *an* anus, *cf* ciliated funnel, *cn* caudal nerve, *in* intestine, *mo* mouth, *mu* musculature, *op* oikoplast area, *sa* stigma, *uc* upper lip cells, and *vs* ventral sense organ

Discussion

Comparative anatomy of the distribution pattern of serotonin-lir cells

A comparison of the distribution pattern of cells that react positively with antibodies against the signaling molecule serotonin among diverse tunicate species revealed conspicuous similarities and differences. In ascidians, comprising tunicates with sessile adults, serotonin-like immunoreactive (serotonin-lir) cells form a band stretching from the peripharyngeal band into the endostyle, where two bilaterally symmetric rows of positively labeled cells extend into the retropharyngeal band and continue into the esophagus (see **Fig. 6**). A modification of this general ascidian pattern occurs in aplousobranchiate species and in *Ciona intestinalis,* a genus that has been traditionally referred to the

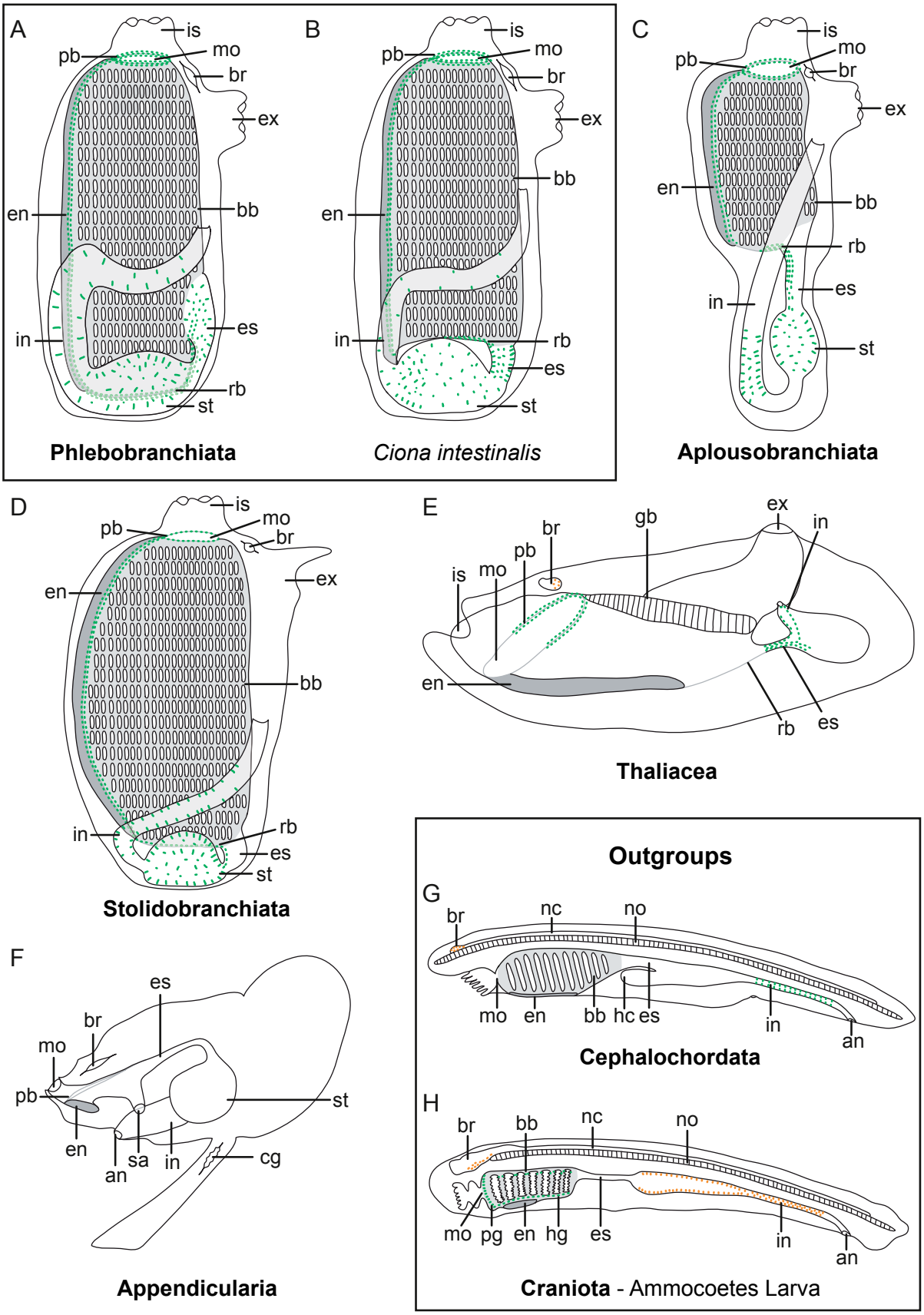

Fig. 6: Schematic representation of the distribution pattern of serotonin-lir cells in tunicates and two out-groups (Cephalochordata and Craniota). Elongated and approximately spherical serotonin-lir cells are displayed in green, serotonin-lir neurons are shown in orange. *an* anus, *bb* branchial basket, *br* brain, *cg* caudal ganglion, *en* endostyle, *es* esophagus, *ex* excurrent siphon, *gb* gill bar, *hc* hepatic cecum, *hg*

hypobranchial groove, *in* intestine, *is* incurrent siphon, *mo* mouth, *nc* nerve cord, *no* notochord, *pb* peripharyngeal band, *pg* pseudobranchial groove, *rb* retropharyngeal band, *sa* stigma, *st* stomach, *ta* tail, *tr* trunk, and *vn* visceral nucleus

taxon Phlebobranchiata (e.g., Millar 1970, Monniot and Monniot 2001). In aplousobranchiate ascidians and *C. intestinalis* the rows of serotonin-lir cells in the retropharyngeal band are discontinuous. The band of serotonin-lir cells ends in the endostylar appendix and serotonin-lir cells are seen again in the more posterior parts of these animals. In all phlebobranchiate ascidians examined and the aplousobranchiate *Clavelina lepadiformis* several rows of serotonin-lir cells are situated in the peripharyngeal band, while in the stolidobranchiate *Botryllus schlosseri* and the aplousobranchiate *Diplosoma listerianum* only a single row of positively labeled cells is present. In phlebobranchiate ascidians the retropharyngeal band contains diverse rows of serotonin-lir cells, comparable to the serotonin-lir cells in the dorsal half of the retropharyngeal bands in aplousobranchiate ascidians and *Ciona intestinalis*. In the stolidobranchiate *B. schlosseri*, on the other hand, only a single row is present.

The distribution of serotonin-lir cells has been described for additional ascidian species. Pennati and co-authors investigated larvae and juveniles of the phlebobranchiate *Phallusia mammilata* and found serotonin-lir cells in the peripharyngeal band, endostyle, and intestine (Pennati et al. 2001). Using antibody staining, Georges (1985) could demonstrate the presence of serotonin-lir in the endostyles, esophagus, and intestine of the phlebobranchiate species *Ascidiella aspersa* (Müller, 1776), *Ascidia mentula* Müller, 1776*, Ciona intestinalis,* and *Phallusia mammilata* but not in the neural complex. Tiozzo and co-authors had already described the pattern of serotonin-lir in *Botryllus schlosseri* (Tiozzo et al. 2009), which we confirmed and to which we could add the presence of serotonin-lir cells in the esophagus and retropharyngeal band and the observation that serotonin-lir cells in the endostyle and in the intestinal tract are of distinct morphologies. Sakharov and Salimova (1982) investigated solitary stolidobranchiate ascidian species and showed that in *Styela clava* Herdman, 1881, *S. rustica* Linnaeus, 1767, and *Molgula retortiformis* Verrill, 1871 serotonin-lir cells form two bilaterally symmetrical rows in the endostyles. Therefore, the observed pattern in the endostyles of these stolidobranchiate ascidians corresponds exactly with the one described for *B. schlosseri*, however the authors did not report the distribution pattern of serotonin-lir cells outside the endostyle.

While the adults of the sessile ascidian species are quite comparable in regards to their respective patterns of serotonin-lir cell distributions, the planktonic tunicates differ in several respects. Adult appendicularians, as far as they have been investigated, lack serotonin-lir cells in their pharynx and intestinal tract entirely. *Oikopleura dioica* also lacks serotonin-lir cells in the brain but Stach (2005) reported the presence of few serotonin-lir cells in the brain of the congeneric species *O. fusiformis* Fol, 1872*,* but could not detect any labeling in *O. rufescens* Fol, 1872 using antibodies against serotonin. Thaliaceans on the other hand display more similarities to sessile ascidians. In the blastozooid of the salp *Thalia democratica* serotonin-lir cells are present in the peripharyngeal band and the digestive tract, while such cells are missing from the endostyle and retropharyngeal band. A similar distribution

of serotonin-lir in the peripharyngeal band, digestive tract and brain has been described for the oozoid of *T. democratica* (Pennati et al. 2012). In the doliolid *Dolium nationalis* Borgert, 1893 serotonin-lir was demonstrated in the intestine, brain, and dorsal part of the peripharyngeal band, erroneously labeled ciliated funnel (Stach 2005).

From a phylogenetic perspective the comparison to the distribution pattern of serotonin-lir cells in cephalochordates and agnathan craniates is of interest. Neither in cephalochordates (Candiani et al. 2001) nor in larval nor adult lampreys (Barreiro-Iglesias et al. 2009; Sakharov and Salimova 1980) serotonin-lir cells were detected in the endostyle or esophagus (see Fig. 6). Both groups, however possess serotonin-lir cells in their central nervous systems. In cephalochordates serotonin-lir cells are – amongst others – located in the anterior part of the brain, where they are part of the anterior eye (Wicht and Lacalli 2005). In larval cephalochordates, serotonin-lir cells occur in two distinct clusters in the anterior brain (Holland and Holland 1993). A similar cluster has been described from larval lamprey (Hay-Schmidt 2001) and from different larval ascidians, belonging to phlebobranchiate and stolidobranchiate species (Stach 2005). In general, serotonin-lir in the central nervous systems of protostome and deuterostome invertebrates is a widespread phenomenon (see e.g., Hay-Schmidt 2001, Stach et al. 2012, Richter et al. 2015).

The detailed comparisons of serotonin-lir cells in tunicate species are now available from a wider range of taxonomic groups (see Table 2) therefore allowing for a preliminary phylogenetic evaluation of potential characters. The similarities and differences in the observed distribution patterns of serotonin-lir cells suggest that serotonin-lir in different body regions can behave as an independent character during evolution and is therefore in principle a potential character for phylogenetic analysis (e.g., Wiley and Liebermann 2014). It is intriguing that the higher taxonomic units within Tunicata show highly similar patterns of serotonin-lir. While ascidians e.g., show no serotonin-lir in their brains, they express serotonin in a band of cells stretching from the peripharyngeal band, through the endostyle, the retropharyngeal band, the esophagus all the way to the intestine. There is little variation in this pattern among ascidians, with the exception of a short interruption of the serotonin-lir of this band in the retropharyngeal band of the aplousobranch ascidians *Clavelina lepadiformis* and *Diplosoma listerianum*. Here again it is noteworthy, that such an interruption also occurs in *Ciona intestinalis* and that there exists a taxonomic dispute, whether *Ciona* should be classified with Aplousobranchiata or with Phlebobranchiata (Kott 2005). The two thaliacean species, the salp *Thalia democratica* and the doliolid *Doliolum nationalis* also show similar patterns of serotonin-lir, featuring serotonin-lir in the brains, the dorsal part of the peripharyngeal bands, and the intestines respectively. The three species in Appendicularia, finally, show a largely reduced pattern of serotonin-lir, without any detectable serotonin-lir in *O. dioica* and *O.rufescens* adult stages and merely few serotonin-lir cells in the brain of *O. fusiformis*. While the observation that the distribution pattern of serotonin-lir agrees considerably well with classical taxonomic groupings, phylogenetic interpretation remains inconclusive. The outgroup comparison shows that serotonin-lir was present in the brains, but this is also the case in thaliacean tunicates. Ascidian larvae on the other hand possess serotonin-lir in their brains similar to cephalochordates and lampreys (see Stach 2005, 2014). Therefore one could consider the lack of

Table 2: Presence of serotonin-like immunoreactivity in distinct body regions of different chordate species

Character / Taxon	Brain	Peripharyngeal band	Endostyle	Retropharyngeal band	Esophagus	Gastrointestinal tract
Phlebobranchiata						
Ciona intestinalis	-	+	+	-	+	+
Ascidia mentula	-	+	+	?	?	+
Ascidiella aspersa	-	+	+	?	?	+
Ascidiella scabra	-	+	+	+	+	+
Phallusia mammillata	-	+	+	?	+	+
Corella parallelogramma	-	+	+	+	+	+
Perophora japonica	-	+	+	+	+	+
Stolidobranchiata						
Botryllus schlosseri	-	+	+	+	+	+
Styela rustica	?	?	+	?	?	?
Styela clava	?	?	+	?	?	?
Molgula retortiformis	?	?	+	?	?	?
Aplousobranchiata						
Clavelina lepadiformis	-	+	+	-	+	+
Diplosoma listerianum	-	+	+	-	+	+
Thaliacea						
Thalia democratica	+	+ (in dorsal half)	-	-	+	+
Doliolum nationalis	+	+ (in dorsal half)	-	+	+	+
Appendicularia						
Oikopleura dioica	-	-	-	-	-	-
Oikopleura fusiformis	(+)	-	-	-	-	-
Oikopleura rufescens	-	-	-	-	-	-
Cephalochordata						
Branchiostoma floridae	+	-	-	-	-	+
Craniota						
Lampetra fluviatilis	+	?	?	?	?	+
Lampetra planeri	+	+	?	?	-	+
Petromyzon marinus	+	+	-	-	-	+

All tunicate species were post metamorphic, *Thalia democratica* was in blastozooid stage, craniate data were from late larval or juvenile stages.

+ present; - absent; ? data are missing; for the retropharyngeal band - symbolizes absence of serotonin-lir cells in the ventral half

References: *A. mentula, A. aspersa* (Georges 1985), *P. mammillata* (Pennati et al. 2001), *S. rustica, S. clava, M. retortiformis* (Sakharov & Salimova 1982), *T. democratica* Oozooid (Pennati et al. 2012), *D. nationalis* Oozooid, *O. fusiformis, O. rufescens* (Stach 2005), *B. lanceolatum* (Moret 2004, Hecht & Lacalli 2005), *B. floridae* (Candiani et al. 2001, Holland & Holland 1993), *L. fluviatilis* (Baumgarten et al. 1973), *L. planeri* (Sakharov & Salimova 1980), *P. marinus* (Barreiro-Iglesias et al. 2009)

serotonin-lir in the brains of adult ascidians as a secondarily derived autapomorphic character, possibly related to the sessility in the post metamorphic stages. If Appendicularia is indeed a taxon comprised of neotenic species as many researchers suggest (Garstang 1928, Lohmann 1956, Stach and Turbeville 2002, Stach 2007, Stach et al 2008), the neotenic stage could have retained an adult brain in the more larval organized remainder of the body. To the contrary, the thaliacean species would have to be considered as regaining a larval character in their mature oozooid stage. No matter, which set of character we evaluate under a phylogenetic paradigm, we will need ad hoc hypotheses to explain the contradictory character distribution. This is even the case, if we map the characters on a molecular phylogenetic hypothesis, with the added difficulty that the most taxon rich current phylogenetic hypotheses based on molecular data drastically differ in their respective branching patterns of major tunicate taxa (see e.g. Tsagkogeorgas et al 2009, Govindarajan et al 2011). Thus, a well-supported phylogenetic hypothesis of tunicates still awaits the analysis of additional molecular and morphological data.

Serotonin-lir cell types

Based on light-microscopically observed morphology, we could distinguish three different types of cells that were immunopositive with antibodies against serotonin. These were more or less spherical serotonin-lir cells, elongated serotonin-lir cells, and serotonin-lir neurons.

In the peripharyngeal bands, the endostyles, the retropharyngeal bands, the esophagus, and stomachs, but not in the intestines of tunicates we identified serotonin-lir cells of nearly spherical shape. For *Ciona intestinalis*, *Corella parallelgogramma*, and *Ascidia mentula* Nilsson et al. (1988) showed the presence of serotonin-lir cells between the 7th and 8th zone using electron-microscopic of immune-gold labeled specimens and suggested an enterochromaffin function. Cells of similarly spherical appearance have been demonstrated (among others) in molluscs (e.g. Doran et al. 2004; Willows et al. 1997; McKenzie et al. 1998), echinoderms (Wada et al. 1997), and vertebrates (König et al. 2009; Barreiro-Iglesias et al. 2009; Naruse et al. 2005), where they have been implicated in the control of ciliary beating and mucus secretion. The distribution pattern of the spherical serotonin-lir cells in tunicates is consistent with the hypothesis that these cells serve a similar function in tunicates.

Elongated serotonin-lir cells have been found in the esophagus, stomach, and intestine of most tunicate species examined (see Table 1). In the intestine elongated serotonin-lir cells are the only serotonin-lir cells detectable. No elongated serotonin-lir cells were found in the adults of appendicularian species and the aplousobranch ascidian *Diplosoma listerianum*, while another aplousobranch species *Clavelina lepadiformis* possesses elongated serotonin-lir cells in stomach and intestine and *C. oblonga* Herdman, 1880 features elongated serotonin-lir cells in the stomach of the larval stage (Stach 2005). Similarly located and shaped serotonin-lir cells have been described from cephalochordates (Candiani et al. 2001, Holland and Holland 1993) and from several vertebrate species from different taxa, such as elasmobranchs (Chiba 1998), amphibians, and sauropsids (Trandaburu and Trandaburu 2007). These cells are known as enterochromaffin cells in craniates and are involved in hormonal regulation of feeding. Based on their similarity with enterochromaffin cells, we suggest that the elongated serotonin-

lir cells of tunicates could correspond to enterochromaffin cells in cephalochordates and craniates.

Neurons consist typically of a soma that contains the nucleus and neurites propagating electric excitations (Richter et al. 2010). While serotonin-lir neurons are present in the brains of most invertebrate and vertebrate taxa (e.g., Hay-Schmidt 2000, Stach et al. 2012, Candiani et al. 2001, Moret et al. 2004, Bogdanski et al. 1963, Kiyasova and Gaspar 2011) they are mostly absent from the brains of metamorphosed tunicates. With the exception of Thaliaceans (Welsh and Loveland 1968, present study, Stach 2005) and a reduced signal in one of three appendicularian species (present study, Stach 2005), serotonin-lir cells have not been found in adult tunicates. Larval stages of several ascidian species from different taxonomic groups on the other hand possess serotonin-lir in their brains (De Bernardi et al. 2006; Stach 2005). From a functional point of view it might be interesting to point out that a major function of serotonin-lir neurons from a wide variety of animal species, such as leeches (Nusbaum and Kristan 1986), nematodes (e.g., Hardaker et al. 2001), molluscs (Lewis et al. 2011), and vertebrates (e.g., Harris-Warrick and Cohen 1985) has been shown to be the initiation of motor activity. Because ascidians as adults are sessile organisms, they may have reduced this pathway for the generation of locomotory patterns. That the scenario is probably not so simple becomes obvious, if the two pelagic tunicate groups are considered more carefully. In most phylogenetic hypotheses, thaliaceans are derived from a sessile ascidian-like ancestor (Tsagkogeorga et al. 2009, Govindarajan et al. 2011). It can therefore be hypothesized that Thaliacea have regained serotonin-lir neurons in connection with their acquiring a more active life-style. However, this is not the case for appendicularians, for which also good arguments have been presented, that this group could be derived from sessile ascidian-like ancestors (Stach and Turbeville 2002, Tsagkogeorga et al. 2009, Stach et al. 2008). It might be hypothesized that appendicularians as neotenic organisms have retained several larval features but at the same time retained also adult features. The case of *O. fusiformis* with a reduced complement of serotonin-lir cells, then might be considered a rudimentary feature.

Funding

This study was funded by the Deutsche Forschungsgemeinschaft (DFG) grant STA655/4-1 and the Elsa-Neumann-Stipendium des Landes Berlin.

Compliance with ethical standards

Conflict of interest

The authors declare that they have no conflict of interest. This article does not contain any studies with human participants performed by any of the authors. All applicable international, national, and/ or institutional guidelines for the care and use of animals were followed.

References

Abitua PB, Wagner E, Navarrete IA, Levine M (2012) Identification of a rudimentary neural crest in a non-vertebrate chordate. Nature 492:104-107

Barreiro-Iglesias A, Aldegunde M, Anadón R, Rodicio MC (2009) Extensive presence of serotonergic cells and fibers in the peripheral nervous system of lampreys. J Comp Neurol 512:478-499

Baumgarten HG, Björklund A, Lachenmayer L, Nobin A, Rosengren E (1973) Evidence for the existence of serotonin-, dopamine-, and noradrenaline-containing neurons in the gut of *Lampetra fluviatilis*. ZZellforsch 141:33-54

Bogdanski DF, Bonomi L, Brodie BB (1963) Occurence of serotonin and catecholamines in brain and peripheral organs of various vertebrate classes. Life Sci 2:80-84

Bone, Q. (1998) The biology of pelagic tunicates. OUP, Oxford

Candiani S, Augello A, Oliveri D, Passalacqua M, Pennati R, De Bernardi F, Pestarino M (2001) Immunocytochemical localization of serotonin in embryos, larvae and adults of the lancelet, *Branchiostoma floridae*. Histochem J 33:413-420

Chiba A (1998) Ontogeny of serotonin-immunoreactive cells in the gut epithelium of the cloudy dogfish, *Scyliorhinus torazame*,with reference to coexistence of serotonin and neuropeptide Y. Gen Comp Endocr 111:290-298

De Bernardi F, Pennati R, Candiani S, Zega G, Groppelli S, Pestarino M (2006) Serotonin in the morphogenesis of ascidian nervous system. Caryologia 59:375-379

Dehal P, Satou Y, Campbell RK, Chapman J, Degnan B, De Tomaso A, Davidson B, Di Gregorio A, Gelpke M, Goodstein DM, Harafuji N, Hastings KEM, Ho I, Hotta K, Huang W, Kawashima T, Lemaire P, Martinez D, Meinertzhagen IA, Necula S, Nonaka M, Putnam N, Rash S, Saiga H, Satake M, Terry A, Yamada L, Wang H-G, Awazu S, Azumi K, Boore J, Branno M, Chin-bow S, DeSantis R, Doyle S, Francino P, Keys DN, Haga S, Hayashi H, Hino K, Imai KS, Inaba K, Kano S, Kobayashi K, Kobayashi M, Lee B-I, Makabe KW, Manohar C, Matassi G, Medina M, Mochizuki Y, Mount S, Morishita T, Miura S, Nakayama A, Nishizaka S, Nomoto H, Ohta F, Oishi K, Rigoutsos I, Sano M, Sasaki A, Sasakura Y, Shoguchi E, Shin-i T, Spagnuolo A, Stainier D, Suzuki MM, Tassy O, Takatori N, Tokuoka M, Yagi K, Yoshizaki F, Wada S, Zhang C, Hyatt PD, Larimer F, Detter C, Doggett N, Glavina T, Hawkins T, Richardson P, Lucas S, Kohara Y, Levine M, Satoh N, Rokhsar DS (2002) The draft genome of *Ciona intestinalis*: insights into chordate and vertebrate origins. Science 298:2157-2167

Delsuc F, Brinkmann H, Chourrout D, Philippe H (2006) Tunicates and not cephalochordates are the closest living relatives of vertebrates. Nature 439:965-968

Diogo R, Kelly RG, Christiaen L, Levine M, Ziermann JM, Molnar JL, Noden DM, Tzahor E (2015) A new heart for a new head in vertebrate cardiopharyngeal evolution. Nature 520:466-473

Doran SA, Koss R, Tran CH, Christopher KJ, Gallin WJ, Goldberg JI (2004) Effect of serotonin on ciliary beating and intracellular calcium concentration in identified populations of embryonic ciliary cells. J Exp Biol 207:1415-1429

Dunn CW, Hejnol A, Matus DQ, Pang K, Browne WE, Smith SA, Seaver E, Rouse GW, Obst M, Edgecombe GD, Sorensen MV, Haddock SHD, Schmidt-Rhaesa A, Okusu A, Kristensen RM, Wheeler WC, Martindale MQ, Giribet G (2008) Broad phylogenomic sampling improves resolution of the animal tree of life. Nature 452:745-749

Edgecombe GD, Giribet G, Dunn CW, Hejnol A, Kristensen RM, Neves RC, Rouse GW, Worsaae K, Sørensen MV (2011) Higher-level metazoan relationships: recent progress and remaining questions. Org Divers Evol 11:151-172

Garstang W (1928) The morphology of the tunicata, and its bearings on the phylogeny of the Chordata. Q J Microsc Sci 72:51-187

Georges D (1985) Presence of cells resembling serotonergic elements in four species of tunicates. Cell Tissue Res 242:341-348

Govindarajan AF, Bucklin A, Madin LP (2011) A molecular phylogeny of the thaliacea. J Plankton Res 33:843-853

Hardaker LA, Singer E, Kerr R, Zhou G, Schafer WR (2001) Serotonin modulates locomotory behavior and coordinates egg-laying and movement in *Caenorhabditis elegans*. J Neurobiol 49: 303-313

Hay-Schmidt A (2000) The evolution of the serotonergic nervous system. P Roy Soc Lond B Bio 267:1071-1079

Holland ND, Holland LZ (1993) Serotonin-containing cells in the nervous system and other tissues during ontogeny of a lancelet, *Branchiostoma floridae*. Acta Zool 74:195-204

Imai KS, Levine M, Satoh N, Satou Y (2006) Regulatory blueprint for a chordate embryo. Science 312:1183-1187

Jefferies RPS (1986) The ancestry of the vertebrates. Cambridge University Press, London

Kiyasova V, Gaspar P (2011) Development of raphe serotonin neurons from specification to guidance. Eur J Neurosci 34:1553-1562

König P, Krain B, Krasteva G, Kummer W (2009) Serotonin increases cilia-driven particle transport via an acetylcholine-independent pathway in the mouse trachea. PloS one 4:e4938

Kott P (2005) Catalogue of tunicata in Australian waters. Australian Biological Resources Study, Australian Government, Department of the Environment and Heritage

Kowalewsky A (1866) Entwicklungsgeschichte der einfachen Ascidien. Mem l'Acad St Petersb, sér.7 10:1-19

Krieger J, Sombke A, Seefluth F, Kenning M, Hansson BS, Harzsch S (2012) Comparative brain architecture of the European shore crab *Carcinus maenas* (Brachyura) and the common hermit crab *Pagurus bernhardus* (Anomura) with notes on other marine hermit crabs. Cell Tissue Res 348:47-69

Lacalli TC, Holland LZ (1998) The developing dorsal ganglion of the salp *Thalia democratica*, and the nature of the ancestral chordate brain. Philos T Roy Soc B 353:1943-1967

Lemaire P (2011) Evolutionary crossroads in developmental biology: the tunicates. Development 138: 2143-2152

Lewis SL, Lyons DE, Meekins TL, Newcomb JM (2011) Serotonin influences locomotion in the nudibranch mollusc *Melibe leonina.* Biol Bull 220: 155-160

Lohmann H (1956) Erste Klasse der Tunicaten: Appendiculariae. In: Lohmann H, Kükenthal W, Krumbach T (eds) Handbuch der Zoologie, vol2, De Gruyter, Leipzig, pp. 15-202

Maisey JG (1986) Heads and tail: a chordate phylogeny. Cladistics 2:201-256

Mayer G, Whitington PM, Sunnucks P, Pflüger H-J (2010) A revision of brain composition in Onychophora (velvet worms) suggests that the tritocerebrum evolved in arthropods. BMC Evol Biol 10:255

McKenzie JD, Caunce M, Hetherington M, Winlow W (1998) Serotonergic innervation of the foot of the pond snail *Lymnaea stagnalis* (L.). J Neurocytol 27:459-470

Millar RH (1970) British ascidians. Tunicata: Ascidiacea: keys and notes for the identification of the species. Synopses of the British Fauna, no. 1, Academic Press, London

Monniot F, Monniot C (2001) Ascidians from the tropical western Pacific. Zoosystema 23:201-383

Moreno TR, Rocha RM (2008) Phylogeny of the Aplousobranchia (Tunicata: Ascidiacea). Rev Bras Zool 25:269-298

Moret F, Guilland J-C, Coudouel S, Rochette L, Vernier P (2004) Distribution of tyrosine hydroxylase, dopamine, and serotonin in the central nervous system of amphioxus (*Branchiostoma lanceolatum*): Implications for the evolution of catecholamine systems in vertebrates. J Comp Neurol 468:135-150

Naruse H, Gomi T, Kimura A, Adriaensen D, Timmermans J-P (2005) Structure of the respiratory tract of the red-bellied newt *Cynops pyrrhogaster*, with reference to serotonin-positive neuroepithelial endocrine cells. Anato Sci Int 80:97-104

Nilsson O, Fredriksson G, Öfverholm T, Ericson LE (1988) Electron-microscopic immunocytochemistry of 5-hydroxytryptamine in the ascidian endostyle. Cell Tissue Res 253:137-143

Nusbaum MP, Kristan WB (1986) Swim initiation in the leech by serotonin-containing interneurones, cells 21 and 61. J Exp Biol 122: 277-302

Pennati R, Dell´Anna A, Zega G, De Bernardi F (2012) Immunohistochemical study of the nervous system of the tunicate *Thalia democratica* (Forsskal, 1775). Eur J Histochemy 56:e16

Pennati R, Groppelli S, Sotgia C, Candiani S, Pestarino M, De Bernardi F (2001) Serotonin localization in *Phallusia mammillata* larvae and effects of 5-HT antagonists during larval development. Dev Growth Differ 43:647-656

Richter S, Loesel R, Purschke G, Schmidt-Rhaesa A, Scholtz G, Stach T, Vogt L, Wanninger A, Brenneis G, Doring C, Faller S, Fritsch M, Grobe P, Heuer C, Kaul S, Moller O, Muller C, Rieger V, Rothe B, Stegner M, Harzsch S (2010) Invertebrate neurophylogeny: suggested terms and definitions for a neuroanatomical glossary. Front Zool 7:29

Richter S, Stach T, Wanninger A (2015) Perspective — Nervous system development in bilaterian larvae: testing the concept of 'primary larvae'. In: Schmidt-Rhaesa A, Harzsch S, Purschke G (eds) Structure and Evolution of Invertebrate Nervous Systems, OUP, Oxford, pp. 313-324

Richter S, Wirkner CS (2014) A research program for evolutionary morphology. J Zool Syst Evol Res 52:338-350

Romer AS (1972) The vertebrate as a dual animal — somatic and visceral. Evol Biol 6:121-156

Sakharov DA, Salimova NB (1980) Serotonin neurons in the peripheral nervous system of the larval lamprey, *Lampetra planeri*. A histochemical, microspectrofluorimetric and ultrastructural study. Zool Jahrb Allg Zool 84:231-239

Sakharov DA, Salimova N (1982) Serotonin-containing cells in the ascidian endostyle. Experientia 38:802-803

Schmidt-Rhaesa A, Harzsch S, Purschke G (2015) Structure and evolution of invertebrate nervous systems. OUP, Oxford

Scholtz G (2013) Versuch einer analytischen Morphologie. Bildwelten des Wissens. Kunsthistorisches Jahrbuch für Bildkritik. 9:30-44

Schindelin J, Arganda-Carreras I, Frise E, Kaynig V, Longair M, Pietzsch T, Preibisch S, Rueden C, Saalfeld S, Schmid B, Tinevez J-Y, White DJ, Hartenstein V, Eliceiri K, Tomancak P, Cardona A (2012) Fiji: an open-source platform for biological-image analysis. Nat Meth 9:676-682

Stach T (2005) Comparison of the serotonergic nervous system among Tunicata: implications for its evolution within Chordata. Org Divers Evol 5:15-24

Stach T (2007) Ontogeny of the appendicularian *Oikopleura dioica* (Tunicata, Chordata) reveals characters similar to ascidian larvae with sessile adults. Zoomorphology 126:203-214

Stach T (2008) Chordate phylogeny and evolution: a not so simple three taxon problem. J Zool 276:117-141

Stach T (2014) Deuterostome phylogeny – a morphological perspective. In: Wägele JW, Bartolomaeus T (eds) Deep Metazoan Phylogeny: The Backbone of the Tree of Life, Walter de Gruyter GmbH, Berlin, Boston, pp. 425–457

Stach T (2015) Science behind, around, and after trees. BioScience 65:118-119

Stach T, Braband A, Podsiadlowski L (2010) Erosion of phylogenetic signal in tunicate mitochondrial genomes on different levels of analysis. Mol Phylogenet Evol 55:860-870

Stach T, Gruhl A, Kaul-Strehlow S (2012) The central and peripheral nervous system of *Cephalodiscus gracilis* (Pterobranchia, Deuterostomia). Zoomorphology 131:11-24

Stach T, Turbeville JM (2002) Phylogeny of Tunicata inferred from molecular and morphological characters. Mol Phylogenet Evol 25:408-428

Stach T, Winter J, Bouquet J-M, Chourrout D, Schnabel R (2008) Embryology of a planktonic tunicate reveals traces of sessility. P Natl A Sci 105:7229-7234

Swalla BJ, Cameron CB, Corley LS, Garey JR (2000) Urochordates are monophyletic within the deuterostomes. Syst Biol 49:52-64

Swalla BJ, Smith AB (2008) Deciphering deuterostome phylogeny: molecular, morphological and palaeontological perspectives. Philos T Roy Soc B 363:1557-1568

Tiozzo S, Murray M, Degnan BM, De Tomaso AW (2009) Development of the neuromuscular system during asexual propagation in an invertebrate chordate. Dev Dynam 238:2081-2094

Trandaburu T, Trandaburu I (2007) Serotonin (5-hydroxytryptamine, 5-HT) immunoreactive endocrine and neural elements in the chromaffin enteropancreatic system of amphibians and reptiles. Acta Histochem 109:237-247

Tsagkogeorga G, Turon X, Hopcroft RR, Tilak M-G, Feldstein T, Shenkar N, Loya Y, Huchon D, Douzery EJP, Delsuc F (2009) An updated 18S rRNA phylogeny of tunicates based on mixture and secondary structure models. BMC Evol Biol 9:187

Van Soest RWM (1981) A monograph of the order Pyrosomatida (Tunicata, Thaliacea). J Plankton Res 3:603-631

Wada Y, Mogami Y, Baba S (1997) Modification of ciliary beating in sea urchin larvae induced by neurotransmitters: beat-plane rotation and control of frequency fluctuation. J Exp Biol 200:9-18

Harris-Warrick RM, Cohen AH (1985) Serotonin modulates the central pattern generator for locomotion in the isolated lamprey spinal cord. J Exp Biol 116: 27-46

Welsh JH, Loveland RE (1968) 5-Hydroxytryptamine in the ascidian, *Ciona intestinalis* L. Comp Biochem Physiol 27:719-722

Wicht H, Lacalli TC (2005) The nervous system of amphioxus: structure, development, and evolutionary significance. Can J Zoolog 83:122-150

Wiley EO, Lieberman BS (2011) Phylogenetics: Theory and Practice of Phylogenetic Systematics. Wiley, Hoboken

Willows AO, Pavlova GA, Phillips NE (1997) Modulation of ciliary beat frequency by neuropeptides from identified molluscan neurons. J Exp Biol 200:1433-1439

Zeng L, Jacobs MW, Swalla BJ (2006) Coloniality has evolved once in stolidobranch ascidians. Integr Comp Biol 46:255-268

4.2 Supplementary material

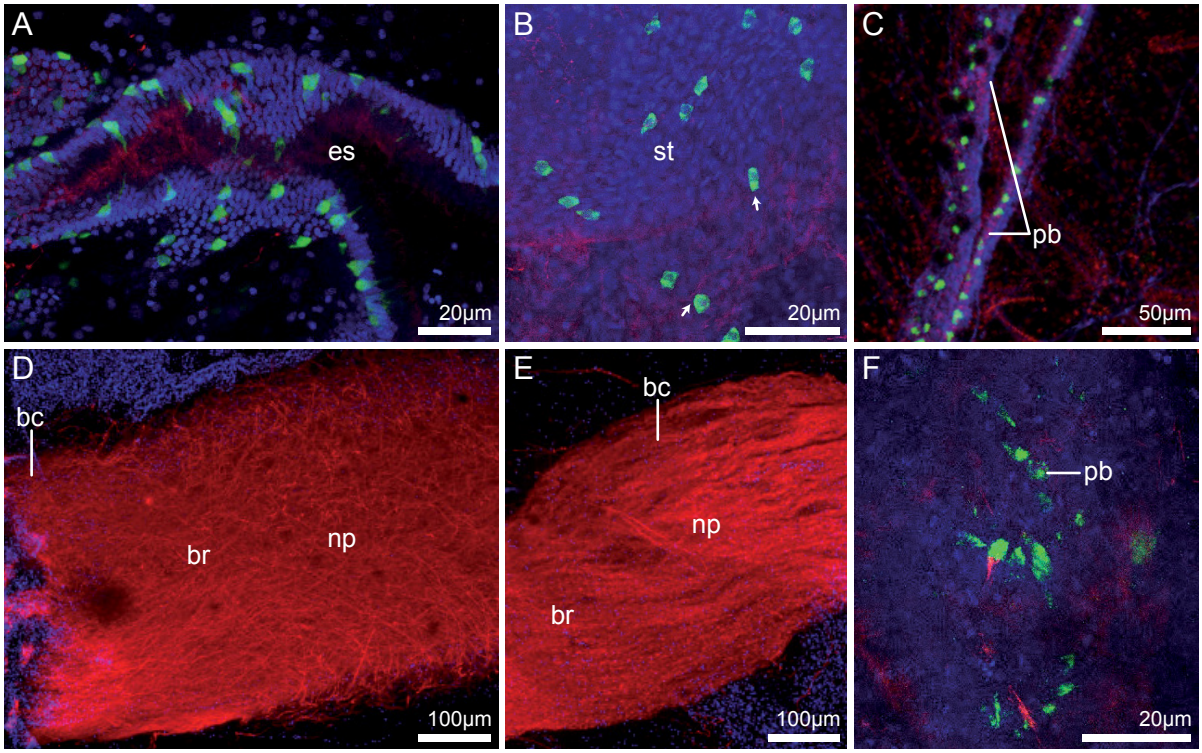

Supplementary Figure 7: Z-projections of confocal laser scanning micrographs of different ascidian species. Localization of antibodies against serotonin (green), against tyrosinated-α-Tubulin (red), and of DAPI and Hoechst (blue). **A** Lateral view of the esophagus (es) of the phlebobranch ascidian *Ascidiella scabra*, anterior is to the left, dorsal to the top. **B** Lateral view of the stomach (st) of the phlebobranch ascidian *Corella parallelogramma*, anterior is to the left, dorsal is to the top. Arrows indicate neurites that are in close proximity to serotonin-lir cells. **C** Lateral view of the peripharyngeal band (pb) of the phlebobranch ascidian *Perophora japonica*, anterior is to the right, ventral to the top. **D, E** Z-projections of two longitudinal vibratome sections of 75 µm thickness through the brain (br) of *Ciona intestinalis*, anterior is to the right, left side of animal is to the top. The brain is divided into the outer cortex (bc) and an inner neuropil (np). Note that no serotonin-like immunoreactivity is present in the brain. **F** Oblique lateral view of the peripharyngeal band of the aplousobranch ascidian *Clavelina lepadiformis*, anterior is to the right

5 Serotonin-like immunoreactivity in Thaliacea

5.1 Publication

This is a post-peer-review, pre-copyedit version of an article published in *Zoomorphology*. The final authenticated version is available online at:

http://dx.doi.org/10.1007/s00435-018-0416-9.

Distribution and evolution of serotonin-like immunoreactive cells in Thaliacea (Tunicata)

Authors

Katrin Braun

Humboldt-Universität zu Berlin, Institut für Biologie, Vergleichende Zoologie, Philippstrasse 13, Haus 2, 10115 Berlin, Germany, katrin.braun@hu-berlin.de

Thomas Stach

Humboldt-Universität zu Berlin, Institut für Biologie, Molekulare Parasitologie, Philippstrasse 13, Haus 14, 10115 Berlin, Germany

Abstract

Thaliacea are marine planktonic animals within the taxon Tunicata. The species-poor taxon is characterized by diverse life cycles, with sexually (blastozooid) and asexually (oozooid) reproducing generations, that usually evolved polymorph phenotypes. While recent molecular phylogenetic studies indicate that tunicates might be closest living relatives to planktonic craniates, additional insights into the evolution of the nervous systems of planktonic tunicates are overdue.

To test the hypothesis that polymorphism in the different stages induces different distribution patterns of neurotransmitters, we comparatively conducted immunostaining experiments utilizing antibodies against serotonin and tyrosinated-α-tubulin, and confocal laser scanning microscopy in planktonic Thaliacea. We considerably increase the available data on serotonin-like immunoreactive (serotonin-lir) in Thaliacea and found that the pattern of distribution of serotonin-lir cells clearly differs between oozooid and blastozooid stages. Thereby, we reveal that the distribution of serotonin-lir cells in different tissues of thaliaceans can be considered as independent characters.

Further, we test the potential phylogenetic signal present in serotonin-lir in thaliaceans, propose a phylogenetic mapping of conceptualized characters, and analyze the evolution of serotonin-lir cells.

Comparing our results with data from previous studies indicated that it was necessary to reevaluate already described distribution patterns of serotonin-lir. Due to the complex life-cycles of Salpida and Doliolida, erroneous descriptions of the localization of serotonin-lir occur in thaliacean literature. To facilitate the evaluation of data on serotonin-lir in thaliaceans for future readers, we suggest depicting whole-mount stainings of complete animals.

Keywords

Urochordates, 5-HT, tunicate phylogeny, salps, confocal microscopy, comparative immunohistology

Introduction

Thaliaceans are marine planktonic animals that constitute one of the five major tunicate taxa. Within the 2500 described tunicate species Thaliacea account for only 70 species. Thaliacea can be identified by their translucent tunic and the positions of the excurrent and incurrent siphons on opposite poles of the animals (Kott 2005). Within Thaliacea three taxa are distinguished: Pyrosomatida, Doliolida, and Salpida (Piette and Lemaire 2015). Pyrosomes are animals that form clonal colonies that swim feebly through the water column utilizing a jet produced by the exhaled water current of the common excurrent opening of the colony. Bright bioluminescence is another typical characteristic of pyrosomes. Doliolids are usually very small (less than 1 mm) barrel-shaped animals with highly complicated life cycles. The third taxon, Salpida, is the best known within Thaliacea. Salps are common in seas all over the world and due to their asexual reproduction occur in high numbers at the sea shores when environmental conditions are beneficial for them (reviewed in Bone 1998).

While in traditional taxonomy Thaliacea was regarded as a basal group within Tunicata with their planktonic life style representing an ancestral plesiomorphic state (e.g. Berrill 1936, Garstang 1928, Lacalli 1999), recent molecular studies on tunicate phylogeny concur that thaliaceans are derived from a sessile ascidian-like ancestor (e.g. Delsuc et al. 2018, Govindarajan et al. 2011, Kocot et al. 2018, Stach and Turbeville 2002, Tsagkogeorga et al. 2009). Within Thaliacea diverse life cycles have evolved. As is common in colonial tunicates, Salpida and Doliolida reproduce sexually and asexually in consecutive generations but the two generations differ drastically in their respective phenotypes (Chamisso 1819, Krohn 1846). The sexually produced embryo develops into the solitary generation (oozooid) that asexually produces a long chain of buds at a specialized ventral organ, the stolo prolifer. The buds (blastozooids) remain aggregated and usually are fertilized by other buds of the same chain. Therefore, blastozooids reproduce sexually. Each fertilized blastozooid carries at least one embryo that again develops into a mature oozooid (Ihle 1956). In doliolids life cycles are even more complicated. Similar to salp embryos, doliolid embryos develop into a larva that develops into a solitary oozooid. The mature oozooid degenerates its internal organs – is then called old nurse – and develops buds at the ventral stolo prolifer. From there, the buds move to a dorsal posterior extension, the caudal peduncle (Godeaux et al. 1998). According to their position in the caudal peduncle these blastozooid buds develop into sterile tropho- or gastrozooids and phorozooids, or fertile gonozooids. Gonozooids are fertilized by other gonozooids of the same chain (Godeaux 2003). The life cycle of Pyrosomatida resembles the one present in colonial ascidians, but pyrosomes develop directly, without a larval stage as present in colonial ascidians (Huxley 1860, Godeaux et al. 1998).

When Delsuc and co-workers (2006) presented molecular phylogenetic evidence that tunicates might be the closest living relatives to Craniota, a taxon with elaborated central nervous systems, the nervous systems of the supposedly primitive tunicates attracted renewed research interest. In an evolutionary context, the central nervous system of thaliaceans is especially informative to study, because among tunicates thaliaceans do not reflect the sessile ascidian life style. The central nervous system of thaliaceans consequently is equipped with probable adaptations to the planktonic life style such as the presence of additional neuropils, eyes, and nerve fiber tracts (Braun and Stach 2018). In the sessile

ascidians, the central nervous system consists of a comparatively simple brain (sensu Richter et al. 2010) that is divided into a central neuropil and a surrounding layer of neuronal somata (cortex). In Salpida additional optical neuropils can be developed that connect the eyes to the main part of the brain (Lacalli and Holland 1998, Braun and Stach 2017). A brain-associated neural gland that is typical of tunicates is reduced in Salpida, but present in Pyrosomatida and Doliolida (Braun and Stach 2018).

In order to gain additional insight into the evolution of tunicate nervous systems, we conducted immunostaining experiments utilizing antibodies against neurotransmitters and confocal laser scanning microscopy. In a previous study on the distribution of the neurotransmitter and tissue hormone serotonin it was shown that at least three different serotonin-like immunoreactive (serotonin-lir) cell types are present in tunicates that are specifically distributed in certain tissues probably performing different functions (Braun and Stach 2016). For sessile ascidians serotonin-lir was detected in the peripharyngeal band, retropharyngeal band, esophagus, stomach, and intestine, but not in the brain (e.g. Georges 1985, Pennati et al. 2001, Braun and Stach 2016). In the other planktonic taxon, Appendicularia, serotonin-lir seems to be completely reduced (Braun and Stach 2016) with the exception of *Oikopleura fusiformis* Fol, 1872 where few serotonin-lir neurons were reported to be present (Stach 2005). In thaliaceans serotonin-lir was described in the brain, peripharyngeal band, esophagus, and intestine (Braun and Stach 2016, Pennati et al. 2012, Stach 2005). Valero-Gracia and co-workers (2016) additionally located serotonin-lir cells in the pyloric gland of the pyrosome *P. verticillata*.

In Salpida and Doliolida brain morphology differs even within the same species e.g. in respect to the numbers and presence of nerves, the shapes of brains, or numbers and shapes of eyes (Braun and Stach 2017, 2018). Yet, comparative studies on differences in distribution patterns of neurotransmitters between two stages of the same species are almost entirely missing for Thaliacea, with the exception of studies on serotonin-lir in *T. democratica*. For this species immunohistochemical results for the nervous system on both stages have been published, but by different investigators (Pennati et al. 2012 – oozooid, Braun and Stach 2016 – blastozooid, Valero-Gracia et al. 2016 – oozooid and blastozooid). Comparing the results of these studies indicates that in *T. democratica* the distribution patterns within the two stages are quite similar, nearly identical. Extrapolating from the variability of the anatomy between different stages one would expect that blastozooids and oozooids also differ in the distribution patterns of neurotransmitters, such as serotonin. To test this hypothesis, we comparatively conducted immunohistological staining experiments with antibodies against serotonin in seven different thaliacean species belonging to the three thaliacean taxa. Thereby, we considerably increase the available data on serotonin-lir in Thaliacea for two pyrosome species, one salp species (both stages), oozooids of two salp species, and one doliolid species (old nurse (oozooid) and gonozooid stage).

Serotonin-lir has been shown to carry phylogenetic information in diverse metazoan taxa (Brenneis and Scholtz 2015, Moret et al. 2004, Schmidt-Rhaesa et al. 2015, Stemme et al. 2017). Previous descriptions of serotonin-lir in tunicates have demonstrated that serotonin-lir serves as a valuable character for phylogenetic analysis within Tunicata (Braun and Stach 2016, Georges 1985). In our present study we further test the potential phylogenetic signal present in serotonin-lir in thaliaceans and present an attempt to reconstruct the evolution of serotonin-lir cells in an evolutionarily important subtaxon of Tunicata.

Material and methods

Collection localities of all specimens are listed in **Table 1**. *Iasis cylindrica, Thalia democratica, Salpa fusiformis* and *Doliolum nationalis* were collected from the water column using a plankton net during a 15 minutes drift tow at 10m depth. Further specimens of *Salpa fusiformis* were provided from the EMBRC-France marine station in Villefranche-sur-Mer. *Pyrosoma atlanticum* was collected from the water column deploying a tucker trawl at 1000m depth that was opened at 300m depth. *Pyrostremma agassizi* and *Pyrosomella verticillata* were secured from the water column deploying a tucker trawl at 1200m depth that was opened at 800m depth on the R/V SONNE expedition SO258 leg 1.

Confocal laser scanning microscopy

For immunohistochemical analysis, specimens were fixed in 4% paraformaldehyde in PBS for 40min at room temperature. Samples were rinsed in PBS and stored in PBS containing 0.05% NaN_3 at 4°C for no longer than 6 months after fixation. All specimens were rinsed three times for 5min in PBS, three times for 10min and four times for 30min in PBTx (PBS containing 0.5% Bovine Serum Albumine (BSA), 0.3% Triton-X-100, and 1.5% Dimethyl Sulfoxide (DMSO)). Samples were blocked with 5% Normal Goat Serum (NGS) in PBTx twice for 30min. Incubation in primary antibodies against serotonin (5-HT (Serotonin) Rabbit; ImmunoStar, Hudson, Wisconsin, USA) and against tyrosinated-α-tubulin (Anti-Tubulin, Tyrosine antibody produced in mouse; Sigma, St. Louis, Missouri, USA) was carried out in preincubation fluid at a dilution of 1:100 (serotonin) and 1:1000 (tyrosinated-α-Tubulin) at 4°C for at least 2.5 days. Samples were rinsed three times for 10min and again four times for 30min in PBTx at room temperature. Preincubation was carried out twice for 30min in 5% NGS diluted in PBTx. Specimens were incubated over night at room temperature in darkness in secondary antibodies Alexa Fluor® 488 goat anti-rabbit IgG (Molecular Probes, Eugene, Oregon, USA) and Cy™3 AffiniPure Goat Anti-Mouse IgG (Jackson ImmunoResearch Laboratories, Inc., Philadelphia, Pennsylvania, USA) diluted in preincubation fluid at a concentration of 1:100 each. All specimens were washed in PBS three times for 10min and labeled with 4'6-Diamidino-2-Phenylindole (DAPI) for at least 1h, and Hoechst 33342 (Sigma, St. Louis, Missouri, USA) for at least 15min. Samples were rinsed in PBS for 10min twice, for 30min again, and dehydrated through an ethanol series. All specimens and sections were cleared with Murray's fluid (2 parts benzyl benzoate: 1 part benzyl alcohol) and mounted in Murray's fluid on microscope slides. Every staining experiment was performed together with two different controls, one with primary antibodies omitted, the second with secondary antibodies omitted. Specimens treated with antibodies against tyrosinated α-tubulin and serotonin, and with DAPI and Hoechst were examined using a Leica TCS SPE confocal laser scanning microscope (Leica Microsystems, Heidelberg, Germany). Appropriate filter settings were applied to record stacks of confocal optical sections. FIJI software (Schindelin et al. 2012) and Adobe Photoshop CS3 software were used for the analysis of images.

Table 1: Information on examined specimens

Species	Family	Stage	Origin	# Specimens examined
Doliolum nationalis Borgert, 1893	Doliolidae	oozooids (old nurses) and blastozooids (gonozooids)	Atlantic Ocean, West Palm Beach, USA	5 6
Iasis cylindrica (Cuvier, 1804)	Salpidae	oozooids	Atlantic Ocean, West Palm Beach, USA	4
Salpa fusiformis Cuvier, 1804	Salpidae	oozooids and blastozooids	Atlantic Ocean, West Palm Beach, USA; Villefranche-sur-Mer, France	4 6
Thalia democratica (Forskål, 1775)	Salpidae	oozooids	Atlantic Ocean, West Palm Beach, USA	4
Pyrostremma agassizi (Ritter & Byxbee, 1905)	Pyrosomatidae	adult zooids	Pacific Ocean, Osborne Seamount	7
Pyrosoma atlanticum Péron, 1804	Pyrosomatidae	adult zooids	Indian Ocean, Afanasy Nikitin Seamount	7
Pyrosomella verticillata (Neumann, 1909)	Pyrosomatidae	adult zooids	Pacific Ocean, Osborne Seamount	6

Light microscopy

For light microscopy *D. nationalis* was fixed in a cold solution of Karnovsky's primary fixative (Karnovsky 1965), consisting of 2% glutaraldehyde, 2% paraformaldehyde, 1.52% NaOH and 1% d-glucose, dissolved in 2.25% sodium hydrogen phosphate buffer (pH 7.4), *P. atlanticum* was fixed in 10% formaldehyde and kept in 70% ethanol.

Specimens for light microscopy were dehydrated in a graded series of ethanol, embedded in epoxy resin (Araldite; Fluka). Then specimens were serially sectioned with a thickness of 0.5µm -0.7µm. Sectioning was performed on a Leica Ultracut S. Semithin sections were stained using 0.5% toluidine blue in a solution of 1.5% sodium bicarbonate and 40% glycerol.

Semithin sections stained with toluidine blue were digitally recorded (distance of sections from *D. nationalis* 3.5µm, from *P. atlanticum* 5µm) using a Zeiss AxioCam HRc camera mounted on a Zeiss Axioskop 2 plus microscope. Complete images were optimized for contrast and light balance using Adobe Photoshop CC Software and were used for 3d reconstructions.

The 3d models of the animals were created in Amira 5.4.3 (FEI Visualization Sciences Group, Berlin, Germany) based on the images of the serial semithin sections. Images were aligned in Amira. The resulting stack of images was used for the reconstruction of the internal anatomy of *D. nationalis* and *P. atlanticum*.

Results

Doliolida

Doliolids are small barrel-shaped tunicates with highly complex life cycles. Among doliolids *Doliolum nationalis* is frequently occurring in the marine plankton. In the solitary asexual generation (oozooid) serotonin-lir is only detectable in the brain (**Figs. 1A & B**). Few serotonin-lir cells are situated in the brain cortex and serotonin-lir is also visible in the neuropil. Somata of these cells are spherically shaped and measure approximately 6µm in diameter.

In the aggregate sexual generation (blastozooid, gonozooid) serotonin-lir is visible in the brain, the characteristic dorsal spiral of the peripharyngeal band, the retropharyngeal band, and the esophagus (**Figs. 1C-G**, see also interactive 3d reconstruction in Supplementary Figure 1A for internal anatomy). In the brain neurons measuring approximately 6µm in diameter are situated in the cortex and serotonin-lir is also present in the neuropil (**Fig. 1C**). In the dorsal part of the peripharyngeal band elongated serotonin-lir cells are located in a single row (**Fig. 1D**). These cells measure 15µm in length, but merely 4-5µm in width. In the retropharyngeal band and esophagus positively labeled cells form a row of more or less spherical cells, measuring 5-6µm in diameter (**Figs. 1 E& F**).

Pyrosomatida

Pyrosomes are small tunicates as individual zooids, but they can form big colonies. They are particularly known for their brilliant bioluminescence. Specimens belonging to the species *Pyrostremma agassizi* can be recognized by their thin and transparent tunic that forms triangular denticulations on the exterior of a colony. Serotonin-lir cells in *P. agassizi* are positioned in the peripharyngeal band, in the endostyle, and in the esophagus, but not in the brain **(Figs. 2A-E)**. In the peripharyngeal band and esophagus one row of positively labeled cells is detectable, while in the endostyle two bilaterally symmetrical rows are developed. Serotonin-lir cells in the peripharyngeal band, endostyle, and esophagus are more or less spherical with diameters of approximately 8µm, 10µm, and 7µm (**Figs. 2C-E**). Stainings with antibodies against tyrosinated-α-tubulin suggest that nerves make contact with some serotonin-lir cells or run in close spatial relation to these immunopositively labeled cells (see arrows in Fig. 1C).

Pyrosoma atlanticum is a common pyrosome that builds large colonies in which the zooids are irregularly arranged. In *P. atlanticum* serotonin-lir is detectable in the peripharyngeal band, the endostyle, the dorsal half of the retropharyngeal band, and the esophagus (**Figs. 2F-J**). In all mentioned body parts serotonin-lir cells are more or less spherically shaped. A single row of positively labeled cells measuring 5µm in diameter is present in the peripharyngeal band. In the endostyle two bilaterally symmetrical rows consisting of serotonin-lir cells that measure 11µm in diameter are detectable. In the retropharyngeal band and esophagus serotonin-lir cells measure 7µm in diameter and these cells form a single row (**Figs. 2H-J**). Serotonin-lir could not be detected in the brain of the animals (**Fig. 2G**).

Roundish and laterally flattened zooids that are strictly arranged in parallel rows in a colony with a smooth tunic are typical for the pyrosome *Pyrosomella verticillata*. Serotonin-lir in *P. verticillata* is located in the peripharyngeal band, endostyle, retropharyngeal band, and esophagus (**Figs. 2K-P**). The identical distribution pattern of serotonin-lir cells is already visible in small buds (**Fig. 2K**). In the brain serotonin-lir cells are not detectable (**Fig. 2L**). In the peripharyngeal and retropharyngeal band a single

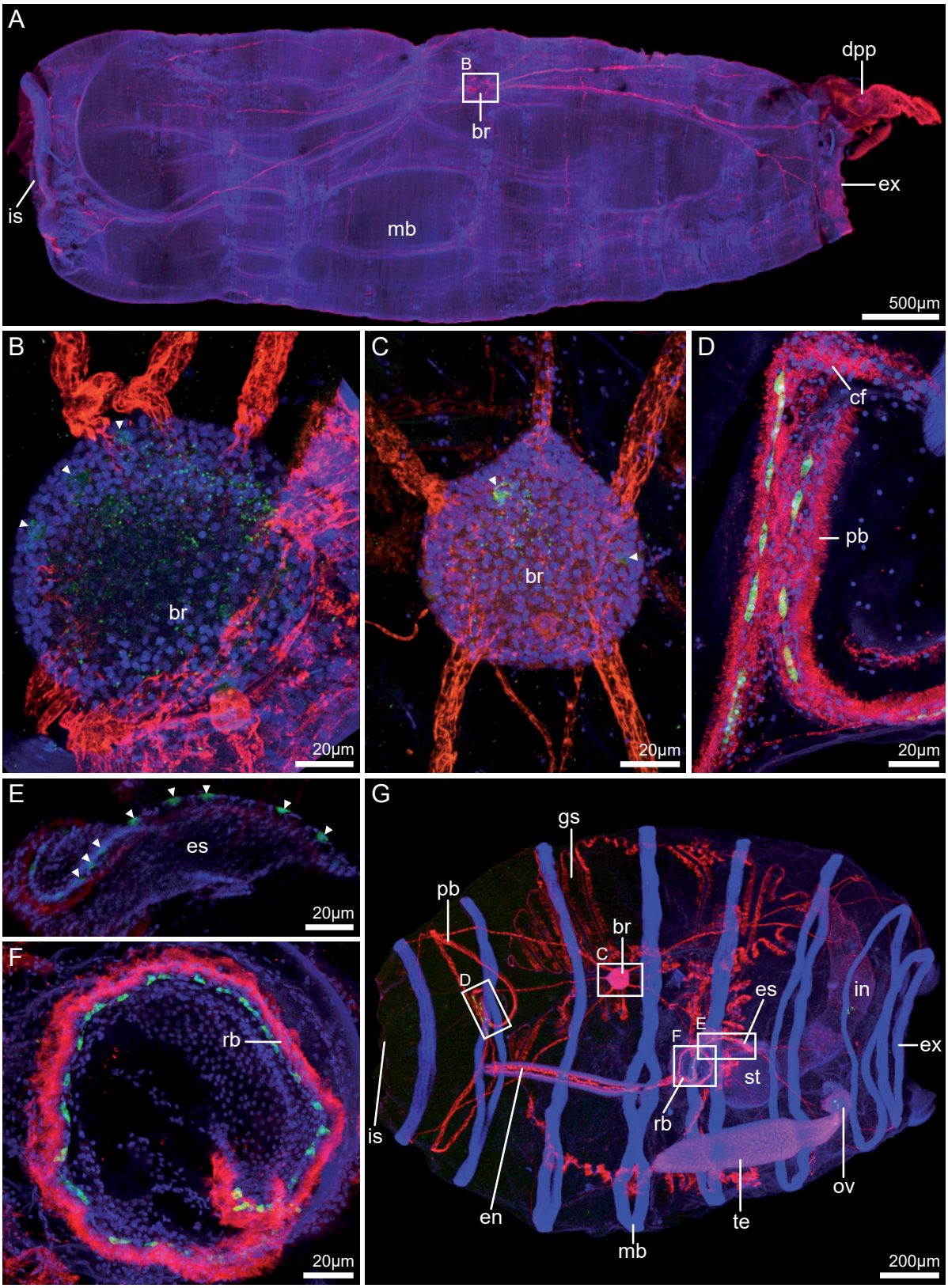

Fig. 1: Z-projections of confocal laser scanning micrographs of immunohistochemical stainings with antibodies against serotonin (green) and tyrosinated-α-tubulin (red), and with DAPI and Hoechst (blue) in *Doliolum nationalis*. **A, B:** Localization of serotonin-lir in the oozoid stage. **A:** Lateral view of an entire animal, anterior to the left, dorsal to the top. In the old oozooid (old nurse) internal organs are degenerated while muscle bands (mb) increase and a dorsal posterior process (dpp) with a chain of buds is formed. **B:** Higher magnification of the brain (br), dorsal view, anterior to the top, area of magnification marked with a white rectangle in **A**. Few neurons with a weak immunoreactivity

against serotonin are situated in the brain cortex (arrowheads). **C-G:** Localization of serotonin-lir in the blastozooid stage. **C-F:** Details of areas with serotonin-lir cells, positions shown with white rectangles in **G**. **C:** Dorsal view on the brain, anterior to the top. Serotonin-lir neurons are present in the brain cortex (arrowheads). **D:** Elongated serotonin-lir cells are situated in the dorsal part of the peripharyngeal band (pb) in the characteristic dorsal spiral. **E:** Serotonin-lir cells are positioned in the esophagus (es) (arrowheads). **F:** Serotonin-lir in the retropharyngeal band (rb). **G:** Dorsal view of complete individual, anterior to the left. Serotonin-lir is detectable in the brain, in the dorsal part of the peripharyngeal band, in the retropharyngeal band, and in the esophagus of the animal. cf: ciliated funnel, en: endostyle, ex: excurrent siphon, gs: gill slits, in: intestine, is: incurrent siphon, ov: ovary, st: stomach, te: testis.

Fig. 2: Z-projections of confocal laser scanning micrographs of three pyrosome species stained with antibodies against serotonin (green), tyrosinated-α-tubulin (red) and with DAPI and Hoechst (blue). **A-E:** Serotonin-lir in *Pyrostremma agassizi*, lateral view, anterior to the top, dorsal to the left. **A:** Complete individual shown, serotonin-lir cells form a band-like pattern that extends from the prolonged peripharyngeal band (pb) to the endostyle (en) (arrowheads). A cluster of serotonin-lir cells is visible in the esophagus (es). **B-E:** Details of areas marked in **A. B:** Higher magnification of the brain (br). Serotonin-lir is not visible in the brain but in the peripharyngeal band beneath the brain. **C:** A single row of serotonin-lir cells is situated in the peripharyngeal band. Neurites make contact with peripharyngeal band in close proximity to serotonin-lir cells (arrows). **D:** Two rows of bilaterally symmetrical serotonin-lir cells are located in the endostyle. **E:** Several rows of serotonin-lir cells are present in the esophagus. **F-J:** Localization of serotonin-lir cells in *Pyrosoma atlanticum*, lateral view, anterior to the top, dorsal to the left. **F:** Entire individual, serotonin-lir cells are present in the peripharyngeal band, endostyle, dorsal half of the retropharyngeal band (rb), and esophagus (arrowheads). **G-J:** Higher magnification of areas marked in **F**. **G:** Serotonin-lir cells are not present in the brain but in the peripharyngeal band ventral to the brain. **H:** Serotonin-lir cells are scattered in the peripharyngeal band. **I:** Two bilaterally symmetrical rows of serotonin-lir cells are present in the endostyle. **J:** A single row of serotonin-lir cells is visible in the esophagus. **K-P:** Serotonin-lir in *Pyrosomella verticillata*, lateral view, anterior to the top, dorsal to the left. **K:** Complete individual, serotonin-lir is located in the peripharyngeal band, endostyle, retropharyngeal band, and esophagus (arrowheads). The same distribution of serotonin-lir cells is already present in the young bud (bu). **L:** Serotonin-lir is not detectable in the brain or ciliated funnel (cf) but in the peripharyngeal band ventral to the brain. **M:** A single row of serotonin-lir cells is positioned in the peripharyngeal band. **N:** Two rows of elongated serotonin-lir cells are present in the endostyle. **O:** In the retropharyngeal band serotonin-lir are scattered. P: Several rows of elongated serotonin-lir cells are positioned in the esophagus. bb: branchial basket, ex: excurrent siphon, gs: gill slits, in: intestine, is: incurrent siphon, ov: ovary, st: stomach, te: testis.

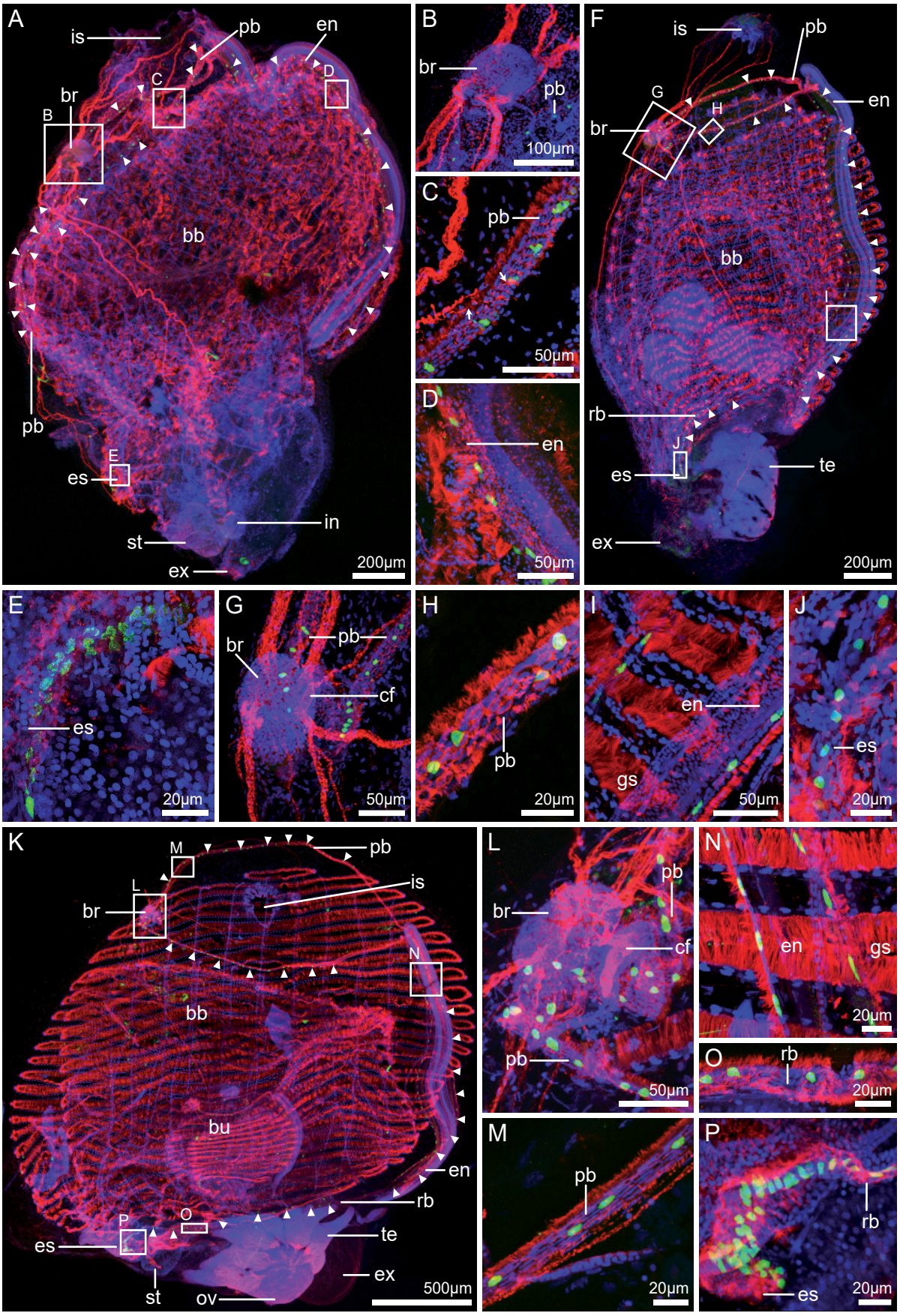
A
is
pb
en
br
C
D
B
bb
pb
E
es
in
st
ex
200µm
B
br
pb
100µm
C
pb
50µm
D
en
50µm
F
is
pb
en
G
H
br
bb
I
rb
J
es
te
ex
200µm
E
es
20µm
G
br
pb
cf
50µm
H
pb
20µm
I
en
gs
50µm
J
es
20µm
K
M
pb
L
is
br
N
bb
bu
en
rb
P
O
es
te
ex
st
ov
500µm
L
br
pb
cf
pb
50µm
M
pb
20µm
N
en
gs
20µm
O
rb
20µm
P
rb
es
20µm

Fig. 2

row of serotonin-lir cells is located with more or less spherical cells measuring 10µm (peripharyngeal band) and 6µm (retropharyngeal band) in diameter (**Figs. 2M & O**). In the endostyle two rows of bilaterally symmetrical serotonin-lir cells are situated that are elongated and measure 15µm in length and approximately 4µm in width (**Fig. 2N**). Several rows of elongated serotonin-lir cells are located in the esophagus. These cells measure approximately 10µm in length (**Fig. 2P**).

Salpida

Salps are the best known group of Thaliacea since they appear in high numbers at the coastlines at certain times of the year. In the asexual oozooid of *Iasis cylindrica* serotonin-lir cells are present in the posterior part of the peripharyngeal band, the brain, and in the esophagus (**Figs. 3A-D**). In the brain serotonin-lir cells are mainly localized in the ventral and anterior part of the neural cortex. The more or less spherical cell somata measure approximately 5µm in diameter. While several rows of irregularly arranged bottle-shaped serotonin-lir cells are positioned in the esophagus, in the peripharyngeal band several rows of elongated serotonin-lir cells are present (**Figs. 3C & D**). Serotonin-lir cells in the peripharyngeal band measure approximately 11µm in length, in the esophagus these cells measure approximately 20µm. In the latter a long extension toward the lumen of the esophagus is formed (**Fig. 3D**). In the asexual oozooid stage of *Thalia democratica* serotonin-lir cells are located in the brain, the dorsal half of the peripharyngeal band, and in the esophagus (**Figs. 3E-H**). Serotonin-lir cells are mainly accumulated in a cluster anteriomedian in the brain. Few serotonin-lir somata are situated bilaterally symmetrical in the posterior brain cortex. Immunopositively labeled cells have a spherical shape and measure approximately 5µm in diameter (**Fig. 3F**). In the peripharyngeal band elongated serotonin-lir cells measure approximately 12µm in length and 3-4 µm in width (**Fig. 3G**). In contrast, serotonin-lir cells in the esophagus are spherically shaped and measure up to 10µm in diameter (**Fig. 3H**). The sexual blastozooid stage of *Salpa fusiformis* shows serotonin-lir cells in the brain, the dorsal half of the peripharyngeal band, and the esophagus **(Figs. 4A-D)**. Serotonin-lir cell somata are visible in the brain cortex. These cells are located in the anterior part and on the right ventral side of the brain. Positively labeled cells in the brain are spherical in shape and measure approximately 5µm in diameter **(Fig. 4B)**. Several rows of serotonin-lir cells are present in the dorsal half of the peripharyngeal band. In that region serotonin-lir cells are bottle-shaped and measure approximately 13µm in length and about 3 µm in width (**Fig.4C**). In the esophagus more or less spherical and elongated serotonin-lir cells are visible. Spherical cells measure 6µm in diameter, while elongated cells measure approximately 8µm in length and roughly 3 µm in width.

In the asexual oozooid stage of *S. fusiformis* serotonin-lir cells are situated in the brain, the dorsal part of the peripharyngeal band, at the transition of the retropharyngeal band and esophagus, and in the esophagus **(Figs. 4E-H)**. Serotonin-lir in the brain is located on the left side and in the posterior part of the brain, in the cortex. Positively labeled cells are more or less spherical and measure approximately 5µm in diameter (**Fig.4F**). In the peripharyngeal band serotonin-lir cells constitute several rows and are elongated, measuring 12µm in length and approximately 4 µm in width (**Fig.4G**). Bottle-shaped serotonin-lir cells are embedded in the esophageal wall and measure approximately 11µm in length (**Fig.4H**).

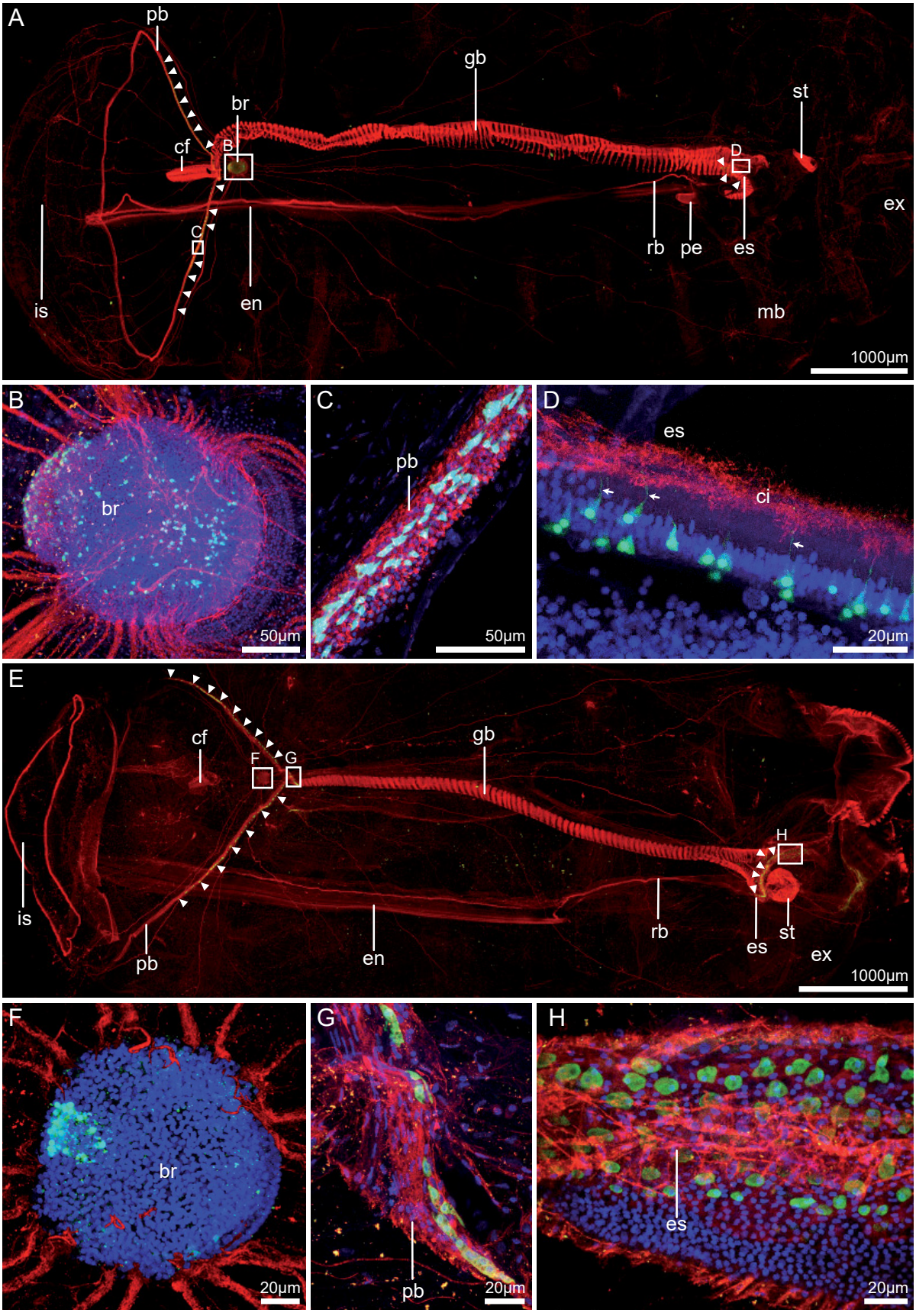

Fig. 3: Z-projections of confocal laser scanning micrographs in the oozooids of two salp species stained with antibodies against serotonin (green), tyrosinated-α-tubulin (red) and with DAPI and Hoechst (blue). All micrographs show dorsal views, anterior to the left. **A-D:** Serotonin-lir in the asexual oozooid stage of *Iasis cylindrica*. **A:** Micrograph of a complete oozooid reveals that serotonin-lir is confined

to three areas – the brain (br), peripharyngeal band (pb), and esophagus (es) (arrowheads). Details of these areas are shown in **B-D**. **B:** Serotonin-lir neurons are positioned in the anterior and ventral part of the brain. **C:** Several rows of serotonin-lir cells are present in the peripharyngeal band. **D:** Bottle-shaped serotonin-lir cells with long thin necks (arrows) are positioned in the esophagus. These cells taper toward the lumen of the esophagus. **E-F:** Localisation of serotonin-lir in the asexual oozooid stage of *Thalia democratica*. **E:** Entire individual shows serotonin-lir cells in the peripharyngeal band, brain, and esophagus (arrowheads). **F-G:** Higher magnification of areas marked in **E**. **F:** Serotonin-lir neurons are localized anteromedian in the brain cortex. **G:** Several rows of elongated serotonin-lir cells are present in the peripharyngeal band. **H:** Approximately spherical serotonin-lir cells are located in the esophagus forming several rows. cf: ciliated funnel, ci: cilia, en: endostyle, ex: excurrent siphon, gb: gill bar, is: incurrent siphon, mb: muscle band, pe: pericardium, rb: retropharyngeal band, st: stomach.

Fig. 4: Z-projections of confocal laser scanning micrographs of immunohistochemical stainings with antibodies against serotonin (green) and tyrosinated-α-tubulin (red), and with DAPI and Hoechst (blue) in *Salpa fusiformis*. All images are dorsal views on the specimens, with anterior to the left. **A-D:** Serotonin-lir in the sexual blastozooid stage. **A:** Complete individual, serotonin-lir are located in the brain (br), peripharyngeal band (pb), and esophagus (es) (arrowheads). Details of areas with serotonin-lir are marked with rectangles and shown in **B-D**. **B:** Serotonin-lir neurons are located in the anterior part and on the right side of the ventral part of the brain. **C:** Several rows of bottle-shaped and elongated serotonin-lir cells are present in the peripharyngeal band. **D:** Several rows of serotonin-lir cells border the esophagus. **E-H:** Localization of serotonin-lir in the asexual oozooid stage. **E:** Entire individual with serotonin-lir cells positioned in the brain, in the peripharyngeal band, at the transition between retropharyngeal band and esophagus, and in the esophagus (arrowheads). Higher magnifications of these areas are shown in **F-H**. **F:** Serotonin-lir neurons are localized in the posterior and left part of the brain cortex. **G:** Several rows of elongated and approximately spherical serotonin-lir cells are situated in the peripharyngeal band. **H:** Bottle-shaped serotonin-lir cells are located in the esophageal wall tapering toward the lumen of the esophagus. cf: ciliated funnel, en: endostyle, ex: excurrent siphon, gb: gill bar, is: incurrent siphon, mb: muscle band, pe: pericardium, rb: retropharyngeal band, st: stomach, vn: visceral nucleus.

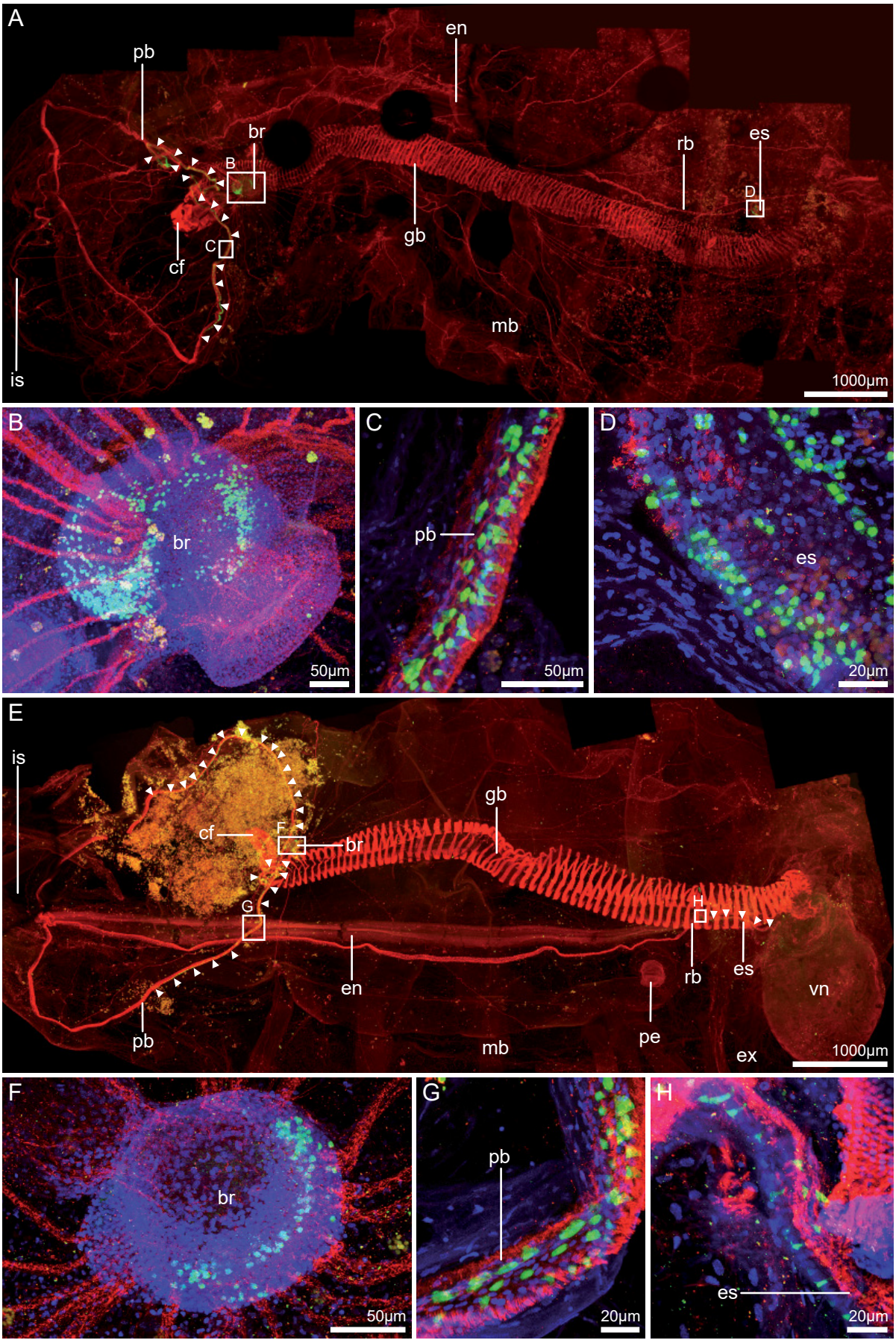
A
pb
en
br
B
rb
es
D
gb
C
cf
mb
is
1000µm
B
br
50µm
C
pb
50µm
D
es
20µm
E
is
gb
cf
F
br
G
H
en
rb
es
vn
pb
mb
pe
ex
1000µm
F
br
50µm
G
pb
20µm
H
es
20µm

Fig. 4

Discussion

Serotonin-lir cells types in Thaliacea

Immunohistological analysis of specimens belonging to the taxon Thaliacea reveals that all previously from other tunicate taxa described serotonin-lir cell types are present in thaliaceans: elongated cells, approximately spherical cells, and serotonin-lir neurons. Elongated serotonin-lir cells are mainly found in the digestive tract of tunicates, but also in other body parts with serotonin-lir, e.g. ciliary bands of the branchial basket (Braun and Stach 2016). Elongated serotonin-lir cells in the esophagus of thaliaceans probably correspond to enterochromaffin cells in craniates which hormonally regulate feeding (Chiba 1998, Trandaburu and Trandaburu 2007). Furthermore elongated serotonin-lir cells in thaliaceans are detectable in the peripharyngeal band, endostyle, and retropharyngeal band. In tunicates the localization of approximately spherical cells is described for the peripharyngeal band, endostyle, retropharyngeal band, esophagus and stomach, but not for the intestine (Braun and Stach 2016). The function of these cells might be analogous to that in other taxa such as molluscs (Doran et al. 2004) or echinoderms (Wada et al. 1997) which would indicate that spherical serotonin-lir cells might also secret mucous and control ciliary beating in thaliaceans. We discovered spherical serotonin-lir cells in the peripharyngeal band, endostyle, retropharyngeal band, and esophagus. The third serotonin-lir cell type present in tunicates, serotonin-lir neurons, is known to initiate motor activity, e.g. in leeches (Nusbaum and Kristan 1986), molluscs (Lewis et al. 2011), and craniates (Harris-Warrick and Cohen 1985) the supposed sister taxon of Tunicata. In Thaliacea, serotonin-lir neurons are only present in Doliolida and Salpida. The exact position of serotonin-lir neurons differs on the intraspecific level and also at the interspecific level. A comparison of serotonin-lir in the brains of the oozooids of *I. cylindrica* and *S. fusiformis* shows that serotonin-lir neurons can be more dispersed in the brain cortex as seen in *I. cylindrica*, but that serotonin-lir cells can also be restricted to a specific area of the brain cortex, e.g. the posterior half of the brain cortex, as seen in *S. fusiformis* (**Figs. 3B & 4F**). Positions of serotonin-lir neurons also vary in different life-history stages. In the salp *S. fusiformis* distribution patterns of serotonin-lir neurons differ considerably between consecutive generations. While in the blastozooid most serotonin-lir neurons are located in the anterior part of the brain, serotonin-lir neurons in the oozooid are present in the posterior part of the brain (**Figs. 4B & 4F**).

Comparison of the distribution of serotonin-lir cells comparison of the distribution pattern of serotonin-lir cells in different tissues of different tunicate taxa shows similarities to a certain extent, but regarding some characters clear variations between species are present. Thus, the distribution of serotonin-lir cells in specific tissues can be regarded as independently evolved characters that probably carry phylogenetic information. Also, within Thaliacea serotonin-lir shows many similarities. However, the distribution of serotonin-lir cells coincides even more between Salpida and Doliolida. In both taxa serotonin-lir cells are completely missing in the endostyle and in the ventral half of the peripharyngeal band, while serotonin-lir is located in the brain. On the contrary, in pyrosomes serotonin-lir cells are not present in the brain, but usually form a continuous band extending from the peripharyngeal band, to the endostyle, retropharyngeal band, and esophagus. Therefore, the distribution pattern of serotonin-lir cells in pyrosomes closely resembles the one present in ascidians, with the exception, that serotonin-

lir cells are missing from the stomach and intestine (Braun and Stach 2016), which is the case for most investigated thaliaceans. Serotonin-lir in the retropharyngeal band differs between species of the same taxon. In some pyrosome species serotonin-lir cells are continuously localized in a band-like pattern along the retropharyngeal band (*P. verticillata*), while in *P. agassizi* serotonin-lir cells are not detectable in the retropharyngeal band. Interestingly, *P. atlanticum* possesses serotonin-lir cells in the dorsal part of the retropharyngeal band, similar to the presence of serotonin-lir cells in aplousobranch ascidians (Braun and Stach 2016). In most salp species serotonin-lir cells are not detectable in the retropharyngeal band, but in the oozooid of *S. fusiformis* serotonin-lir cells are visible at the transition of retropharyngeal band and esophagus. These observations indicate that the localization of serotonin-lir cells in specific tissues of thaliaceans can be considered as independently evolved characters "(Pogue and Mickevich 1990).

The distribution patterns of serotonin-lir cells agree well within thaliacean taxa, and classical tunicate taxa. However, mapping serotonin-lir on recently published molecular phylogenies (Delsuc et al. 2018 and Kocot et al. 2018) remains ambiguous because character distribution is inconclusive, due to homoplasies (**Fig. 5**). In the molecular tunicate phylogenies published by Delsuc and co-workers (2018) and Kocot and co-workers (2018) Thaliacea form the sister group to a taxon consisting of Aplousobranchiata and Phlebobranchiata. With Aplousobranchiata, Phlebobranchiata, and Pyrosomatida showing no serotonin-lir in the brains the question remains, whether the homoplastic localization of serotonin-lir neurons in the brains of Doliolida and Salpida is a regained character or a plesiomorphic character that is retained from the last common ancestor of Tunicata and Craniota. Because serotonin-lir in the brain is only present in Doliolids and Salpida it is more parsimonious to assume that serotonin-lir neurons were regained in the stem lineage of Doliolida and Salpida and therefore were present in the last common ancestor of Doliolida and Salpida. This evolutionary scenario can be explained with the more active planktonic life style of specimens belonging to these two taxa. For several taxa, it has been shown that serotonergic neurons regulate motor activity (e.g. Nusbaum and Kristan 1986, Lewis et al. 2011). A reason why serotonin-lir neurons are not detectable in the brains of the equally planktonic pyrosomes might be that they do not move actively by muscular activity as zooids as do the other two groups. Doliolids and salps move by jet propulsion that is created by contractions of their muscles bands that are situated beneath the epidermis. In pyrosomes muscles are nearly completely reduced and hardly used for movement activity. Instead, they move through the water column using the jet propulsion of the excurrent siphons created by the combined ciliary activity of the branchial baskets of the entire colony (Bone 1998).

In the pyrosome *P. verticillata* we could not detect serotonin-lir cells in the pyloric gland as previously described (Valero-Gracia et al. 2016). A closer look at the presented images of the aforementioned study shows that the authors detected a band-like pattern with a single row of serotonin-lir cells in the posterior part of the branchial basket that coincides with the band-like pattern we detected in the retropharyngeal band and esophagus of *P. verticillata*. We suggest that this pattern has erroneously been assigned to the pyloric gland, instead of the retropharyngeal band and esophagus. From the morphology of the pyloric gland we would expect that serotonin-lir should not be visible as a band-

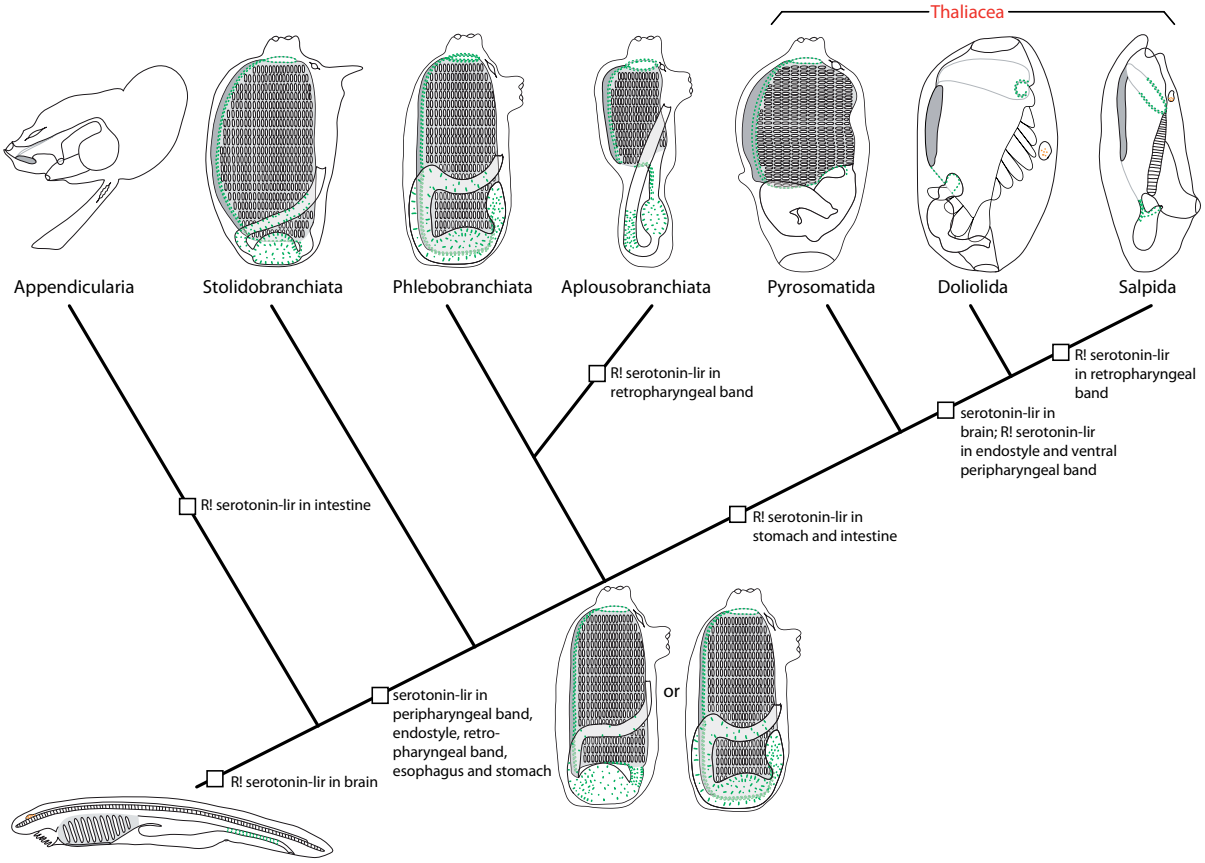

Fig. 5: Schematic representations of localization of serotonin-lir cells and inferred ancestral states plotted on the phylogeny of major tunicate and thaliacean taxa based on the molecular phylogeny by Kocot and coworkers (2018). The presence of serotonin-lir cells in outgroup taxa is represented by a scheme of serotonin-lir in Cephalochordata (Candiani et al. 2001, Holland and Holland 1993). Serotonin-lir neurons are depicted in orange, serotonin-lir cells in non-neural tissue is displayed in green. R! represents the reduction of serotonin-lir cells in the specified tissue.

like pattern, but rather as a dendriform pattern (see also interactive 3d reconstruction in Supplementary Fig. 1B for internal anatomy of pyrosomes).

Complex life-cycles strategies

Within tunicates Thaliacea is the taxon with manifold life-cycle strategies. Among Thaliacea, doliolids possess the most complex life-cycles. Doliolida and Salpida develop through two different alternating generations (asexual and sexual stages). Additionally, in doliolids buds with individuals that perform different tasks in the colony are produced and therefore, even within the same generation, the morphology of individuals can differ drastically. These life-cycle strategies in Thaliacea are especially interesting from a developmental point of view, since in doliolids the same genotype in buds produced by one individual creates polymorphic phenotypes, and in salps the same genotype develops two generations with drastically distinct morphologies. On the other hand complex life-cycle strategies also cause problems in scientific studies, when definitions and terms are not consistently used. In 1819, Adelbert von Chamisso was the first scientist who discovered that the two different salp generations

belong to a single species naming the different generations of salps "proles solitaria" – the solitary asexual generation, oozooid – and "proles gregata" – the aggregate sexual generation, blastozooid (Chamisso 1819). In our study we use the terms oozooid and blastozooid referring to Delage and Hérouard (1898). Because of the distinct morphologies of the different stages it is mandatory to not only carefully identify the species, but also to correctly identify the generations of the investigated animals. Simply identifying an oozooid by its solitary occurrence might be misleading, because mature solitary blastozooids also occur individually when they broke free from the chain. Additional information, such as whether the investigated animal bears embryos (indicative of blastozooids) or possesses a chain with immature blastozooids (indicative of oozooids) is mandatory. Erroneous identifications of generations are widespread in thaliacean literature and even led to contradictory and confusing descriptions regarding patterns of serotonin-lir. E.g., serotonin-lir for oozooids of *T. democratica* has first been described by Pennati et al. (2012). Comparing their Fig. 1 with their Fig. 3 shows that in this study serotonin-lir was shown for blastozooids; this is conclusively seen in the number of muscle bands, which is 4 in blastozooids as opposed to 5 in oozooids. Recently another study on serotonin-lir in *T. democratica* was published, in which the authors described serotonin-lir in "adult oozooids" (Valero-Gracia et al. 2016), while their study depicted an animal possessing three eyes as integrative part of the brain. Three eyes, however, are typical of blastozooids of this species whereas oozooids possess a single horseshoe-shaped eye (see Braun and Stach 2017 and references therein). Furthermore, comparing serotonin-lir in the brain of the oozooid of *T. democratica* from the present study (Fig. 3F) with images provided by Valero-Gracia and co-workers (2016) it is clear that the pattern of immunopositively labeled cells differs. On the other hand, it conforms well to the distribution pattern of serotonin-lir neurons in the blastozooid of *T. democratica* shown in Braun and Stach (2016). The same problem appears in descriptions of serotonin-lir in doliolids. The first study reporting serotonin-lir in doliolids was labeled as serotonin-lir in oozooids of *D. nationalis* (Stach 2005). However, from the whole-mount images shown in this study, it is clear that the study actually depicts a blastozooid.

Because different generations differ drastically in their anatomy, we expected differences in the cells as well. Indeed, we found in the present study that this is the case and that the pattern of distribution of serotonin-lir cells can differ clearly between oozooid and blastozooid stages. Comparisons with published studies indicated that it was necessary to reevaluate already described distribution patterns of serotonin-lir, correct erroneous attributions, and recommend publication of whole-mount stainings of complete animals in order to facilitate future corrections.

Acknowledgements

The authors would like to thank Stefano Tiozzo for expert collection and fixation of specimens of *Salpa fusiformis*. We are thankful to the invaluable help of Woody Lee and Scott Jones from the Smithsonian Marine Station in Fort Pierce, Florida in securing specimens of *Iasis cylindrica*, *Salpa fusiformis*, *Thalia democratica* and *Doliolum nationalis*. We are also indebted to Prof. Valerie Paul and Prof. Mary Rice for generously providing access to the facilities of the Smithsonian Marine Station. We are much obliged to the scientific party and the crew of FS SONNE during the cruise SO258/1, especially to Dr. Nina Furchheim and Reinhard Werner for collecting and fixing specimens of *Pyrostremma agassizi*, *Pyrosoma atlanticum,* and *Pyrosomella verticillata*. We are grateful for the access to the Leica SPE CLSM granted by Dr. Carsten Lüter (Museum für Naturkunde Berlin). Funding by the Deutsche Forschungsgemeinschaft (DFG), the German Academic Exchange Service (DAAD), and the Elsa-Neumann-Stipendium des Landes Berlin are gratefully acknowledged.

Funding

This study was funded by the Deutsche Forschungsgemeinschaft (DFG) grant STA655/4-1, the German Academic Exchange Service (DAAD), and the Elsa-Neumann-Stipendium des Landes Berlin.

Compliance with ethical standards

Conflict of interest

The authors declare that they have no conflict of interest. This article does not contain any studies with human participants performed by any of the authors. All applicable international, national, and/or institutional guidelines for the care and use of animals were followed.

References

Bone Q (1998) The biology of pelagic tunicates. OUP, Oxford

Berrill NJ (1936) II - Studies in tunicate development. Part V - The evolution and classification of ascidians. Philos Trans R Soc B 226:43-70. https://doi.org/10.1098/rstb.1936.0002

Braun K, Stach T (2016) Comparative study of serotonin-like immunoreactivity in the branchial basket, digestive tract, and nervous system in tunicates. Zoomorphology 135:351-366. https://doi.org/10.1007/s00435-016-0317-8

Braun K, Stach T (2017) Structure and ultrastructure of eyes and brains of *Thalia democratica* (Thaliacea, Tunicata, Chordata). J Morphol 278:1421-1437. https://doi.org/10.1002/jmor.20722

Braun K, Stach T (2018) Morphology and evolution of the central nervous system in adult tunicates. Manuscript submitted for publication.

Brenneis G, Scholtz G (2015) Serotonin-immunoreactivity in the ventral nerve cord of Pycnogonida – support for individually identifiable neurons as ancestral feature of the arthropod nervous system. BMC Evol Biol 15:136. https://doi.org/10.1186/s12862-015-0422-1

Candiani S, Augello A, Oliveri D, Passalacqua M, Pennati R, De Bernardi F, Pestarino M (2001) Immunocytochemical localization of serotonin in embryos, larvae and adults of the lancelet, *Branchiostoma floridae*. Histochem J 33:413-420. https://doi.org/10.1023/A:1013775927978

Chamisso AV (1819) De animalibus quibusdam e classe vermium Linnaeana in circumnavigatione terrae auspicante Comite N. Romanzoff duce Ottone de Kotzebue annis 1815. 1816. 1817. 1818. peracta observatis. Fasciculus primus. De Salpa. Dümmler Verlag, Berlin

Chiba A (1998) Ontogeny of serotonin-immunoreactive cells in the gut epithelium of the cloudy dogfish, *Scyliorhinus torazame*, with reference to coexistence of serotonin and neuropeptide Y. General and Comparative Endocrinology 111:290-298. https://doi.org/10.1006/gcen.1998.7104

Delage Y, Hérouard E (1898) Les procordés. Schleicher Frères (eds.) Traité de Zoologie Concrète. T.8. Masson, Paris

Delsuc F, Brinkmann H, Chourrout D, Philippe H (2006) Tunicates and not cephalochordates are the closest living relatives of vertebrates. Nature 439:965-968. https://doi.org/10.1038/nature04336

Delsuc, F., Philippe, H., Tsagkogeorga, G., Simion, P., Tilak, M.-K., Turon, X., López-Legentil, S., Piette, J., Lemaire, P., Douzery, E. J. P. (2018). A phylogenomic framework and timescale for comparative studies of tunicates. bioRxiv. doi: 10.1101/236448

Doran SA, Koss R, Tran CH, Christopher KJ, Gallin WJ, Goldberg JI (2004) Effect of serotonin on ciliary beating and intracellular calcium concentration in identified populations of embryonic ciliary cells. J Exp Biol 207:1415-1429. https://doi.org/10.1242/jeb.00924

Garstang W (1928) The morphology of the Tunicata, and its bearings on the phylogeny of the Chordata. Q J Microsc Sci 72:51-187

Georges D (1985) Presence of cells resembling serotonergic elements in four species of tunicates. Cell Tissue Res 242:341-348

Godeaux J (2003) History and revised classification of the order Cyclomyaria (Tunicata, Thaliacea, Doliolida). Bull Inst Roy Sci Nat Belgique Biol 73: 191-222

Godeaux JEA, Bone Q, Braconnot JC (1998) Anatomy of Thaliacea. In: Bone Q (ed) The biology of pelagic tunicates. OUP, Oxford

Govindarajan AF, Bucklin A, Madin LP (2011) A molecular phylogeny of the Thaliacea. J Plankton Res 33:843-853. https://doi.org/10.1093/plankt/fbq157

Harris-Warrick RM, Cohen AH (1985) Serotonin modulates the central pattern generator for locomotion in the isolated lamprey spinal cord. J Exp Biol 116:27-46

Holland ND, Holland LZ (1993) Serotonin-containing cells in the nervous system and other tissues during ontogeny of a lancelet, *Branchiostoma floridae*. Acta Zool 74:195-204. https://doi.org/10.1111/j.1463-6395.1993.tb01234.x

Huxley TH (1860) XVI. On the anatomy and development of Pyrosoma. Trans Linn Soc Lond 23:193-250. https://doi.org/10.1111/j.1096-3642.1860.tb00130.x

Ihle JEW (1956) Dritte und letzte Ordnung der Thaliacea: Desmomyaria. In: Krumbach T (ed) Handbuch der Zoologie. Fünfter Band. Zweite Hälfte. Walter de Gruyter, Berlin, pp 401-544

Karnovsky MJ (1965) A formaldehyde-glutaraldehyde fixative of high osmolality for use in electron microscopy. J Cell Biol 27:137A

Kocot KM, Tassia MG, Halanych KM, Swalla BJ (2018) Phylogenomics offers resolution of major tunicate relationships. Mol Phylogenet Evol 121:166-173. https://doi.org/10.1016/j.ympev.2018.01.005

Kott P (2005) Catalogue of tunicata in Australian waters. Australian Biological Resources Study, Canberra

Krohn A (1846) Observations sur la génération et le développement des Biphores (Salpa). – Annales des Sciences naturelles. Troisième série. Zoologie 6: 110-132

Lacalli TC (1999) Tunicate tails, stolons, and the origin of the vertebrate trunk. Biol Rev 74:177-198

Lacalli TC, Holland LZ (1998) The developing dorsal ganglion of the salp *Thalia democratica*, and the nature of the ancestral chordate brain. Philos Trans R Soc B 353:1943-1967. https://doi.org/10.1098/rstb.1998.0347

Lewis SL, Lyons DE, Meekins TL, Newcomb JM (2011) Serotonin influences locomotion in the nudibranch mollusc *Melibe leonina*. Biol Bull 220:155–160. https://doi.org/10.1086/BBLv220n3p155

Moret F, Guilland J-C, Coudouel S, Rochette L, Vernier P (2004) Distribution of tyrosine hydroxylase, dopamine, and serotonin in the central nervous system of amphioxus (*Branchiostoma lanceolatum*): implications for the evolution of catecholamine systems in vertebrates. J Comp Neurol 468:135-150. https://doi.org/10.1002/cne.10965

Nusbaum MP, Kristan WB (1986) Swim initiation in the leech by serotonin-containing interneurones, cells 21 and 61. J Exp Biol122:277–302

Pennati R, Dell´Anna A, Zega G, De Bernardi F (2012) Immunohistochemical study of the nervous system of the tunicate *Thalia democratica* (Forsskal, 1775). Eur J Histochem 56:e16. https://doi.org/10.4081/ejh.2012.16

Pennati R, Groppelli S, Sotgia C, Candiani S, Pestarino M, De Bernardi F (2001) Serotonin localization in *Phallusia mammillata* larvae and effects of 5-HT antagonists during larval development. Dev Growth Differ 43:647-656. https://doi.org/10.1046/j.1440-169X.2001.00608.x

Piette J, Lemaire P (2015) Thaliaceans, the neglected pelagic relatives of ascidians: a developmental and evolutionary enigma. Q Rev Biol 90:117-145. https://doi.org/10.1086/681440

Pogue MG, Mickevich MF (1990) Character definitions and character state delineation: the bete noir of phylogenetic inference. Cladistics 6:319-361. https://doi.org/10.1111/j.1096-0031.1990.tb00549.x

Richter S, Loesel R, Purschke G, Schmidt-Rhaesa A, Scholtz G, Stach T, Vogt L, Wanninger A, Brenneis G, Doring C, Faller S, Fritsch M, Grobe P, Heuer C, Kaul S, Moller O, Muller C, Rieger V, Rothe B, Stegner M, Harzsch S (2010) Invertebrate neurophylogeny: suggested terms and definitions for a neuroanatomical glossary. Front Zool 7:29. https://doi.org/10.1186/1742-9994-7-29

Schindelin J, Arganda-Carreras I, Frise E, Kaynig V, Longair M, Pietzsch T, Preibisch S, Rueden C, Saalfeld S, Schmid B, Tinevez J-Y, White DJ, Hartenstein V, Eliceiri K, Tomancak P, Cardona A (2012) Fiji: an open-source platform for biological-image analysis. Nat Meth 9:676-682. https://doi.org/10.1038/nmeth.2019

Schmidt-Rhaesa A, Harzsch S, Purschke G (2015) Structure and evolution of invertebrate nervous systems. OUP, Oxford

Stach T (2005) Comparison of the serotonergic nervous system among Tunicata: implications for its evolution within Chordata. Org Divers Evol 5:15-24. https://doi.org/10.1016/j.ode.2004.05.004

Stach T, Turbeville JM (2002) Phylogeny of Tunicata inferred from molecular and morphological characters. Mol Phylogenet Evol 25: 408-428. https://doi.org/10.1016/s1055-7903(02)00305-6

Stemme T, Stern M, Bicker G (2017) Serotonin-containing neurons in basal insects: In search of ground patterns among tetraconata. J Comp Neurol 525:79-115. https://doi.org/10.1002/cne.24043

Trandaburu T, Trandaburu I (2007) Serotonin (5-hydroxytryptamine, 5-HT) immunoreactive endocrine and neural elements in the chromaffin enteropancreatic system of amphibians and reptiles. Acta Histochemica 109:237-247. https://doi.org/10.1016/j.acthis.2006.10.005

Tsagkogeorga G, Turon X, Hopcroft RR, Tilak M-G, Feldstein T, Shenkar N, Loya Y, Huchon D, Douzery EJP, Delsuc F (2009) An updated 18S rRNA phylogeny of tunicates based on mixture and secondary structure models. BMC Evol Biol 9:187. https://doi.org/10.1186/1471-2148-9-187

Valero-Gracia A, Marino R, Crocetta F, Nittoli V, Tiozzo S, Sordino P (2016) Comparative localization of serotonin-like immunoreactive cells in Thaliacea informs tunicate phylogeny. Front Zool 13:45. https://doi.org/10.1186/s12983-016-0177-6

Wada Y, Mogami Y, Baba S (1997) Modification of ciliary beating in sea urchin larvae induced by neurotransmitters: beat-plane rotation and control of frequency fluctuation. J Exp Biol 200:9-18

5.2 Supplementary material

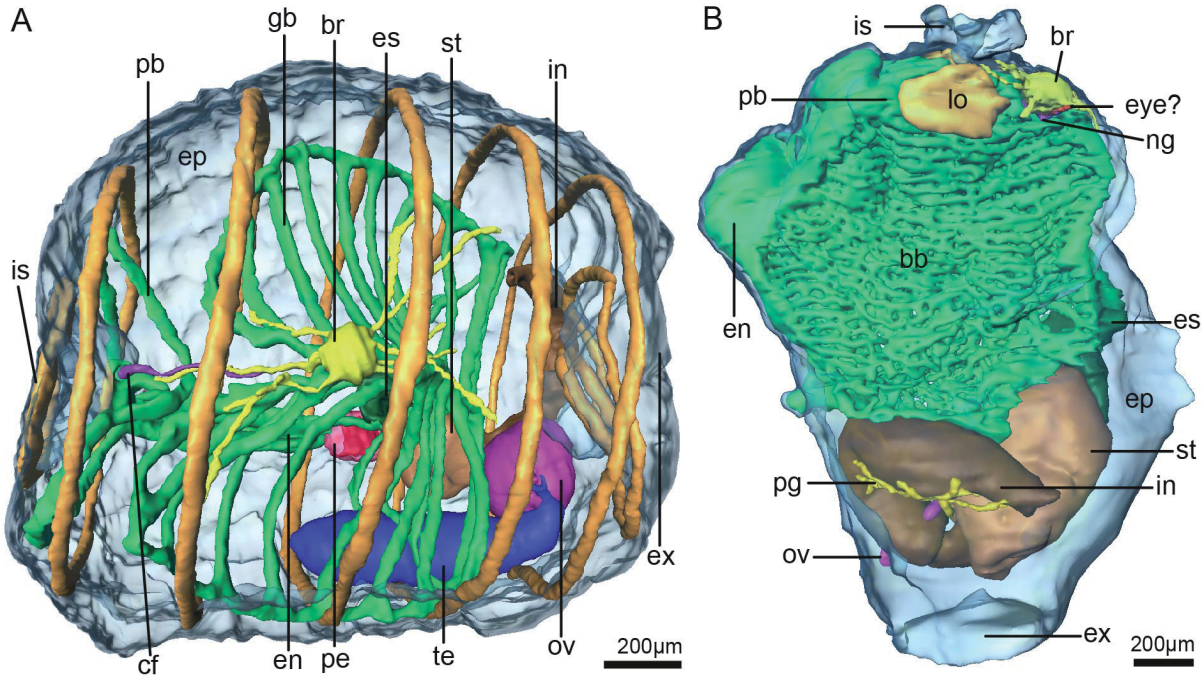

Supplementary Fig. 1: Interactive 3d model of the internal anatomy of the blastozooid stage of *D. nationalis* and of *P. atlanticum* based on serial sections for light microscopy. **A:** Anatomy of *D. nationalis*, dorsal view anterior to the top. The ciliated funnel (cf) opens into the branchial basket (bb – not completely shown in the 3d reconstruction) in close spatial relation to the dorsal spiral of the peripharyngeal band (pb). **B:** Internal anatomy of *P. atlanticum*, view from the left side, anterior to the top. The pyloric gland (pg) is dendritically shaped. Originating from the stomach (st), the pyloric gland forms several branches that connect with the posterior intestinal wall. br: brain, en: endostyle, ep: epidermis, es: esophagus, ex: excurrent siphon, in: intestine, is: incurrent siphon, lo: light organ, ng: neural gland, ov: ovary, pe: pericardium, te: testis.

6 Eye and brain of *Thalia democratica*

6.1 Publication

This is the peer reviewed version of the following article:

Braun, K., & Stach, T. (2017). Structure and ultrastructure of eyes and brains of *Thalia democratica* (Thaliacea, Tunicata, Chordata). *Journal of Morphology*, 278(10), 1421-1437,

which has been published in final form at:

https://doi.org/10.1002/jmor.20607 and https://doi.org/10.1002/jmor.20722.

Structure and ultrastructure of eyes and brains of *Thalia democratica* (Thaliacea, Tunicata, Chordata)

Katrin Braun

Humboldt-Universität zu Berlin, Institut für Biologie, Vergleichende Zoologie, Philippstrasse 13, Haus 2, 10115 Berlin, Germany

Thomas Stach

Humboldt-Universität zu Berlin, Institut für Biologie, Molekulare Parasitologie, Philippstrasse 13, Haus 14, 10115 Berlin, Germany, thomas.stach@hu-berlin.de, telephone: 0049-(0)30 2093 6590, fax: 0049-(0)30 2093 6002

Research highlights

In two salp stages, we report for the first time detailed 3D-structure and ultrastructure of drastically different cerebral eyes: three looking in different directions vs. a single unusual horseshoe-shaped eye. We discuss evolutionary implications.

Abstract

Salps are marine planktonic chordates that possess an obligatory alternation of reproductive modes in subsequent generations. Within tunicates, salps represent a derived life cycle and are of interest in considerations of the evolutionary origin of complex anatomical structures and life history strategies. In the present study the eyes and brains of both the sexual, aggregate blastozooid and the asexual, solitary oozooid stage of *Thalia democratica* (Forskål, 1775) were digitally reconstructed in detail based on serial sectioning for light and transmission electron microscopy. The blastozooid stage of *T. democratica* possesses three pigment cup eyes, situated in the anterior ventral part of the brain. The eyes are arranged in a way that the optical axes of each eye point towards different directions. Each eye is an inverse eye that consists of two different cell types: pigment cells (pigc) and rhabdomeric photoreceptor cells (prcs). The oozooid stage of *T. democratica* is equipped with a single horseshoe-shaped eye, positioned in the anterior dorsal part of the brain. The opening of the horseshoe-shaped eye points anteriorly. Similar to the eyes of the blastozooid, the eye of the oozooid consists of pigc and prcs. Prcs possess apical microvilli that form a densely packed presumably photosensitive receptor part adjacent to the concave side of the pigc. We suggest correspondences of the individual eyes in the blastozooid stage to respective parts of the single horseshoe-shaped eye in the oozooid stage and hypothesize that the differences in visual structures and brain anatomies evolved as a result of the aggregate life style of the blastozooid as opposed to the solitary life style of the oozooid.

Keywords

salp, urochordate, rhabdomeric, ciliary photoreceptor, central nervous system (cns)

Introduction

"To suppose that the eye… could have been formed by natural selection, seems, I freely confess, absurd in the highest possible degree" (Darwin 1859)
"… it is no wonder the eye has evolved at least 40 times independently around the animal kingdom" (Dawkins 1995).

In natural selection Darwin had convincingly suggested a plausible mechanism that could account for the hierarchy and diversity observed in nature. The evolution of eyes however had puzzled Darwin and he felt eye evolution difficult to reconcile with his theory (Darwin 1859). Almost 150 years of research after Darwin, eye evolution on the other hand seemed so easy that scientists saw no difficulties in eyes evolving numerous times independently (Nilsson and Pelger 1994, Dawkins 1995). Biologists' interest in eyes across the animal kingdom has never diminished, in fact this interest considerably increased with the discovery of *Pax6* as the "master control gene of the eye" (e.g. Gehring 1996) and the ensuing hypothesis that eyes evolved only once in the animal kingdom (Gehring 1996, Gehring and Ikeo 1999). While this discovery fostered molecular evo-devo research programs which continue to thrive and produce intriguing insights regarding the molecular level of eye evolution (Oakley and Speiser 2015, Ramirez et al. 2016), modern morphological investigations, that illuminate the phenotypic level of eye evolution beyond model species, have lagged behind. Comparative morphological investigations, however, are necessary to assess the evolutionary anatomical disparity, to formulate homology hypotheses on this organismal level, and to understand the functional adaptations of this sensory organ. Salps belong to tunicates, a group of marine animals, that according to recent molecular phylogenetic studies, are considered to be the sister group of vertebrates (Delsuc et al. 2006, 2008, Lowe et al. 2015; but see Stach 2014). While ascidians, with a tadpole-like larva and a sessile adult, have been in the focus of evo-devo studies during the past decades other groups of tunicates have attracted less interest (e.g. Lemaire 2011). Salps are peculiar tunicates in the plankton of tropical and temperate oceans world-wide (Van Soest 1998). They are almost completely transparent, with the visceral nucleus, the muscle bands, and pigments of their eyes often being the only visible feature. Salps are characterized by their metagenetic life-cycles, meaning subsequent generations alternate between modes of reproduction: while one generation reproduces sexually, the other reproduces asexually. Moreover, the two generations differ in appearance and anatomy (Chamisso 1819, Glaubrecht and Dohle 2012, Piette and Lemaire 2015). Most studies on the anatomy of salp eyes and brains are more than 100 years old (e.g., Ussow 1876, Brooks 1893, Göppert 1893, Metcalf 1898, Redikorzew 1905), with the notable exception of Lacalli and Holland (1998) who investigated the development of the brain in the oozooid stage of *Thalia democratica* (Forskål, 1775). Similar to the brains of adult ascidians, the brains of salps are constituted of a central neuropil and a surrounding cortex of neuronal cell somata (reviewed in Bone 1998). Based on electron microscopic investigations, Lacalli and Holland (1998) showed that a neural gland, that in ascidians is associated with the brain, and a hypophysial duct are missing in the oozooid stage. These authors also showed that the brain of oozooid stages is symmetrical with three clusters of motoneurons being the most conspicuous feature in the brain. Electron microscopic investigations into the anatomy of the brain of blastozooid stages are nearly entirely lacking, except for

Gorman et al. (1971) who showed a single TEM image of a photoreceptor cell.

Regarding eye anatomy in salps, it had soon been established that the asexual oozooids in various salp species possess a single horseshoe-shaped eye that appears uniform across species in light microscopic aspects, whereas the hermaphroditic blastozooids feature several pigment cup eyes that show more variability across species (e.g., Ussow 1876, Brooks 1893, Göppert 1893, Metcalf 1898, Redikorzew 1905). While these pioneering studies were meticulous in demonstrating the organization of eyes in salps, questions remained due to technical limitations as well as to conceptual problems not clarified at the time. Based on light microscopic investigations, the eyes of salps had been described as rhabdomeric and to be an integral part of the brain. Indeed the electron microscopic investigation of Gorman et al. (1971) showed that the photoreceptor cells (prcs) of *T. democratica* (refered to as *Salpa democratica*) bear microvilli, but the authors did not describe neurites in the prcs nor did they elaborate on the ultrastructure of the pigment cells. Moreover, it remained unclear whether the specimens being investigated were in blastozooid or oozooid stage. From an evolutionary perspective, descriptions of the salps' prcs as rhabdomeric are incongruous to the ciliary nature of prcs in ascidians (Eakin and Kuda 1970), vertebrates (Cohen 1963, Lamb 2013), and the anterior larval eye of cephalochordates (Lacalli et al. 1994). Nevertheless, a direct evolutionary link had also been suggested for the light sensitive cells with cephalochordates as primitive, tunicates intermediary, and vertebrates as advanced (Brooks 1893), but other authors suggested that salp eyes as outgrowths of the central nervous systems were homologous to vertebrate lateral eyes (Todaro 1893). Still others rejected this hypothesis of homology while simultaneously claiming that the eyes of salps were intermediate between larval ascidian eyes and the pineal eyes of vertebrates (Redikorzew 1905). However, because the eyes of the two life history stages are so dramatically different, the question whether corresponding structures of the eyes can be identified between the stages arises. This in effect, is addressing the problem of "ontogenetic homology" (sensu Haszprunar 1992). Another open question concerns the cellular composition of the eyes in salps. Whereas most authors found a single type of photoreceptor cells (e.g., Brooks 1893, Göppert 1893, Metcalf 1898), Redikorzew described two distinct types of photoreceptor cells and in addition asserted that a third type of cells, supportive cells, were present in the retina of salps (Redikorzew 1905).

Despite the phylogenetic importance of tunicates in general and the fascinating life history traits of salps in particular, more recent investigations than the one from Gorman and co-authors (1971) into the anatomy of eyes in salps are missing (see also reviews by Madin 1995, Bone 1998, and Mackie and Burighel 2005). Because the higher resolution of confocal laser scanning microscopy and electron microscopy and because electron microscopy of serial sections are necessary in order to ascertain the microvillar nature of apical cell extensions in prcs and to rule out vestigial cilia, we investigated the eyes and brains of blastozooid and oozooid stages using digital 3D-reconstructions based on complete series of semithin sections in combination with preparations for transmission electron microscopy with the aim to resolve the discrepancies discussed above. Moreover, since the diversity of structures observed in animal eyes has proved to be closely linked to the functional needs of their bearers (e.g., Nilsson 2009, Banks et al. 2015, Fergus et al. 2015, Glaeser and Paulus 2015), we decided to focus

specifically on the morphological level which not only enables us to suggest homology hypotheses but also to draw functional inferences.

Materials and methods

Blastozooid (aggregate stage) specimens of *Thalia democratica* (Forskål, 1775) were obtained from the coastal waters around the Mediterranean island Ibiza (Spain) in March 2014. A plankton net was towed across the surface waters of the Cala Llenya, Cala Vadella, Penyal de s'Aguila, and the Punta Grassio. Oozooid stages were collected off West Palm Beach in the Gulf Stream employing a plankton net during a 15 minutes drift tow at 10m depth in May 2016.

Specimens were fixed for ca. 12h (blastozooid stages) or 2h (oozooid stages) in a cold solution of Karnovsky's primary fixative (Karnovsky 1965), consisting of 2% glutaraldehyde, 2% paraformaldehyde, 1.52% NaOH and 1.2g d-glucose, dissolved in 2.25% sodium hydrogen phosphate buffer (pH 7.4). Specimens were subsequently rinsed in three changes of buffer and stored in buffer solution for two weeks (blastozooid stages) or processed further immediately. Following primary fixation in Karnovsky's fixative specimens were post-fixed for 2h in 1% OsO_4 solution at room temperature and, following dehydration in a graded series of ethanol, embedded in epoxy resin (Araldite; Fluka). One specimen (blastozooid stage) was serially sectioned for light microscopy (0.7µm), another specimen (blastozooid) was serially sectioned for transmission electron microscopy (60nm). An additional specimen of both stages was serially sectioned alternating between semithin sections (0.5µm) and ultrathin sections (60nm). Sectioning was performed on a Leica Ultracut S. Semithin sections were stained using 1% toluidine blue in a solution of 1% sodium tetraborate (borax). Ultrathin sections were stained with 2% uranylacetate and 2.5% lead citrate in an automatic stainer (courtesy of Dr. Björn Quast, Universität Bonn and Dr. Alexander Gruhl, MPI Bremen).

For immunohistochemical visualization of the nervous system, specimens were fixed in 4% paraformaldehyde in phosphate-buffered saline (PBS: 0.01M, pH 7.4) for 40min at room temperature. Samples were rinsed in PBS and stored in PBS containing 0.05% NaN_3 at 4°C for no longer than 6 months after fixation. Specimens were incubated in primary antibodies against tyrosinated α-tubulin (Anti-Tubulin, Tyrosine antibody produced in mouse; Sigma, St. Louis, Missouri, USA) and secondary antibodies Cy™3 AffiniPure goat anti-mouse IgG (Jackson ImmunoResearch Laboratories, Inc., Philadelphia, Pennsylvania, USA); nuclei were labeled using 4'6-Diamidino-2-Phenylindole, Dihydrochloride (DAPI dihydrochloride, Thermo Fisher Scientific Inc., Waltham, Massachusetts, USA). Details can be found in Braun and Stach (2016). Every staining experiment was performed together with two different controls: one with primary antibodies omitted and the second with secondary antibodies omitted.

Light microscopy

Semithin sections stained with toluidine blue were digitally recorded (distance 2-2.1µm) using a Zeiss AxioCam HRc camera mounted on a Zeiss Axioskop 2 plus microscope. Images were processed using

Adobe Photoshop CS5 Software and were used for 3D-reconstructions.

Transmission electron microscopy

Stained ultrathin sections were examined under a Zeiss EM9 transmission electron microscope, operated at 80kV.

Confocal Laser Scanning Microscopy

Specimens treated with antibodies against tyrosinated α-tubulin and DAPI were examined using a Leica TCS SPE confocal laser scanning microscope (Leica Microsystems,Heidelberg, Germany). Appropriate filter settings were applied to record stacks of confocal optical sections. Stacks of confocal images of the brains of both life cycle stages were processed with Amira 5.4.3 software (FEI Visualization Sciences Group, Berlin, Germany) to create a three-dimensional (3D) model of the nervous system. Based on the tyrosinated-α-tubulin and DAPI channel output of the confocal microscope the surfaces were generated using the "Volren" command.

The output of the DAPI channel of the brains of both stages was additionally used to count the approximate numbers of the respective cells. For that purpose these data were processed in Imaris 8.3.1 (Bitplane AG, Zurich, Switzerland) using the "Add new Spots" command.

Digital 3D-reconstruction

The 3D-models of the brains of the blastozooid and oozooid stages of *T. democratica* were created in Amira 5.4.3 (FEI Visualization Sciences Group, Berlin, Germany) based on the images of the serial semithin sections. Images were aligned in Amira. The resulting stack of images was used for the reconstruction of the brains with associated nerves, motoneurons, microvilli, photoreceptor cells (prc), and pigment cells (pigc). The numbers of pigc and prc were counted using the profiles of the respective nuclei while going through the aligned stack of images in Amira.

Results

Salps are characterized by a metagenetic life cycle with two distinctly dimorphic stages, the sexually reproducing aggregate form or blastozooid (Figs. 1A, C) and the asexually reproducing solitary form or oozooid (Figs. 1B, D). In both stages the brain is situated in the dorsal midline anteriorly to the main body muscles. The brains and associated eyes are easily visible even without magnifying optics due to the opaque whitish appearance of the brain and the presence of often red, sometimes brown or black pigments in the eyes (Figs. 1E, F). With the aid of a dissecting microscope nerve fibers can be seen radiating from the brain.

Anatomy of the blastozooid brain

In the blastozooid the brain is ovoid to pear-shaped with the slightly narrower portion pointing anteriorly and a pair of bilaterally symmetrical ventrolateral brain appendages. The brain in the blastozooid measures approximately 90µm in length and up to 60µm in diameter (Figs. 1E, G, 2A, B). Automatic

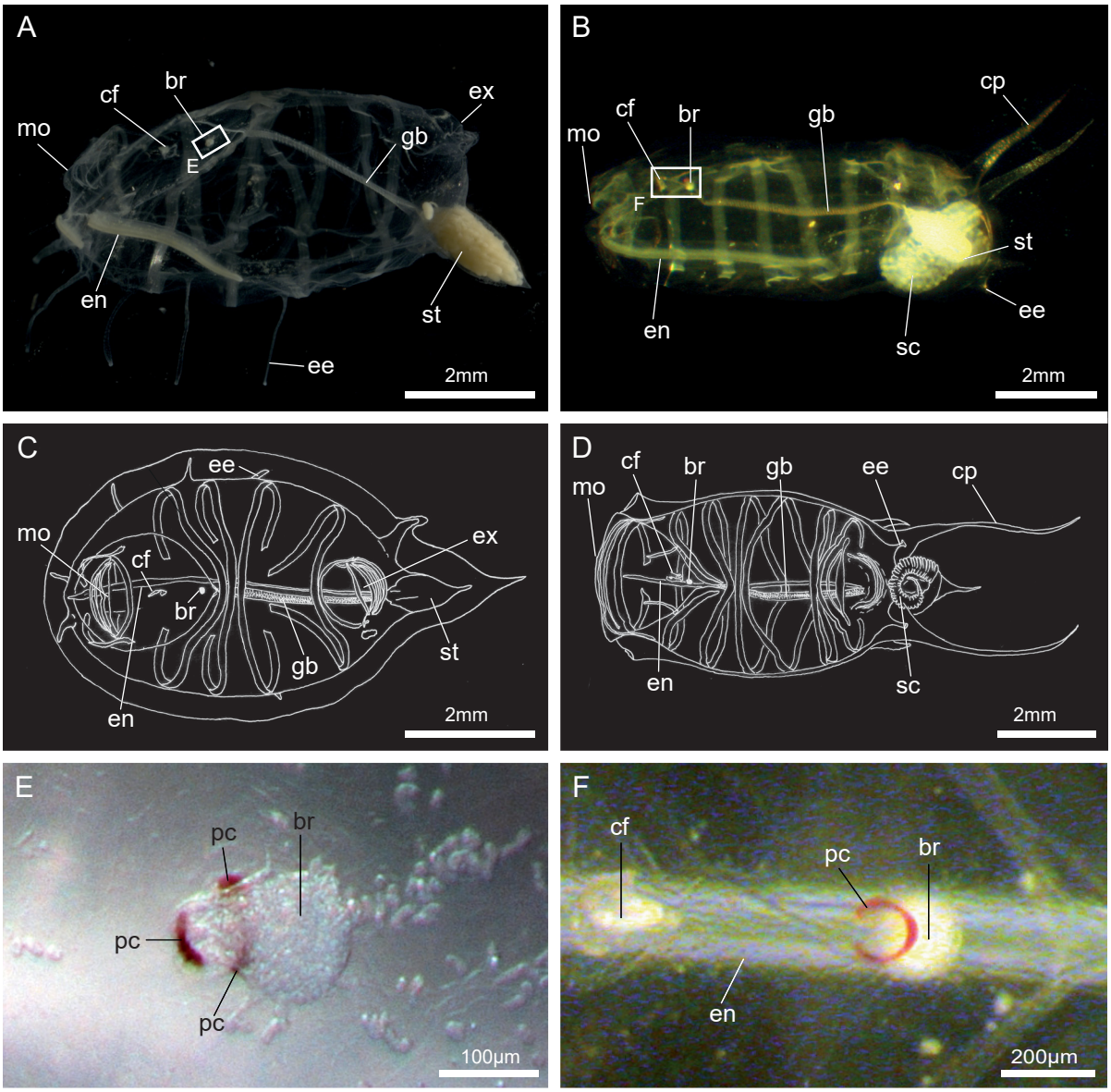

Fig. 1: *Thalia democratica*, comparison of the anatomy of the sexual aggregate blastozooid (left side) and the asexual solitary oozooid (right side) stage. **A:** Stereomicroscopical picture of a whole blastozooid, about 6mm in length. View from left side, anterior is to the left, ventral is at the bottom. **B:** Stereomicroscopical picture of a whole oozooid, about 7mm in length. View from left side, anterior is to the left, ventral is at the bottom. **C, D:** Schematic drawings of the anatomy of blastozooid (**C**) and oozooid (**D**) stages. Dorsal view, anterior is to the left. **E, F**: Higher magnification of areas marked in **A** and **B**. Detail of the brain (br) and red pigment cells (pc) of the eyes of blastozooid (E) and oozooid (F) stage. cf: ciliated funnel, cp: caudal peduncle, ee: extension of epithelium, en: endostyle, ex: excurrent siphon, gb: gill bar, mo: mouth, sc: stolonic chain of blastozooids, st: stomach

counts of the nuclei showed that the brain consists of no more than 1500 cells. In two specimens eight distinct nerves emanate bilaterally symmetrical from each side of the posterior part of the brain. Most of these fibers project towards the muscle bands. A conspicuous pair of nerves originates from the ventral side of the main posterior portion of the brain, arches anteriorly and projects parallel anteriorly to innervate the lip region around the mouth opening. These nerves are called right respectively left ventral anterior nerve. Confocal laser scanning microscopical localization of nuclei utilizing DAPI

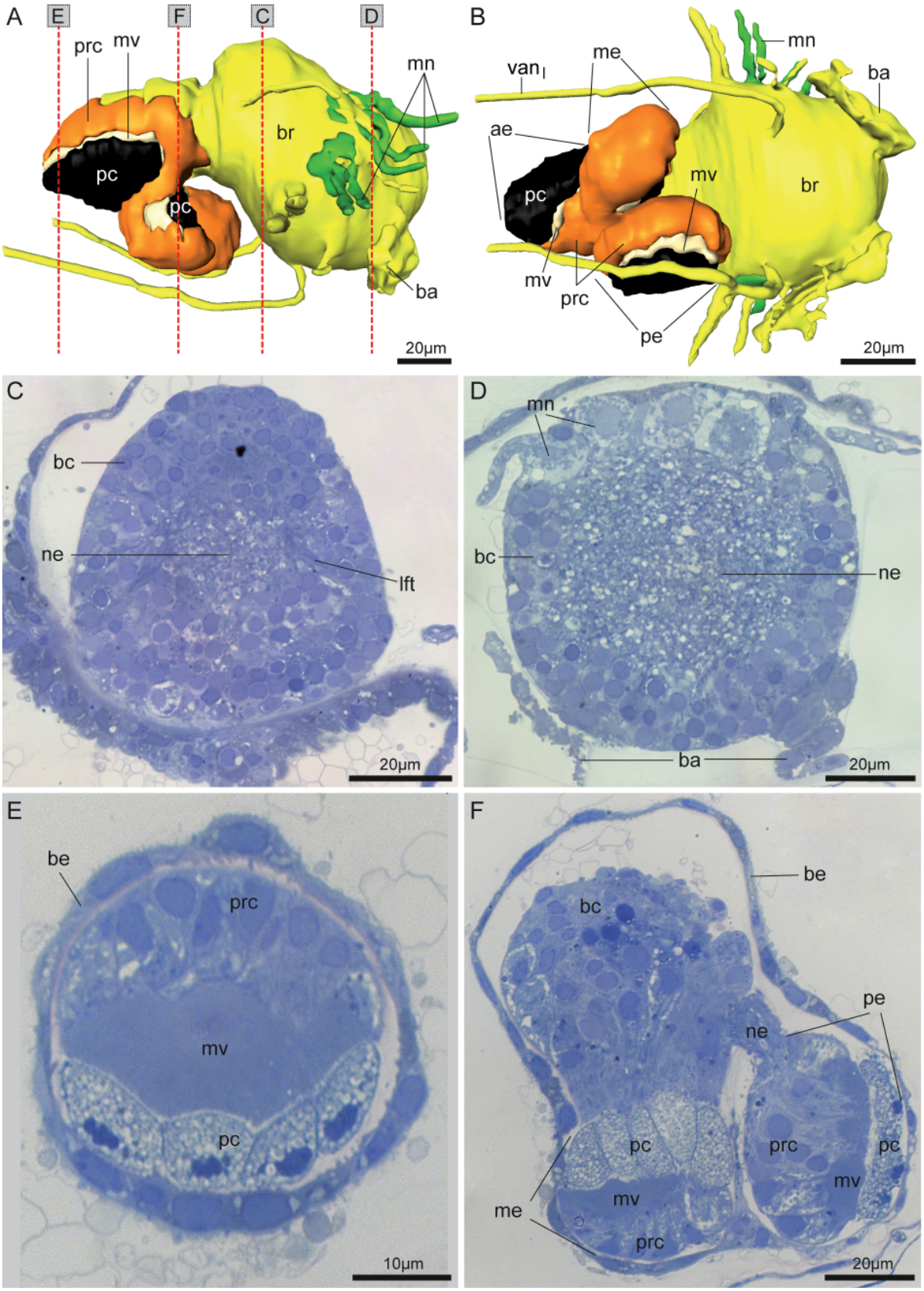

Fig. 2: *Thalia democratica*, brain anatomy of the blastozooid based on light microscopy. **A, B**: 3D-reconstructions of the brain (br) and adjacent nerves (yellow) based on serial semithin sections. Pigment cells (pc, black) form eyecups, microvilli (mv, cream-colored) of the photoreceptor cells (prc, orange) project into the concave side of the pigment cells. Motoneurons (mn, green) leave the brain on the dorsal side. **A**: Left view on the brain, anterior is to the left. Section planes of **C-F** are indicated

by dashed red lines. **B**: Ventral view on the brain, anterior is to the left. Interactive 3D-reconstruction is available in the online version. **C-F**: Light micrographs of cross sections through the brain. Dorsal is at the top, right is to the right. **C**: Somata of the nerve cells are arranged peripherally in a brain cortex (bc) surrounding the central neuropil that is formed by numerous neurites (ne). Some nerve tracts can be observed (e.g. lateral fiber tract (lft)). **D**: In the brain cortex on the dorsal side of the brain conspicuously large nerve somata are located, the motoneurons (mn). **E**: The anterior eye (ae) is constituted of pigment cells (pc) that possess numerous translucent vesicles and photoreceptor cells (prc) that bear microvilli (mv) at their apical side. **F**: The median eye (me) and the posterior eye (pe) are of the same composition as the anterior eye. Nerve fibers connect the photoreceptor cells with the brain. The eyes and the brain are surrounded by a brain epithelium (be). ba: brain appendages, vanl: left ventral anterior nerve

and neurites utilizing antibodies against tyrosinated α-tubulin indicate that the perinuclear somata comprise a superficial cortex in the brain (Fig. 6A). This general histological arrangement is verified in histological sections of the brain stained with toluidine blue (Figs. 2C, D). These serial sections reveal the central neuropil and peripheral arrangement of nuclei in the cortex. Symmetrical fiber tracts can be seen in cross sections just posterior to the first lateral nerves (Figs. 2C, 6B) running from the center to the ventral periphery, but no more structural differentiation is discernible in the central neuropil. Further the light microscopic analysis reveals the distinctly larger somata of the motoneurons which are also distinguished by the lighter appearance of their cytoplasm (Fig. 2D). Three pigmented eyes are located in the anterior ventral part of the brain of the blastozooid (Figs. 2A, B see also 3D-pdf in online version); however this is not clearly visible in the confocal laser scanning micrograph (Fig. 6A).

Anatomy of the eyes of the blastozooid stage

The blastozooid stage possesses three pigment-cup eyes situated in the anterior ventral part of the brain (Fig. 2; see also 3D-pdf in digital version of Fig. 2B). From anterior to posterior the three eyes are the anterior eye, the median eye, and the posterior eye. The anterior eye is ovoid, whereas the median and the posterior eyes are spherical but somewhat flattened. The eyes are connected to the main posterior part of the brain via a narrower neck-like region (Fig. 2F). The eyes are an integral part of the brain and the entire structure – brain and eyes – is surrounded by the epithelium of the epidermis (Figs. 2C-F, 3A, C). The digital 3D-reconstructions, based on complete serial sections of the brain and eyes, show the detailed arrangement of the eyes (Figs. 2A, B) and demonstrate that the optical axis of each eye points towards a different direction. The optical axis of the anterior eye is oriented obliquely towards the dorsal right side, slightly posteriorly; the optical axis of the median eye points anteriorly and slightly to the left side; and the optical axis of the posterior eye aims almost directly towards the left side, slightly to the posterior of the animal (see also Fig. 7). Light micrographs of toluidine blue stained semithin sections show that the three eyes consist of two different cell types: Pigment cells (pigc) and photoreceptor cells (prc). In addition, the eyes are connected to the posterior part of the brain via neurite bundles. The neurites enter the eye through the neck-like region and contact the eyes via their respective concave side, thus each eye is an inverse eye. While there are differences in size and cell number in each eye, the general arrangement of pigc and prc is the same. The anterior eye is the largest,

measuring about 45µm in length and approximately 20µm in diameter. The median and the posterior eye are considerably smaller. The median eye measures approximately 20µm in all dimensions, but the layer of pigc is ovoid with the longer axis measuring about 20µm and 10µm in height. In the posterior eye the layer of pigc comprises almost a circle with a diameter of 20µm, whereas the entire posterior eye is about 30µm in diameter yet somewhat flattened. While the shape of these structures can be seen in the depictions of the digital 3D-reconstructions from various angles in Figures 2A and B, they can be better appreciated in the 3D-pdf (Fig. 2B) in the online version. Histologically, the pigc are cuboidal with a prominent nucleus at their basal sides. The cytoplasm is relatively electron dense and filled with numerous pigment vesicles which in toluidine-stained preparations appear very lightly stained and electron lucent in TEM preparations. The vesicles range from 0.2µm in diameter to 0.8µm and contain a floccular precipitation (Fig. 3C). Moreover, pigc feature thin, thread-like cellular processes that sheath the prc of the respective eye and interdigitate between stacks of the microvilli (see arrowheads in Figs. 3A, C). Immediately adjacent to the pigc on their apical sides, i.e., on the concave side of the cup-shaped layer formed by the pigc, is a layer of almost homogenous appearance (Figs. 2E, F). These are the stacks of photoreceptive microvilli of the prc. The microvilli originate from the apical cell membrane (Fig. 3A, B, B', D, see also Supplementary Figure A, B). In the serial sections of three different individuals in blastozooid stage no ciliary structures were present. The prc are columnar cells, the tallest being situated in the centers of the eyes, the shorter ones more to the periphery of the eyes. Prc are equipped with a prominent nucleus, situated centrally or basally in the cells (Figs. 3B, B'), numerous mitochondria (Figs. 3A, B, D), extensive arrays of endoplasmic reticulum (Fig. 3A), and occasionally vesicles that stain lightly in toluidine-stained histological sections (Fig. 2F). At the basal side of the prc the cells taper, thereby probably forming a short neurite (Figs. 3B, B'; Supplementary Figure C). At this position numerous profiles through neurites are found (Figs. 3A, B; Supplementary Figure C). The number of pigc in two specimens in the anterior eye was 13, in the median eye 5, and in the posterior eye 16. The number of prc is more difficult to ascertain unambiguously, but in the anterior eye we counted 52 and 85 in the two specimens respectively, in the median eye 14 and 18, and in the posterior eye 53 and 49 prc.

Anatomy of the connection between eyes and central neuropil in the blastozooid stage

The internal architecture of the brain of the blastozooid reflects the central role of the optical system. Confocal laser scanning micrographs of anti-tyrosinated-tubulin stained specimens reveal an anterior neuropil situated immediately posterior and slightly dorsal to the anterior eye. This anterior optical neuropil (aon; Fig. 6B) is connected to all three eyes. Its major input is from the anterior eye, but connections to the median eye on the left side and to the posterior eye on the right side exist (Fig. 6B; see also supplemental stack of clsm-micrographs). A pair of conspicuous neurite bundles projects to a second neuropil that is situated posterior to the aon. From this posterior optical neuropil a pair of neurite bundles connects laterally on both sides to the anterior cluster of giant motoneurons (Figure 6B). Medially, a pair of lateral fiber tracts projects to the central neuropil of the brain (Fig. 2C, 6B).

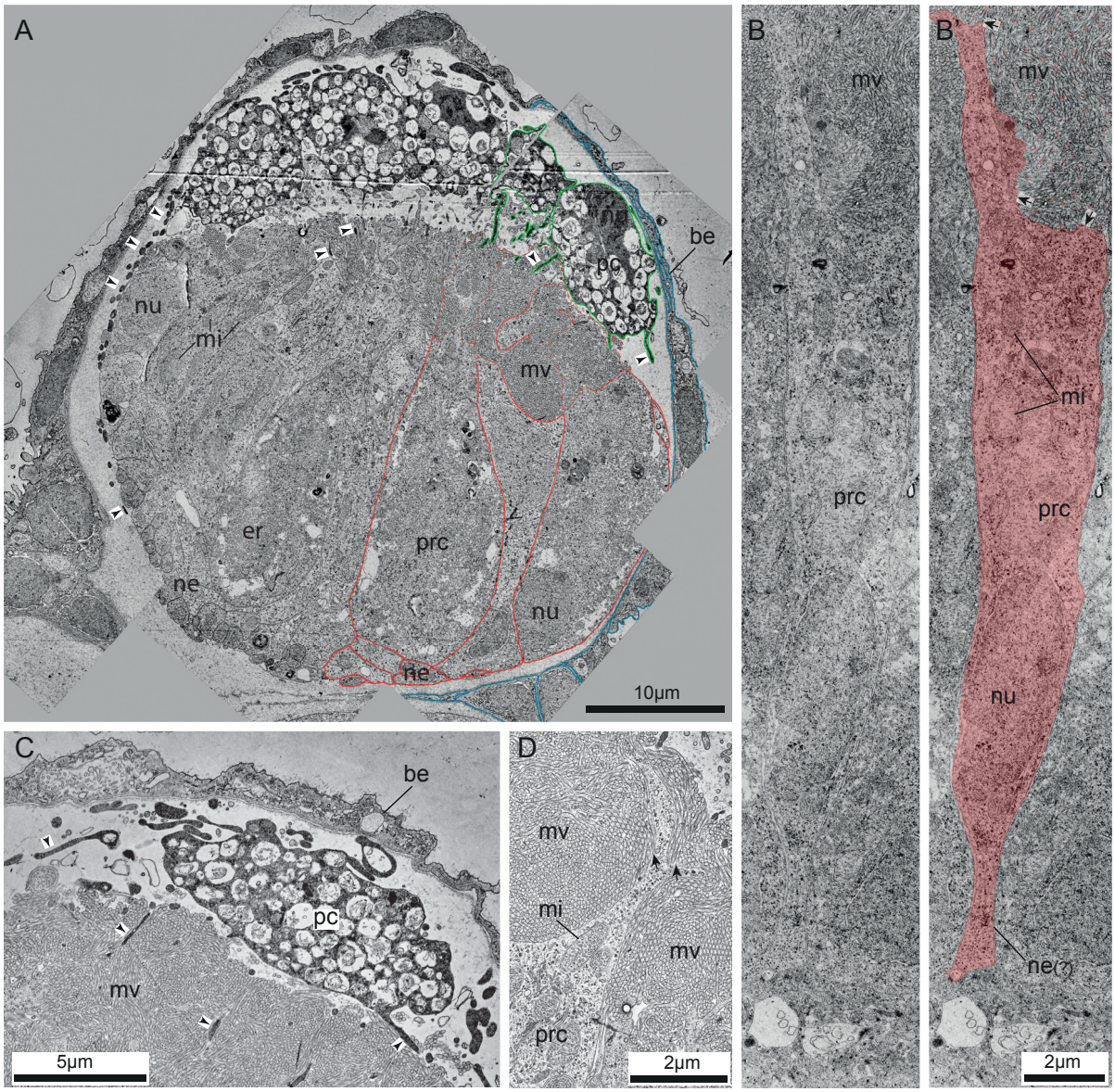

Fig. 3: *Thalia democratica*, transmission electron micrographs of the eyes of the blastozooid. **A**: Ultrastructure of the anterior eye. Two pigment cells (pc) are edged with green, three photoreceptor cells (prc) are edged with red and the brain epithelium (be) is partly edged with blue. From the pigment cells processes project through the stacks of microvilli (see arrowheads). **B, B'**: One photoreceptor cell is shown in detail. The nucleus (nu) is located at the basal side. The cell is equipped with many mitochondria (mi), apical microvilli (mv) and a short neurite (ne). Arrows show connections of microvilli with the cytoplasm on the apical side of the photoreceptor cell. **C**: Ultrastructure of a pigment cell. The cytoplasm of the cell appears electron dense while the pigment vesicles are mostly electron light. Numerous processes pass through the microvilli of the photoreceptor cells (arrowheads). **D**: Higher magnification of the apical region of a photoreceptor cell. Numerous densely packed microvilli originate from the apical side of the cell (see arrows). The same cell is shown in even higher magnification in the Supplementary Figure B. er: endoplasmatic reticulum

limbs of the horseshoe-shaped layer formed by the pigc, are two separate layers of almost homogenous appearance (Fig. 4C). At the posterior end at the connection of the two horseshoe limbs the layer of pigc is shallowly M-shaped in cross sectional aspect (Fig. 4D). While prc are seen dorsal and ventral

Anatomy of the oozooid brain

The brain of the oozooid stage in *Thalia democratica* is divided into an almost completely spherical ventral part that possesses a pair of bilaterally symmetrical ventrolateral brain appendages and a comparatively large dorsal outgrowth that contains the conspicuous u-shaped eye (Figs. 1F, 4A, B). The ventral part has a diameter of 120µm. The whole brain consists of no more than 4500 cells. Ten nerves radiate from it on both sides, bilaterally symmetrically arranged, in a plane that is tilted at an angle of approximately 30° compared to the horizontal plane of the animal (Figs. 4A, B see also 3D-pdf in online version). These nerves project towards the body muscles, the sphincters around the incurrent and excurrent openings, and the sensory cells in the epithelium. Comparable to the brain of the blastozooid, confocal laser scanning microscopical localization of nuclei utilizing DAPI and neurites utilizing antibodies against tyrosinated α-tubulin show that the perinuclear somata form a superficial cortex in the brain (Fig. 6C). Again, this general histological arrangement is verified in histological sections of the brain stained with toluidine blue (Figs. 4C, D). Thus, these sections reveal the central neuropil and peripheral arrangement of nuclei in the cortex. The single horseshoe-shaped, pigmented eye, with the opening of the horseshoe pointing anteriorly, occupies the dorsal part of the brain of the oozooid (Figs. 4A, B), but this is not clearly visible in the confocal laser scanning micrograph (Fig. 6C).

Anatomy of the eyes of the oozooid stage

The eye in the oozooid stage is a large horseshoe-shaped structure constituting the dorsal part of the brain. The length of the eye measures about 130µm and its breadth about 100µm. Like the eyes in the blastozooid stage, the horseshoe-shaped eye of the oozooid is an integral part of the brain. Together with the ventral part of the brain the eye is surrounded by the epithelium of the epidermis (Figs. 4C, D). The digital 3D-reconstruction, based on a complete series of alternating semithin (0.5µm) and ultrathin (60nm) sections of the brain and eye, shows the detailed arrangement of the eye (Figs. 4A, B) and demonstrates that the opening of the horseshoe points anteriorly. The layer formed by the pigment cells (pigc) delimits the horseshoe-shaped eye laterally on both sides with the masses of microvilli in the center of the two limbs of the horseshoe. Posteriorly where the two limbs are connected medially, the layer of pigc becomes horizontal with the presumably photosensitive microvilli ventral to it (Figs. 4A, B see also 3D-pdf in online version). Thus, at the anterior part of the horseshoe the light preferentially enters the eye anteriorly and dorsally, whereas the posterior part detects light from the ventral side of the animal (Fig. 7). As in the eyes of the blastozooid, the horseshoe-shaped eye of the oozooid is inverse. Identical to the three eyes of the blastozooid stage the horseshoe-shaped eye of the oozooid consists of two different cell types: Pigment cells (pigc) and photoreceptor cells (prc) (Figs. 4C, D, 5). The pigc are cuboidal cells with a prominent nucleus at their basal sides. The cytoplasm appears relatively electron dense and is filled with numerous pigment vesicles, which in toluidine-stained preparations appear black and in TEM preparations appear electron dense with a smooth content that occasionally is almost black towards one side of the vesicles (Figs. 5A, B). The vesicles range from 0.2µm in diameter to 0.8µm. Most vesicles are spherical, but rare pear-shaped profiles also occur. Immediately adjacent to the pigment cells on their apical sides, i.e., on the central side of the two

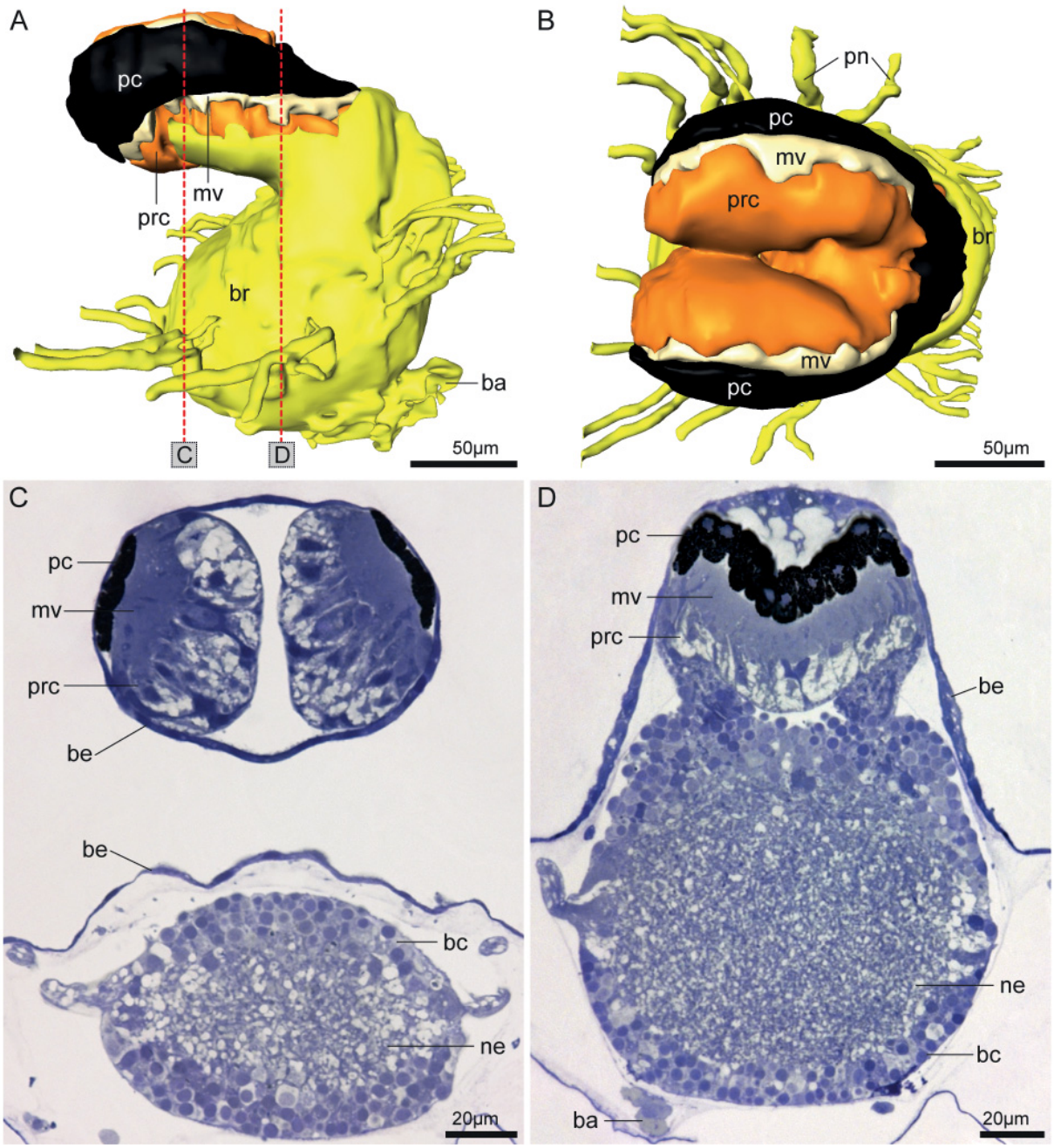

Fig. 4: *Thalia democratica*, brain anatomy of the oozooid based on light microscopy. **A, B**: 3D-reconstructions of the brain (br) and brain nerves (yellow) based on serial semithin sections. Pigment cells (pc, black) form one horseshoe-shaped eyecup, microvilli (mv, cream-colored) of the photoreceptor cells (prc, orange) reach into the concave side of the pigment cup. **A**: Left view on the brain, anterior is to the left. Section planes of **C** and **D** are represented by dashed red lines. **B**: Dorsal view on the brain, anterior is to the left. The opening of the horseshoe points anteriorly. Interactive 3D-reconstruction is available in the online version. **C, D**: Light micrographs of cross sections through the brain. Dorsal is at the top, right is to the left. The eye consists of pigment cells and photoreceptor cells with numerous microvilli. Both, brain and eye are enclosed in a brain epithelium (be). **C**: A superficial layer of nerve cell somata, the brain cortex (bc), surrounds the neurites (ne) that form the central neuropil. At the anterior limbs of the horseshoe the photoreceptor cells of the two limbs are not connected. **D**: At the connection of both horseshoe limbs the pigment cells are M-shaped. Pigment vesicles appear dark black. Photoreceptor cells are positioned ventrally and dorsally from the "M". Neurite bundles that connect the photoreceptor cells with the brain are clearly visible. ba: brain appendages, pn: peripheral nerves

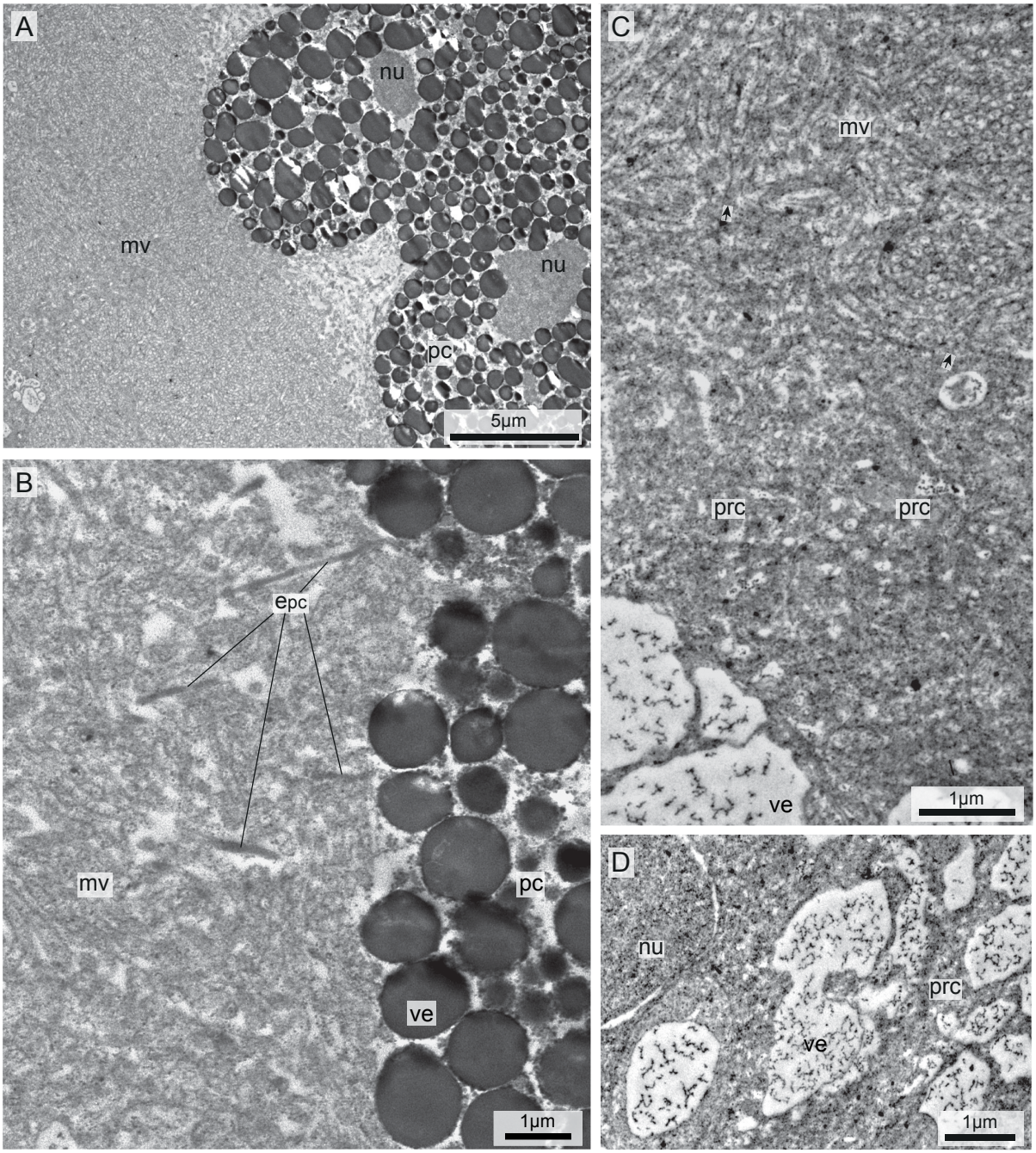

Fig. 5: *Thalia democratica*, ultrastructure of the horseshoe-shaped eye of the oozoid. **A**: Detail of microvilli (mv) and pigment cells (pc). Microvilli are densely packed. Nuclei (nu) of the pigment cells are located basally, pigment vesicles (ve) are electron dense. **B**: Higher magnification of apical side of one pigment cell and adjacent microvilli. Pigment vesicles appear electron dense with almost black content to one side of the cell. Thin extension of (probably) the pigment cells (epc) run through the stacks of microvilli. **C**: Detail of two photoreceptor cells (prc). Numerous densely packed microvilli project from the apical side of the photoreceptor cells (see arrows). **D**: Higher magnification of a photoreceptor cell. Various vesicles are situated on the basal side of the cell. Vesicles are electron light and contain floccular precipitation.

of the shallow M formed by the pigc, the layer of homogenous appearance is located only ventral to it. The prc are columnar cells, the shorter ones more to the dorsal and ventral side of the horseshoe limbs

(Fig. 4C) or laterally at the posterior end of the horseshoe (Fig. 4D). The prc possess apical microvilli without detectable ciliary structures throughout the whole series of sections (Fig. 5C). Rarely thin, thread-like fibers between stacks of the microvilli are probably extensions of pigc (Fig. 5B). The prc are equipped with prominent nuclei, situated centrally in the cells, and numerous basal vesicles that stain lightly in toluidine-stained histological sections and electron light in ultrathin sections with a small amount of floccular precipitations (Figs. 4C, D, 5D). The number of pigc in the horseshoe-shaped eye was at least 63, the number of prc at least 160. Technical limitations impede description of further ultrastructural details.

Anatomy of the connection between eyes and central neuropil in the oozooid stage

In the oozooid a pair of fan-shaped neurite bundles from the two limbs of the horseshoe-shaped eye converge and project into anteriorly and ventrally directed neurite bundles that bend backwards and "disperse" into the paraxial neuropils (Figure 6D, see also supplemental stack of clsm-micrographs). Dorsal in the brain, yet immediately ventral to the horseshoe-shaped eye, the two paraxial neuropils (Lacalli and Holland 1998) are visible (Fig. 6E). A pair of lateral fiber tracts (Figure 6E) in the central neuropil projects from the dorsal posterior medial brain towards the anterior pair of clusters of motoneurons (c3 of Lacalli and Holland 1998).

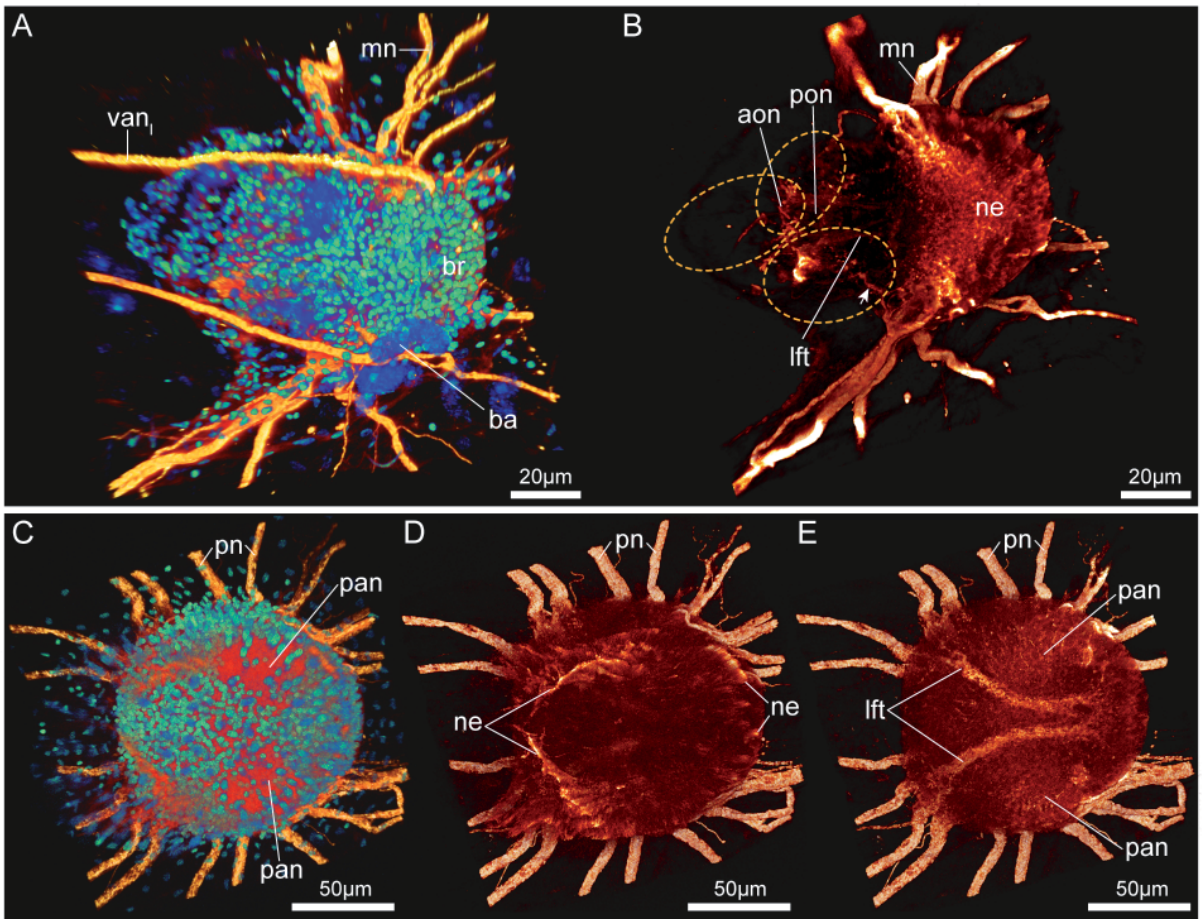

Fig. 6: *Thalia democratica*, 3D-rendered signal of confocal laser scanning micrographs of the brain (br). Immunostaining against tyrosinated a-tubulin (orange/red) and nuclear staining utilizing DAPI (blue/green). **A, B**: 3D-rendering of the brain in the blastozooid stage. Ventral view, anterior is to the left. **A**: Nuclei are arranged in an outer brain cortex. **B**: Dorsal half of 3D-rendered tyrosinated- α-Tubulin

channel shown. The eyes (position indicated by grey dotted ellipses) are connected to an anterior optical neuropil (aon). Neurite bundles (double arrowheads) connect the aon with a posterior optical neuropil (pon). From the posterior optical neuropil two lateral fiber tracts (lft) project into the central neuropil. On each side the posterior optical neuropil is connected via neurite bundles (short arrows) to the cluster of motoneurons (mn). **C-E**: 3D-renderings of the brain in the oozooid stage. Dorsal view, anterior is to the left. **C**: Nuclei are arranged in an outer brain cortex. Two paraxial neuropils (pan) are visible. **D**: Tyrosinated- α-Tubulin channel only. Fan-shaped neurite bundles connect prc positioned at the two limbs of the horseshoe-shaped eye to the paraxial neuropils. **E**: Tyrosinated- α-Tubulin channel only; dorsal half of clsm-stack omitted. A conspicuous pair of lateral fiber tracts horizontally draws through the brain. ae: anterior eye, ba: brain appendages, me: median eye, ne: neurites, pe: posterior eye, pn: peripheral nerves, vanl: left ventral anterior nerve

Discussion

Tunicates, as the potential sister taxon to vertebrates (Delsuc et al. 2006, Tsagkogeorga et al. 2009, see also review by Stach 2014), have attracted considerable interest from evolutionary biologists with a clear focus on ascidians (e.g., Lemaire 2011, Diogo et al. 2015, Kusakabe 2017). Recently, appendicularians gained appreciation (Seo et al. 2001, Stach et al. 2008, Denoeud et al. 2010, Albalat and Cañestro 2016), while the more arcane planktonic taxa pyrosomes, doliolids, and salps (together constituting the taxon Thaliacea) remain relatively obscure (Piette and Lemaire 2015), though molecular tools are currently developed to investigate the evolution of their complex life cycles (Jue et al. 2016).

Comparison of brain morphologies of T. democratica

Brain size in the oozooid is larger than in the blastozooid stage. The number of neurons that build up the brains is approximately three times higher in the oozooid stage compared to the number in the blastozooid stage. Also, the number of emanating nerves is higher in the oozooid than in the blastozooid and the positions of the radiating nerves of the brain differ in the two stages. While in the blastozooid most nerves originate from the side, in the oozooid the nerves leave the brain in a plane that is tilted at an angle of 30°. One pair of nerves in the blastozooid stage, the right and left ventral anterior nerves, has an unusual course: they leave the brain from the ventral side bend anteriorly in a sharp curve and extend anteriorly. These right and left ventral anterior nerves are unique for the blastozooid of *T. democratica* and have to our knowledge not been described for *T. democratica* or other thaliacean species.

The brains are ganglion like in their organization (terminology according to Richter et al. 2010) with a central neuropil and a peripheral cortex and are similar to the brains of sessile ascidians in that respect (e.g. Burighel and Cloney 1997). However, the brains of the two life cycle stages in *T. democratica* differ also in their internal anatomy. This is most obvious in the eyes which we will discuss below. In the blastozooid a group of bilaterally symmetrically arranged motoneurons in the ventral posterior part are discernible by their larger size and lighter cytoplasm. Such conspicuous cells are lacking in the oozooid stage.

Besides the central neuropils in both stages, additional smaller neuropils are identifiable. In the blastozooid stage two smaller neuropils are positioned dorsoanterior in the brain, immediately dorsal to the eyes. Because of their close connection with the eyes, we named them anterior and posterior optical neuropils. In the oozooid stage the two paraxial neuropils are situated dorsally and posteriorly in the brain. These paraxial neuropils are therefore situated in close proximity to the posterior end of the horseshoe-shaped eye and might be implicated in the procession of optical stimuli. The paraxial neuropils had been described by Lacalli and Holland (1998). A pair of lateral fiber tracts (lft) is present in both stages in *T. democratica*. In the blastozooid stage lft run ventroanteriorly between the dorsal side of the central neuropil and the posterior optical neuropil. In the oozooid stage lft are stretching obliquely from the anterior cluster of motoneurons (c3 according to Lacalli and Holland 1998) to the posterior side of the central neuropil. While the course of lft differs in the two stages, processing of optical inputs is a likely major function in both cases.

Lacalli and Holland (1998) provided a detailed analysis of the developing brain and the brain anatomy in the early oozooid stage of *T. democratica*. Our data are generally in accordance with their findings with the exception that the number of nerves emerging from the brain in the older oozooids of our study is higher (see 3D-pdf in Fig. 4B in online version). While this difference is most likely due to the ontogenetic stage of the specimens examined, it makes a definitive attribution of the numbering system for individual nerves used by Lacalli and Holland (1998) difficult. Lacalli and Holland (1998) demonstrated that the ganglion-like anatomy derived from an earlier neural tube-like stage. Following the argumentation of Nelson (1978), this observation can be interpreted as supportive of the hypothesis that salps are evolutionarily derived from an ascidian-like sessile ancestor. Similarly, we suggest that the overall simplicity of the brains in both stages is reminiscent of the sessile ascidian-like ancestor, and the traces of internally discernible regionalization (conspicuous motoneurons, lateral fiber tracts, brain appendages, optic and paraxial neuropils) might be a consequence of the more active planktonic mode of life. Contrary to this trend, *T.* democratica, like appendicularians (Olsson et al. 1990), lacks a neural gland that is typically a part of the neural complex in ascidians (e.g. Mackie and Burighel 2005), although *T. democratica* possesses a ciliated funnel in both stages anterior to the brain.

Comparison of eye morphologies of T. democratica

In terms of histological composition the eyes of both life cycle stages of *T. democratica*, blastozooid and oozooid, are composed of two different cell types only: photoreceptor cells (prc) and pigment cells (pigc). No cornea or crystal cone were present in the eye cells, making the interpretation of Ussow (1876) obsolete and thereby confirming observations and interpretations of other researchers, such as Göppert (1893), Metcalf (1898), and Redikorzew (1905). The improved resolution of modern light microscopy and electron microscopy showed that only a single type of prc is present in the eyes of *T. democratica*. Depending on the shape of the eye and the position of the prc in the eye, the overall shape of prc might differ, yet the ultrastructure in the respective life cycle stage seems the same in all prc. The retina in the eye of *T. democratica* therefore is composed of prc only, contrary to the claim of Redikorzew (1905), who not only mentioned two differently shaped prc, but who also described

"Stützzellen" – supportive cells – in the eyes of salps. The prc in the cerebral eyes of both life cycle stages are most probably primary sensory cells with their own basal neurites, although we cannot be completely decisive on this issue due to methodological limitations of our study.

We confirm Gorman and Co-authors (1971) observation that the eyes of *T. democratica* are lensless, and affirm that the presumably photosensitive enlarged membrane arrays are provided by the apical side of the prc, adding that this is the case in both the sexual aggregate and asexual solitary stage. Thus prc are rhabdomeric cells, different in this respect from the ciliary prc in the brains of larval ascidians (Dilly 1964, Eakin and Kuda 1970, Kusakabe and Tsuda 2007), the ciliary prc in the anterior larval eye of cephalochordates (Lacalli et al. 1994, Wicht and Lacalli 2005), or the prc in the retinas of the paired vertebrate eyes (De Robertis 1960, Wolken 1963) and more similar to rhabdomeric prc of cephalochordates (e.g., Lacalli and Stach 2016), enteropneusts (Braun et al. 2015), echinoids (Ullrich-Lüter et al. 2011), or even arthropods (e.g., Reimann and Richter 2007, Müller et al. 2007). It is noteworthy in this context that the epidermal ocelli surrounding the oral siphon of the ascidian *Ciona intestinalis* possess rhabdomeric prc (Dilly and Wolken 1973) which thus differ from the larval prc in *C. intestinalis* (Dilly 1964, Eakin and Kuda 1970, Kusakabe and Tsuda 2007). On a molecular level, the distinction between ciliary and rhabdomeric prc is also found in the respective opsins (Arendt 2003, Porter et al. 2012), but from an evolutionary point of view, it is significant that both types of prc or opsins can be found in the same species (see e.g., tabulation in Schmidt-Rhaesa 2007, Porter et al. 2012). By analysing the genomic sequences of *C. robusta* (published as the genome of *C. intestinalis* – see Brunetti et al. 2015, Pennati et al. 2015) and *C. savignyi,* Porter and co-authors identified the first rhabdomeric opsin genes in tunicates (Porter et al. 2012). However, this r-opsin has not been characterized further and therefore it is unknown to which prc or even cell type this r-opsin belongs. On another biological level, the prc in the cerebral eyes of *T. democratica* are of the inverse type, i.e. their basal poles with the extending neurites are oriented towards the light. This is similar to the condition observed in the paired lateral eyes of vertebrates but fundamentally different from the arrangement of prc in larval ascidians or the ocelli around the oral siphon in *Ciona* species. This character state distribution therefore shows that prc-type and orientation towards light evolve independently.

There is a slight difference in the ultrastructure of the prc of the oozooid of *T.democratica* compared to prc of the blastozooid. In the oozooid more vesicles with electron lucent content were present around or basal to the nuclei. Thus, these vesicles are on the side of light penetration, i.e. the light passes through these vesicles, before it falls onto the light sensitive microvilli. Because the vesicles do not form an obvious lens shape they might be considered as a screen, filtering out harmful electromagnetic waves (Nilsson 2009, Furchheim 2016).

In both life cycle stages the pigc are characterised by thin extensions that extend around the retina but also between the microvilli. These extensions might separate packages of microvilli from individual cells and could therefore increase the ability to detect local differences in brightness in the respective eyes.

Functional aspects of the 3D-arrangement of eyes of T. democratica

The detailed digital 3D-reconstruction of the eyes of the two different life cycle stages of the salp *T. democratica* makes it possible to digitally isolate the pigment layer and the presumably photosensitive areas of the photoreceptor cells. The geometric arrangement of these two structures determines the possible initial interaction with incident light. This is visualized in Figure 6, where based on the distribution of shading pigment layer the preferential direction of light falling on the light sensitive photoreceptive is depicted as yellow lines and arrows. (A better understanding of the relation of the sub-structures of the eyes can be gained from the 3D-pdfs in the online version). Like other structures, animal eyes have served as inspiration for technical solutions (Lee and Szema 2005, Song et al. 2013, Deng et al. 2016). However, technical solutions, like most eyes, are usually radially symmetrical. Deviations from this rule in animals can be seen e.g., in mesopelagic fishes (Warrant and Locket 2004) or crustaceans (Nilsson 1996) but rarely in technical solutions (Kingslake and Johnson 2010). Technical optical instruments usually solve a single specific problem, whereas biological light detectors often cater towards several needs (Nilsson 1996). In the case of the three eyes of the blastozooid stage of *T. democratica*, each eye in itself has the shape of a simple pigment-cup eye (Fig. 7E). The configuration of relatively wide aperture and low numbers of prc in each eye indicates that these eyes do not form images, but in combination will serve as sensitive detectors for the direction of incoming light. Because of the unusual, not radially symmetric configuration of the eye in the oozooid stage of *T. democratica* (Fig. 7F), the functional interpretation hardly can go further than suggesting that the horseshoe-shaped eye is the optimal compromise solution between a detector of light direction and material economy as has eloquently been done by Göppert (1893, p. 271) already. The present detailed study has shown that the different parts of the horseshoe-shaped eye seem to "look" into different directions, therefore nervous integration of the signal from prc from different areas of the eye might lead to an even better local detection of light directionality.

One genotype, two eyes – correspondences in the different eyes of T. democratica

Because both life cycle stages share a common genotype and despite morphological differences also similarities in their anatomical organizations the question arises whether the eyes of the different stages share similarities that could justify hypotheses of correspondence ("ontogenetic homology" sensu Haszprunar 1992). Indeed, direct comparison of the 3D-reconstructions of the eyes in dorsal view show that the arrangement of the three individual eyes of the blastozooid stage is in fact comparable to the horseshoe-shaped eye in the oozooid. The respective positions of individual eyes of the blastozooid suggest that each might correspond to a part of the horseshoe-shaped eye in the oozooid (Figs. 6A, B). Metcalf (1898) described that the eye in ontogenetically earlier blastozooid stages is horseshoe-shaped coinciding with the shape of the eyes in oozooid stages. Thus, we hypothesize that during ontogeny the horseshoe-shaped eye precursor in the blastozooid separates and migrates anteriorly to form the three individual eyes of the mature blastozooid. A reason for this unusual change of visual systems in one individual might be the mode of locomotion. The solitary oozooid has more individual control over its position and movement in the water column compared to the aggregate blastozooid.

Besides the horseshoe-shaped eye in *T. democratica*, the eyes of all examined solitary stages of thaliacean

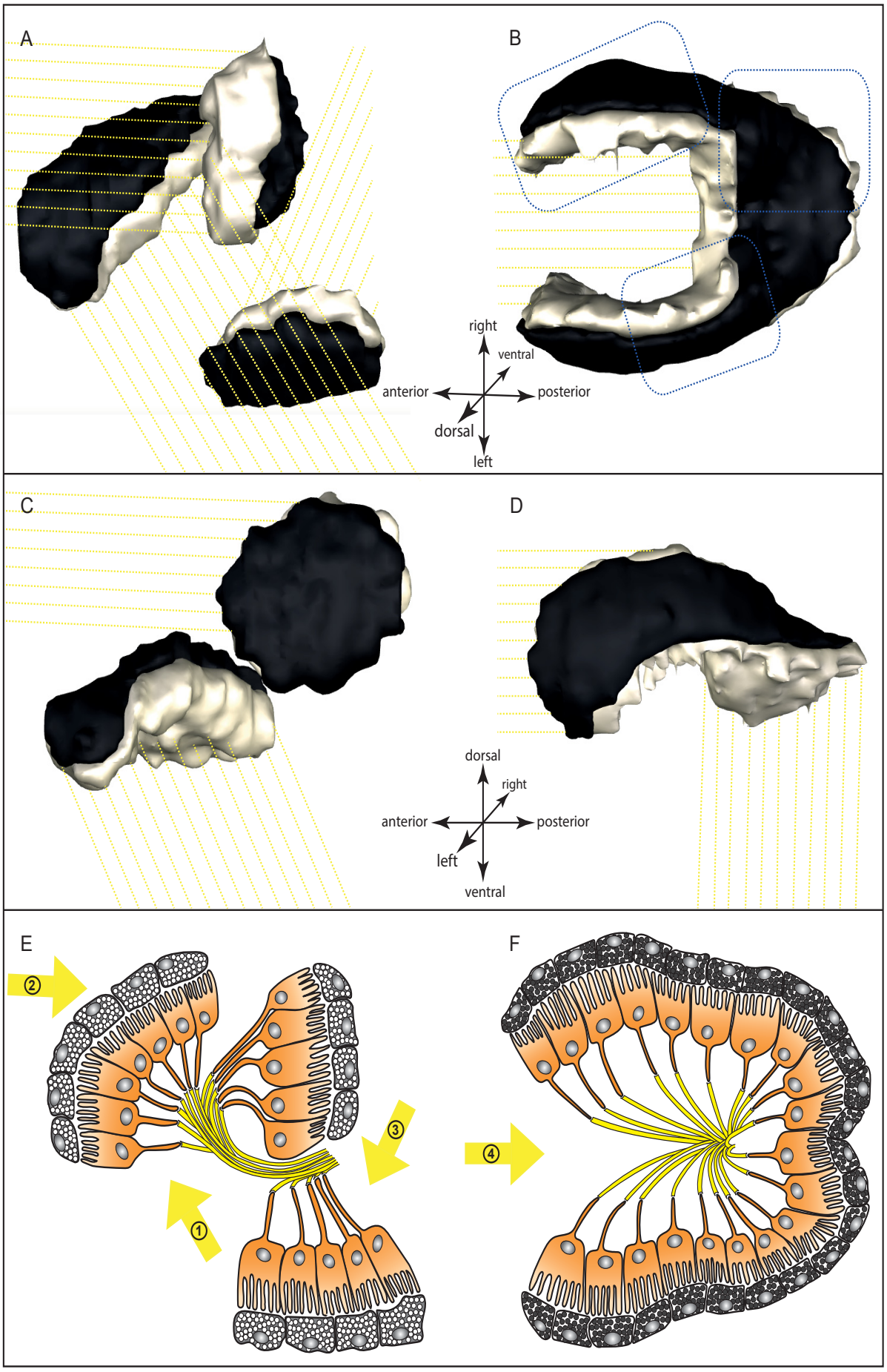
A
B
right
ventral
anterior
posterior
dorsal
left
C
D
dorsal
right
anterior
posterior
left
ventral
E
F
②
③
①
④

Fig. 7:

Fig. 7: *Thalia democratica*, comparison of the eyes of the blastozooid (left side) and oozooid (right side) stage. **A-D**: 3D-reconstructions of digitally isolated pigment cells (black) and microvilli (cream-colored) based on serial semithin sections. Pigment cells form the eyecups in which the microvilli of the photoreceptor cells (not shown) rage into. Direction of incoming light of each eye is indicated by yellow dashed lines. **A, B**: Dorsal view on the eyes, anterior is to the left. **A**: The optical axis of the anterior eye is oriented obliquely towards the dorsal right side, slightly posteriorly. The median eye points anteriorly and slightly to the left side. The optical axis of the posterior eye is oriented towards the left side, slightly to the posterior of the animal. B: The optical axis of the horseshoe-shaped eye points anteriorly. Blue dashed rectangles mark areas that potentially correspond to individual eyes in **A. C, D**: View on the eyes from the left side, dorsal is to the top, anterior is to the left. **C**: The optical axis of the anterior eye points dorsally, slightly to the posterior. **D**: At the connection of both horseshoe limbs microvilli are also arranged ventrally. Therefore the optical axis is also oriented to the ventral side. **E-F**: Interpretative schematic representations of longitudinal sections through the eyes including nerve connections, nerve tracts (in yellow), and direction of incoming light (yellow arrows). **E**: All three eyes of the blastozooid consist of two different cell types: pigment cells and photoreceptor cells (orange). Pigment cells are equipped with electron dense cytoplasm and numerous electron light pigment vesicles. Arrow 1 shows optical axis of the anterior eye, arrow 2 of the median eye, and arrow 3 of the posterior eye. **F**: The horseshoe-shaped eye of the oozooid is also composed of pigment cells and photoreceptor cells. Pigment cells bear numerous electron dense pigment vesicle. Arrow 4 indicates the optical axis of the eye.

species so far are similarly horseshoe-shaped with the opening of the horseshoe pointing anteriorly. In contrast the shape and orientation of the investigated eyes of thaliacean species in blastozooid stages differ considerably (e.g. Metcalf 1898, reviewed in Madin 1995). Therefore, the horseshoe-shaped eye is the "more general" one (sensu Nelson 1978), we can infer that following Nelson's rule the horseshoe-shaped eye is the plesiomorphic condition (Nelson 1978).

Evolutionary considerations concerning the eyes of T. democratica

"Es ist überhaupt empfehlenswert, davor zu warnen, sich in allzu großem Maße phylogenetischen Betrachtungen hinzugeben" (Redikorzew 1905, p. 232. It is profoundly recommendable to warn against indulging too much in phylogenetic observations).

We follow Redikorzew's warning and keep the evolutionary considerations brief. Cerebral eyes are present in the brains of cephalochordates, ascidian larvae, and in the diencephalic paired eyes of craniates. In ascidian larvae and the paired lateral eyes of vertebrates, the prc are of the ciliary type. In cephalochordates, rhabdomeric eyes are present in the central nervous system, e.g. in form of the Hesse ocelli and Joseph cells, but it is an anterior eye with ciliary prc that is probably homologous to the lateral eyes of vertebrates (Lacalli et al. 1994, Vopalensky et al. 2012). Although tunicate phylogeny is far from being resolved, most recent phylogenies indicate that salps are derived from sessile ascidian-like ancestors (Stach and Turbeville 2002, Tsagkogeorga et al. 2009, Govindarajan et al. 2011). Adult ascidians have ganglion-like brains without cerebral eyes (e.g., Huus and Knudsen 1950, Burighel and Cloney 1997), though behavioural experiments indicate that ascidian brains are light sensitive (Hecht 1918). The complex rhabdomeric eyes as the main visual organs in the brain of adult salps are a secondary phenomenon within tunicates and the rhabdomeric cerebral eyes can be interpreted as an

apomorphic feature of salps. Although we lack detailed knowledge of the eyes of pyrosomes (Neumann 1956, Bone 1998), it seems likely that cerebral rhabdomeric eyes are an apomorphic character of thaliaceans as a whole or a synapomorphic character of Salpida and Pyrosomatida.

Author contributions

TS designed the study, sectioned specimens, performed electron microscopy. KB sectioned specimens, realized 3D-reconstruction, performed confocal laser scanning microscopy. Both authors wrote the manuscript.

Acknowledgements

We thank Priv.-Doz. Dr. Carsten Müller (Universität Greifswald) for collecting and kindly providing the fixed blastozooid stages used in this study. We are grateful for access to the Leica SPE CLSM granted by Priv.-Doz. Dr. Carsten Lüter (Museum für Naturkunde Berlin). Financial support by the Deutsche Forschungsgemeinschaft (DFG), the German Academic Exchange Service (DAAD) and the Elsa-Neumann-Stipendium des Landes Berlin is gratefully acknowledged. We are thankful to the invaluable help of Woody Lee and Scott Jones from the Smithsonian Marine Station in Fort Pierce, Florida in securing specimens. We are also indebted to Prof. Valerie Paul and Prof. Mary Rice for generously providing access to the facilities of the Smithsonian Marine Station.

References

Arendt D. 2003. Evolution of eyes and photoreceptor cell types. Int J Dev Biol 47:563-571.

Banks MS, Sprague WW, Schmoll J, Parnell JAQ, Love GD. 2015. Why do animal eyes have pupils of different shapes?. Science Advances 1.

Bone Q. 1998. Nervous system, sense organs, and excitable epithelia. In: Bone Q editor. The biology of pelagic tunicates. Oxford, New York,Tokyo: Oxford University Press. p 55-80.

Braun K, Kaul-Strehlow S, Ullrich-Lüter E, Stach T. 2015. Structure and ultrastructure of eyes of tornaria larvae of *Glossobalanus marginatus*. Org Divers Evol 15:423-428.

Braun K, Stach T. 2016. Comparative study of serotonin-like immunoreactivity in the branchial basket, digestive tract, and nervous system in tunicates. Zoomorphology 135(3):351-366.

Brooks WK. 1893. The genus Salpa. Memoirs from the Biological Laboratory of the Johns Hopkins University II. Baltimore: The Johns Hopkins Press. p 1-303.

Brunetti R, Gissi C, Pennati R, Caicci F, Gasparini F, Manni L. 2015. Morphological evidence that the molecularly determined *Ciona intestinalis* type A and type B are different species: *Ciona robusta* and *Ciona intestinalis*. J Zool Syst Evol Res 53:186-193.

Burighel P, Cloney RA. 1997. Urochordata: Ascidiacea. In: Harrison FW, Ruppert EE, editors. Microscopic anatomy of invertebrates. Hemichordata, Chaetognatha, and the invertebrate chordates. New York, Chichester, Weinheim, Brisbane, Singapore, Toronto: Willey-Liss, Incorporation. p 221-347.

Chamisso AV. 1819. De animalibus quibusdam e classe Vermium Linnaeana in circumnavigatione terrae. Fasciculus primus. De Salpa. Berlin: Dümmler.

Cohen AI. 1963. Vertebrate retinal cells and their organization. Biol Rev 38(4):427-459.

Darwin C. 1859. The origin of species. Edition from 1985 edn. London: Penguin Book.

Dawkins R. 1995. River out of Eden: a Darwinian view of life. New York: Basic Books.

De Robertis E. 1960. Some observations on the ultrastructure and morphogenesis of photoreceptors. J Gen Physiol 43(6):1-13.

Delsuc F, Brinkmann H, Chourrout D, Philippe H. 2006. Tunicates and not cephalochordates are the closest living relatives of vertebrates. Nature 439(7079):965-968.

Deng Z, Chen F, Yang Q, Bian H, Du G, Yong J, Shan C, Hou X. 2016. Dragonfly-eye-inspired artificial compound eyes with sophisticated imaging. Adv Funct Mater 26(12):1995-2001.

Dilly N. 1964. Studies on the receptors in the cerebral vesicle of the ascidian tadpole, 2. The ocellus. Q J Microsc Sci s3-105(69):13-20.

Dilly PN, Wolken JJ. 1973. Studies on the receptors in *Ciona intestinalis*. IV. The ocellus in the adult. Micron 4:11-29.

Eakin RM, Kuda A. 1970. Ultrastructure of sensory receptors in ascidian tadpoles. Z Zellforsch 112(3):287-312.

Fergus JLB, Johnsen S, Osborn KJ. 2015. A unique apposition compound eye in the mesopelagic hyperiid amphipod *Paraphronima gracilis*. Curr Biol 25(4):473-478.

Forskål P. 1775. Descriptiones animalium, avium, amphibiorum, piscium, insectorum, vermium, quae in itinere orientali observavit. Petrus Forskål. Post mortem auctoris edidit Carsten Niebuhr. Adjuncta est materia medica kahirina atque tabula Maris Rubri geographica. Ex-officina Mölleri.

Furchheim N. 2016. Funktionelle Morphologie der Lichtsinnesorgane rezenter Brachiopoda [dissertation]. Berlin: Humboldt-Universität zu Berlin. p 121.

Gehring WJ. 1996. The master control gene for morphogenesis and evolution of the eye. Genes Cells 1(1):11-15.

Gehring WJ, Ikeo K. 1999. Pax 6: mastering eye morphogenesis and eye evolution. Trends Genet 15(9):371-377.

Glaubrecht M, Dohle W. 2012. Discovering the alternation of generations in salps (Tunicata, Thaliacea): Adelbert von Chamisso's dissertation "De Salpa " 1819 – its material, origin and reception in the early nineteenth century. Zoosyst Evol 88:317-363.

Glaeser G, Paulus HF. 2015. The evolution of the eye. Cham: Springer International Publishing.

Göppert E. 1893. Untersuchungen über das Sehorgan der Salpen. Morph Jahrbuch. Bd. 19. Heft 3. p 250-294.

Gorman ALF, McReynolds JS, Barnes SN. 1971. Photoreceptors in primitive chordates: fine structure, hyperpolarizing receptor potentials, and evolution. Science 172(3987):1052-1054.

Govindarajan AF, Bucklin A, Madin LP. 2011. A molecular phylogeny of the Thaliacea. J Plankton Res 33:843-853.

Haszprunar G. 1992. The types of homology and their significance for evolutionary biology and phylogenetics. J Evol Biol 5(1):13-24.

Hecht S. 1918. The photic sensitivity of *Ciona intestinalis*. J Gen Physiol 1(2):147-166.

Huus J, Knudsen J. 1950. Tunicata. In: Fridriksson Å, Tuxen SL, editors. The Zoology of Iceland. Copenhagen, Reykjavik: Munksgaard, Ejnar. p 1-25.

Jue NK, Batta-Lona PG, Trusiak S, Obergfell C, Bucklin A, O'Neill MJ, O'Neill RJ. 2016. Rapid evolutionary rates and unique genomic signatures discovered in the first reference genome for the Southern Ocean salp, *Salpa thompsoni* (Urochordata, Thaliacea). Genome Biol Evol 8(10):3171-3186.

Karnovsky MJ. 1965. A formaldehyde-glutaraldehyde fixative of high osmolality for use in electron microscopy. J Cell Biol 27: 137A.

Kingslake R, Johnson RB. 2010. Lens design fundamentals. Oxford: Elsevier Inc.

Kusakabe T, Tsuda M. 2007. Photoreceptive systems in ascidians. Photochem Photobiol 83(2):248-252.

Lacalli TC, Holland LZ. 1998. The developing dorsal ganglion of the salp *Thalia democratica*, and the nature of the ancestral chordate brain. Philos Trans R Soc Lond B 353:1943-1967.

Lacalli TC, Holland ND, West JE. 1994. Landmarks in the anterior central nervous system of amphioxus larvae. Philos Trans R Soc Lond B 344:165-185.

Lacalli TC, Stach T. 2016. Acrania (Cephalochordata). In: Schmidt-Rhaesa A, Harzsch S, Purschke G, editors. Structure & evolution of invertebrate nervous systems. Oxford: Oxford University Press. p 719-728.

Lamb TD. 2013. Evolution of phototransduction, vertebrate photoreceptors and retina. Prog Retin Eye Res 36:52-119.

Lee LP, Szema R. 2005. Inspirations from biological optics for advanced photonic systems. Science 310(5751):1148-1150.

Lemaire P. 2011. Evolutionary crossroads in developmental biology: the tunicates. Development 138(11):2143-2152.

Lowe CJ, Clarke DN, Medeiros DM, Rokhsar DS, Gerhart J. 2015. The deuterostome context of chordate origins. Nature 520(7548):456-465.

Mackie GO, Bone Q. 1977. Locomotion and propagated skin impulses in salps (Tunicata: Thaliacea). Biol Bull 153(1):180-197.

Mackie GO, Burighel P. 2005. The nervous system in adult tunicates: current research directions. Can J Zool 83:151-183.

Madin LP. 1995. Sensory ecology of salps (Tunicata, Thaliacea): more questions than answers. Mar Freshw Behav Physiol 26(2-4):175-195.

Metcalf MM. 1898. The eyes and subneural gland of salpa. Memoirs from the Biological Laboratory of the Johns Hopkins University II. Baltimore: The Johns Hopkins Press. p 305-371.

Müller CHG, Sombke A, Rosenberg J. 2007. The fine structure of the eyes of some bristly millipedes (Penicillata, Diplopoda): additional support for the homology of mandibulate ommatidia. Arthropod Struct Dev 36(4):463-476.

Nelson G. 1978. Ontogeny, phylogeny, paleontology, and the biogenetic law. Syst Zool 27:324-345.

Neumann G. 1956. 1. Ordnung der Thaliaceae: Pyrosomida. In: Handbuch der Zoologie: eine Naturgeschichte der Stämme des Tierreichs. Bd.5:2 Tunicata. Berlin: Walter de Gruyter & Co. p 226-323.

Nilsson D-E. 1996. Eye design, vision and invisibility in planktonic invertebrates. In: Zooplankton: Sensory Ecology and Physiology. Amsterdam: Overseas Publishers Association. p 149-162.

Nilsson D-E. 2009. The evolution of eyes and visually guided behaviour. Philos Trans R Soc Lond B Biol Sci 364:2833-2847.

Nilsson D-E, Pelger S. 1994. A pessimistic estimate of the time required for an eye to evolve. Proc R Soc London B Biol Sci 256(1345):53-58.

Oakley TH, Speiser DI. 2015. How complexity originates: the evolution of animal eyes. Annu Rev Ecol Evol Syst 46:237-260.

Olsson R, Holmberg K, Lilliemarck Y. 1990. Fine structure of the brain and brain nerves of *Oikopleura dioica* (Urochordata, Appendicularia). Zoomorphology 110:1-7.

Pennati R, Ficetola F, Brunetti R, Caicci F, Gasparini F, Griggio F, Sato A, Stach T, Kaul-Strehlow S, Gissi C, Manni L. 2015. Remarkable morphological differences between larvae of the *Ciona intestinalis* species complex: hints for a valid taxonomic definition of distinct species. PLoS ONE 10:e0122879.

Piette J, Lemaire P. 2015. Thaliaceans, the neglected pelagic relatives of ascidians: a developmental and evolutionary enigma. Q Rev Biol 90(2):117-145.

Porter ML, Blasic JR, Bok MJ, Cameron EG, Pringle T, Cronin TW, Robinson PR. 2012. Shedding new light on opsin evolution. Proc R Soc Lond B Biol Sci 279:3-14.

Ramirez MD, Pairett AN, Pankey MS, Serb JM, Speiser DI, Swafford AJ, Oakley TH. 2016. The last common ancestor of most bilaterian animals possessed at least nine opsins. Genome Biol Evol 8(12):3640-3652.

Redikorzew W. 1905. Über das Sehorgan der Salpen. Gegenbaurs Morphol Jahrb. Bd. 34. p 204-239.

Reimann A, Richter S. 2007. The nauplius eye complex in 'conchostracans'(Crustacea, Branchiopoda: Laevicaudata, Spinicaudata, Cyclestherida) and its phylogenetic implications. Arthropod Struct Dev 36(4):408-419.

Richter S, Loesel R, Purschke G, Schmidt-Rhaesa A, Scholtz G, Stach T, Vogt L, Wanninger A, Brenneis G, Doring C, Faller S, Fritsch M, Grobe P, Heuer CM, Kaul S, Møller OS, Müller CHG, Rieger V, Rothe BH, Stegner MEJ, Harzsch S. 2010. Invertebrate neurophylogeny: suggested terms and definitions for a neuroanatomical glossary. Front Zool 7(1):29.

Schmidt-Rhaesa A. 2007. The evolution of organ systems. Oxford: Oxford University Press.

Song YM, Xie Y, Malyarchuk V, Xiao J, Jung I, Choi K-J, Liu Z, Park H, Lu C, Kim R-H, Li R, Crozier KB, Huang Y, Rogers JA. 2013. Digital cameras with designs inspired by the arthropod eye. Nature 497(7447):95-99.

Stach T. 2014. Deuterostome phylogeny – a morphological perspective. In: Wägele JW, Bartolomaeus T, editors. Deep metazoan phylogeny: the backbone of the tree of life. Berlin, Boston: Walter de Gruyter GmbH. p 425–457.

Stach T, Turbeville JM. 2002. Phylogeny of Tunicata inferred from molecular and morphological characters. Mol Phylogen Evol 25:408-428.

Todaro F. 1893. Sull' organo visivo delle Salpe. Atti d Acad Lincei (5), Rend. II: 374-381.

Tsagkogeorga G, Turon X, Hopcroft R, Tilak M, Feldstein T, Shenkar N, Loya Y, Huchon D, Douzery E, Delsuc F. 2009. An updated 18S rRNA phylogeny of tunicates based on mixture and secondary structure models. BMC Evol Biol 9:187.

Ullrich-Lüter EM, Dupont S, Arboleda E, Hausen H, Arnone MI. 2011. Unique system of photoreceptors in sea urchin tube feet. Proc Natl Acad Sci 108(20):8367-8372.

Ussow M. 1876. Beiträge zur Kenntnis der Organisation der Tunicaten. Mém soc imp sci nat Moscou 18:1-54.

Van Soest RWM. 1998. The cladistic biogeography of salps and pyrosomas. In: Bone Q, editor. The biology of the pelagic tunicates. Oxford, New York, Tokyo: Oxford University Press. p 231-249.

Vopalensky P, Pergner J, Liegertova M, Benito-Gutierrez E, Arendt D, Kozmik Z. 2012. Molecular analysis of the amphioxus frontal eye unravels the evolutionary origin of the retina and pigment cells of the vertebrate eye. Proc Natl Acad Sci 109:15383-15388.

Warrant EJ, Locket NA. 2004. Vision in the deep sea. Biol Rev 79(3):671-712.

Wicht H, Lacalli TC. 2005. The nervous system of amphioxus: structure, development, and evolutionary significance. Can J Z 83:122-150.

Wolken JJ. 1963. Structure and molecular organization of retinal photoreceptors. J Opt Soc Am 53(1):1-19.

6.2 Supporting Information

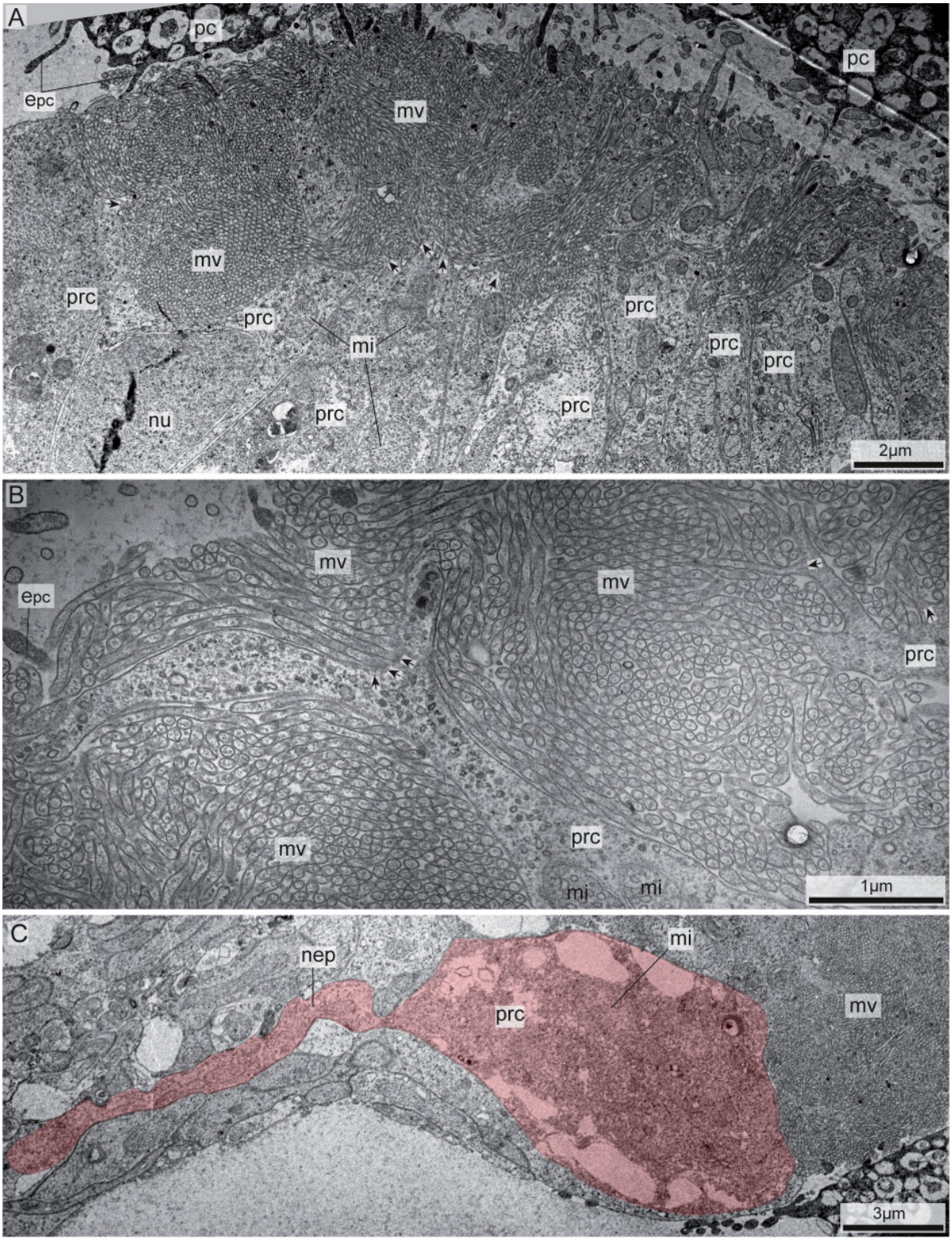

Supporting Information Figure: Ultrastructure of the eye of the blastozooid stage of *T. democratica*. **A**: Transmission electron micrograph of at least seven photoreceptor cells (prc) and several pigment cells (pc). Microvilli (mv) of the photoreceptor cells largely fill the space on the concave side of the pigment cup formed by the pigment cells. Arrows indicate examples where microvilli are clearly connected with the cytoplasm of the photoreceptor cells. **B**: Higher magnification of the photoreceptor cell shown in Fig. 3D. It is clearly visible that some microvilli are attached to the cytoplasm of the apical region of the photoreceptor cell (see arrows). **C:** Detail of a prc that tapering into a basal neurite-

like process (nep). epc: extension of the pigment cells, mi: mitochondria, nu: nucleus

Supplementary Movie 1: Movie generated from stack of 51 confocal laser scanning micrographs of the brain of the blastozooid stage of *Thalia democratica*. Distance between confocal levels is 1.4 µm. Immunostaining against tyrosinated-α-Tubulin (red) and nuclear staining utilizing DAPI (blue).

Supplementary Movie 2: Movie generated from stack of 94 confocal laser scanning micrographs of the brain of the oozooid stage of *Thalia democratica*. Distance between confocal levels is 1.5 µm. Immunostaining against tyrosinated-α-Tubulin (red) and nuclear staining utilizing DAPI (blue).

7 The central nervous system in adult tunicates

7.1 Publication

This is the pre-peer reviewed version of the following article:

Braun, K., & Stach, T. (2018). Morphology and evolution of the central nervous system in adult tunicates. *Journal of Zoological Systematics and Evolutionary Research*, 1-22,

which has been published in final form at:

https://doi.org/10.1111/jzs.12246.

Morphology and evolution of the central nervous system in adult tunicates

Authors

Katrin Braun

Humboldt-Universität zu Berlin, Institut für Biologie, Vergleichende Zoologie, Philippstrasse 13, Haus 2, 10115 Berlin, Germany

Thomas Stach

Humboldt-Universität zu Berlin, Institut für Biologie, Molekulare Parasitologie, Philippstrasse 13, Haus 14, 10115 Berlin, Germany, thomas.stach@hu-berlin.de

Abstract

Tunicata, comprising approximately 2500 marine invertebrate species, has recently been proposed to be the sister taxon to Craniota. Phylogenetic interrelationships of higher tunicate taxa are controversial and it remains unclear, whether traces of a fish-like ancestor with an active mode of life can be found in present day tunicates.

To answer this question, we investigated the morphology of the central nervous systems of 18 tunicate species, belonging to the five major tunicate taxa. Therefore, we reconstructed three-dimensional anatomical models of the neural complexes, and additionally conducted immunohistological staining experiments using antibodies against tyrosinated-α-tubulin. While the reconstructions of the neural complexes are consistent with previous studies of select species, they also reveal an unappreciated variation of the tunicate nervous systems, especially on the interspecific level. Presence and number of brain nerves i.e., paired anterior and posterior nerves, lateral and ventral visceral nerves, as well as the presence of a dorsal strand vary among representatives of a higher taxon, but can be very similar to species within another taxon. We ameliorated the availability of data on the neuroarchitecture of tunicate species providing detailed descriptions of the neural complexes of adult specimens. Moreover, we formulated a set of neuroanatomical characters and showed in a phylogenetic analysis that neuroanatomical characters are parsimony-informative, but are insufficient to resolve phylogenetic relationships on their own. In order to understand neuroanatomical character evolution we plotted our data on a recently published phylogenetic hypothesis showing that the evolution of the neural complex is clearly correlated with the evolution of life-history strategies.

Keywords

Cerebral ganglion, urochordates, brain evolution, phylogeny, ascidians

Introduction

Tunicates comprise about 2500 described species that are exclusively marine and unique amongst all metazoans in their ability to produce cellulose (Shenkar & Swalla 2011). The life cycles of these animals are intriguingly diverse (Glaubrecht & Dohle 2012, Lemaire & Piette 2015). Some tunicates, like the best-known ascidians are sessile as adults. Others such as salps and pyrosomes (Thaliacea) or larvaceans (Appendicularia) are pelagic. Some species are colonial while others are solitary (Zeng, Jacobs, & Swalla 2006). There are groups with extraordinary polymorphisms and even heterogenetic modes of reproduction, reminiscent of parasitic invertebrates rather than chordates. Thus, it was unexpected when molecular phylogenies overturned the traditional view that the fish-like lancelets (Cephalochordata) and vertebrates (Craniota or Vertebrata) formed a monophyletic clade (Notochordata-hypothesis; see e.g. Ax 2001, Stach 2008) to the exclusion of Tunicata (Delsuc, Brinkmann, Chourrout, & Philippe 2006, Dunn et al. 2008, Edgecombe et al. 2011). As an alternative view, these molecular phylogenies supported a sister group relationship between Tunicata and Craniota, forming the so-called Olfactores, to the exclusion of Cephalochordata. Therefore, instead of a stepwise evolution of craniate characters, the new, molecular based phylogeny was interpreted as the sudden occurrence of a fish-like ancestor in the stem lineage of chordates (Swalla & Smith 2008; but see Stach 2014). While raising interest in tunicate evolution in general, the Olfactores-hypothesis poses the question, whether remnants of the formerly active, fish-like mode of life can be found in present day tunicates.

Arguably the most complex organ system evolved in the animal kingdom is the nervous system. Moreover, the nervous system is considered to be evolutionarily conservative with a tendency to change slower than other organ systems (Fritzsch, Sonntag, Dubuc, Ohta, & Grillner 1990, Gilland & Baker 2005). It is little surprising that the complexity of the nervous system has repeatedly been used as a valuable source for phylogenetic inferences (Loesel 2011, Nieuwenhuys et al. 2014, Schmidt-Rhaesa, Harzsch, & Purschke 2015). Because the nervous system is also the central organ system in control of patterns of activity it could preserve traces of a more actively living ancestor.

The central nervous systems of tunicates have been studied in several species and it has been found to consist of an anterior, dorsal brain or ganglion. The brain possesses an outer brain cortex, where somata of nerve cells are located and an inner neuropil, where nerve fibers are arranged (Koyama & Kusunoki 1993; Lacalli & Holland 1998; Olsson, Holmberg, & Lilliemarck 1990; Zaniolo, Lane, Burighel, & Manni, 2002). In general, tunicate brains are equipped with paired anterior and posterior nerves, and an unpaired ventral visceral nerve (Huus 1956, Manni & Pennati 2016). In addition to the brain, ascidian larvae possess a visceral ganglion (Meinertzhagen & Okamura 2001), whereas in appendicularians a caudal ganglion is developed (Søviknes, Chourrout, & Glover 2007, Stach, Winter, Bouquet, Chourrout, & Schnabel 2008). In most tunicate species the brain is associated with a neural gland that together with the brain forms the neural complex. Yet, the function of the neural gland remains controversial (e.g. Burighel, Lane, Zaniolo, & Manni 1998, Nozaki & Gorbman 1992, Ruppert 1990). The neural gland is connected to the branchial basket via the gland duct and a ciliated funnel that might form a dorsal tubercle. Moreover, the neural gland features a posterior extension, the dorsal strand (Ruppert 1990). While there are detailed studies on the neuroanatomy of tunicates available,

these are limited to certain stages or taxa and no systematic attempt utilizing a phylogenetic framework has been conducted.

In Appendicularia the neural complex of adults of *Oikopleura dioica* Fol, 1872 has been described based on transmission electron microscopy (Holmberg 1982, Holmberg 1984, Olsson et al. 1990). For thaliaceans data of the brain anatomy of salps are available. Most investigations date back to the late 19th or the beginning of the 20th century (Göppert 1893, Metcalf 1898, Redikorzew 1905, Ussow 1876). For *Thalia democratica* (Forskål, 1775) (Braun & Stach 2017, Lacalli & Holland 1998) and *Salpa maxima* Forskål, 1775 (Fedele 1933) more recent studies were conducted. However, for pyrosomes and doliolids only brief descriptions of the brain and eye of *Pyrosomella verticillata* (Neumann, 1909) and the neural complex of *Doliolina mülleri* (Krohn, 1852) exist (Uljanin 1884). In the phlebobranch ascidian species *Ciona intestinalis* (Linnaeus, 1767) the larval central nervous system is well studied (e.g. Imai & Meinertzhagen 2007, Ryan, Lu, & Meinertzhagen 2018, Takamura, Minamida, & Okabe 2010) while the adult central nervous system lagged behind (Dahlberg et al. 2009, Mackie 1995) and light-microscopical investigations are still producing new insights (Osugi, Sasakura, & Satake 2017). In stolidobranch ascidians, the morphology of the neural complex of two species has been examined: the brain of the colonial *Polyandrocarpa misakiensis* Watanabe & Tokioka, 1972 for adult animals (Koyama & Kusunoki 1993) and the anatomy of the brain in larvae and the neural complex in adults of the colonial species *Botryllus schlosseri* (Pallas, 1766) (e.g. Manni, Lane, Sorrentino, Zaniolo, & Burighel 1999, Zaniolo et al. 2002). Still, detailed comparative analyses of the morphology of the neural complexes with a broader taxon sampling, similar technical standards, and a consistent methodological-phylogenetic framework is missing. Little is known, e.g., about exact numbers of nerves branching off the brains, brain sizes, numbers of neurons that build up the brains, subdivisions of the brains in additional neuropils, exact positions and shapes of neural glands, dorsal strands and dorsal tubercles (see reviews by Bone 1998, Mackie & Burighel 2005, Manni & Pennati 2016). Consequently, it remains unclear, to what extent morphological similarities might be used to support hypotheses of homology between the neural complexes of tunicates.

In order to more carefully evaluate the potential of the neural complex as a phylogenetically important character that allows evolutionary conclusions, we comparatively explored the detailed anatomies of the central nervous system in 18 tunicate species, belonging to 14 different families of the five major tunicate taxa. Based on complete serial sections for light microscopy, we reconstructed 20 virtual tunicate neural complexes in 3d and complemented these data with immunohistological stainings of the brain using antibodies against tyrosinated-α-tubulin for 15 species.

Material and methods

Collection localities of all specimens are listed in **Table 1**. Ascidians were collected in the lower intertidal or upper subtidal. *Iasis cylindrica* and *Doliolum nationalis* were collected from the water column using a plankton net during a 15 minutes drift tow at 10m depth. *Pyrosoma atlanticum* was collected from the water column deploying a tucker trawl at 1000m depth that was opened at 300m depth on the R/V SONNE expedition SO258 leg 1. Living specimens of *Oikopleura dioica* were provided from Sars International Centre for Marine Molecular Biology and cultured at Humboldt-University zu Berlin through numerous generations. Salp specimens for scanning electron microscopy came from the collection of the Museum für Naturkunde (Berlin, Germany; Supplementary Table 1). The guidelines for the care and use of animals according to the Directive 2010/63/EU were followed.

Fixation

Before fixation all ascidians were anaesthetized for approximately an hour using menthol crystals. *I. cylindrica*, *D. nationalis*, *P. atlanticum*, and *O. dioica* were fixed directly without anaesthetization.

For light microscopy animals were fixed either in Bouin's solution, an aqueous solution containing 8% formaldehyde, 5% acetic acid, and 1% picric acid, or in a cold solution of Karnovsky's primary fixative (Karnovsky 1965), consisting of 2% glutaraldehyde, 2% paraformaldehyde, 1.52% NaOH and 1.2g d-glucose, dissolved in 2.25% sodium hydrogen phosphate buffer (pH 7.4). *P. atlanticum* was fixed in 10% formaldehyde and kept in 70% ethanol.

For transmission electron microscopy specimens of *O. dioica* were fixed for 40 minutes in a cold solution of Karnovsky's primary fixative (see above). Specimens were subsequently rinsed in three changes of buffer. Specimens were post-fixed for 1h in 1% OsO_4 solution at room temperature.

Specimens for light and transmission electron microscopy were dehydrated in a graded series of ethanol, embedded in epoxy resin (Araldite; Fluka) or in paraffin. For light microscopy specimens were serially sectioned with a thickness of 0.5µm -1µm (Araldite) or 5µm (paraffin: *A. scabra* and *A. mentula*). One specimen of *O. dioica* was serially sectioned for light microscopy (0.7µm); another specimen of *O. dioica* was serially sectioned alternating between semithin sections (0.5µm) and ultrathin sections (60nm). Sectioning was performed on a Leica Ultracut S. Semithin sections were stained using 1% toluidine blue in a solution of 1% sodium tetraborate (borax). Ultrathin sections were stained with 2% uranylacetate and 2.5% lead citrate in an automatic stainer (courtesy of Dr. Björn Quast, Universität Bonn and Dr. Alexander Gruhl, MPI Bremen).

For immunohistochemical visualization of the nervous system, specimens were fixed in 4% paraformaldehyde in PBS for 40min at room temperature. Samples were rinsed in PBS and stored in PBS containing 0.05% NaN_3 at 4°C for no longer than 6 months after fixation. Specimens were incubated in primary antibodies against tyrosinated α-tubulin (Anti-Tubulin, Tyrosine antibody produced in mouse; Sigma, St. Louis, Missouri, USA) and secondary antibodies Cy™3 AffiniPure goat anti-mouse IgG (Jackson ImmunoResearch Laboratories, Inc., Philadelphia, Pennsylvania, USA); nuclei were labeled using 4'6-Diamidino-2-Phenylindole, Dihydrochloride (DAPI dihydrochloride, Thermo Fisher Scientific Inc., Waltham, Massachusetts, USA). Details can be found in Braun &

Table 1: Information on examined specimens; adult stages were used in all species. In doliolids and salps both stages were analyzed

Species	Family	Order	Origin	Number of specimens examined	Fixations and Methods
Aplidium turbinatum (Savigny, 1816)	Polyclinidae	Aplousobranchiata	Kristineberg, Sweden	1	Bouin, LM
Clavelina lepadiformis (Müller, 1776)	Clavelinidae	Aplousobranchiata	Helgoland, Germany	6	Karnovsky, PFA, LM, CLSM
Diplosoma listerianum (Milne-Edwards, 1841)	Didemnidae	Aplousobranchiata	Helgoland, Germany	6	Karnovsky, PFA, LM, CLSM
Distaplia stylifera (Kowalevsky, 1874)	Holozoidae	Aplousobranchiata	Fort Pierce, USA	9	Karnovsky, PFA, LM, CLSM
Ascidiella aspersa (Müller, 1776)	Ascidiidae	Phlebobranchiata	Helgoland, Germany	5	Bouin, PFA, LM
Ascidiella scabra (Müller, 1776)	Ascidiidae	Phlebobranchiata	Helgoland, Germany Kristineberg, Sweden	10	Bouin, PFA, LM, CLSM
Ascidia mentula Müller, 1776	Ascidiidae	Phlebobranchiata	Kristineberg, Sweden	1	LM
Ciona intestinalis (Linnaeus, 1767)	Cionidae	Phlebobranchiata	Helgoland, Germany Kristineberg, Sweden	15	Bouin, PFA, LM, CLSM
Corella parallelogramma (Müller, 1776)	Corellidae	Phlebobranchiata	Kristineberg, Sweden	9	Bouin, PFA, LM, CLSM
Perophora japonica Oka, 1927	Perophoridae	Phlebobranchiata	Helgoland, Sweden	8	Bouin, PFA, LM, CLSM
Botryllus schlosseri (Pallas, 1766)	Styelidae	Stolidobranchiata	Kristineberg, Sweden	20	Karnovsky, PFA, LM, CLSM
Dendrodoa grossularia (Van Beneden, 1846)	Styelidae	Stolidobranchiata	Kristineberg, Sweden	10	Bouin, PFA, LM, CLSM
Styela clava Herdman, 1881	Styelidae	Stolidobranchiata	Helgoland, Germany Texel, Netherlands	9	Bouin, PFA, LM, CLSM
Molgula manhattensis (De Kay, 1843)	Molgulidae	Stolidobranchiata	Texel, Netherlands	10	Bouin, PFA, LM, CLSM
Oikopleura dioica Fol, 1872	Oikopleuridae	Appendicularia	Bergen, Norway	24	Karnosky, PFA, LM, TEM, CLSM
Doliolum nationalis Borgert, 1893	Doliolidae	Thaliacea	West Palm Beach, USA	15	Karnosky, PFA, LM, CLSM
Iasis cylindrica (Cuvier, 1804)	Salpidae	Thaliacea	West Palm Beach, USA	8	Karnovsky, PFA, LM, CLSM
Pyrosoma atlanticum Péron, 1804	Pyrosomatidae	Thaliacea	Indian Ocean, Afanasy Nikitin Seamount	9	Formaldehyde, PFA, LM, CLSM

CLSM: confocal laser scanning microscopy, LM: light microscopy, PFA: paraformaldehyde, TEM: transmission electron microscopy

Stach (2016). Every staining experiment was performed together with two different controls: one with primary antibodies omitted and the second with secondary antibodies omitted.

Light microscopy

Semithin sections stained with toluidine blue (Araldite) or Azan (paraffin) were digitally recorded (distance between sections 1-2µm) using a Zeiss AxioCam HRc camera mounted on a Zeiss Axioskop 2 plus microscope. Complete images were optimized for contrast and light balance using Adobe Photoshop CC Software and were used for 3d reconstructions.

Transmission electron microscopy

Stained ultrathin sections were examined under a Zeiss EM900 transmission electron microscope, operated at 80kV and recorded with a 2k slow scan CCD camera.

Scanning electron microscopy

For SEM, specimens were critical point dried in a Balzers Union CPD 030. Dried specimens were sputter coated with gold in a Balzers Union SCD 040 sputter coater and viewed with a LEO 1430.

Confocal Laser Scanning Microscopy

Specimens treated with antibodies against tyrosinated α-tubulin and DAPI were examined using a Leica TCS SPE confocal laser scanning microscope (Leica Microsystems, Heidelberg, Germany). Appropriate filter settings were applied to record stacks of confocal optical sections. Stacks of confocal images of the brains were processed with Amira 5.4.3 software (FEI Visualization Sciences Group, Berlin, Germany) to create a three-dimensional (3d) model of the nervous system. Based on the tyrosinated-α-tubulin channel output of the confocal microscope the surfaces were generated using the "Volren" command.

The output of the DAPI channel of the brains was additionally used to count the approximate numbers of the respective cells. For that purpose these data were processed in Imaris 8.3.1 (Bitplane AG, Zurich, Switzerland) using the "Add new Spots" command.

Digital 3d reconstruction

The 3d models of the brains were created in Amira 5.4.3 (FEI Visualization Sciences Group, Berlin, Germany) based on the images of the serial semithin sections. Images were aligned in Amira. The resulting stack of images was used for the reconstruction of the brains with associated nerves, neural gland, gland duct, dorsal tubercle and dorsal strand.

Phylogenetic analysis

We used the latest versions of Mesquite (https://mesquiteproject.wikispaces.com) to compile a data matrix for neuroanatomical characters and PAUP (http://phylosolutions.com/paup-test/) to analyze this matrix. A parsimony analysis was conducted using the branch-and-bound option. The strict consensus

and the majority rule consensus tree was calculated from this search. Statistical support for nodes is reported as Jackknife-values based on 100 replicates with 50% character deletion and bootstrap percentages based on 100 replicates using a full heuristic search strategy with default settings.

Results

Phlebobranchiata

The neural complex of the solitary ascidian *Ascidiella scabra* is characterized by a long brain and a notably extensive neural gland situated ventral from the brain. The brain has a diameter of 200µm and a length of 1mm in an animal of 1.1cm in size. It is composed of a central neuropil and an outer layer of somata, the brain cortex (**Fig. 1A**). Two anterior, two posterior, and a single ventral visceral nerve branch off the brain. The anterior nerves mainly innervate muscles of the incurrent siphon and the peripharyngeal band, the posterior nerves project toward the muscles of the excurrent siphon and muscles of the lateral body walls, and the ventral visceral nerve extends toward the digestive tract. The latter runs in close spatial relation to the dorsal strand forming a dorsal strand plexus (**Fig. 1B**, see also interactive 3d pdf online). Stainings with antibodies against tyrosinated-α-tubulin reveal that there are no discernible fiber tracts in the brain of *A. scabra* (**Fig. 1C**). Automatic counts of the DAPI-stained nuclei showed that the brain is composed of approximately 4000 cells. Immunohistological techniques confirm the morphology of the neural complex in *A. scabra* inferred from histological serial sections. The neural gland measures 700µm in breadth and 1mm in length. The dorsal tubercle is heart-shaped and connected to the neural gland via a thin gland duct. The dorsal strand extends from the posterior part of the neural gland to the ventroposterior side of the animal.

The closely related solitary ascidian species *Ascidiella aspersa* is equally equipped with a neural gland ventral to the brain (Supplementary Fig. 1A). At a total body length of 1.5mm the elongated brain measures 100µm in diameter and 220µm in length. It is divided into a central neuropil and an outer brain cortex (Supplementary Fig. 1B). Two anterior, two posterior and one ventral visceral nerve exit the brain. The neural gland measures 75µm in diameter and 200µm in length. It possesses a heart-shaped dorsal tubercle and a dorsal strand that ends blindly ventral from the brain (Supplementary Fig. 1B, see also interactive 3d pdf online). The dorsal strand curves around the right posterior nerve and is not associated with the ventral visceral nerve.

Ascidia mentula is a solitary ascidian species that possesses a large neural gland (850µm in diameter, 2.5mm in length) positioned ventral from the brain (Supplementary Fig. 1C). In the brain, nerve fibers are arranged in the central neuropil and somata of the neurons in an outer brain cortex. The brain is elongated and measures 300µm in diameter and 1mm in length at an individual body size of 1.7cm. It possesses eight anterior nerves, two lateral nerves and eight posterior nerves. The neural gland duct is extended because the dorsal tubercle is positioned comparatively distant from the brain and therefore is not visible in the 3d reconstruction (Supplementary Fig. 1D, see also interactive 3d pdf online). The dorsal tubercle is heart-shaped. A dorsal strand is missing.

In the solitary ascidian species *Corella parallelogramma* the neural gland is situated ventral to the

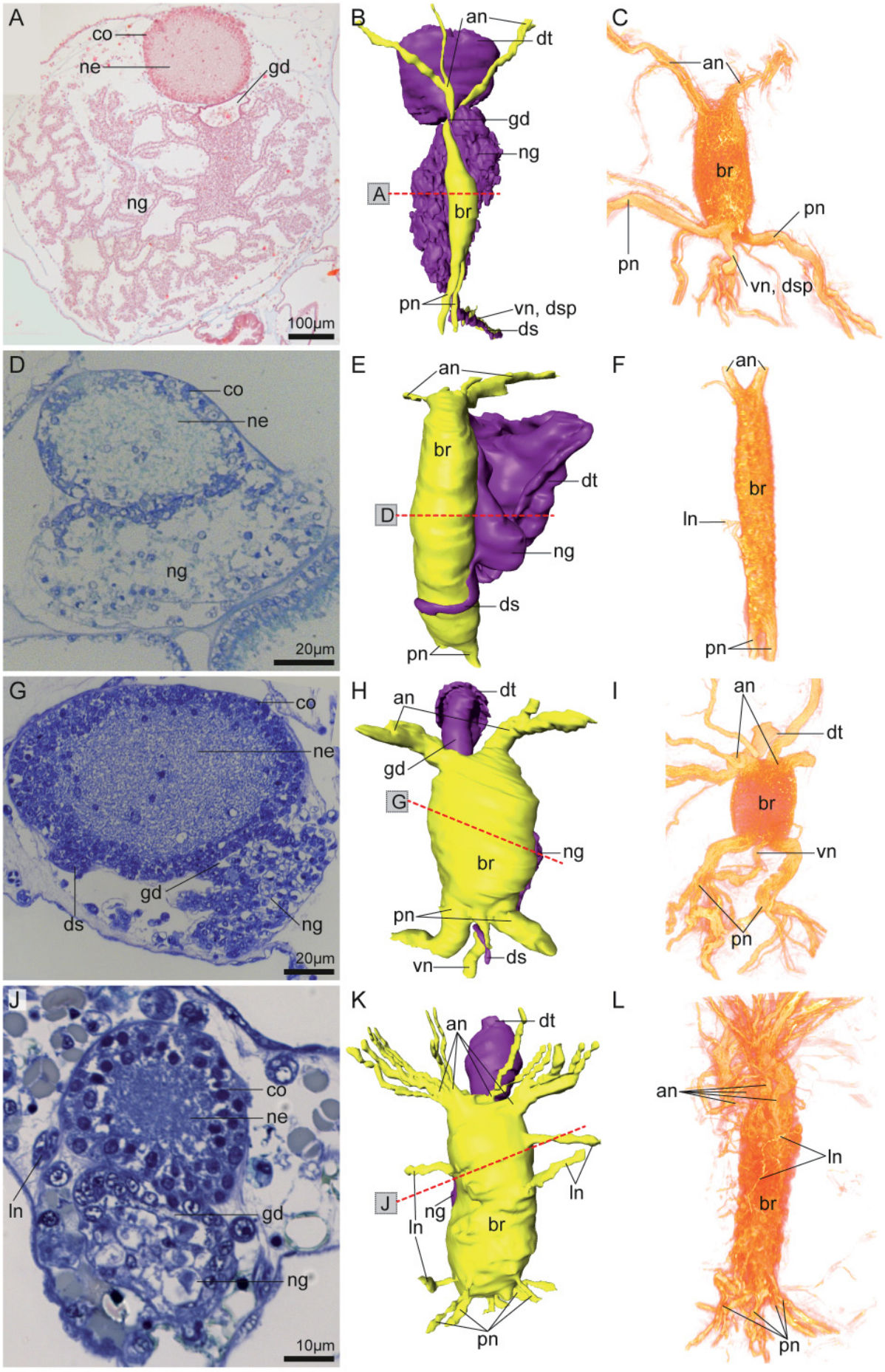
A
co
ne
gd
ng
100µm
B
an
dt
gd
ng
A
br
pn
vn, dsp
ds
C
an
br
pn
pn
vn, dsp
D
co
ne
ng
20µm
E
an
br
dt
D
ng
ds
pn
F
an
br
ln
pn
G
co
ne
gd
ds
ng
20µm
H
an
dt
gd
G
ng
br
pn
vn
ds
I
an
dt
br
vn
pn
J
co
ne
ln
gd
ng
10µm
K
an
dt
ln
J
ng
ln
br
pn
L
an
ln
br
pn

Fig. 1:

Fig. 1: Anatomy of the neural complex in Phlebobranchiata. **A, D, G, J:** Light micrographs of cross sections through the neural complexes; dorsal to the top, right to the right. The brain (br) is divided into a brain cortex (bc) and neuropil. **B, E, H, K:** 3d reconstructions of brains and nerves (yellow) and associated neural gland (ng), dorsal tubercle (dt) and dorsal strand (ds) (purple) based on serial semithin sections; dorsal view, anterior to the top. Section planes from **A, D, G, J** are indicated by dashed red lines. Interactive 3d models available in online version. **C, F, I, L:** 3d rendered signal of confocal laser scanning micrographs of brains. Immunostaining against tyrosinated-α-tubulin (orange/red), view from dorsal, anterior to the top, except from **L:** view from right side, anterior to the top. **A-C:** Neuroanatomy of *Ascidiella scabra*. The neural gland is extensive and situated ventral to the brain. A dorsal strand and dorsal strand plexus (dsp) are developed. **D-F:** Morphology of neural complex in *Corella parallelogramma*. **E:** A ventral neural gland is associated with a large intricate dorsal tubercle and a dorsal strand that ends blindly on the dorsal side of the brain. **F:** An unpaired lateral nerve (ln) is visible exiting the brain on its left side. **G-I:** Architecture of neural complex in *Ciona intestinalis*. In this specimen the dorsal tubercle is shaped simple and the dorsal strand ends shortly behind the brain. **J-L:** Morphology of neural complex in *Perophora japonica*. A ventral visceral nerve is not developed. The ventral neural gland is equipped with a simple dorsal tubercle and a very short dorsal strand that terminates on the ventral side of the brain. an: anterior nerve, gd: gland duct, ne: neurites, pn: posterior nerve, vn: ventral visceral nerve.

brain (**Fig. 1D**). The brain is elongated and divided into a central neuropil and an outer brain cortex. In an animal measuring 3.5mm in length, the brain measures 50µm in diameter and 150µm in length. Two anterior and two posterior nerves emanate from the brain. Anterior nerves mainly innervate the muscles in the incurrent siphon and the peripharyngeal band, while posterior nerves innervate the muscles of the excurrent siphon. A ventral visceral nerve is not developed. However, stainings with antibodies against tyrosinated-α-tubulin reveal that there is a single unpaired lateral nerve leaving the brain on the left side (**Fig 1F**) running toward the branchial basket. Conspicuous tracts are not detectable in the brain of *C. parallelogramma*. Utilizing DAPI stainings, automatic counts of the nuclei showed that the brain is composed of approximately 3000 cells. The neural gland of *C. parallelogramma* measures 50µm in diameter and 150µm in length. A short gland duct connects the neural gland with the large dorsal tubercle that is heart-shaped. The dorsal strand is present but ending in close spatial relation to the brain on its dorsal side (**Fig. 1E**, see also interactive 3d pdf online).

Ciona intestinalis is a solitary ascidian and a well-known model organism. Its neural complex is composed of an elongated brain and a neural gland positioned ventral to it (**Fig. 1G**). At an individual's body size of 2.2mm, brain size measures 80µm in diameter and 180µm in length. The brain is composed of a central neuropil and an outer brain cortex with two anterior, two posterior and a single ventral visceral nerve are developed. The anterior nerves extend toward the musculature of the incurrent siphon, the peripharyngeal band and oral tentacles, and ventrolateral body musculature, the posterior nerves run for the muscles of the excurrent siphon and the dorsolateral body muscles, and the ventral visceral nerve takes course toward the branchial basket and digestive tract of the animals. The ventral visceral nerve is associated with the dorsal strand, thereby constituting a dorsal strand plexus (**Fig. 1H**, see also interactive 3d pdf online). Neural complexes of *C. intestinalis* stained with DAPI and antibodies against tyrosinated-α-tubulin show that the brain possesses approximately 10 000 cells.

Careful analysis of single images in the complete stack of confocal images demonstrates that there are two anterior nerves leaving the brain and branching off again in close spatial relation to the brain. Because the antibodies stain tubulin in cilia and nerve fibers, the dorsal tubercle is visible (**Fig. 1I**). In *C. intestinalis* fiber tracts in the brain could not be observed. Immunohistoligical investigations verify the overall morphology of the brain deduced from light microscopical analysis. The neural gland measures 60µm in diameter and 90µm in length. It is equipped with an intricate heart-shaped dorsal tubercle, although this is not depicted in the 3d model, and a dorsal strand. In this specimen the dorsal strand ends posterior to the brain in close spatial relation to it, however, there are some individuals described that had an extended dorsal strand ending close to the gonads (Groepler 2016, Mackie 1995). In the colonial ascidian species *Perophora japonica* small zooids are connected via stolons. The neural complex is constituted of an elongated brain and a neural gland positioned ventral to it. The brain consists of a central neuropil and an outer layer of somata – the brain cortex (**Fig. 1J**). It measures 30µm in diameter and 80µm in length at a body size of 900µm. Four anterior nerves project mainly toward the musculature of the incurrent siphon and the peripharyngeal band, four posterior nerves mainly innervate the musculature of the excurrent siphon, and four lateral nerves run toward the branchial basket. Ventral nerves are not detectable (**Fig. 1K**, see also interactive 3d pdf in online version). Immunohistological techniques showed that the fibers in the neuropil do not show signs of organization, i.e. conspicuous tracts in the brain were not observable. Automatic counts of cell numbers revealed that approximately 2000 cells build up the brain of *P. japonica*. Stacks of confocal laser scanning micrographs of the brain labeled with antibodies against tyrosinated-α-tubulin confirm the morphology of the brain shown in the digital 3d reconstruction (**Figs. 1K, L**). The neural gland of *P. japonica* measures 30µm in diameter and 50µm in length. The dorsal strand is very short, ending blindly close to the brain on its ventral side. A short gland duct connects the neural gland to the dorsal tubercle that is simple in shape.

Aplousobranchiata

Specimens of the colonial ascidian *Clavelina lepadiformis* possess a more or less spherical brain that is composed of a central neuropil and an outer brain cortex (**Fig. 2A**). The neural gland is located on the ventral side of the brain. In an animal measuring 2.6mm in length the size of the brain is 100µm in diameter. In *C. lepadiformis* four anterior nerves project mainly toward the incurrent siphon and peripharyngeal band, six lateral nerves extend into the branchial basket, the esophagus, and digestive tract, four posterior nerves mainly innervate the muscles of the excurrent siphon and a single ventral visceral nerve runs toward the digestive tract and gonads. The ventral visceral nerve sheaths the dorsal strand on the dorsal side where the two converge; more distant from the brain, the ventral visceral nerve continues on the ventral side. Thus, the ventral visceral nerve constitutes a dorsal strand plexus (**Fig. 2B**, see also interactive 3d pdf online). Nuclei stainings with DAPI reveal that the brain is composed of approximately 4000 cells. Additionally, applying antibodies against tyrosinated-α-tubulin shows that the neuropil is void of any form of organization, i.e. specific tracts in the brain are not present (**Fig. 2C**). The morphology of the brain inferred from morphological data is in accordance with the data

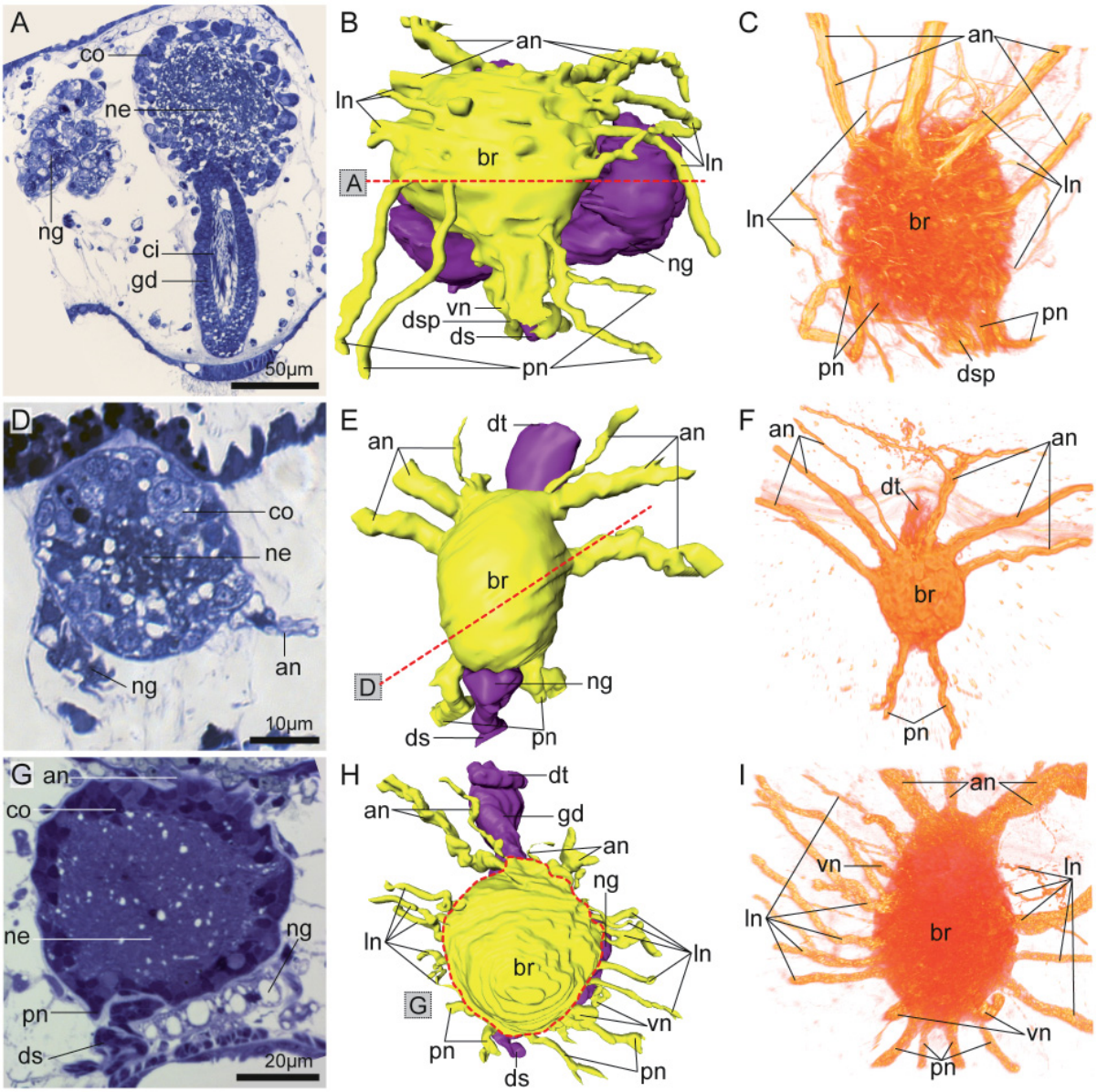

Fig. 2: Anatomy of the neural complex in Aplousobranchiata. **A, D, G:** Light micrographs of semithin sections through the neural complexes, **A, D** oblique cross sections, dorsal to the top, right to the right; **G** longitudinal section, anterior to the top, right to the right. A central neuropil and an outer brain cortex (bc) are visible. **B, E, H:** 3d reconstructions of brains (br) and nerves (yellow) and associated neural gland (ng), dorsal tubercle (dt) and dorsal strand (ds) (purple) based on serial semithin sectioning, dorsal view, anterior to the top. Dashed red lines show section planes from **A, D, G**. Interactive 3d reconstructions available in the online version. **C, F, I:** signal of confocal laser scanning micrographs of brains. Immunostaining against tyrosinated-α-tubulin (orange/red), dorsal view, anterior to the top. **A-C:** Neural complex in *Clavelina lepadiformis*, the ventral visceral nerve (vn) accompanies the dorsal strand forming a dorsal strand plexus (dsp). The neural gland is positioned on the ventral side of the brain. It opens through a simple dorsal tubercle into the branchial basket. **D-F:** Neural complex morphology in *Diplosoma listerianum*. Lateral nerves or a ventral visceral nerve are not developed. The neural gland is elongated and located on the ventral side of the brain. **G-I:** Neural complex in *Distaplia stylifera*, four ventral visceral nerves are present. The neural gland is positioned ventral to the brain. The dorsal tubercle is simple and a short dorsal strand exits the neural gland ending abruptly posterior to the brain. an: anterior nerve, ci: cilia, gd: gland duct, ln: lateral nerve, ne: neurites, pn: posterior nerve.

from immunohistological techniques. The neural gland of *C. lepadiformis* is horizontally elongated. In diameter it measures 70µm, in breadth 190µm. The dorsal tubercle opens into the branchial basket as a simple, funnel shaped hole in close spatial relation to the brain. The dorsal strand is very long, extending into the gonads of the animals.

Diplosoma listerianum are small colonial ascidians. In *D. listerianum* the neural complex consists of a brain that is more or less spherically shaped and an associated neural gland on the ventral side. With an animal size of 850µm the brain measures 30µm in diameter and is divided into a central neuropil and an outer layer of somata (**Fig. 2D**). Six anterior nerves and two posterior nerves branch off the brain. While the anterior nerves mainly run toward the incurrent siphon and branchial basket the posterior nerves project toward the excurrent siphon and digestive tract. An unpaired ventral visceral nerve and lateral nerves are missing (**Fig. 2E**, see also interactive 3d pdf online). Immunolabelings with antibodies against tyrosinated-α-tubulin show six anterior nerves and two posterior nerves. Fiber tracts in the brain were not detectable (**Fig. 2F**). Automatic counts of the DAPI-stained nuclei showed that the brain is composed of approximately 300 cells. A relatively long neural gland stretches on the ventral side of the brain (15µm in diameter, 50µm in length). It features a simply shaped dorsal tubercle and a long dorsal strand that extends into the gonads.

In the colonial ascidian species *Distaplia stylifera* the brain has an ovoid shape and associated with it a neural gland that is positioned ventral to the brain. The brain is composed of a central neuropil and an outer brain cortex. It measures 60µm in diameter in an animal measuring 1.1mm in length (**Fig. 2G**). Four anterior, ten lateral, four posterior and four ventral nerves emanate from the brain (**Fig. 2H**, see also interactive 3d pdf online). The anterior nerves mainly extend into the incurrent siphon and peripharyngeal band, the lateral nerves into the branchial basket, the posterior nerves into the excurrent siphon and the ventral nerves into the digestive tract. In stainings with antibodies against tyrosinated-α-tubulin the brain appears approximately pear-shaped. Furthermore, automatic counts in immunohistological investigations showed that there are approximately 2500 cells located in the brain and that conspicuous fiber tracts are not present in the brain of *D. stylifera*. The number of nerves in CLSM micrographs is identical to the number of the respective nerves in the histology-based 3d model (**Fig. 2I**). The associated neural gland is flat and measures only 15µm in depth, 50µm in breadth and 40µm in length. The dorsal tubercle is simple and the dorsal strand is present but ending in close proximity to the brain. A dorsal strand plexus is not developed.

Aplidium turbinatum is a colonial ascidian with a body that is divided into three parts – thorax, abdomen, and postabdomen. The neural complex consists of an ovoid brain and a neural gland positioned on the ventral side of the brain. The brain consists of an outer brain cortex and a central neuropil. In an animal that measures 5.2mm in length, the brain measures 60µm in diameter (Supplementary Fig. 1E). Six anterior nerves, four posterior nerves, and a single conspicuously thick ventral visceral nerve leave the brain. The small ovoid neural gland measures 45µm in diameter. The dorsal tubercle is simply shaped and a dorsal strand is not present (Supplementary Fig. 1F, see also interactive 3d pdf online).

Stolidobranchiata

Specimens of the small colonial ascidian species *Botryllus schlosseri* possess an exceptional brain with numerous nerves branching off. These are twelve anterior nerves, twelve lateral nerves, four posterior nerves and two ventral visceral nerves (**Figs. 3B**, see also interactive 3d pdf online, **C**). The anterior nerves mainly innervate the muscles of the incurrent siphon and the peripharyngeal band, the lateral nerves run toward the branchial basket, posterior nerves extend toward the excurrent siphon and the ventral nerves extend toward the digestive tract. The brain is divided into a central neuropil and an outer brain cortex (**Fig. 3A**). It is more or less spherically shaped, with a diameter of 30µm in animals with a body size of 500µm. Automatic cell counts utilizing DAPI stained brains showed that the brain consists of approximately 2000 cells. Neuropils labeled with antibodies against tyrosinated-α-tubulin showed no organization in conspicuous fiber tracts. Immunohistological data and histological serial sections are in accordance regarding the overall brain anatomy (**Fig. 3C**). The neural gland, dorsal tubercle, and dorsal strand are located dorsomedian from the brain. The neural gland is ovoid with a diameter of 10µm and a length of 40µm. The dorsal tubercle is developed as a simple hole. The dorsal strand ends in close spatial relation, immediately posterior to the brain.

Individuals belonging to the species *Dendrodoa grossularia* are solitary flat ascidians. The neural complexes of these animals contain an elongated brain (100µm in diameter, 200µm in length at an individual size of 1.5mm in diameter) and a neural gland that is positioned dorsally on the right side of the brain. The brain is composed of an outer layer of somata and a central neuropil (**Fig. 3D**). Four anterior nerves, two lateral nerves, two posterior nerves and a single ventral visceral nerve emanate from the brain (**Fig. 3E**, see also interactive 3d pdf online). In stainings with antibodies against tyrosinated-α-tubulin only seven of nine nerves were labeled (**Fig. 3F**). Both lateral nerves are not visible in the CLSM micrographs, either because their signal was too weak to be detected or because of penetration problems. In the brain no organized fiber tracts were detected. Automatic counts show that the brain is composed of approximately 3500 cells. The neural gland measures 80µm in diameter and 100µm in length. It is connected to an intricate dorsal tubercle via a short gland duct. A short dorsal strand is present that ends on the right side of the brain. In our specimen a dorsal strand plexus is not developed along the short dorsal strand, but it has been described by Mackie (1995).

Styela clava are solitary ascidians that are equipped with a tough leathery tunic. The neural complex is composed of an elongated brain and an extensive neural gland dorsal to the brain with parts of the gland protruding laterally on both sides of the brain. The brain consists of an outer brain cortex and a central neuropil (**Fig. 3G**). It measures 300µm in diameter and 600µm in length in an individual of 9mm body length. Two anterior, two posterior, and a ventral visceral nerve leave the brain in *S. clava* (**Figs. 3H**, see also interactive 3d pdf online, **I**). The anterior nerves innervate the muscles in the incurrent siphon, the peripharyngeal band and oral tentacles, and ventrolateral muscles of the mantle; posterior nerves innervate muscles of the excurrent siphon and dorsolateral mantle muscles, whereas the ventral visceral nerve extends toward the digestive tract. Lateral nerves or fiber tracts in the brain are not detectable. Automatic counts of the nuclei showed that the brain is composed of approximately 3000 cells. Immunohistological techniques show no indication that the neuropil is organized in fiber

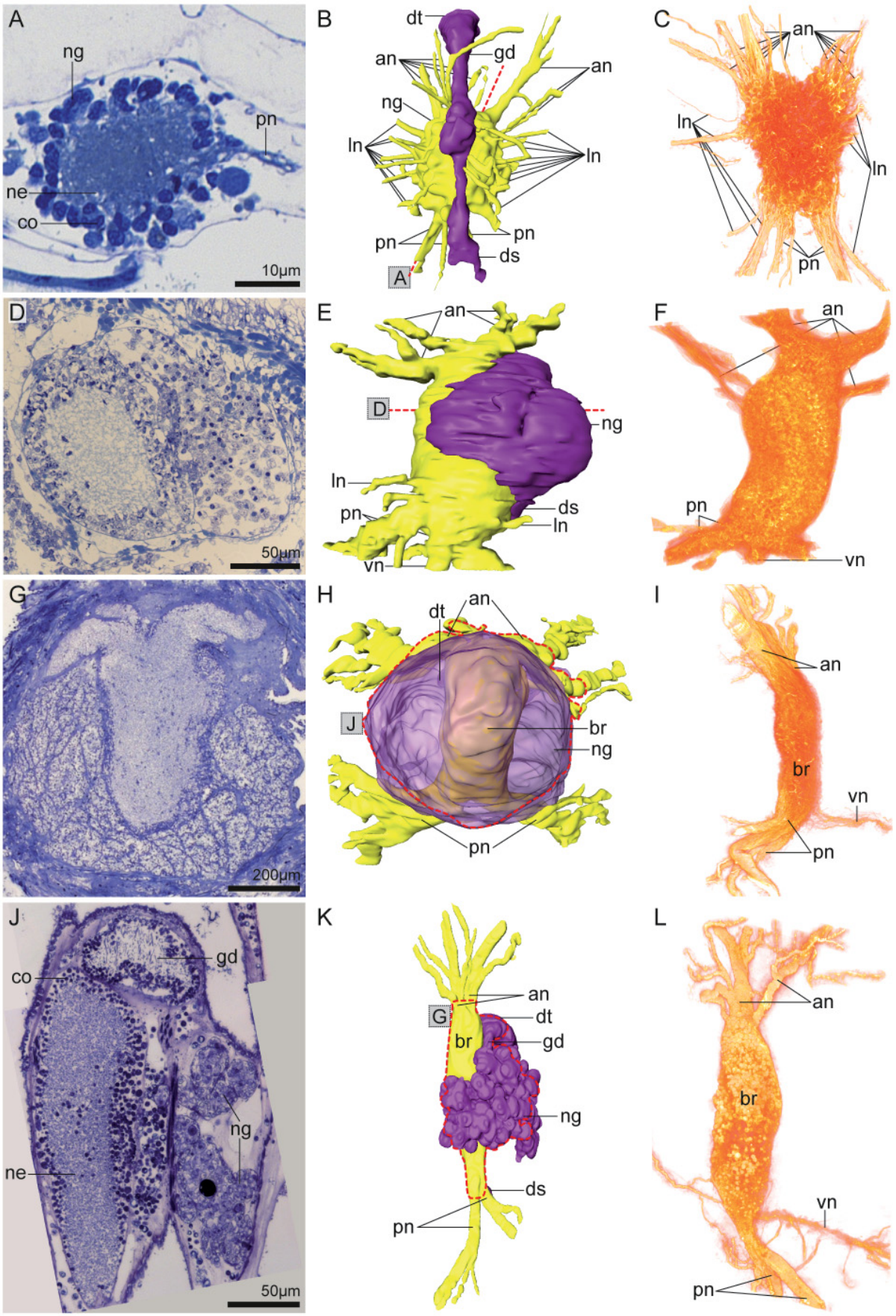

Fig. 3: Anatomy of the neural complex in Stolidobranchiata. **A, D, G, J:** Light micrographs of semithin sections through the neural complex, **A, D** oblique cross sections, dorsal to the top, right to the right; **G, J** longitudinal sections, anterior to the top, right to the right. Brains (br) of stolidobranch ascidians

are composed of a central neuropil where neurites (ne) are concentrated and an outer brain cortex (bc) where somata are situated. **B, E, H, K:** 3d reconstructions of brains and nerves (yellow), neural gland (ng), dorsal tubercle (dt), and dorsal strand (ds) (purple) based on serial semithin sections for light microscopy, dorsal view, anterior to the top. Section planes from **A, D, G, J** are illustrated by dashed red lines. Interactive 3d models are available online. **C, F, I, L:** 3d rendered signal of confocal laser scanning micrographs of brains. Immunostaining against tyrosinated-α-tubulin (orange/red); **C, F:** view from dorsal, anterior to the top; **I**, **L:** view from right side, anterior to the top. **A-C:** Morphology of the neural complex of *Botryllus schlosseri*. Two ventral visceral nerves (vn) branch off the brain. A small neural gland is located dorsal from the brain. **D-F:** Neural complex in *Dendrodoa grossularia*, the neural gland is shifted to the right side of the brain. An intricate dorsal tubercle and a short dorsal strand are present. **F:** Lateral nerves (ln) shown in **G** are not detectable. **G-I:** Morphology of neural complex in *Styela clava*. The ventral visceral nerve connects with the dorsal strand, forming a dorsal strand plexus. The neural gland is extensive and possesses an intricate dorsal tubercle. **J-L:** Anatomy of neural complex in *Molgula manhattensis*. The ventral visceral nerve is closely associated with the dorsal strand, so that a dorsal strand plexus is present. The neural gland is positioned dorsal, to the right side of the brain. The dorsal tubercle is intricate. an: anterior nerve, gd: gland duct, pn: posterior nerve.

tracts, but these data support the brain morphology inferred from histological serial sections. In size the neural gland measures 700µm in length and breadth and 500µm in depth. It possesses a short gland duct to connect the gland to the heart-shaped dorsal tubercle. Furthermore, the long dorsal strand extends toward the gonads. The dorsal strand is accompanied by the ventral visceral nerve on its left side. A dorsal strand plexus is developed.

In the solitary ascidian *Molgula manhattensis* the brain is elongated and associated with a neural gland positioned to its dorsolateral side. The major part of the neural gland is located on the right side of the brain. Brain size measures 70µm in diameter and 220µm in length in an individual with a total body length of 1.8mm. Within the brain most nerve somata are situated in an outer layer, while nerve fibers are located in a central neuropil (**Fig. 3J**). There are two anterior nerves projecting mainly into the incurrent siphon and peripharyngeal band, two posterior nerves mainly extending toward the excurrent siphon and branchial basket, and a single ventral visceral nerve that runs along the outer wall of the branchial basket toward the digestive tract. Lateral nerves are not developed (**Fig. 3K**, see also interactive 3d pdf online). Automatic cell counts in immunohistological analyses of neural complexes showed that approximately 6000 cells constitute the brain of. *M. manhattensis*. Stainings with antibodies against tyrosinated-α-tubulin revealed that the fibers in the neuropil do not show signs of organization, i.e. no conspicuous fiber tracts were present. Moreover, the immunohistological data confirmed the overall anatomy inferred from the histological sections (**Fig. 3L**). The size of the neural gland is 170µm in length 150µm in breadth and 90µm in depth. A short and thin gland duct connects the neural gland with the heart-shaped dorsal tubercle. A long dorsal strand is present that is associated with the ventral visceral nerve forming a dorsal strand plexus.

Thaliacea

Belonging to the taxon Doliolida, individuals of the species *Doliolum nationalis* possess a complex life cycle. The neural complex of the sexual generation (blastozooid, gonozooid) consists of an ovoid brain and a small neural gland on its ventral side. The brain only measures 40µm in diameter at an animal size of 700µm. It contains an outer brain cortex and a small central neuropil (**Fig. 4A**). Five anterior, two lateral, and four posterior nerves branch off the brain. A single unpaired anterior nerve leaves the brain anteromedian and runs in close spatial relation to the gland duct terminating close to the ciliated funnel. Ventral nerves, fiber tracts in the brains, eyes, or statocytes are not present (**Fig. 4B,** see also interactive 3d pdf online**, C**). The anterior nerves innervate the first three muscle bands, peripharyngeal band, and lip region. Lateral nerves run toward the gill slits of the branchial basket. Posterior nerves innervate the fourth to eighth muscle bands and cloacal opening. The brain of the blastozooid contains approximately 700 cells. The neural gland only measures 10µm in diameter. It is equipped with a neural gland duct that runs approximately 400µm anteriorly into a simply shaped dorsal tubercle. A dorsal strand is missing.

In the asexual generation (oozooid, nurse) of *D. nationalis* the neural complex is situated dorsomedian in the animal. The brain is ovoid in shape and measures 60µm in diameter in an animal with a body size of 2.5mm. Ventral to the brain a small neural gland is located. The brain is composed of an outer brain cortex and a central neuropil (**Fig. 4D**). Five anterior nerves and four posterior nerves emanate from the brain. Similar to the blastozooid stage, the brain of an oozooid possesses a single unpaired anterior nerve (**Fig. 4E,** interactive 3d model available in online pdf file, **4F**). The anterior nerves innervate the muscles anterior to the brain and the lip region, while posterior nerves innervate muscles posterior to the brain and the region of the cloacal opening. After leaving the brain, all nerves take an unusual course: They curve to the dorsal side cross the musculature and run beneath the epidermis, dorsal to the muscle fibers. Lateral and ventral nerves, brain tracts, eyes, or statocytes are not developed. In the oozooid stage the brain comprises of approximately 2000 cells. The neural gland measures 10µm in diameter. A neural gland duct extends anteriorly toward the dorsal tubercle. A dorsal strand is not present.

Specimens of the species *Iasis cylindrica* are planktonic salps that have alternating generations. In the sexual aggregate generation (blastozooid) the brain is equipped with a pigmented eye as an integrative part of the brain. The brain is composed of a central neuropil and a superficial brain cortex (Supplementary Fig. 1G, H). It is more or less spherical in shape; on its dorsal side a thin isthmus composed of neurites connects the eye to the main part of the brain. On the ventrolateral side some neurons protrude from the cortex. A neural gland is not developed, although the animals possess a simple dorsal tubercle anterior to the brain. The brain measures 110µm in diameter at a body length of 8.9mm. Two anterior, twelve lateral, and two posterior nerves emanate from it (Supplementary Fig. 1I, see also interactive 3d pdf online). Based on light microscopical analysis, the single ovoid eye dorsal to the brain is constituted of cylindrical photoreceptor cells in the center and shading pigment cells that appear black in light microscopic aspects. Pigment cells surround the photoreceptor cells laterally, anteriorly, and posteriorly. Furthermore, on the posterior part of the brain on its dorsal side

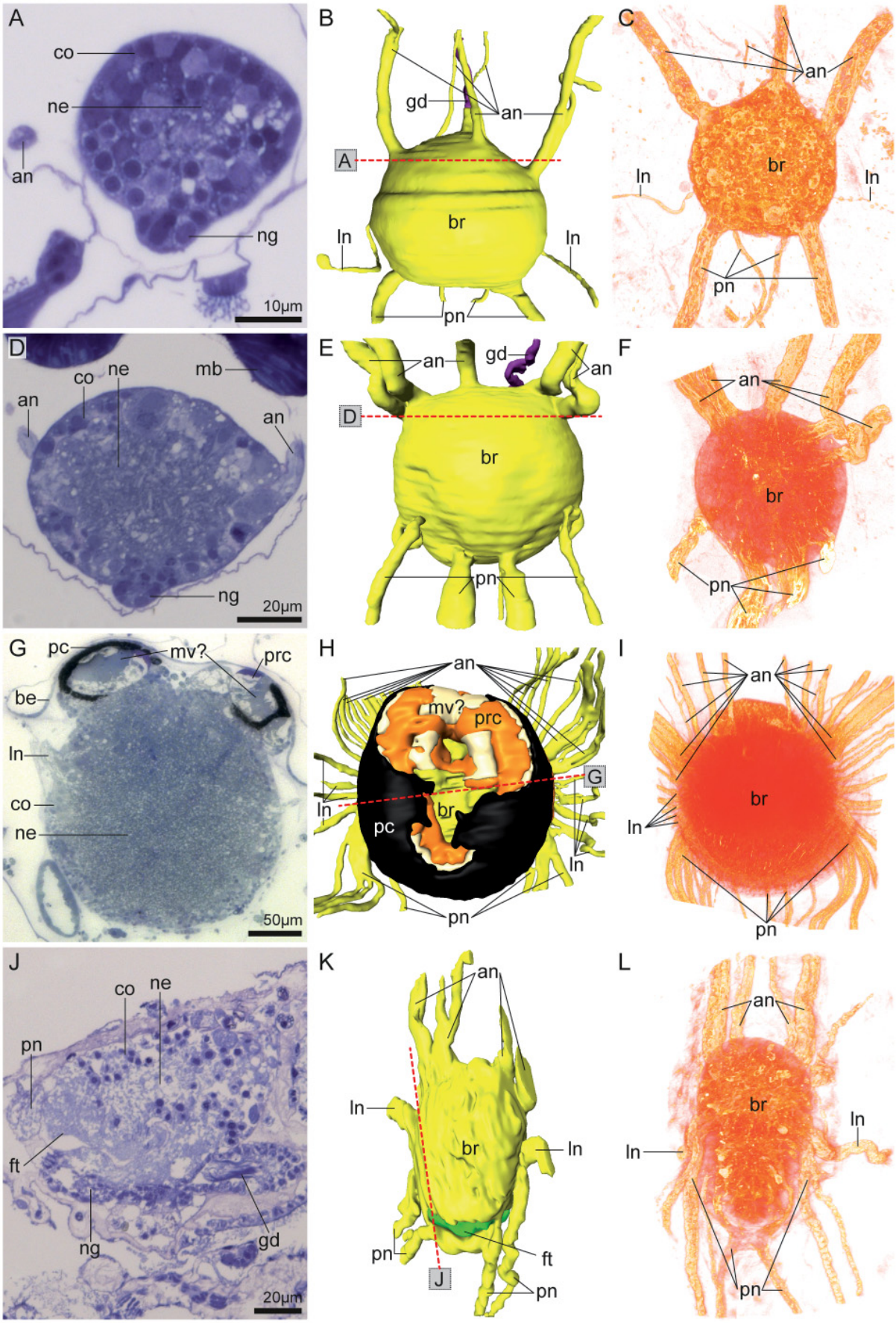

Fig. 4: Anatomy of the neural complex in Thaliacea. **A, D, G, J:** Light micrographs of cross sections through the neural complexes, dorsal to the top, right to the right. Brains are composed of a central neuropil and a superficial layer of somata, brain cortex (bc). **B, E, H, K:** 3d reconstructions of brains

(br), nerves (yellow), an integrated presumable eye (green), pigment cells (pc, black), photoreceptor cells (prc, orange), presumable microvilli (mv?, cream-colored), neural glands (ng), and gland ducts (gd) (purple); based on serial sections for light microscopy, dorsal view, anterior to the top. Red dashed lines indicate section planes from **A, D, G, J**. Interactive 3d models available in online version. **C, F, I, L:** Immunostainings against tyrosinated-α-tubulin (orange/red) are shown as 3d rendered signal of confocal laser scanning micrographs of the brains, view from dorsal, anterior to the top. **A-C:** Neuroanatomy of the sexual blastozooid generation of *Doliolum nationalis*. An unpaired anterior nerve (an) and a small neural gland are developed. **D-F:** Morphology of neural complex of the asexual oozooid generation of *D. nationalis*. All nerves take a dorsal course and run between the epidermis and the massive muscle bands (mb). An unpaired anterior nerve and a small neural gland are present. **G-I:** Architecture of brain in the oozooid stage of *Iasis cylindrica*. A horseshoe-shaped eye is present as an integrated part of the brain. A neural gland is missing. **J-L:** Morphology of the neural complex in *Pyrosoma atlanticum*. Filamentous tissue (ft) represents the remnant of the eye according to Neumann (195?). An elongated neural gland is located ventral to the brain. A simple dorsal tubercle opens into the branchial basket. be: brain epithelium, gd: gland duct, ln: lateral nerve, ne: neurites, pn: posterior nerve.

some cells reminiscent of photoreceptor cells are positioned, but they are not shaded by pigment cells (Supplementary Fig. 1H).

The brain of the asexual stage (oozooid) of *I. cylindrica* is approximately spherical. A horseshoe-shaped eye with the opening of the horseshoe directed anteriorly is an integral part of the brain; it is situated on the dorsal side of the brain. The brain is divided into a central neuropil and an outer layer of somata (cortex) (**Fig. 4G**). In an animal that measures 9.3mm in length the brain measures 220µm in diameter and length. Bilaterally symmetrical, twelve anterior nerves, eight lateral nerves, and four posterior nerves branch off the brain to mainly extend toward the muscle bands of the animal. Additionally, anterior nerves innervate the peripharyngeal band and lip region, while posterior nerves innervate the cloacal opening and digestive tract. On the ventrolateral part of the brain two symmetrical brain appendages are visible (**Fig. 4H**, see also interactive 3d pdf online). A neural gland is missing but a simple dorsal tubercle with a slit-like opening is developed anterior to the brain (Supplementary Fig. 2A). Stainings with antibodies against tyrosinated-α-tubulin reveal two paraxial neuropils in the eye region (Supplementary Fig. 1J) and lateral fiber tracts on the ventral side of the brain (Supplementary Fig. 1K). Automatic counts of nuclei utilizing DAPI calculated that the brain is composed of approximately 8000 cells. The eye is built up of photoreceptor cells and pigment cells. Pigment cells are visible as cells with black content in toluidine-stained preparations and they confine the eye laterally and posteriorly. In the posterior eye region pigment cells cover photoreceptor cells dorsally without contacting the pigment cells of the opposite side of the horseshoe, leaving a narrow gap in this posterior part (Supplementary Fig. 1K).

Pyrosoma atlanticum are colonial planktonic thaliaceans within the taxon Pyrosomatida that are famous for their bioluminescence. The neural complex of the animals comprises an ovoid brain with an elongated neural gland on the ventral side of the brain. The brain measures 50µm in diameter and

80µm in length in zooids of 1.5mm in body length. It is divided into a neuropil and an outer brain cortex (**Fig. 4J**). A filamentous tissue in the ventroposterior part of the brain (**Fig. 4J**) that in living animals can be seen as red-pigmented areas probably corresponds to the pyrosome eye described by Neumann (1909). However, we could not identify photoreceptor cells or pigment cells. Four anterior nerves, two lateral nerves, and two posterior nerves leave the brain. The bilaterally symmetrical posterior nerves that are positioned closer to the median line of the brain converge again after having left the brain before diverging again, thereby forming an x-shape in dorsal view (**Figs. 4K**, see also interactive 3d pdf online, **L**). Therefore, these posterior nerves leave open a region through which light might penetrate onto the presumable eye. Anterior nerves mainly project toward the incurrent siphon and peripharyngeal band, lateral nerves run toward the digestive tract, and posterior nerves extend toward the excurrent siphon. Immunolabelings with antibodies against tyrosinated-α-tubulin show lateral fiber tracts in the ventral part of the brain (Supplementary Fig. 1L). Nuclei stainings with DAPI showed that the brain consists of approximately 2000 cells. Immunohistological data also confirm numbers and positions of nerves. The neural gland of *P. atlanticum* is elongated and situated ventral to the brain. It measures 80µm in length and 40µm in diameter at its greatest expansion. It is connected to a simple dorsal tubercle by a short gland duct. A dorsal strand is not detectable.

Appendicularia

Specimens of *Oikopleura dioica* are small planktonic tunicates that build filter-feeding houses. The neural complex of *O. dioica* has aptly been described by Olsson et al. (1990) and Holmberg (1982). Our results confirm the morphology of the neural complex reported in these studies (**Fig 5A-D**). We add that the entire brain measures 10µm in diameter and 40µm in length in an animal with a trunk length of 270µm. The small neural gland is positioned on the right side of the brain **(Fig. 5A, C**). It measures 30µm in length, 20µm in breadth and 7µm in depth. The opening of the dorsal tubercle into the pharynx is simply shaped and connected to the neural gland by a short gland duct. A dorsal strand is not developed. CLSM micrographs of immunohistochemical stainings with antibodies against tyrosinated-α-tubulin indicate that a thin neuropil is lined by somata (**Fig 5D**). Automatic counts of nuclei resulted in approximately 150 cells that are located in the neural complex. Transmission electron micrographs reveal a neuropil (**Fig. 5B**) that approximately measures 5µm in diameter.

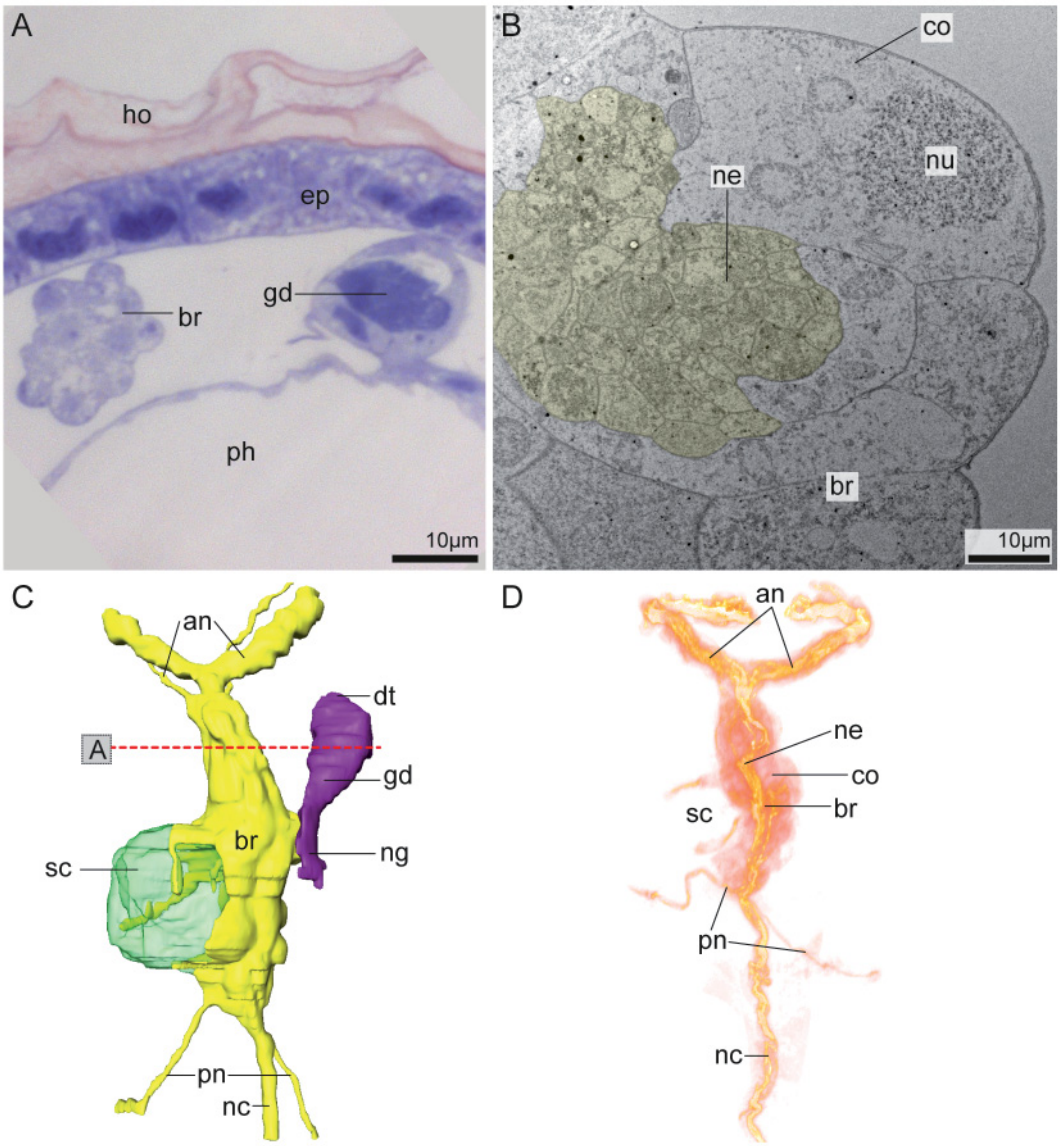

Fig. 5: The neural complex in *Oikopleura dioica*. **A:** Light micrograph of a cross section through the neural complex, dorsal to the top, right to the right. **B:** Transmission electron micrograph of the brain (br). It is composed of a central region where neurites (ne) are concentrtated (neuropil, yellow colored area) and a superficial layer of somata (brain cortex, bc). **C:** 3d reconstruction of brain and nerves (yellow) and associated neural gland (ng), gland duct (gd) and dorsal tubercle (dt) (purple) based on serial semithin sections, dorsal view, anterior to the top. Section plane from **A** indicated by a dashed red line. Interactive 3d model available in online version. The neural gland, gland duct and dorsal tubercle are situated on the right side of the brain. **D:** 3d rendered signal of confocal laser scanning micrographs of the brain. Immunostaining against tyrosinated-α-tubulin (orange/red), view from dorsal, anterior to the top. an: anterior nerve, ep: epidermis, ho: house remnant, nc: nerve cord, nu: nucleus, ph: pharynx, pn: posterior nerve, sc: statocyste.

Table 2: Character matrix, showing the distribution of different neuronal characters in adults of different tunicate, one cephalochordate (*B. lanceolatum*), and one vertebrate (*P. marinus*) species. For *T. democratica, I. cylindrica,* and *D. nationalis* both stages are presented (variations shown as "blastozooid" & "oozooid")

character taxon	Brain divided into cortex and neuropil	Anterior nerves	Unpaired antero-median nerve	Number of anterior nerve pairs	Posterior nerves	Number of posterior nerve pairs	Lateral nerves	Unpaired lateral nerve	Number of lateral nerve pairs	Posterior neural tube	Ventral visceral nerves
Branchiostoma lanceolatum	-	+	?	>1	?	?	+	?	?	+	-
Petromyzon marinus	-	+	?	>1	?	?	+	?	?	+	-
Oikopleura dioica	+	+	-	>1	+	1	-	-	n.a.	+	-
Molgula manhattensis	+	+	-	1	+	1	-	-	n.a.	-	+
Dendrodoa grossularia	+	+	-	>1	+	1	+	-	1	-	+
Styela clava	+	+	-	1	+	1	-	-	n.a.	-	+
Botryllus schlosseri	+	+	-	>1	+	>1	+	-	>2	-	+
Perophora japonica	+	+	-	>1	+	>1	+	-	2	-	-
Ciona intestinalis	+	+	-	1	+	1	-	-	n.a.	-	+
Corella parallelo-gramma	+	+	-	1	+	1	+	+	n.a.	-	-
Ascidia mentula	+	+	-	>1	+	>1	+	-	1	-	-
Ascidiella scabra	+	+	-	1	+	1	-	-	n.a.	-	+
Ascidiella aspersa	+	+	-	1	+	1	-	-	n.a.	-	+
Clavelina lepadiformis	+	+	-	>1	+	>1	+	-	>2	-	+
Distaplia stylifera	+	+	-	>1	+	>1	+	-	>2	-	+
Aplidium turbinatum	+	+	-	>1	+	>1	-	-	n.a.	-	+
Diplosoma listerianum	+	+	-	>1	+	1	-	-	n.a.	-	-
Pyrosoma atlanticum	+	+	-	>1	+	>1	+	-	1	-	-
Thalia democratica	+	+	-	1&>1	+	1&>1	+	-	2&>2	-	-
Iasis cylindrica	+	+	-	1&>1	+	1&>1	+	-	>2	-	-

character taxon	Number of ventral visceral nerves	Dorsal tubercle	Shape of dorsal tubercle	Neural gland duct	Length of neural gland duct	Neural gland	Ventral position of neural gland	Neural gland shifted to the right or dorsomedian	Neurite tract	Dorsal strand	Dorsal strand plexus	Adult brain with eyes	Adult brain with statocyte	Brain appendages
B. lanceolatum	n.a.	+	simple	+	short	+	+	n.a.	+	-	-	+	-	-
P. marinus	n.a.	+	simple	+	short	+	+	n.a.	+	-	-	+	-	-
O. dioica	n.a.	+	simple	+	short	+	-	right	-	-	-	-	+	-
M. manhattensis	1	+	intricate	+	short	+	-	right	-	+	+	-	-	-
D. grossularia	1	+	intricate	+	short	+	-	right	-	+	+	-	-	-
S. clava	1	+	intricate	+	short	+	-	dorsomedian	-	+	+	-	-	-
B. schlosseri	>1	+	simple	+	short	+	-	dorsomedian	-	+	-	-	-	-
P. japonica	n.a.	+	simple	+	short	+	+	n.a.	-	+	-	-	-	-
C. intestinalis	1	+	intricate	+	short	+	+	n.a.	-	+	+	-	-	-
C. parallelogramma	n.a.	+	intricate	+	short	+	+	n.a.	-	+	-	-	-	-
A. mentula	n.a.	+	intricate	+	elongated	+	+	n.a.	-	-	-	-	-	-
A. scabra	1	+	intricate	+	short	+	+	n.a.	-	+	+	-	-	-
A. aspersa	1	+	intricate	+	short	+	+	n.a.	-	+	-	-	-	-
C. lepadiformis	1	+	simple	+	short	+	+	n.a.	-	+	+	-	-	-
D. stylifera	>1	+	simple	+	short	+	+	n.a.	-	+	-	-	-	-
A. turbinatum	1	+	simple	+	short	+	+	n.a.	-	-	-	-	-	-
D. listerianum	n.a.	+	simple	+	short	+	+	n.a.	-	+	-	-	-	-
P. atlanticum	n.a.	+	simple	+	short	+	+	n.a.	+	-	-	+	-	-
T. democratica	n.a.	+	simple	-	n.a.	-	n.a	n.a.	+	-	-	+	-	+
I. cylindrica	n.a.	+	simple	-	n.a.	-	n.a	n.a.	+	-	-	+	-	+
D. nationalis	n.a.	+	simple	+	elongated	+	+	n.a.	-	-	-	-	-	-

+ present; - absent; ? data are missing; n.a. character not applicable; References: *B. lanceolatum* (Wicht & Lacalli 2005), *P. marinus* (Richardson, Admiraal & Wright 2010), *T. democratica* (Braun & Stach 2017)

Discussion

The term neurophylogeny conveys the promise that nervous systems can constitute a valuable source of information to elucidate phylogenetic and evolutionary questions. This is especially true for tunicates, because molecular phylogenies (Delsuc et al. 2006, Swalla & Smith 2008, Kocot, Tassia, Halanych, & Swalla 2018) supported a sister group relationship between tunicates and vertebrates and inferred that tunicates derived from an actively free-swimming fish-like ancestor. It is therefore surprising that broad comparative anatomical studies of adult tunicate nervous systems have not been conducted in a modern conceptual framework (see reviews by Mackie & Burighel 2005, Manni & Pennati 2016). Light microscopic studies in several selected species have been performed in the beginning of the 20th century (see Huus 1956, and Drach 1948 for review), but in the more recent era, few studies limited to specific taxa and stages have been published (e.g. Braun & Stach 2017, Burighel, Sorrentino, Zaniolo, Thorndyke, & Manni 2001, Mackie 1995, Olsson et al. 1990). This is quite contrary to investigations of the free-swimming larval stages, especially in the two model species *Ciona robusta* and *Halocynthia roretzi* (e.g. Ryan et al. 2018, Takamura et al. 2010). Here we ameliorated this situation and presented a detailed description of the neural complexes of adult specimens of 15 tunicate species covering all major tunicate clades, allowing for detailed comparisons, considerations of homology hypotheses, and evolutionary inferences.

In several species the anatomy of the adult neural complex has been analyzed in some detail (e.g., Koyama & Kusunoki 1993, Manni et al. 1999, Lacalli & Holland 1998; see also recent review by Manni & Pennati 2016). While these studies already demonstrated a considerable diversity of structures within the nervous system, in modern publications these anatomical studies are generally summarized as a brain consisting of a cortex of neuronal somata surrounding a compact neuropil; five main nerves leaving the brain: two anterior nerves, two, posterior nerves, and a single posterior-ventral visceral nerve; and associated with the brain a neural gland that is a sac-like organ, opening via a ciliated duct and a funnel-shaped dorsal tubercle into the prebranchial region (e.g., Burighel & Cloney 1997, Manni & Pennati 2016). Indeed, because the larval nervous system aroused more interest, one review drily states, that "The adult ascidian brain, by contrast, tends to be seen as a relatively uninteresting structure" (Mackie & Burighel 2005). Our investigations improved traditional light microscopical approaches by adding serial sectioning techniques and computer assisted 3d reconstructions and combined them with immunohistological stainings and confocal laser scanning microscopy (CLSM). Overall, we confirm previous anatomical studies but demonstrated that variability is considerable especially on the interspecific level.

Computer assisted 3d reconstructions of complete serial sections of neural complexes gave the most detailed picture of these anatomical structures. However, because this technique is time-consuming only few individuals of a species have been studied in this way. CLSM on the other hand, allowed us to corroborate the findings from the 3d reconstructions in several (up to 10) specimens of the same species. The variation among individuals of the same species is minor. The shapes and positions of the brain, the neural gland, the neural gland duct, the dorsal tubercle, and the dorsal strand were highly similar in all specimens of the same species examined. Some of these characters, e.g., the position of the neural

gland or the shape of the dorsal tubercle, have been widely used as characters for species identification (e.g., Berrill 1950, Kott 1985, 1990, 1992, 2001, Van Name 1945, Monniot & Monniot 1972), which of course agrees with our assessment. While with one exception the numbers and positions of the nerves leaving the brain were identical in all specimens of the same species, the exact course after leaving the brain could differ. E.g., in *C. intestinalis* the right anterior nerve branches into two nerves shortly after exiting the brain while in another specimen this division is located more distant from the brain **(Figs. 1 H, L)**. The exception mentioned above was *D. grossularia,* where the 3d reconstructed specimen possessed a pair of lateral nerves that was not detectable in the CLSM experiments. Here we suspect that staining experiments failed to visualize the fine lateral nerves either because of a weak immunoreactivity or penetration problems of the antibodies. In conclusion, the comparisons of our anatomical data demonstrate that the variation concerning characters of the neural complex within a species is limited and therefore, these characters are in principle valuable for phylogenetic evaluation. Comparison of neural complexes of different tunicate species revealed enough similarities to support specific hypotheses of homology. Moreover, the comparison also showed that the neural complex consists of several characters that show clear interspecific variation, can therefore evolve independently, and consequently can be used in order to infer phylogenetic relationships. The main part of the neural complex consists of a brain that is organized as a ganglion (sensu Richter et al. 2010), i.e. possesses a central neuropil and a cortex where most of the neuronal somata are located. Conspicuous nerves are leaving the brain. We consider the paired nerves that leave the brain anteriorly and project toward the group of oral sphincters and the peripharyngeal band as homologous and following Julin (1881) we named them anterior nerves. Besides their connection to the sphincter muscles the anterior nerves carry sensory fibers to the oral tentacles where they probably receive input from the coronal organ (Burighel et al. 2003, Rigon et al. 2013). In species in which lateral nerves are not developed, the anterior nerves that extend toward the peripharyngeal band are branched sending out nerves to the ventral mantle musculature. In these cases the dorsal mantle musculature is innervated by branches of the posterior nerves. There are usually one or two pairs of anterior nerves, but in *A. mentula*, *B. schlosseri*, *D. listerianum*, and *A. turbinatum* additional anterior nerves are developed. The additional anteromedian nerve exiting the brain in *Doliolum nationalis* has no corresponding counterpart in other tunicate taxa. In the investigated species one or two pairs of posterior nerves are present, with the exception of *A. mentula*, where four pairs of posterior nerves occur.

The tunicate brain in most taxa is associated with a more or less extensive glandular structure, the neural gland. This gland opens in most taxa via a more or less extensive tube-like channel through a ciliated funnel into the branchial basket in the dorsal midline, just posterior to the mouth opening. This ciliated funnel is elevated and thus the structure is called the dorsal tubercle. The dorsal tubercle can be just that, a simple funnel shaped opening or the funnel can be narrowed, curved, with horns enrolled or even more complex. While the functions of this brain associated gland and its duct and opening are still unclear (Ruppert 1990, Gorbman 1999), the presence of gonadotropin stimulating hormones (Chang, Lui, & Chen 1982, Tsutsui, Yamamoto, Ito, & Oka 1998, Kah et al. 2007) and the anatomical similarities especially in developmental stages have been taken as evidence to homologize the neural

gland with the adenohypophysis in vertebrates and Hatschek's pit and groove in cephalochordates (Stach 1996, Gorbman 1999, Burighel et al. 1998; but see Ruppert 1990 for a conflicting hypothesis). Within tunicates, all these elements just mentioned vary to a certain extent and are therefore evolutionarily independent. E.g., the neural gland itself is in most species quite extensive and situated on the ventral side of the brain. This incidentally is the plesiomorphic condition as revealed by outgroup-comparison. In stolidobranch ascidians, however, the neural gland can be found on the right side of the brain or, in some cases (*S. clava*, *B. schlosseri* in our study) even on the dorsal side of the brain. In several species the neural gland is somewhat reduced (*B. schlosseri*), almost completely reduced to a few cells at the blind end of the duct connected to the ciliated funnel (*O. dioica*), or entirely reduced (*I. cylindrica*), although transmission electron microscopic studies are lacking for salps, and peculiarly a dorsal tubercle – yet without a gland duct – is present.

The dorsal tubercle on the other hand is also variable. The simple funnel-shape is found, e.g., in all aplousobranch species, but also in the colonial phlebobranch *P. japonica* and the colonial stolidobranch *B. schlosseri* with their miniaturized zooids. At the other end of the anatomical sophistication of the dorsal tubercle, very similar u-shaped forms can be found in the larger solitary ascidians. Thus, u-shaped and more elaborately structured dorsal tubercles derived from the u-shape are present in Phlebobranchiata and Stolidobranchiata. Usually, the peculiarly isolated dorsal tubercles in salp species are relatively simple, yet they also vary between a simple funnel shape, a more elongated, slit-like form and a complex intricate shape (see Supplementary Figure 2).

The central neuropil in the tunicate brains did show no sign of obvious subdivisions or internal structures with the techniques applied, although several immunohistochemical markers have been tested (see e.g., Braun & Stach 2016). Only in the planktonic pyrosomes and salps a pair of lateral fiber tracts has been identified using immunohistochemical staining against tyrosinated-α-tubulin. Interestingly, both of these taxa reportedly possess elaborate optical sensory structures in form of eyes. While these eyes are well documented in the salp species (Braun & Stach 2017 and references therein), the reports for pyrosomes are more circumstantial and modern anatomical investigations are warranted (see Neumann 1956).

We conceptualized the documented character distribution in form of a cladistic character matrix for the 19 tunicate and two outgroup taxa and 25 neural complex characters, of which 19 were parsimony informative (see **Table 2**). Given the low number of characters compared to the number of taxa, we did not expect to resolve phylogenetic relationships within tunicate taxa, but gauge the potential contribution of neural complex characters toward such a goal. A branch and bound search using this limited character matrix resulted in 30 equally parsimonious trees. The strict consensus of these trees (see Supplementary Figure 4) shows a monophyletic Tunicata, Salpida, and a group consisting of solitary ascidians excluding *Ascidia mentula*. While the two former are found in traditional systematic classifications (e.g., Drach 1948, Hyman 1959, Ax 2001), and are also recovered in molecular phylogenetic analyses (Tsagkogeorga et al. 2009, Govindarajan et al. 2011), the latter is obviously not monophyletic. Tree length of the most parsimonious solutions was 36 with a consistency index of 0.64, indicating a comparatively low level of homoplasy. Whereas the explanatory power of this narrow set

of characters is poor, there are potential synapomorphies in features of the overall neural architecture from the present analysis that support traditional monophyletic taxa such as Thaliacea (neurite tracts, cerebral eyes, reduction of ventral visceral nerve and dorsal strand) as well as Stolidobranchiata (neural gland not ventral to brain). However, none of these synapomorphies are without homoplasy. Thus, we conclude that phylogenetic signal is present in the neural complex characters data, yet it is insufficient to resolve internal tunicate phylogenetic relationships. While this does demonstrate that these characters can be parsimony informative and will proof useful additions in larger analyses, it does not replace other morphological or molecular phylogenetic approaches. In any case, because character transformation is an important part of evolutionary analyses, we plotted our densely sampled neural complex data on a recently published phylogenetic hypothesis (Kocot et al. 2018) in order to track character transformations and their potential relation to life-history evolution within tunicates (Fig. 6, Supplementary Fig. 3).

Tracing neural complex character transformations in this way reveals that the evolution of the neural complex is clearly correlated with the evolution of the life-history strategies reconstructed in the stem lineage of a taxon. An instructive example for this is seen in the evolution of a holoplanktonic life-history

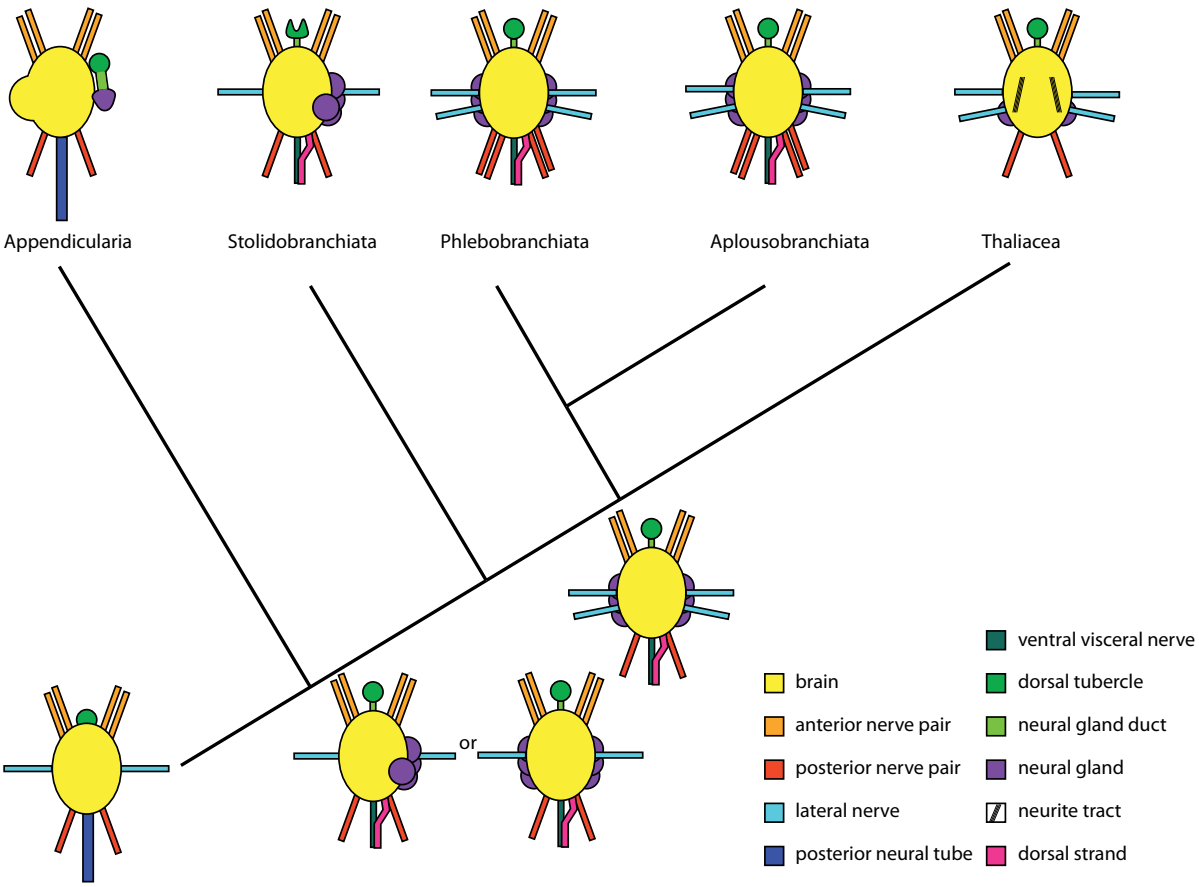

Fig.6: Schematic representations of neural complexes, and inferred ancestral states plotted on the phylogeny of higher tunicate taxa based on a recent molecular phylogenetic analysis (Kocot et al. 2018, see also supplementary Fig. 3 for a more detailed representation).

strategy in the last common ancestor of Thaliacea. Here, the reconstruction implies that concordant with the life-habit change toward more motility in the stem lineage of Thaliacea the evolution of lateral fiber tracts is seen. In addition, a more complex optical system in form of cerebral eyes has evolved. All of these transformations attest to the need for a more elaborate central nervous coordination in the planktonic forms. Within Thaliacea we then reconstruct the reduction of anterior and posterior nerves, and also of the neural gland together with the gland duct in the stem lineage of Salpida. Surprisingly, the dorsal tubercle, i.e. the opening of the neural gland-duct system is still present in salps and may be quite extensive and diverse in different salp species (Supplementary Fig. 2). Transmission electron microscopic investigations of the dorsal tubercle in any salp species are lacking (Mackie and Burighel 2005, Bone 1998) but would be imperative to rule out the possibility that remnants of the neural gland or the gland duct are still present. Such an investigation might yield additional arguments to suggest functions for this subsystem of the neural complex. Incidentally, while in spite of its miniature size, the neural complex of appendicularians is also relatively complex, it shows marked differences to the neural complex in thaliaceans. Both taxa are holoplanktonic, yet appendicularians lack eyes, but instead feature a statolith as an apomorphic trait in the adults and a posterior neural tube as a plesiomorphic character inherited with little change from the last common ancestor of Chordata.

Tunicate diversity offers also opportunities to analyze concepts about the correlation of evolutionary transformations of nervous system anatomy with miniaturization. Asexual reproduction leading to a colonial mode of life has occurred several times independently within tunicates (Lemaire 2011). In the sessile ascidians e.g., this mode of reproduction evolved at least three times independently once in each of the higher taxa Aplousobranchiata, Phlebobranchiata, and Stolidobranchiata (Stach & Turbeville 2002, Brown & Swalla 2012). Despite displaying great morphological variety, the colonial sessile ascidians share some remarkable similarities. Most obviously, the individual zooids are considerably smaller (in the mm range) compared to the sessile solitary ascidians, which are usually in the cm to dm range in size. In addition, larvae of colonial species are relatively large, often in the same size range as the zooids, are brooded over a longer period, and spend only a short time swimming freely in the water, often only minutes. Solitary species to the contrary possess considerably smaller larvae that develop freely in the water column, and spend a longer time actively swimming in the water, usually hours to days. Morphologically, brains of adult miniaturized colonial ascidian species show similarities in the development of additional anterior, posterior, lateral, ventral visceral nerves, and a dorsal tubercle that is shaped as a simple ciliated funnel. These similarities probably have to be evaluated as cases of convergent evolution because of similar life-habit changes toward living as small zooids in colonies.

In many vertebrate taxa, brain-to-body mass ratios roughly yield a linear correlation at least if related species are compared (van Dongen 1998, Roth & Dicke 2005). We investigated, whether a similar correlation exists across tunicates or subtaxa thereof. As an approximation we tabulated brain length versus body length, number of neurons versus body length as well as number of neurons versus body length. In general, there is an apparent correlation between brain length and body length (see Supplementary Fig. 5). Clearly, the smaller specimens, including the small colonial species, have smaller brains. Whether phylogenetic position (and therefore evolutionary trends) influences this correlation,

cannot be asserted based on the relatively low sample size in our current study. The observed strength of the correlation (r^2= 0.74) (brain length/body length) might be also misleading, because of the low number of species and individuals analyzed. With these limitations in mind, our data indicate that this correlation applies to tunicate species independent of their taxonomic position.

If one considers neuron counts instead of brain length as a variable, (see Supplementary Table 2) the linear correlation is considerably weaker (r^2=0.16). It is tempting to interpret the relatively high neuron number to brain length ratio in *C. intestinalis* as a sign of increased neuronal capacity, although it is difficult to see the role of such an increased capacity in the life of a sessile filter feeder. Maybe, this can be attributed to an ancestry of a more active, free-swimming ancestor, often implied in the Olfactores-hypothesis (Swalla & Smith 2008). This would, however, necessitate the retaining of a plesiomorphic condition in the nervous system of *C. intestinalis*. *C. intestinalis* has on occasion been considered as an early branching taxon within tunicates (Plough 1978) but this is not supported in the recent molecular phylogenies, supporting the close relationship between Tunicata and Vertebrata (i.e., the Olfactores-hypothesis).

Acknowledgements

We are grateful for access to the tunicate collection and to the Leica SPE CLSM granted by Priv.-Doz. Dr. Carsten Lüter (Museum für Naturkunde Berlin). Financial support by the Deutsche Forschungsgemeinschaft (DFG), the German Academic Exchange Service (DAAD) and the Elsa-Neumann-Stipendium des Landes Berlin is gratefully acknowledged. We are thankful to the invaluable help of Woody Lee and Scott Jones from the Smithsonian Marine Station in Fort Pierce, Florida in securing specimens of *Iasis cylindrica* and *Doliolum nationalis*. We are also indebted to Prof. Valerie Paul and Prof. Mary Rice for generously providing access to the facilities of the Smithsonian Marine Station. We are much obliged to Dr. Nina Furchheim for collecting and fixing specimens of *Pyrosoma atlanticum* during the R/V SONNE expedition SO258 leg 1.

References

Ax, P. (2001). *Das System der Metazoa III: Ein Lehrbuch der phylogenetischen Systematik*: Spektrum Akademischer Verlag.

Berrill, N. J. (1950). *The Tunicata – with an account of the British species*. London: The Ray Society.

Bone, Q. (1998). *The biology of pelagic tunicates*. Oxford: Oxford University Press.

Braun, K., & Stach, T. (2016). Comparative study of serotonin-like immunoreactivity in the branchial basket, digestive tract, and nervous system in tunicates. *Zoomorphology, 135*(3), 351-366. doi: 10.1007/s00435-016-0317-8.

Braun, K., & Stach, T. (2017). Structure and ultrastructure of eyes and brains of *Thalia democratica* (Thaliacea, Tunicata, Chordata). *Journal of Morphology, 278*(10), 1421-1437. doi: 10.1002/jmor.20722

Brown, F. D., & Swalla, B. J. (2012). Evolution and development of budding by stem cells: Ascidian coloniality as a case study. *Developmental Biology, 369*(2), 151-162. doi: 10.1016/j.ydbio.2012.05.038

Burighel, P., & Cloney, R. (1997). Urochordata: Ascidiacea. In F. W. Harrison & E. E. Ruppert (Eds.), *Microscopic Anatomy in Invertebrates, Vol. 15, Hemichordata, Chaetognatha, and the invertebrate chordates*. New York: Wiley-Liss.

Burighel, P., Lane, N. J., Fabio, G., Stefano, T., Zaniolo, G., Carnevali, M. D. C., & Manni, L. (2003). Novel, secondary sensory cell organ in ascidians: In search of the ancestor of the vertebrate lateral line. *The Journal of Comparative Neurology, 461*(2), 236-249. doi: 10.1002/cne.10666

Burighel, P., Lane, N. J., Zaniolo, G., & Manni, L. (1998). Neurogenic role of the neural gland in the development of the ascidian, *Botryllus schlosseri* (Tunicata, Urochordata). *Journal of Comparative Neurology, 394*(2), 230-241. doi: 10.1002/(SICI)1096-9861(19980504)394:2<230::AID-CNE7>3.0.CO;2-3

Burighel, P., Sorrentino, M., Zaniolo, G., Thorndyke, M. C., & Manni, L. (2001). The peripheral nervous system of an ascidian, *Botryllus schlosseri*, as revealed by cholinesterase activity. *Invertebrate Biology, 120*(2), 185-198. doi: 10.1111/j.1744-7410.2001.tb00123.x.

Chang, C. Y., Chu, Y., & Chen, D. (1982). Immunocytochemical demonstrations of luteinizing hormone (LH) in Hatschek's pit of Amphioxus (*Branchiostoma belcheri* Gray). *Kexue Tongbao, 27*, 1233-1234.

Dahlberg, C., Auger, H., Dupont, S., Saakura, Y., Thorndyke, M. C., & Joly, J.-S. (2009). Refining the *Ciona intestinalis* model of central nervous system regeneration. *PLoS One, 4*(2), e4458-e4458.

Delsuc, F., Brinkmann, H., Chourrout, D., & Philippe, H. (2006). Tunicates and not cephalochordates are the closest living relatives of vertebrates. *Nature, 439*(7079), 965-968. doi: 10.1038/nature04336

Drach, P. (1948). Embranchement des Céphalochordés. In P. P. Grassé (Ed.), *Traité de zoologie, vol. 11* (pp.931-1037). Paris: Masson & Cic.

Dunn, C. W., Hejnol, A., Matus, D. Q., Pang, K., Browne, W. E., Smith, S. A., . . . Giribet, G. (2008). Broad phylogenomic sampling improves resolution of the animal tree of life. *Nature, 452*(7188), 745-749. doi: 10.1038/nature06614

Edgecombe, G. D., Giribet, G., Dunn, C. W., Hejnol, A., Kristensen, R. M., Neves, R. C., . . . Sørensen, M. V. (2011). Higher-level metazoan relationships: recent progress and remaining questions. *Organisms Diversity & Evolution, 11*(2), 151-172. doi: 10.1007/s13127-011-0044-4

Fedele, M. (1933). Sul ritmo muscolare somatico delle Salpe. *Bollettino della Societa Italiana di Biologia Sperimentale, 8*, 475-478.

Fritzsch, B., Sonntag, R., Dubuc, R., Ohta, Y., & Grillner, S. (1990). Organization of the six motor nuclei innervating the ocular muscles in lamprey. *The Journal of Comparative Neurology, 294*(4), 491-506. doi: 10.1002/cne.902940402

Glaubrecht, M., & Dohle, W. (2012). Discovering the alternation of generations in salps (Tunicata, Thaliacea): Adelbert von Chamisso's dissertation "De Salpa " 1819 – its material, origin and reception in the early nineteenth century. *Zoosystematics and Evolution, 88*(2), 317-363. doi: 10.1002/zoos.201200024

Gilland, E., & Baker, R. (2005). Evolutionary patterns of cranial nerve efferent nuclei in vertebrates. *Brain, Behavior and Evolution, 66*(4), 234-254. doi: 10.1159/000088128

Göppert, E. (1893). Untersuchungen über das Sehorgan der Salpen. In C. Gegenbaur (Ed.), *Morphologisches Jahrbuch – Eine Zeitschrift für Anatomie und Entwicklungsgeschichte, Band 19, Heft 3*, (pp. 250-294). Leipzig: Verlag von Wilhelm Engelmann.

Gorbman, A. (1999). Brain – Hatschek's pit relationships in amphioxus species. *Acta Zoologica*, 80(4), 301-305. doi: 10.1046/j.1463-6395.1999.00027.x

Govindarajan, A. F., Bucklin, A., & Madin, L. P. (2011). A molecular phylogeny of the Thaliacea. *Journal of Plankton Research, 33*(6), 843-853. doi: 10.1093/plankt/fbq157

Groepler, W. (2016). *Die Seescheiden von Helgoland*. Hohenwarsleben: Westarp Wissenschaften-Verlagsgesellschaft mbH.

Holmberg, K. (1982). The ciliated brain duct of *Oikopleura dioica* (Tunicata, Appendicularia). *Acta Zoologica, 63*(2), 101-109. doi: 10.1111/j.1463-6395.1982.tb00765.x

Holmberg, K. (1984). A transmission electron microscopic investigation of the sensory vesicle in the brain of *Oikopleura dioica* (Appendicularia). *Zoomorphology, 104*(5), 298-303. doi: 10.1007/BF00312011

Hyman, L. H. (1959). *The invertebrates: smaller coelomate groups, Chaetognatha, Hemi-chordata, Pogonophora, Phoronida, Ectoprocta, Brachipoda, Sipunculida, the coelomate Bilateria. Volume V*: New York: McGraw-Hill Book Company Inc.

Huus, J. (1956). Zweite und letzte Unterklasse der Acopa: Ascidiacea = Tethyoideae = Seescheiden. In T. Krumbach (Ed.), *Handbuch der Zoologie* (pp. 545-692). Berlin: Walter de Gruyter & Co.

Imai, J. H., & Meinertzhagen, I. A. (2007). Neurons of the ascidian larval nervous system in *Ciona intestinalis*: I. central nervous system. *Journal of Comparative Neurology, 501*(3), 316-334. doi: 10.1002/cne.21246

Julin, C. (1881). Recherches sur l'organisation des ascidies simples. *Archives de Biologie*, 2, 59-126.

Kah, O., Lethimonier, C., Somoza, G., Guilgur, L. G., Vaillant, C., & Lareyre, J. J. (2007). GnRH and GnRH receptors in metazoa: A historical, comparative, and evolutive perspective. *General and Comparative Endocrinology, 153*(1), 346-364. doi: 10.1016/j.ygcen.2007.01.030

Karnovsky, M. J. (1965). A formaldehyde-glutaraldehyde fixative of high osmolality for use in electron microscopy. *The Journal of Cell Biology, 27*, 137A.

Kocot, K. M., Tassia, M. G., Halanych, K. M., & Swalla, B. J. (2018). Phylogenomics offers resolution of major tunicate relationships. *Molecular Phylogenetics and Evolution, 121*, 166-173. doi: 10.1016/j.ympev.2018.01.005.

Kott, P. (1985). The Australian Ascidiacea. Part 1, Phlebobranchia and Stolidobranchia. *Memoirs of the Queensland Museum, 23*. Brisbane: Queensland Museum.

Kott, P. (1990). The Australian Ascidiacea. Part 2, Aplousobranchia (1). *Memoirs of the Queensland Museum, 29*. Brisbane: Queensland Museum.

Kott, P. (1992). The Australian Ascidiacea. Part 3, Aplousobranchia (2). *Memoirs of the Queensland Museum, 32*. Brisbane: Queensland Museum.

Kott, P. (2001). The Australian Ascidiacea. Part 4, Aplousobranchia (3), Didemnidae. *Memoirs of the Queensland Museum, 47*. Brisbane: Queensland Museum.

Koyama, H., & Kusunoki, T. (1993). Organization of the cerebral ganglion of the colonial ascidian *Polyandrocarpa misakiensis*. *The Journal of Comparative Neurology, 338*(4), 549-559. doi: 10.1002/cne.903380405

Lacalli, T. C., & Holland, L. Z. (1998). The developing dorsal ganglion of the salp Thalia democratica, and the nature of the ancestral chordate brain. *Philosophical Transactions of the Royal Society of London B: Biological Sciences, 353*. doi: 10.1098/rstb.1998.0347

Lemaire, P. (2011). Evolutionary crossroads in developmental biology: the tunicates. *Development, 138*(11), 2143-2152. doi: 10.1242/dev.048975

Lemaire, P., & Piette, J. (2015). Tunicates: exploring the sea shores and roaming the open ocean. A tribute to Thomas Huxley. *Open Biology, 5*(6). doi: 10.1098/rsob.150053

Loesel, R. (2011). Neurophylogeny: Retracing early metazoan brain evolution. In P. Pontarotti (Ed.), *Evolutionary Biology – Concepts, Biodiversity, Macroevolution and Genome Evolution* (pp. 169-191). Berlin, Heidelberg: Springer Berlin Heidelberg.

Mackie, G. O. (1995). On the 'visceral nervous system' of *Ciona*. *Journal of the Marine Biological Association of the United Kingdom, 75*(1), 141-151. doi: 10.1017/S0025315400015253.

Mackie, G. O., & Burighel, P. (2005). The nervous system in adult tunicates: current research directions. *Canadian Journal of Zoology, 83*, 151-183. doi: 10.1139/Z04-177.

Manni, L., Lane, N. J., Sorrentino, M., Zaniolo, G., & Burighel, P. (1999). Mechanism of neurogenesis during the embryonic development of a tunicate. *Journal of Comparative Neurology, 412*(3), 527-541. doi: 10.1002/(SICI)1096-9861(19990927)412:3<527::AID-CNE11>3.0.CO;2-U.

Manni, L., & Pennati, R. (2016). Tunicata. In A. Schmidt-Rhaesa, S. Harzsch, G. Purschke (Eds.) *Structure and evolution of invertebrate nervous systems* (pp. 699–718). Oxford: Oxford University Press.

Meinertzhagen, I. A., & Okamura, Y. (2001). The larval ascidian nervous system: the chordate brain from its small beginnings. *Trends in Neurosciences, 24*(7), 401-410. doi: 10.1016/S0166-2236(00)01851-8

Metcalf, M. M. (1898). The eyes and subneural gland of salpa. *Memoirs from the Biological Laboratory of the Johns Hopkins University II* (pp. 305-371). Baltimore: The Johns Hopkins Press.

Monniot, C., & Monniot, F. (1972). Clé mondiale des genres d'ascidies. *Archives de zoologie expérimentale et générale, 113*, 311-367.

Neumann, G. (1909). Die Pyrosomen. *Dr. H. G. Bronn's Klassen und Ordnungen des Thier-Reichs, wissenschaftlich dargestellt in Wort und Bild*, *Band 3*, Supplement 2, Abteilung 2.

Neumann, G. (1956). Erste Unterklasse der Acopa. Thaliaceae. In T. Krumbach (Ed.), *Handbuch der Zoologie* (pp. 203-323). Berlin: Walter de Gruyter.

Nieuwenhuys, R., Smeets, W. J. A. J., Wicht, H., Donkelaar, H. J., Meek, J., Nicholson, C., . . . Voogd, J. (2014). *The Central Nervous System of Vertebrates.* Berlin, Heidelberg: Springer Berlin Heidelberg.

Nozaki, M., & Gorbman, A. (1992). The question of functional homology of Hatschek's pit of amphioxus (Branchiostoma belcheri) and the vertebrate adenohypophysis. *Zoological Science, 9*(2), 387-395.

Olsson, R., Holmberg, K., & Lilliemarck, Y. (1990). Fine structure of the brain and brain nerves of *Oikopleura dioica* (Urochordata, Appendicularia). *Zoomorphology, 110*, 1-7. doi: 10.1007/BF01632806

Osugi, T., Sasakura, Y., & Satake, H. (2017). The nervous system of the adult ascidian *Ciona intestinalis* Type A (*Ciona robusta*): Insights from transgenic animal models. *PLoS One, 12*(6), e0180227. doi: 10.1371/journal.pone.0180227.

Plough, H. H. (1978). *Sea squirts of the Atlantic Continental Shelf from Maine to Texas*. Baltimore: Johns Hopkins University Press.

Redikorzew, W. (1905). Über das Sehorgan der Salpen. *Gegenbaurs Morphologisches Jahrbuch, 34*, 204-239.

Richardson, M. K., Admiraal, J., & Wright, G. M. (2010). Developmental anatomy of lampreys. *Biological Reviews, 85*, 1-33. doi: 10.1111/j.1469-185X.2009.00092.x

Richter, S., Loesel, R., Purschke, G., Schmidt-Rhaesa, A., Scholtz, G., Stach, T., . . . Harzsch, S. (2010). Invertebrate neurophylogeny: suggested terms and definitions for a neuroanatomical glossary. *Frontiers in Zoology, 7*(1), 29. doi: 10.1186/1742-9994-7-29

Rigon, F., Stach, T., Caicci, F., Gasparini, F., Burighel, P., & Manni, L. (2013). Evolutionary diversification of secondary mechanoreceptor cells in Tunicata. *BMC Evolutionary Biology, 13*(1), 112. doi: 10.1186/1471-2148-13-112

Roth, G., & Dicke, U. (2005). Evolution of the brain and intelligence. *Trends in Cognitive Sciences, 9*(5), 250-257. doi: 10.1016/j.tics.2005.03.005

Ruppert, E. E. (1990). Structure, ultrastructure, and function of the neural gland complex of *Ascidia interrupta* (Chordata, Ascidiacea): clarification of hypotheses regarding the evolution of the vertebrate anterior pituitary. *Acta Zoologica, 71*. doi: 10.1111/j.1463-6395.1990.tb01189.x

Ryan, K., Lu, Z., & Meinertzhagen, I. A. (2018). The peripheral nervous system of the ascidian tadpole larva: Types of neurons and their synaptic networks. *Journal of Comparative Neurology, 526*(4), 583-608. doi: 10.1002/cne.24353

Schmidt-Rhaesa, A., Harzsch, S., & Purschke, G. (2015). *Structure and evolution of invertebrate nervous systems*. Oxford: Oxford University Press.

Shenkar, N., & Swalla, B. J. (2011). Global diversity of ascidiacea. *PLoS One, 6*(6), e20657. doi: 10.1371/journal.pone.0020657

Søviknes, A. M., Chourrout, D., & Glover, J. C. (2007). Development of the caudal nerve cord, motoneurons, and muscle innervation in the appendicularian urochordate *Oikopleura dioica*. *Journal of Comparative Neurology, 503*(2), 224-243. doi: 10.1002/cne.21376

Stach, T. (1996). On the preoral pit of the larval amphioxus (*Branchiostoma lanceolatum*). *Annales des sciences naturelles, Zoologie, Paris*, 17, 129–134.

Stach, T. (2008). Chordate phylogeny and evolution: a not so simple three-taxon problem. *Journal of Zoology, 276*(2), 117-141. doi: 10.1111/j.1469-7998.2008.00497.x

Stach, T. (2014). Deuterostome phylogeny - a morphological perspective. In J.W. Wägele & T. Bartolomaeus (Eds.), *Deep Metazoan Phylogeny: The Backbone of the Tree of Life* (pp. 425-457). Berlin: De Gruyter.

Stach, T., & Turbeville, J. M. (2002). Phylogeny of Tunicata inferred from molecular and morphological characters. *Molecular Phylogenetics and Evolution, 25*(3), 408-428. doi: 10.1016/S1055-7903(02)00305-6

Stach, T., Winter, J., Bouquet, J.-M., Chourrout, D., & Schnabel, R. (2008). Embryology of a planktonic tunicate reveals traces of sessility. *Proceedings of the National Academy of Sciences, 105*(20), 7229-7234. doi: 10.1073/pnas.0710196105

Swalla, B. J., & Smith, A. B. (2008). Deciphering deuterostome phylogeny: molecular, morphological and palaeontological perspectives. *Philosophical Transactions of the Royal Society of London B: Biological Sciences, 363*(1496), 1557-1568. doi: 10.1098/rstb.2007.2246

Takamura, K., Minamida, N., & Okabe, S. (2010). Neural map of the larval central nervous system in the ascidian *Ciona intestinalis*. *Zoological Science, 27*, 191-203. doi: 10.2108/zsj.27.191

Tsagkogeorga, G., Turon, X., Hopcroft, R. R., Tilak, M.-G., Feldstein, T., Shenkar, N., . . . Delsuc, F. (2009). An updated 18S rRNA phylogeny of tunicates based on mixture and secondary structure models. *BMC Evolutionary Biology, 9*, 187. doi: 10.1186/1471-2148-9-187

Tsutsui, H., Yamamoto, N., Ito, H., & Oka, Y. (1998). GnRH-Immunoreactive Neuronal System in the Presumptive Ancestral Chordate,Ciona intestinalis(Ascidian). *General and Comparative Endocrinology, 112*(3), 426-432. doi: 10.1006/gcen.1998.7160

Uljanin, B. N. (1884). *Die Arten des Gattung Doliolum in Golfe von Neapel und den angrenzen den Meeresabschnitten*. Leipzig: Verlag von Wilhelm Engelmann.

Ussow, M. (1876). Beiträge zur Kenntnis der Organisation der Tunicaten. *Mémoires de la Société Imperiale des naturalistes de Moscou, 18*, 1-54.

van Dongen, P. A. M. (1998). Brain size in vertebrates. *The Central Nervous System of Vertebrates: Volume 1 / Volume 2 / Volume 3* (pp. 2099-2134). Berlin, Heidelberg: Springer Berlin Heidelberg. doi: 10.1007/978-3-642-18262-4_23

Van Name, W. G. (1945). The north and south American ascidians. *Bulletin of the American museum of natural history, 84*, 1-476.

Wicht, H., & Lacalli, T. C. (2005). The nervous system of amphioxus: structure, development, and evolutionary significance. *Canadian Journal of Zoology, 83*(1), 122-150. doi: 10.1139/z04-163

Zaniolo, G., Lane, N. J., Burighel, P., & Manni, L. (2002). Development of the motor nervous system in ascidians. *Journal of Comparative Neurology, 443*(2), 124-135. doi: 10.1002/cne.10097

Zeng, L., Jacobs, M. W., & Swalla, B. J. (2006). Coloniality has evolved once in stolidobranch ascidians. *Integrative and Comparative Biology*. doi: 10.1093/icb/icj035

7.2 Supporting Information

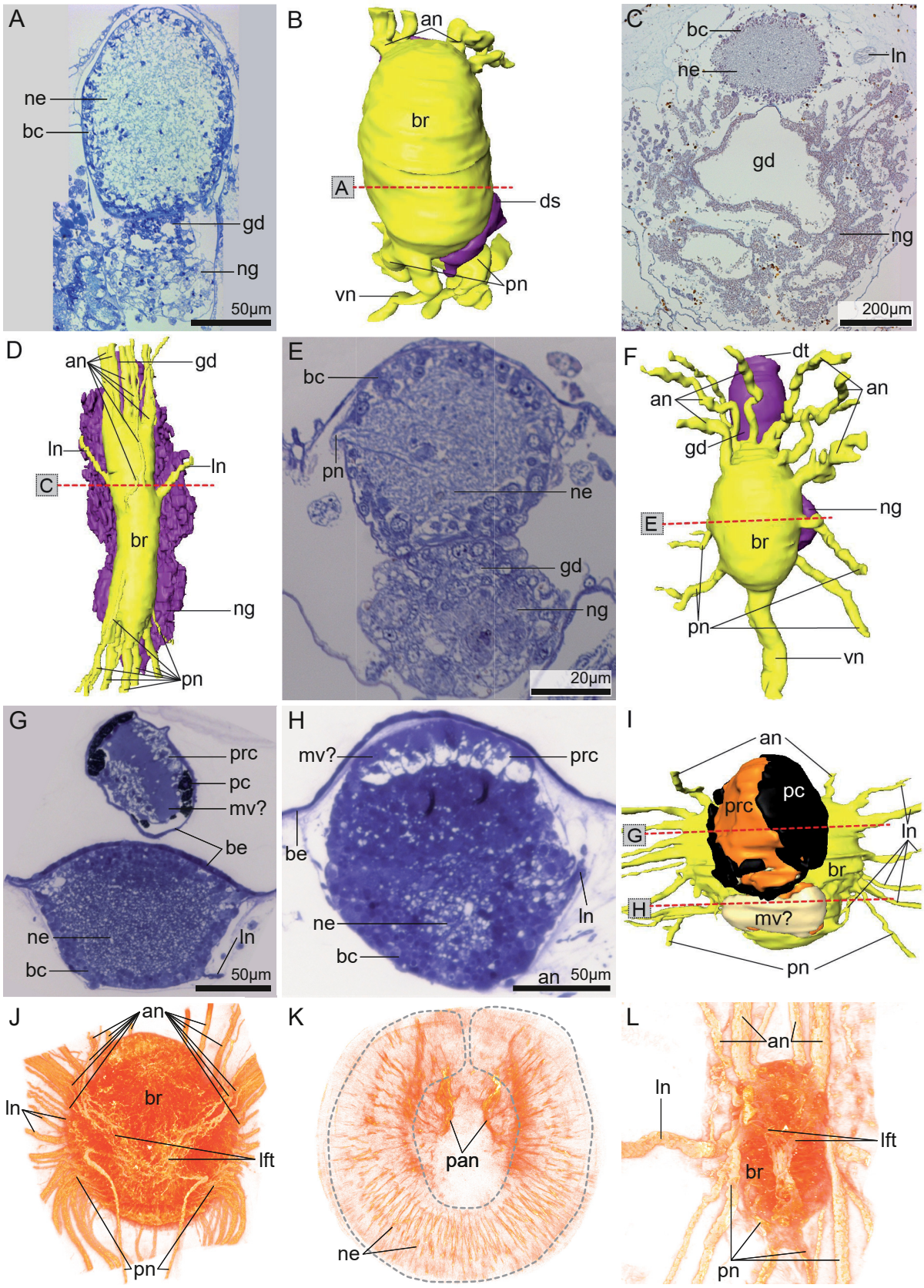

Fig. S1, Supporting information: Additional data on the anatomy of the neural complexes of different tunicate species. A, C, E, G-H: Light micrographs of cross sections of the neural complexes, dorsal to the top, right to the right. Brains (br) possess a central neuropil and a cortex (co). B, D, F, I: 3d

models of the anatomy of the neural complexes. Brains and nerves (yellow), neural gland (ng), dorsal strand (ds), gland duct (gd) and dorsal tubercle (dt) (purple), as well as pigment cells (pc, black), photoreceptor cells (prc, orange) and presumable microvilli (mv?, cream-colored) are depicted, dorsal view, anterior to the top. Section planes from A, C, E, G, H are shown as dashed red lines. Interactive 3d reconstructions online available. A, B: Morphology of the neural complex of Ascidiella aspersa. The neural gland is located ventral to the brain. The dorsal tubercle is intricate, the dorsal strand curves around the right posterior nerve (pn) ending blindly behind it. C, D: Neural complex in Ascidia mentula. The extensive neural gland is located ventral to the brain. A long gland duct connects the neural gland to the distant dorsal tubercle, not shown in the 3d model. E, F: Anatomy of the neural complex in Aplidium turbinatum. A prominent ventral visceral nerve (vn) is developed, but a dorsal strand is missing. The neural gland is positioned ventral and the dorsal tubercle is simply shaped. G-I: Neuroanatomy of the blastozooid generation of Iasis cylindrica. The eye is connected to the brain via a thin neck region. Posterior to the eye presumable photoreceptor cells are detectable that are not shaded by pigment cells. A neural gland is not developed. J-L: Immunostaining against tyrosinated-α-tubulin (orange/red) shown as 3d rendered signal. J, K: Brain of the oozooid stage of I. cylindrica. J: Ventral view, anterior to the top; on the ventral side of the brain lateral fiber tracts (lft) are detectable. K: View from dorsal, anterior to the top; neurites (ne) connect two paraxial neuropils (pan) with photoreceptor cells. J: Ventral view on the brain of Pyrosoma atlanticum, anterior to the top. Bilateral symmetrical fiber tracts run on the ventral side of the brain. an: anterior nerve, be: brain epithelium, ln: lateral nerve.

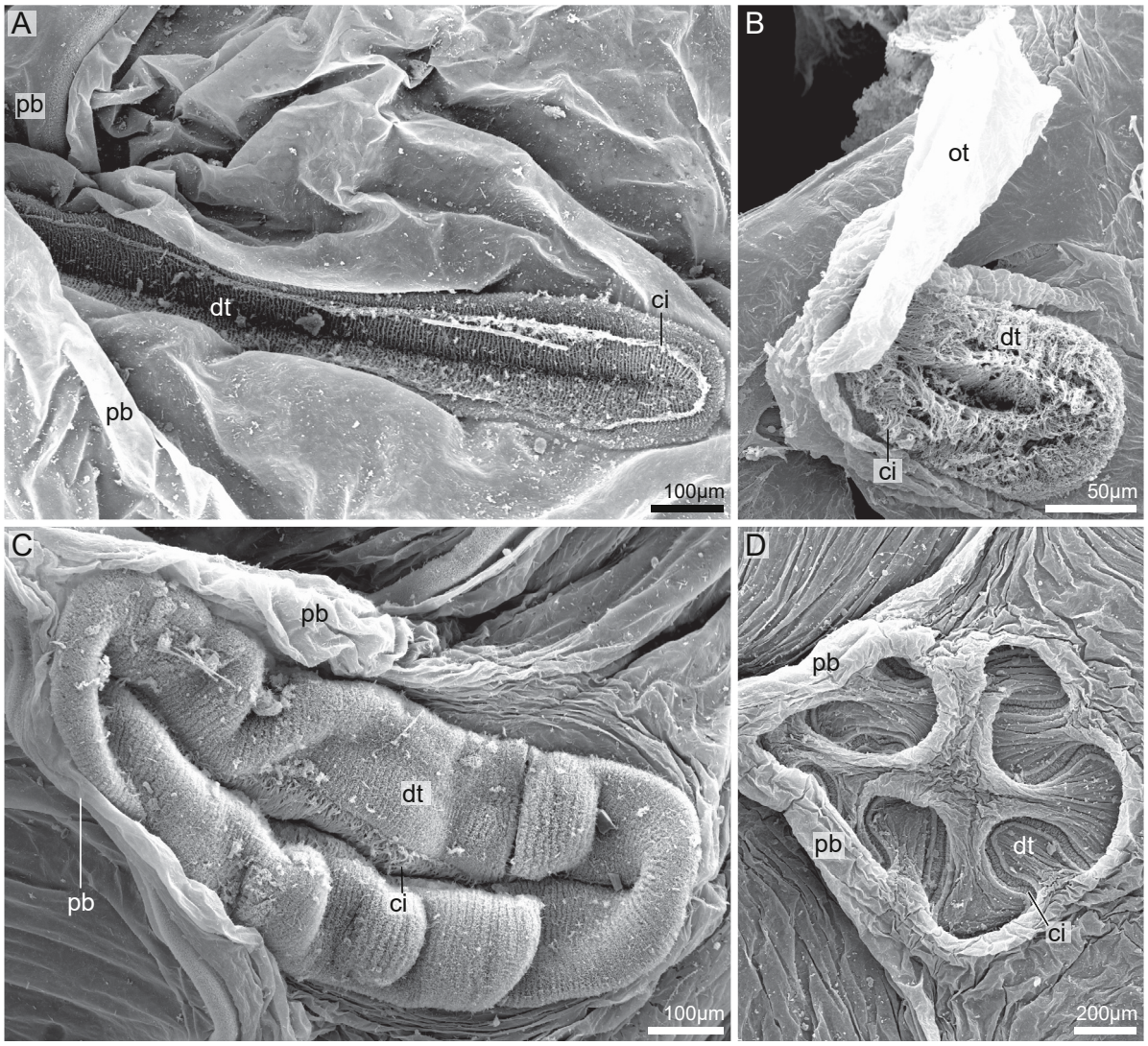

Fig. S2, Supporting information: Scanning electron micrographs of the dorsal tubercles (dt) in four different salp species. Ventral views, anterior to the right. A: Elongated dorsal tubercle with a slit-like opening in the oozooid stage of Iasis cylindrica. The dorsal tubercle is positioned anterior to the transition zone of the gill bar and peripharyngeal band (pb). B: In Thalia democratica the dorsal tubercle of the oozoid is ovoid and positioned at the anterior base of the oral tentacle (ot). C: The dorsal tubercle of the blastozooid stage of Salpa aspera is elongated with a slit-like opening, and framed by the peripharyngeal band. D: Intricate dorsal tubercle in the oozooid stage of Cyclosalpa pinnata. ci: cilia.

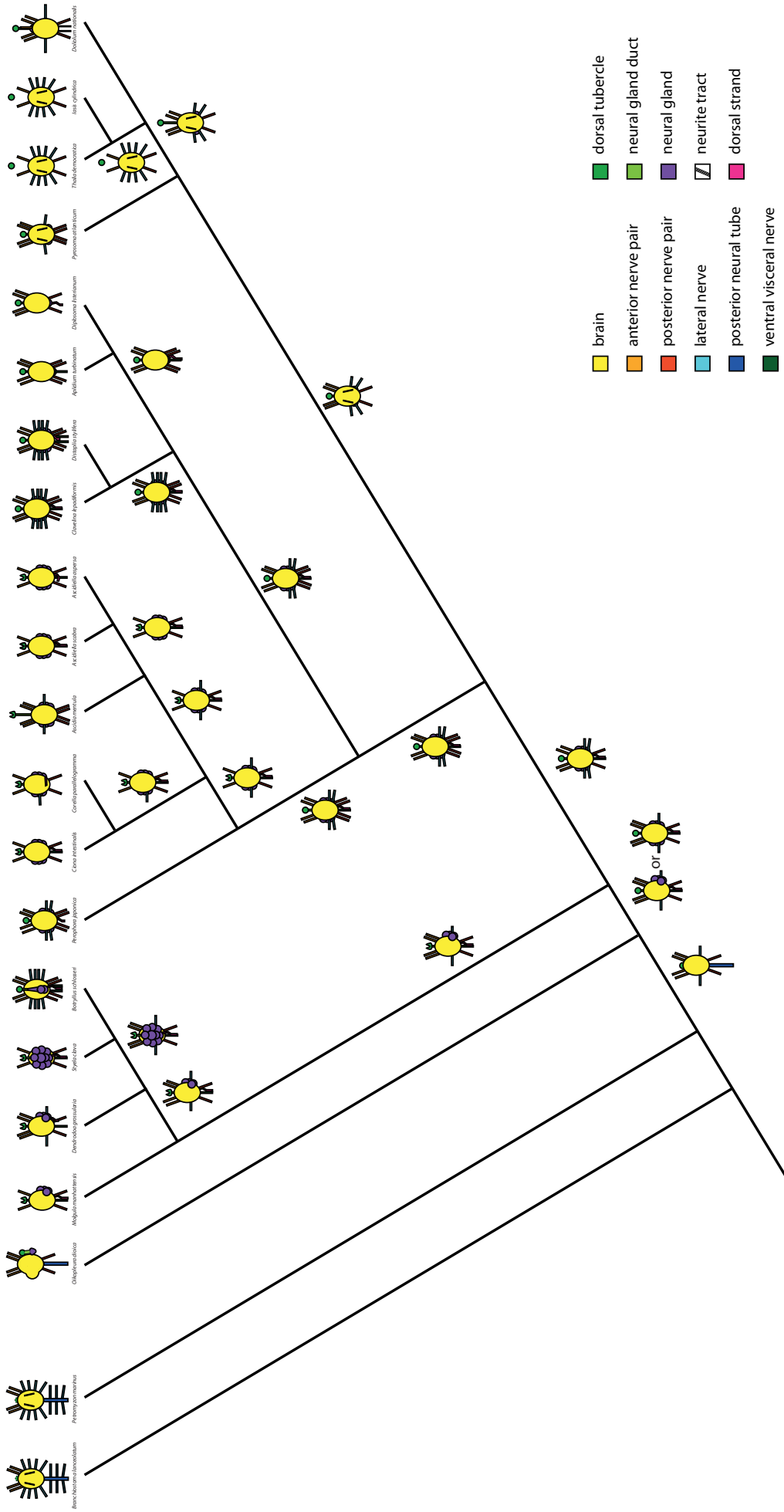

Fig. S3, Supporting information

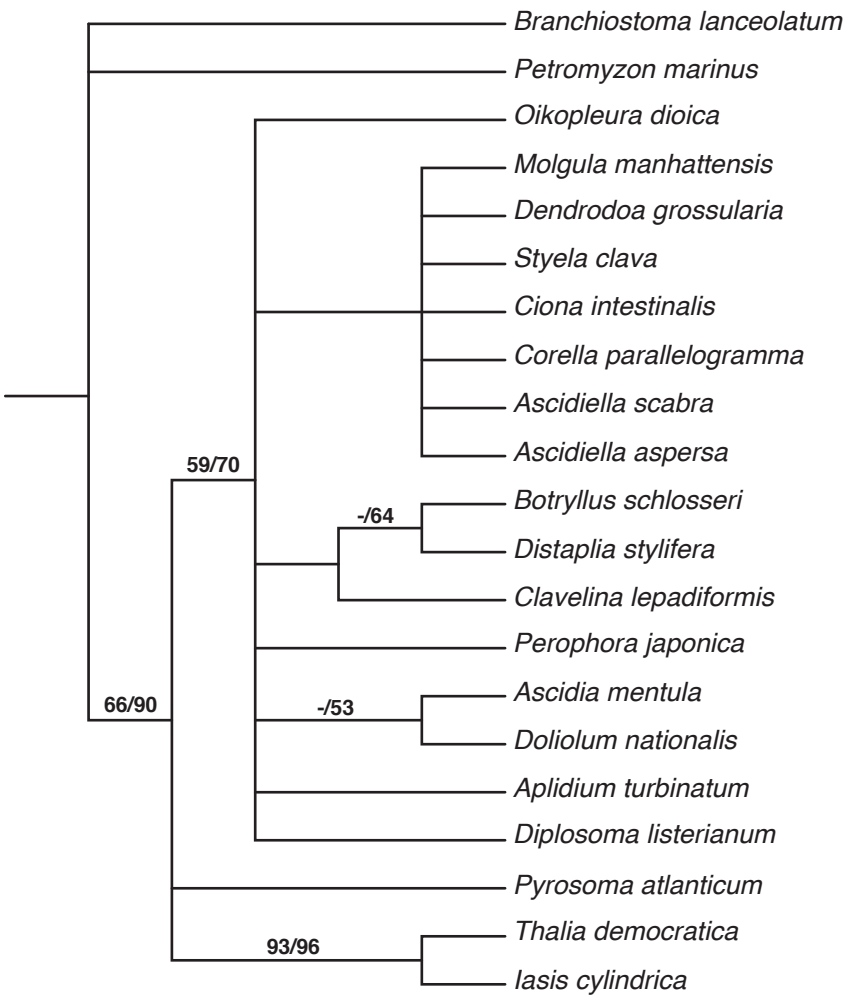

Fig. S4, Supporting information: Strict consensus of 30 equally parsimonious trees found in a branch-and-bound analysis of 25 neuronal characters (19 parsimony informative) coded for 21 species in PAUP. Numbers on branches are jackknife percentages / bootstrap percentages respectively. Tree length = 36, consistency index (CI) = 0.64 CI excluding uninformative characters = 0.61, retention index = 0.81, rescaled consistency index = 0.52.

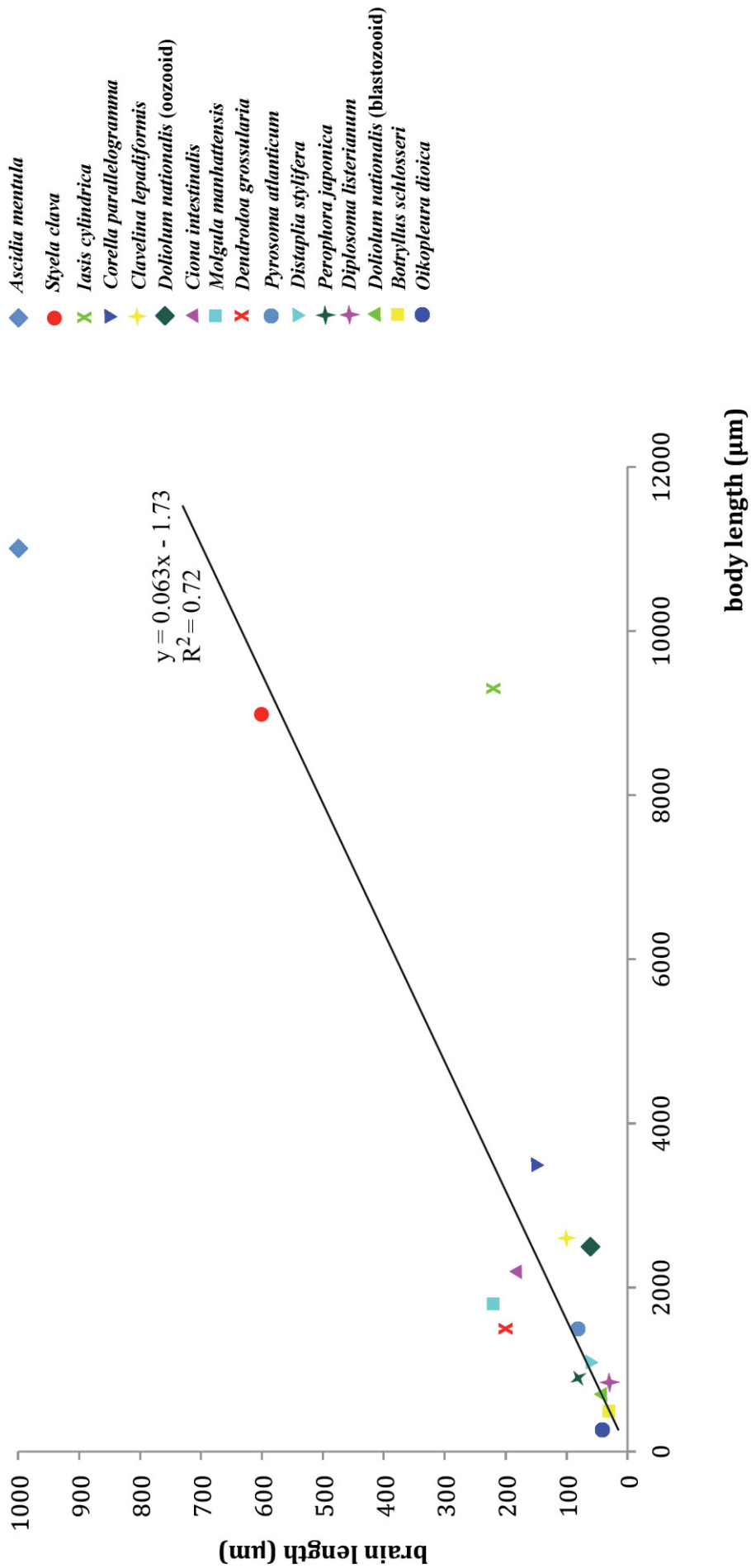

Fig. S5, Supporting information: Diagram of the relationship between total body length (in µm) and brain length (in µm) of 16 tunicates of 15 different species of all 5 major taxa. A graph shows the linear correlation, $y = 0.063x - 1.73$; $R^2 = 0.72$.

Supplementary Table 1: Information on specimens examined with scanning electron microscopy.

Species	Family	Museum accession number[1]	Origin
Iasis cylindrica (Cuvier, 1804)	Salpidae	ZMB Tun 1743	Sierra Leone 6°48'5"N, 14°51'3"W
Salpa aspera Chamisso, 1819	Salpidae	ZMB Tun 1758	Cape Town 56°30'1"S, 14°29'2"O
Cyclosalpa pinnata (Forskål, 1775)	Salpidae	ZMB Tun 553	Messina, harbor
Thalia democratica (Forskål, 1775)	Salpidae	ZMB Tun 1724	off Cape Town

[1] Catalogue number of the Museum für Naturkunde (Berlin, Germany)

Supplementary Table 2: Total body lengths, brain lengths, and automatic counts of nuclei. Nuclei were counted in Imaris 8.3.1 (Bitplane AG, Zurich, Switzerland) based on stacks of confocal laser scanning micrographs of DAPI stained.

Species	Body length [µm]	Brain length [µm]	Cell # in neural complex[1]
Ascidiella scabra	11000	1000	4000
Corella parallelogramma	3500	150	3000
Ciona intestinalis	2200	180	10000
Perophora japonica	900	80	2000
Clavelina lepadiformis	2600	100	4000
Diplosoma listerianum	850	30	300
Distaplia stylifera	1100	60	2500
Botryllus schlosseri	500	30	2000
Dendrodoa grossularia	1500	200	3500
Styela clava	9000	600	3000
Molgula manhattensis	1800	220	6000
Doliolum nationalis (oozooid)	2500	60	2000
D. nationalis (blastozooid)	700	40	700
Iasis cylindrica (oozooid)	9300	220	8000
Pyrosoma atlanticum	1500	80	2000
Oikopleura dioica	270	40	150

[1] Because immunohistochemical staining experiments might not detect every individual cell, we list the highest numbers for each species in our experiments. These are nevertheless approximate numbers of cells.

8 Phylogenetic analysis of Tunicata

8.1 Manuscript

This is the pre-peer reviewed version of the following article:

Braun, K., Leubner, F., & Stach, T. Phylogenetic analysis of phenotypic characters of Tunicata supports basal Appendicularia and monophyletic Ascidiacea,

which was submitted for publication to *Cladistics*. This article may be used for non-commercial purposes in accordance with Wiley Terms and Conditions for Use of Self-Archived Versions.

Title

Phylogenetic analysis of phenotypic characters of Tunicata supports basal Appendicularia and monophyletic Ascidiacea

Authors

Katrin Braun, Vergleichende Zoologie, Institut für Biologie, Humboldt-Universität zu Berlin, Philippstrasse 13, Haus 2, 10115 Berlin, Germany

Fanny Leubner, Animal Evolution and Biodiversity, J-F-Blumenbach Institute for Zoology & Anthropology, Georg-August-University Göttingen, Göttingen, Untere Karspüle 2, 37073 Göttingen Germany

Thomas Stach, thomas.stach@hu-berlin.de, Molekulare Parasitologie, Institut für Biologie, Humboldt-Universität zu Berlin, Philippstrasse 13, Haus 14, 10115 Berlin, Germany

Abstract

With approximately 3000 marine species Tunicata represents the most disparate subtaxon of Chordata. Molecular phylogenetic studies support Tunicata as sister taxon to Craniota rendering it pivotal to understand vertebrate evolution. While successively more molecular data became available to resolve internal tunicate phylogenetic relationships, phenotypic data have not been utilized consistently. Here we address these shortcomings by cladistically analyzing 116 phenotypic characters for 49 tunicate species comprising all higher tunicate taxa, and 5 craniate and cephalochordate outgroup species. In addition, we performed a combined analysis of the phenotypic characters with 18S rDNA-sequence data in 32 OTUs. The strict consensus tree from the analysis of the phenotypic characters recovers monophyletic Appendicularia as sister taxon to the remaining tunicate taxa. “Thaliacea” is found paraphyletic with Pyrosomatida as sister taxon to Ascidiacea and the relationship between Doliolida and Salpida unresolved. Thus, the phenotypic data support the hypothesis that the last common ancestor of Tunicata was free-living, that ascidian sessility is a derived character and that the last common ancestor of Ascidiacea was colonial. The combined analysis, congruent with published purely molecular analyses, recovers Thaliacea monophyletic nested within paraphyletic “Ascidiacea”. Successively up-weighting phenotypic data indicates that phenotypic data contribute disproportionally more to the resulting phylogenetic hypothesis.

Introduction

Tunicata is a taxon that comprises approximately 3000 marine invertebrate species, including the brightly bioluminescent Pyrosomatida, the translucent Salpida with their heterogenic life cycle or the Appendicularia (= Larvacea) that are capable of producing a most delicate, yet at the same time complex extracorporal structure often called a house (Lemaire and Piette, 2015; Shenkar and Swalla, 2011). The best known and most numerous tunicates, however, are the sessile, comparatively unadorned ascidians, most of which live at shallow shores attached to various hard substrata. Tunicata had been considered to be a subgroup of bivalves by early zoologists (e.g., Cuvier, 1840) and it was an unexpected surprise when the discovery of their larval stage, resembling a miniature tadpole, showed that these animals, perhaps uncharismatic at first sight, were in fact chordates (Kowalevsky, 1866). Mirroring this epiphany was the finding based on molecular phylogenetic analyses that supported Tunicata as a sister taxon to Craniota (Delsuc et al., 2006). This so-called Olfactores-hypothesis has been criticized, because rates of sequence evolution are known to be exceptionally high in tunicates and because analyses of internal data conflict had shown that the phylogenetic information content was not as confident inspiring as the statistical support values suggested (Stach, 2014; Tsagkogeorga et al., 2009). Moreover, the Olfactores-hypothesis is in conflict with the interpretation of numerous characters shared by Cephalochordata and Craniota, which had been interpreted as synapomorphies (Stach, 2008). Nevertheless, subsequent molecular studies supported the position of Tunicata as the sister group to vertebrates and this is currently the dominant hypothesis (Delsuc et al., 2018; Giribet, 2018; Kocot et al., 2018).

Until recently, only a couple of genes had been used to infer the molecular phylogenetic interrelationships of tunicate sub-groups (e.g., Stach and Turbeville, 2002; Swalla et al., 2000; Tsagkogeorga et al., 2009; Wada, 1998; see review in Giribet, 2018). Despite their limitations, these studies eventually converged on some points: the planktonic Appendicularia is placed as sister taxon to the remaining Tunicata; the sessile sea-squirts, i.e., "Ascidiacea" turned out to be paraphyletic with the planktonic Thaliacea being nested within this group. The molecular markers moreover supported the monophyly of several other tunicate subtaxa, such as Stolidobranchiata, Aplousobranchiata, Pyrosomatida, Salpida, or Doliolida and clarified the controversial (e.g., Kott, 1985, 1990) position of the genus *Ciona* within Phlebobranchiata and found also some support for the placement of Diazonidae within Aplousobranchiata (Shenkar et al., 2016). Some other groups supported in traditional taxonomies remained either weakly supported or found no support in the molecular systematic studies. Phlebobranchiata, e.g., was found monophyletic in some analyses but paraphyletic with respect to Aplousobranchiata in others. In most analyses, "Pyuridae", traditionally considered to be a "family" within Stolidobranchiata was recovered to be paraphyletic with Styelidae nested within "Pyuridae". While the number of molecular markers has increased considerably with two recently published studies that in parallel supported the phylogenies just outlined (Delsuc et al., 2018; Kocot et al., 2018), the number of species studied remains low considering the diversity found within

Tunicata.

The disparity of morphologies and life history strategies encountered in Tunicata has fascinated researchers early on and numerous scrupulous taxonomic treatises and textbooks bear witness to this attention (e.g., Chamisso, 1819; Godeaux, 2003; Kott, 1985, 1990, 1992, 2001; Monniot and Monniot, 1972, 2001; Van Soest, 1981). While therefore meticulous descriptions of tunicate species abound, attempts to cladistically analyze the distribution of morphological characters remained few and far between. Stach and Turbeville (2002) published a cladistic study of 24 morphological characters for Tunicata at the traditional "family"-level. This study resulted in little resolution, yet the authors discussed several potential character transformations compatible with the morphological evidence and their combined analysis. The most interesting finding in this study had been the possible closer relationship of Appendicularia to Aplousobranchiata, a sister group relationship also supported in the parsimony analysis of 18S rDNA-sequences, cox1-mtDNA sequences combined with morphological characters. Moreno and Rocha (2008) have published the largest morphological data set so far. Their analysis focused on the interrelationships of "genera" in the ascidian subtaxon Aplousobranchiata. Because traditional aplousobranch ascidians comprise only colonial species, the majority of characters analyzed in this study was biologically correlated with coloniality. Therefore, the finding that colonial ascidians from other ascidian groups are closer related to Aplousobranchiata—rendering, e.g., Phlebobranchiata paraphyletic—is probably an artifact of this data matrix. In addition to these cladistic analyses, there were some attempts to phylogenetically analyze individual characters or plot them onto molecular phylogenies (e.g., Vanadium content – Hawkins et al., 1983; sperm morphology – Holland, 1992; secondary mechanoreceptor cells – Rigon et al., 2013; adult neural complex – Braun and Stach, 2018a).

Clearly, morphology with its manifold levels of comparisons can contribute phylogenetic information to substantiate phylogenetic hypotheses and should not be neglected, if one seriously considers the requirement of total evidence as an important corner stone of natural sciences. Along this line of argumentation, we endeavored to compile a data matrix conceptualizing 116 characters into primary homology hypotheses for 49 species, representing all higher tunicate taxa. The characters were chosen to allow for hypotheses of primary homology hypotheses across the entire diversity of tunicate taxa. Among these are characters traditionally used in tunicate taxonomy, such as characteristics of the branchial basket or the morphology of the gonads, but also characters recently compiled in our own research such as the kinds and distribution of serotonergic cells in the nervous system (see also Braun and Stach, 2016, 2018b). Besides being an independent source of evidence for phylogenetic analyses, homology hypotheses of morphological characters are quintessential for any understanding of organismal evolutionary changes beyond the branching pattern of a cladogram. Therefore, the aim of the present study is to establish a broader factual basis to include morphological characters in cladistic considerations concerning tunicate and chordate evolution. In addition to presenting homology hypotheses, we cladistically analyze the data matrix, compare the result

to molecular hypotheses and perform a combined analysis in order to evaluate the respective contributions of the morphological and molecular partition toward the resulting phylogenetic hypothesis.

Material and methods

Collection and rearing

Collection localities for specimens examined as well as applied fixations and microscopic methods are listed in Table 1. Ascidians were collected in the lower intertidal or upper subtidal. Living specimens of *Oikopleura dioica* were provided from Sars International Centre for Marine Molecular Biology and cultured at Humboldt-University zu Berlin through numerous generations. Many specimens for scanning electron microscopy came from the collection of the Museum für Naturkunde (Berlin, Germany; Table 1) and the SEM preparations are kept in the collection Marine Invertebrates.

Fixation

Before fixation ascidians used for light microscopy were anaesthetized for approximately an hour using menthol crystals. *O. dioica* was fixed directly without anaesthetization. The tunic of ascidians was opened before fixation in order to facilitate penetration of the fixative.

For light microscopy animals were fixed either in Bouin's solution, an aqueous solution containing 8% formaldehyde, 5% acetic acid, and 1% picric acid, or in a cold solution of Karnovsky's primary fixative (Karnovsky, 1965), consisting of 2% glutaraldehyde, 2% paraformaldehyde, 1.52% NaOH and 1.2g d-glucose, dissolved in 2.25% sodium hydrogen phosphate buffer (pH 7.4). *P. atlanticum* was fixed in 10% formaldehyde and stored in 70% ethanol.

For scanning electron microscopy specimens were fixed either in 70% ethanol or in 4% paraformaldehyde.

Sectioning

Specimens for light microscopy were dehydrated in a graded series of ethanol and embedded in epoxy resin (Araldite; Fluka). Specimens were serially sectioned with a thickness of 0.5µm -1µm. Two specimens of *O. dioica* were serially sectioned for light microscopy (0.7µm); another specimen of *O. dioica* was serially sectioned alternating between semithin sections (0.5µm) and ultrathin sections (60nm). Sectioning was performed on a Leica Ultracut S. Semithin sections were stained using 1% toluidine blue in a solution of 1% sodium tetraborate (borax).

Treatments with antibodies

Specimens were incubated in primary antibodies against tyrosinated α-tubulin (Anti-Tubulin, Tyrosine antibody produced in mouse; Sigma, St. Louis, Missouri, USA, product number: T9028) and antibodies against serotonin (5-HT (Serotonin) Rabbit; ImmunoStar, Hudson, Wisconsin, USA, product number: 20080) for at least 2.5 days at 4°C. Incubation in secondary antibodies Cy™3 AffiniPure goat anti-mouse IgG (Jackson ImmunoResearch Laboratories, Inc., Philadelphia, Pennsylvania, USA, code: 115-035-003) and Alexa Fluor® 488 goat anti-rabbit IgG (Molecular Probes, Eugene, Oregon, USA, catalogue number: A-11008) was carried out over night at room temperature; nuclei were labeled using 4'6-Diamidino-2-Phenylindole, Dihydrochloride (DAPI dihydrochloride, Thermo Fisher Scientific Inc., Waltham, Massachusetts, USA, catalogue number: D1306). Details can be found in Braun and Stach (2016). Every staining experiment was performed together with two different controls: one with primary antibodies omitted and the second with secondary antibodies omitted.

Light microscopy

Semithin sections stained with toluidine blue (Araldite) or Azan (paraffin) were digitally recorded (distance between sections 1-2µm) using a Zeiss AxioCam HRc camera mounted on a Zeiss Axioscope 2 plus microscope. Complete images were optimized for contrast and light balance using Adobe Photoshop CC Software. Serial sections of *Molgula manhattensis* were used for 3d reconstructions.

Scanning electron microscopy

For SEM, specimens were critical point dried in a Balzers Union CPD 030. Dried specimens were sputter coated with gold in a Balzers Union SCD 040 sputter coater and viewed with a LEO 1430.

Confocal Laser Scanning Microscopy

Specimens treated with antibodies against tyrosinated α-tubulin and serotonin, and DAPI were examined using a Leica TCS SPE confocal laser scanning microscope (Leica Microsystems, Heidelberg, Germany). Appropriate filter settings were applied to record stacks of confocal optical sections.

Digital 3d reconstruction

The 3D model of the anatomy of *Molgula manhattensis* was created in Amira 5.4.3 (FEI Visualization Sciences Group, Berlin, Germany) based on the images of the serial semithin sections. Images were aligned in Amira.

Phylogenetic analysis

We used Mesquite Version 3.10 (Maddison and Maddison, 2018) to compile a data matrix for 116 morphological characters for 54 taxa and PAUP 4.0a (build 161) (Swofford, 2003) to analyze this matrix. All characters were treated as unordered and with equal weight. Gaps were treated as missing. An initial heuristic parsimony analysis was conducted with 100, 500, and 1000 replicates. The length of the most parsimonious trees found in the latter two analyses remained stable at 293 steps. The main analysis was then conducted as a heuristic analysis with 10 000 replicates, TBR branch swapping, and not more than 1000 trees saved at each replicate. This analysis, although analyzing a considerably larger tree space did not result in a shorter tree. The strict consensus and the majority rule consensus tree was calculated from this search. Subsequently we analyzed the data set a second time reweighting characters according to their rescaled consistency index. In addition, we performed a branch-and-bound search with the strict consensus of the main analysis as constraint, searching for optimal trees not compatible with this constraint. This analysis found no further shorter trees, indicating, that we recovered all most parsimonious solutions of our data set. Finally, we also analyzed the matrix with TNT (Goloboff et al., 2008) under the 'traditional search' option (Wagner trees, 1000 random seeds, 10000 replicates, 1000 trees saved per replicate, swapping algorithm TBR) and recovered 24 most parsimonious trees with a length of 293 steps. The strict consensus was identical to the strict consensus of the main heuristic analysis performed in PAUP. Statistical measures of nodal support is reported as Bremer support indices, jackknife values based on 100 replicates with 50% character deletion, and bootstrap percentages based on 100 replicates using the same search strategy as for the main analysis. In a second step we combined the matrix for phenotypic data with an alignment of molecular 18S rDNA sequence data provided by Dr. Frédéric Delsuc (Université de Montpellier) and repeated our main analysis. Treating all characters as unordered and with equal weight an heuristic analysis under the parsimony paradigm was performed as detailed as for the morphological data above. Again, statistical support for nodes is reported as Bremer support indices, jackknife values, and bootstrap percentages. Subsequently, we performed the same analyses but increased the weight of the phenotypic data by a factor of 2, 3, 4, and 5 in order to roughly quantify the influence of the respective data on the outcome of the resulting phylogenetic hypothesis.

Table 1: Information on examined specimens; adult stages were used in all species. In doliolids and salps both stages were analyzed.

Species	Family	Order	Origin	# specimens examined	Museum accession number[1]	Fixations and Methods
***Oikopleura dioica* Fol, 1872**	Oikopleuridae	Appendicularia	Bergen, Norway	3	-	Karnovsky, LM
***Megalocercus huxleyi* (Ritter, 1905)**	Oikopleuridae	Appendicularia	Seychelles, Indian Ocean	1	ZMB 1608	70% ethanol, SEM
***Fritillaria borealis* Lohmann, 1896**	Fritillariidae	Appendicularia	Atlantic Ocean, West Palm Beach, USA	6	-	PFA, CLSM
***Salpa fusiformis* Cuvier, 1804**	Salpidae	Thaliacea	Villa Franca, Mediterranea Sea	2	ZMB 2703	70% ethanol, SEM
***Doliolum denticulatum* Quoy & Gaimard, 1834**	Doliolidae	Thaliacea	Madagascar, Indian Ocean	2	ZMB 3357	70% ethanol, SEM
***Pyrosoma atlanticum* Péron, 1804**	Pyrosomatidae	Thaliacea	0° 0,8506N, 160° 27,3294E	1 colony	-	Formaldehyde, SEM
***Ascidiella scabra* (Müller, 1776)**	Ascidiidae	Phlebobranchiata	Kristineberg, Sweden	2	-	Formaldehyde, SEM
***Ascidia virginea* Müller, 1776**	Ascidiidae	Phlebobranchiata	Kristineberg, Sweden	1	-	Formaldehyde, SEM
***Phallusia nigra* (Savigny, 1816)**	Ascidiidae	Phlebobranchiata	Sinai, Gulf of Suez	1	ZMB 3277	70% ethanol, SEM
***Corella parallelogramma* (Müller, 1776)**	Corellidae	Phlebobranchiata	Tjärnö, Sweden	1	-	Formaldehyde, SEM
***Rhodosoma callense* (Ehrenberg, 1828)**	Corellidae	Phlebobranchiata	Gimsah Bay, Gulf of Suez	1	ZMB 778	70% ethanol, SEM
***Agnezia septentrionalis* (Huntsman, 1912)**	Agneziidae	Phlebobranchiata	Bering Sea	1	ZMB 2913	70% ethanol, SEM

Ciona intestinalis **(Linnaeus, 1767)**	Cionidae	Phlebobranchiata	Kristineberg, Sweden	2	-	Formaldehyde, SEM
Perophora viridis **Verrill, 1871**	Perophoridae	Phlebobranchiata	Newport, USA	5	ZMB 2086	70% ethanol, SEM
Molgula citrina **Alder & Hancock, 1848**	Molgulidae	Stolidobranchiata	Roscoff, Atlantic Ocean	1	ZMB 2566	70% ethanol, SEM
Molgula manhattensis **(De Kay, 1843)**	Molgulidae	Stolidobranchiata	Texel, Netherlands Sylt, Germany	1 9 1	-	Bouin, LM, PFA, CLSM, 70% ethanol, SEM
Halocynthia roretzi **(Drasche, 1884)**	Pyuridae	Stolidobranchiata	Hakodate, Japan	2	ZMB 595	70% ethanol, SEM
Herdmania momus **(Savigny, 1816)**	Pyuridae	Stolidobranchiata	Red Sea	2	ZMB 2357	70% ethanol, SEM
Microcosmus claudicans **(Savigny, 1816)**	Pyuridae	Stolidobranchiata	Rovinj, Croatia	1	ZMB 1135	70% ethanol, SEM
Dendrodoa grossularia **(Van Beneden, 1846)**	Styelidae	Stolidobranchiata	Kristineberg, Sweden	1	-	Bouin, LM
Styela clava **Herdman, 1881**	Styelidae	Stolidobranchiata	Texel, Netherlands	8	-	PFA, CLSM
Styela plicata **(Lesueur, 1823)**	Styelidae	Stolidobranchiata	Messina, Italy	1	ZMB 542	70% ethanol, SEM
Botryllus schlosseri **(Pallas, 1766)**	Styelidae	Stolidobranchiata	Kristineberg, Sweden	1 colony	-	Formaldehyde, SEM
Symplegma brakenhielmi **(Michaelsen, 1904)**	Styelidae	Stolidobranchiata	Fort Pierce, USA	6	-	PFA, CLSM
Kukenthalia borealis **(Gottschaldt, 1894)**	Styelidae	Stolidobranchiata	Bredefjord, Greenland	1 colony	ZMB 3713	70% ethanol, SEM

***Pelonaia corrugata* Goodsir & Forbes, 1841**	Styelidae	Stolidobranchiata	Helgoland, Germany	1	ZMB 1038	70% ethanol, SEM
***Diazona violacea* Savigny, 1809**	Diazonidae	Aplousobranchiata	Naples, Italy	1 colony	ZMB 568	70% ethanol, SEM
***Clavelina lepadiformis* (Müller, 1776)**	Clavelinidae	Aplousobranchiata	Roscoff, Atlantic Ocean, Helgoland, Germany	1	ZMB 1435	70% ethanol, SEM, Karnovsky, LM
***Didemnum maculosum* (Milne Edwards, 1841)**	Didemnidae	Aplousobranchiata	Naples, Italy	1 colony	ZMB 202	70% ethanol, SEM
***Diplosoma listerianum* (Milne Edwards, 1841)**	Didemnidae	Aplousobranchiata	Kristineberg, Sweden	1 colony	-	Formaldehyde, SEM
***Lissoclinum verrilli* (Van Name, 1902)**	Didemnidae	Aplousobranchiata	Fort Pierce, USA	12	-	PFA, CLSM
***Distaplia stylifera* (Kowalevsky, 1874)**	Holozoidae	Aplousobranchiata	Fort Pierce, USA	8	-	PFA, CLSM
***Sycozoa sigillinoides* Lesson, 1830**	Holozoidae	Aplousobranchiata	Kerguelsen, French Southern and Antarctic Lands	1 colony	ZMB 2192	70% ethanol, SEM
***Eudistoma obscuratum* (Van Name, 1902)**	Polycitoridae	Aplousobranchiata	Fort Pierce, USA	6	-	PFA, CLSM
***Polyclinum aurantium* Milne Edwards, 1841**	Polyclinidae	Aplousobranchiata	Blacksod Bay, Ireland	1 colony	ZMB 3613	70% ethanol, SEM
***Polyclinum constellatum* Savigny, 1816**	Polyclinidae	Aplousobranchiata	Fort Pierce, USA	10	-	PFA, CLSM
***Synoicum pulmonaria* (Ellis & Solander, 1786)**	Polyclinidae	Aplousobranchiata	Kristineberg, Sweden	1 colony	-	Formaldehyde, SEM
***Aplidium turbinatum* (Savigny, 1816)**	Polyclinidae	Aplousobranchiata	Kristineberg, Sweden	1	-	Bouin, LM
***Morchellium argus* (Milne Edwards, 1841)**	Polyclinidae	Aplousobranchiata	Roscoff, Atlantic Ocean	1 colony	ZMB 1428	70% ethanol, SEM

***Branchiostoma lanceolatum* (Pallas, 1774)**	Branchiostomidae	Cephalochordata	Helgoland, Germany	2	-	Formaldehyde, SEM

Abbreviations: CLSM: confocal laser scanning microscopy, LM: light microscopy, SEM: scanning electron microscopy, PFA: paraformaldehyde.

[1] Catalogue number of the Museum für Naturkunde (Berlin, Germany)

Results

Phenotypic data

Homology hypotheses for morphological characters were conceptualized into a data matrix for 49 tunicate species and five chordate outgroup species. The tunicate species represented 19 families from the five higher tunicate clades, traditionally afforded the rank of classes. The final character matrix included 116 characters comprising characters regularly used in tunicate, especially ascidian, systematics as well as newly acquired characters. The characters covered the entire phenotype and could be conveniently, though not unambiguously categorized: 23 of the characters were general anatomical characters, 17 characters characterized sexual reproduction, 9 characters concerned asexual reproduction, 22 characters detailed the branchial basket anatomy, ten characters the excretory system and digestive tract, four characters the atrium, six characters conceptualized serotonin-like immunoreactivity (serotonin-lir), and 25 characters the microscopic anatomy of the nervous system. Of the 116 characters, 107 were coded as binary characters and nine as multistate characters. 112 characters were parsimony informative, whereas four characters (character numbers 20, 41, 76, and 93) were parsimony uninformative. These characters were autapomorphies of *Pyrosoma atlanticum* (20 & 41), *Kukenthalia borealis* (76), and *Thalia democratica* (93), respectively. The complete data matrix is seen in Supplementary Table 1 and a concise description for each character is found below.

Phylogenetic analysis of phenotypic characters

The extensive heuristic search conducted in PAUP with parsimony as the optimality criterion and with equal weights attributed to all characters resulted in 147.243 most parsimonious trees. Tree length of these optimal trees was 293 steps, with a consistency index (CI) of 0.46, homoplasy index (HI) of 0.54 and a retention index (RI) of 0.84. The strict consensus tree (Fig. 1) is highly resolved and identical to the strict consensus of 24 most parsimonious trees found with TNT. Monophyly of several traditionally recognized tunicate taxa is supported in this strict consensus tree; strongly supported clades are highlighted with capital letters in this figure and featured Bremer support indices of at least 5 along with jackknife values higher than 0.75 and bootstrap percentages higher than 0.70. Besides the two outgroup taxa Cephalochordata (marked A in Fig. 1) and Craniota (B), these strongly supported taxa were: Tunicata (C), Ascidiacea (G), Stolidobranchiata (I), Botryllinae (J), Didemnidae (H), Appendicularia (D), Salpida (F), Doliolida (E), and Molgulidae (K). All of these strongly supported taxa are characterized by uncontroverted apomorphies – a single one (character 54: kidney) in the case of Molgulidae and up to seven (characters 13: tunic, (18): heart beat reversal, (60): pyloric gland, (61): shape of gastrointestinal tract – u-shaped, (78): larval tunic, (81): larval statocyte, (96): brain divided into cortex and neuropil) in the case of Tunicata.

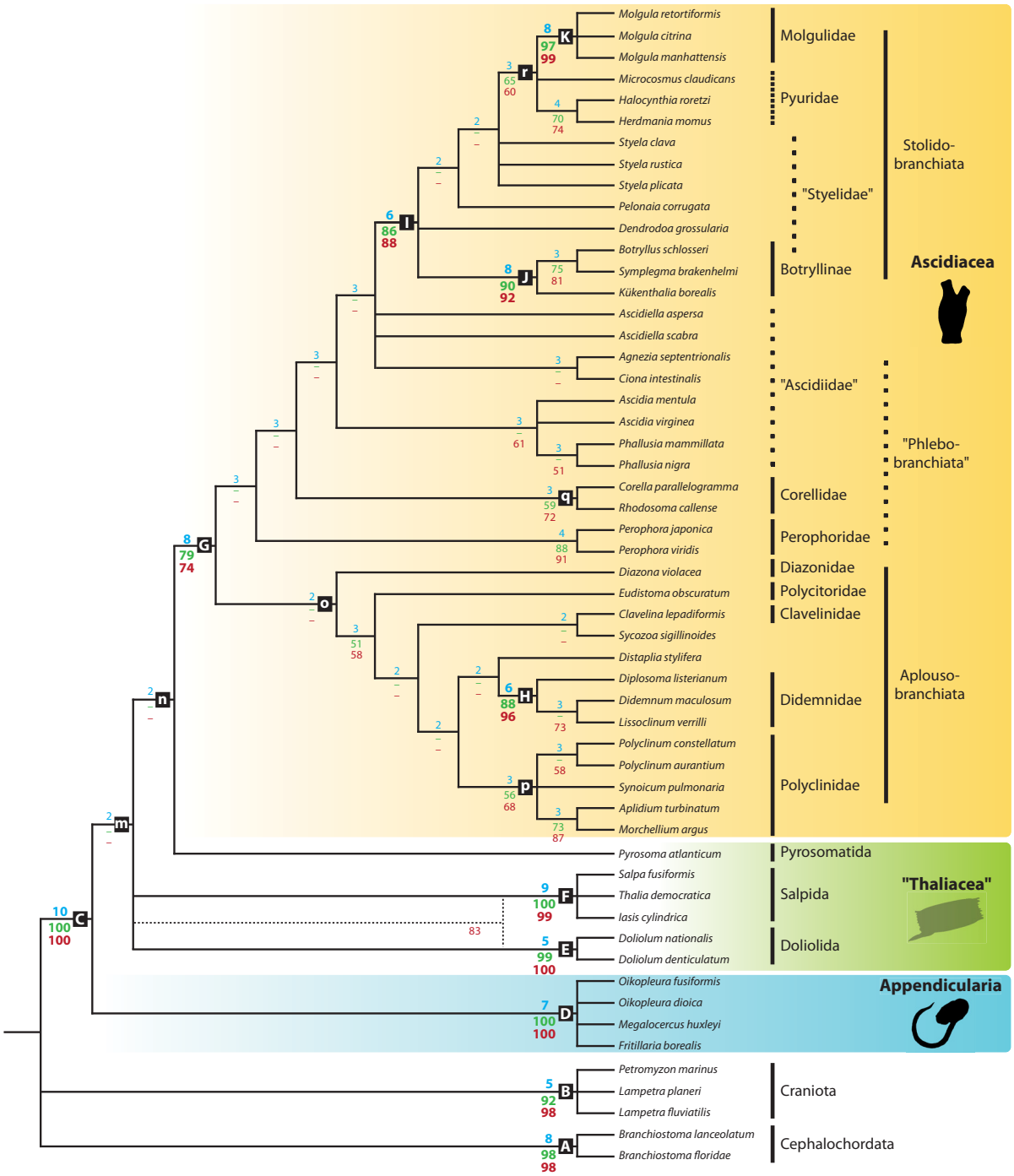

Figure 1. Strict consensus tree of 147.243 equally parsimonious trees found in an heuristic analysis conducted in PAUP analyzing 116 morphological characters (112 parsimony informative) coded for 49 tunicate species and 5 outgroup species. TL = 293, CI = 0.46, RI = 0.81. Numbers indicate Bremer support indices (blue), Jackknife values (green), bootstrap percentages (red). Letters in rectangles refer to monophyla discussed in the text and listed in Table 2. Traditional taxonomic groups are indicated at the top. Quotation marks indicate traditional taxonomic groups found paraphyletic in the present analysis. Note the position of Appendicularia, the monophyly of Ascidiacea, and the paraphyly of "Thaliacea".

Clades supported with uncontroverted apomorphies, but with a Bremer support index below 4 and statistical support indices beneath 0.75 are marked with lower case letters in Figure 1. Clades supported by uncontroverted apomorphies in the parsimony analysis are listed in Table 2 along with these apomorphic characters. Appendicularia (= Larvacea) is the sister taxon to all the remaining tunicates in this analysis. Note that "Thaliacea", a traditionally recognized taxon, comprised of approximately 80 planktonic species moving by jet propulsion, is not found monophyletic in this analysis. Instead the relationship between Doliolida and Salpida is unresolved and Pyrosomatida is sister taxon to the monophyletic Ascidiacea, thereby rendering "Thaliacea" paraphyletic. The single diazonid *Diazona violacea* is the sister taxon to the remaining Aplousobranchiata.

In addition, we conducted a second analysis with reweighting of characters according to the rescaled consistency index from the main analysis with 1000 replicates, TBR branch swapping, and not more than 10 trees saved at each replicate, resulting in 10 most parsimonious trees. The strict consensus was almost identical to the one from our main analysis, the difference being a sister group relationship between Doliolida and Salpida supported with a bootstrap value of 0.83. Tree length of these optimal trees was 109.44 steps, with a consistency index (CI) of 0.66, homoplasy index (HI) of 0.34 and a retention index (RI) of 0.91.

Combination of phenotypic data with molecular sequence data

We used the matrix for phenotypic data described above as the basis for an extended analysis in combination with molecular sequence data. To this end we concatenated the matrix with the aligned 18S rDNA sequence data kindly supplied by Dr. Frédéric Delsuc (Université de Montpellier) published in Tsagkogeorga et al. (2009). Although the matrix of the aligned 18S rDNA sequences possesses the highest taxon overlap with our phenotypic data matrix of all published molecular data matrices, taxon overlap was still less than 100%. We therefore devised the following strategy to combine molecular and phenotypic data: molecular data were appended to the phenotypic data when they were available for the same species. This was the case for 21 species. For 11 more species from the phenotypic data matrix molecular sequences from congeners were available and we combined these into mixed species operational taxonomic units (OTUs). The remaining 23 taxa from the phenotypic data matrix for which no congeneric sequence data were available, were completely removed prior to the analysis. The list of operational taxonomic units and their respective concatenation is detailed in Table 3. The combined data matrix is found in the supplemental data (Supplementary Table 2).

The final data matrix of phenotypic and molecular sequence data thus consisted of 32 taxa and 2121 characters. Besides the 116 phenotypic characters up to 1005 nucleotide positions were present in a taxon, while the remaining characters were gapped positions. 1212 of the 2121 characters were constant and 252 were parsimony uninformative, of which four were phenotypic characters (see above).

Table 2. Monophyletic clades and respective uncontroverted apomorphies, found in the strict consensus of the analysis of the phenotypic data under the parsimony criterion (see Figure 1).

Traditional taxon name	**Letter-label at nodes in Figure 1**	**uncontroverted apomorphy/apomorphies for respective node** (numbers refer to the character numbers in the accompanying data matrix)
Cephalochordata	**A**	**23 (notochord extends from anterior to posterior tip of body), 66 (ventral origin of atrial cavity)**
Craniota	**B**	**94 (adult cerebral eye with lens)**
Tunicata	**C**	**13 (tunic), 18 (heart beat reversal), 60 (pyloric gland), 61 (u-shaped gastrointestinal tract), 78 (larval tunic), 81 (larval statocyte), 96 (brain ganglion-like; i.e., divided into cortex and central neuropil)**
Appendicularia	**D**	**14 (tunic forms elaborate filter house), 35 (round or ovoid stigmata), 105 (caudal ganglion in adults), 115 (statocyte in adult)**
Doliolida	**E**	**12 (continuous muscle bands encircling body), 45 (dorsal organ absent), 114 (unpaired anterior nerve)**
Salpida	**F**	**35 (expanded stigmata), 109 (brain appendages)**
Ascidiacea	**G**	**1 (sessile adults), 36 (transverse orientation of adult stigmata)**
Didemnidae	**H**	**30 (pyloric epicardial budding), 75 (brood chamber in common tunic)**
Stolidobranchiata	**I**	**39 (internal longitudinal vessels not on papillae)**
Botryllinae	**J**	**32 (vascular mesenchymatic budding), 82 (larval photolith)**
Molgulidae	**K**	**54 (kidney)**
Ascidiacea + "Thaliacea"	**m**	**21 (notochord absent in adults), 90 (serotonin-like immunoreactivity in esophagus)**
Ascidiacea + *Pyrosoma atlanticum*	**n**	**64 (rectum in dorsomedian position), 88 (serotonin-like immunoreactivity)**
Aplousobranchiata (incl. *Diazona violacea*)	**o**	**2 (body division into thorax and abdomen)**
Polyclinidae	**p**	**3 (body division into thorax, abdomen, and postabdomen), 31 (postabdominal strobilation)**
Corellidae	**q**	**63 (gastrointestinal tract on right side of the body)**
Molgulidae + Pyuridae	**r**	**8 (oral tentacles branched), 58 (hepatic gland)**

Table 3. Species as operational taxonomic units and their respective concatenation for the analysis of combined phenotypic and molecular data.

Operational Taxonomic Unit (in Figure 2)	**Species used for concatenation** (empty if a single species was used)
Oikopleura (fus&lab)	***Oikopleura fusiformis & O. labradoriensis***
Oikopleura dioica	
Megalocercus huxleyi	
Salpa (fus&thomp)	***Salpa fusiformis & S. thompsoni***
Thalia democratica	
Iasis cylindrica	
Doliolum nationalis	
Doliolum denticulatum	
Pyrosoma atlanticum	
Ascidia (ment&cerat)	***Ascidia mentula & A. ceratodes***
Ascidia (virg&ahod)	***Ascidia virginea & A. ahodori***
Corella (parall&infla)	***Corella parallelogramm & C. inflata***
Phallusia mammillata	
Phallusia nigra	
Perophora (jap&saga)	***Perophora japonica & P. sagamiensis***
Perophora viridis	
Ciona intestinalis	**Note: may be *C. robusta***
Molgula retortiformis	
Molgula citrina	
Molgula manhattensis	

Microcosmus (claud&squa)	*Microcosmus claudicans & M. squamata*
Styela (cla&gib)	*Styela clava & Styela gibsii*
Styela (rust&monte)	*Styela rustica & S. montereyensis*
Styela plicata	
Botryllus schlosseri	
Symplegma (brake&viri)	*Symplegma brakenhielmi & S. viridis*
Halocynthia roretzi	
Herdmania momus	
Pelonaia corrugata	
Clavelina (lepad&meridio)	*Clavelina lepadiformis & C. meridionalis*
Branchiostoma floridae	
Petromyzon marinus	

Phylogenetic analysis of phenotypic characters combined with molecular sequence data

Treating all characters as unordered and with equal weight an heuristic analysis under the parsimony paradigm was performed. We analyzed 10 000 replicates starting from random trees with subsequent tree bisection and reconnection, retaining a single best tree of a tree length of at least 500 at each replicate. This search resulted in a single most parsimonious tree with a tree length of 2388, a consistency index (CI) of 0.57, homoplasy index (HI) of 0.43, and a retention index (RI) of 0.71. The strict consensus tree shown in Fig. 2 is well resolved and is highly similar to the one published by Tsagkogeorga et al. (2009) that was based on a Bayesian analysis of the same molecular sequences, but more taxa were included (see previous paragraph).

The strict consensus tree is highly resolved and finds strong intrinsic statistic support for the monophyly of Tunicata (JK: 1.00, bt: 1.00). Within the targeted in-group, the Tunicata, several higher monophyletic clades are recovered: Appendicularia (JK: 1.00, bt: 1.00), Stolidobranchiata (JK: 1.00, bt: 1.00), Molgulidae (JK: 1.00, bt: 1.00), Styelidae (JK 0.98, bt: 0.97), Thaliacea (JK: 0.90, bt: 0.89), Doliolida (JK: 1.00, bt: 1.00), Salpida (JK: 1.00, bt: 1.00), Ascidiidae (JK: 1.00, bt: 1.0), and Perophoridae (JK: 1.00, bt: 1.00). Aplousobranchiata was represented by the single OTU *Clavelina (lepad&meridio)* and therefore monophyly of Aplousobranchiata was not tested in this analysis. "Phlebobranchiata" is paraphyletic with respect to Thaliacea plus Aplousobranchiata, thus Thaliacea renders "Ascidiacea" also paraphyletic in this analysis. Thaliacea, now recovered monophyletic, is the sister taxon to Aplousobranchiata, which however was represented by a single OTU. Note the identical position of Appendicularia as the sister taxon to the remaining tunicate taxa, as in the analysis of the phenotypic data.

In order to gauge the influence of the different data partitions, molecular data versus phenotypic data, for the outcome of the phylogenetic analysis we gradually increased the weight of the phenotypic data from zero (molecular data only) to equal (1:1) to 5:1. Because the major difference in the purely molecular and the purely phenotypic data is the monophyly of Thaliacea in the molecular analysis (paraphyletic in the phenotypic analysis) and the monophyly of Ascidiacea in the phenotypic analysis (paraphyletic in the molecular analysis), we focus on these two groups in the following paragraph.

If the weight of phenotypic data is doubled (2:1) the result is essentially the same as with the equally weighed data, which in turn is concordant with the analysis of the purely molecular data (Fig. 2). However the bootstrap value for a monophyletic Thaliacea increases from 0.51 in the analysis of purely molecular data to 0.81 in the equal-weights scheme (1:1) and then drops to 0.66 in the analysis with the weight doubled for the phenotypic data (2:1) (Fig. 3). "Ascidiacea" is still paraphyletic under this weighing scheme. At a weight of phenotypic data to molecular data of 3:1, Thaliacea becomes paraphyletic with Salpida, Doliolida, and Pyrosomatida, represented by the single species *Pyrosoma atlanticum*, being successive sister taxa to Ascidiacea (i.e. (Appendicularia (Salpida (Doliolida (*P. atlanticum* + Ascidiacea))))).

Ascidiacea becomes monophyletic under this weighting scheme, with a bootstrap support of 0.66. At a weighting scheme of phenotypic data to molecular data of 4:1, Ascidiacea is monophyletic, with a bootstrap support of 0.94. In this analysis "Thaliacea" is found paraphyletic as in the previous analysis. Finally, at a weighting scheme of phenotypic data to molecular data of 5:1, Ascidiacea is monophyletic, with a bootstrap support of 0.95. Under this weighting scheme "Thaliacea" is again recovered paraphyletic.

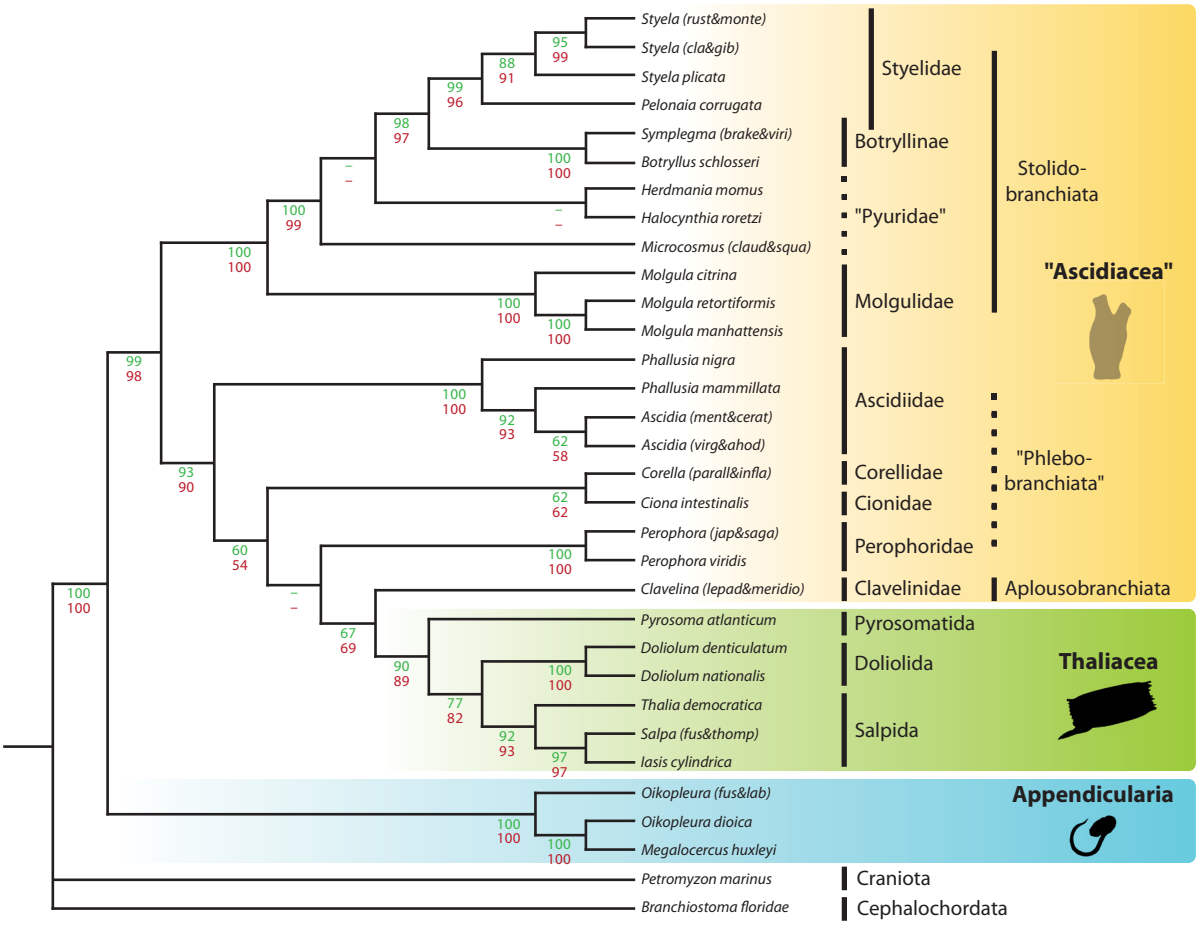

Figure 2. Single most parsimonious tree found in an heuristic analysis conducted in PAUP analyzing 116 morphological characters (112 parsimony informative) combined with 18S rDNA-sequence data resulting in 2121 characters for 32 tunicates (21 species and 11 concatenated species from the same genus; see Table 3 for details) and 5 outgroup species. TL = 2388, CI = 0.57, RI = 0.71. Numbers indicate Jackknife values (green), bootstrap percentages (red). Traditional taxonomic groups are indicated at the top. Quotation marks indicate traditional taxonomic groups found paraphyletic in the present analysis. Note the position of Appendicularia, the paraphyly of "Ascidiacea", and the monophyly of Thaliacea.

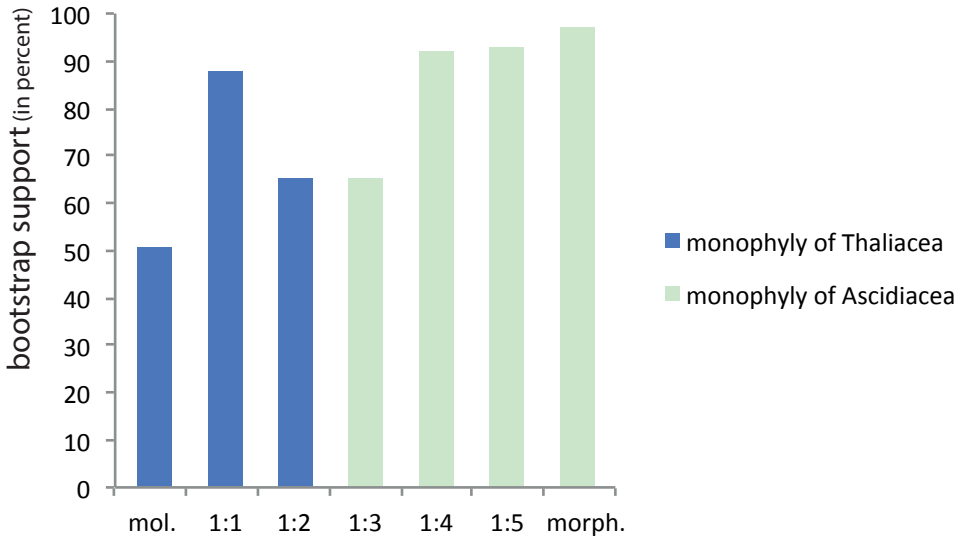

Figure 3. Bootstrap percentages supporting the monophyly of Thaliacea and the monophyly of Ascidiacea at different weighting schemes of phenotypic and molecular data. Number of data in the respective data partitions in the combined data set: phenotypic data: $\#_{(morph)} = 116$, number of sequence sites: $\#_{(mol)} = 2005$; i.e. $\#_{(morph)} : \#_{(mol)} \approx 0.058 \approx 1:17$.

List of characters

General morphology

1. Sessile adults: (0) absent; (1) present. Within tunicates, species belonging to the taxa Phlebobranchiata, Aplousobranchiata, and Stolidobranchiata (ascidians) develop sessile adults after metamorphosis. Adult specimens belonging to the taxa Thaliacea and Appendicularia, as well as species belonging to the outgroup taxa are free-living, actively swimming or planktonic. Although adult cephalochordates are characterized as semi-sessile, they actively burrow in the sediment and are capable to actively change their location via undulatory vigorous swimming (Pietschmann, 1962).

2. Body division: (0) absent; (1) present. Body division is acknowledged here for species with recognizably divided bodies in outer appearance and internal anatomy (e.g., Millar, 1970; Van Name, 1945). Since Cionidae do not display body division in their overall morphology *C. intestinalis* is coded as 0.

3. Number of body parts: (0) two; (1) three. Number of body parts refers to the division of the body into thorax, abdomen, and postabdomen traditionally recognized in ascidians (e.g., Millar, 1966; Van Name, 1945). For *D. stylifera* Kott (1990) described two body parts and a posterior abdominal sac that she does not regard as a homolog of a postabdomen. Van Name (1945) describes three body parts, mentioning however, that the postabdomen only contains gonads, not the heart. We follow Kott's description, because of the absence of the heart from the abdominal sac.

4. Incurrent and excurrent siphon on opposite poles of the animal: (0) absent; (1) present.

5. Lobed incurrent siphon: (0) absent; (1) present. The incurrent siphon of many tunicate species shows more or less conspicuous lobes. Information on character distribution is found in Berrill (1950), Groepler (2016), and Van Name (1945).

6. Numbers of lobes at incurrent siphon: (0) four; (1) six; (2) eight; (3) more than eight. This character is traditionally used in identification keys to distinguish tunicate families (Berrill, 1950; Groepler, 2016; Kott, 1985, 1990, 1992, 2001; Millar, 1966, 1970; Van Name, 1945). In adult *P. mammillata* the number of lobes is difficult to determine because of the irregularly bulbous and extensive external tunic, but counts result in eight or nine lobes. In *P. nigra* eight lobes or more than eight lobes are described for the incurrent siphon (Rocha et al., 2012; Van Name, 1945). Therefore, we coded this character as polymorphic for investigated *Phallusia* species. For *A. septentrionalis* Van Name (1945) counted six or eight lobes, here we also coded this character as polymorphic. Lobes in *D. grossularia* are inconspicuous; the opening of the incurrent siphon is tetragonal (Groepler, 2016). We homologize the tetragonal opening of the incurrent siphon with 4 lobes at incurrent siphons. In *D. nationalis* the oozooids possess eight lobes, while blastozooids possess 12 lobes (Berrill, 1950); we coded the character as polymorphic. See also Fig. 4A-D.

7. Oral tentacles: (0) absent; (1) present. Oral tentacles are located at the transition of mouth opening and branchial basket (Huus, 1956). In planktonic tunicates oral tentacles are not developed, while they are present in all investigated ascidian species. For the outgroup species we consider the velar tentacles present in all five species homologous to oral tentacles in Tunicata.

8. Shape of oral tentacles: (0) simple, unbranched; (1) branched. Information on character distribution is found in Drasche (1884) and Berrill (1950), see also Fig. 4 E-G.

9. Lobed excurrent siphon: (0) absent; (1) present. The excurrent siphon as well as the incurrent siphon in most tunicate species is lobed (see also character 5). We consider a cloacal languet present in some aplousobranch species and in *B. schlosseri* homologous to a lobed excurrent siphon. Information on character distribution is found in Berrill (1950) and Van Name (1945).

10. Number of lobes at excurrent siphon: (0) two; (1) four; (2) six; (3) more than six; (4) cloacal languet. Information on character distribution is found in Berrill (1950) and Van Name (1945).

11. Conspicuous circular muscle bands for locomotion: (0) absent; (1) present. This character is only present in Salpida and Doliolida (Ihle, 1956).

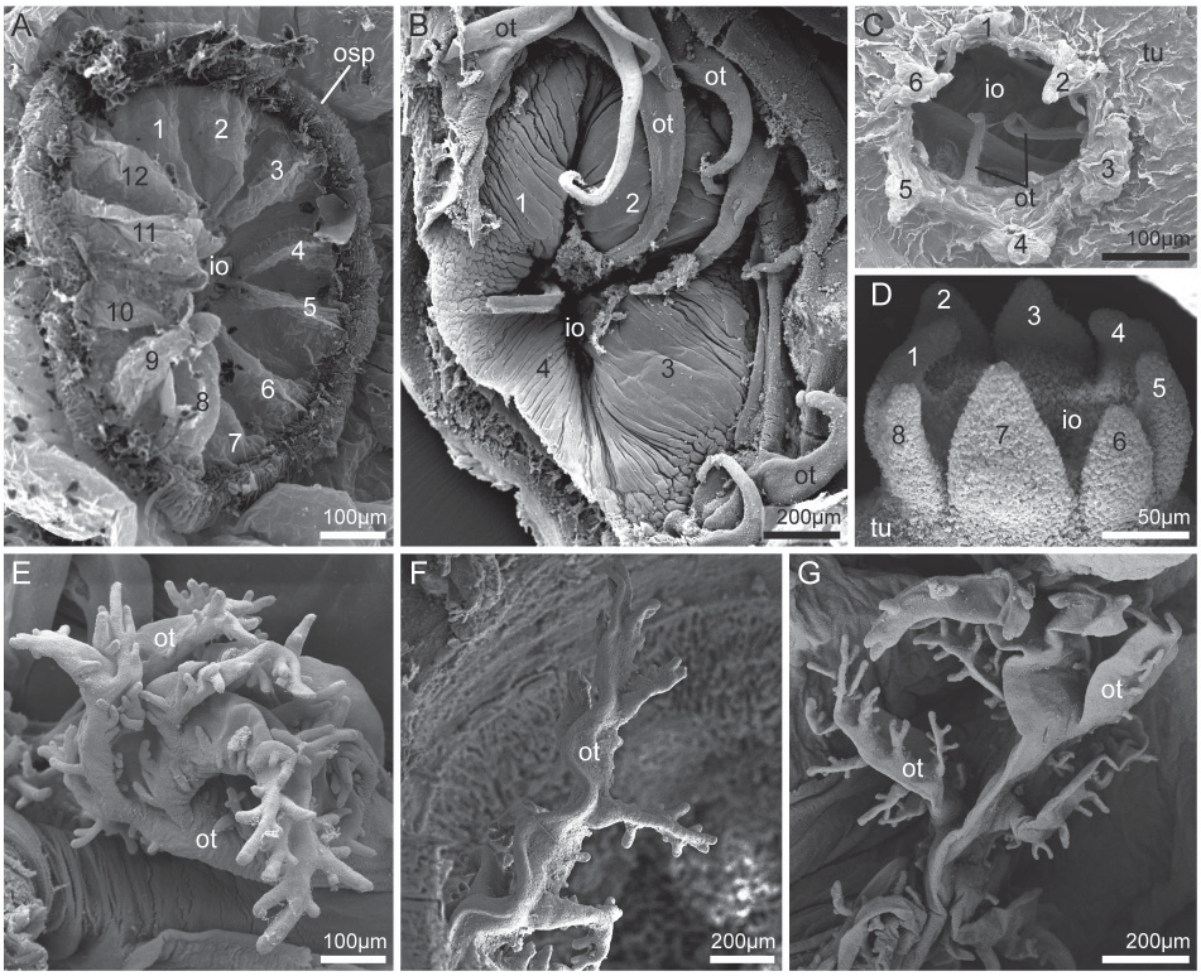

Figure 4. Scanning electron micrographs of incurrent siphons and oral tentacles (ot). **A-D:** Lobed incurrent siphons of different tunicate species. **A:** The incurrent siphon of *Doliolum denticulatum* possesses 12 lobes. **B:** The incurrent siphon of *Kükenthalia borealis* consists of four lobes. Oral tentacles are simple, without branching. **C:** The incurrent siphon of *Diplosoma listerianum* forms six lobes, oral tentacles are simple in shape. **D:** Incurrent siphons of *Morchellium argus* possess eight conspicuous lobes. **E-G:** Branched oral tentacles in three different stolidobranch species. **E:** In *Molgula manhattensis* oral tentacles are branched. **F:** Oral tentacle of *Microcosmus claudicans*. **G:** Oral tentacle of *Herdmania momus*. io: incurrent opening, osp: oral sphincter, tu: tunic.

12. Shape of circular muscle bands: (0) discontinuous; (1) continuous. In species of Doliolida muscle bands are continuous while in the investigated members of Salpida muscle bands are discontinuous on the ventral side (Ihle, 1956).

13. Tunic: (0) absent; (1) present. The tunic is an extracellular covering produced by the epidermis and containing cellulose. Tunicates are the only animals able to produce cellulose (Hirose et al., 1999; Lohmann, 1956; Shenkar and Swalla, 2011).

14. Shape of tunic: (0) simple cover of epidermis; (1) elaborate, multi-chambered filter-feeding house. In Appendicularia the tunic additionally functions as a complex filtering system to concentrate food particles from the water column (Flood and Deibel, 1998; Körner, 1952).

15. Calcareous spicules in tunic: (0) absent; (1) present. For additional protection against predators some ascidians deposit calcareous spicules into the tunic. The tunic of species in Didemnidae is usually equipped with copious amounts of calcareous spicules; however, the didemnid *D. listerianum* possesses no spicules visible in a dissecting microscope (Berrill, 1950). In *H. momus* and *K. borealis* calcareous spicules are also present in the tunic (Lambert and Lambert, 1987; Van Name, 1945).

16. Epicardium: (0) absent; (1) present. Epicardia are internal sacs lined completely by an epithelium. Ontogenetically they are derived from the posterior ventral part of the pharynx, from a paired rudiment. Extent and form in the adults may vary. Berrill (1950) homologized excretory cells and organs with epicardia. These however develop from vacuolized blood cells and the homology to epicardia remains uncertain. We follow in this respect Groepler's argument (Groepler, 2016), although we realize that Berrill's hypothesis should be investigated with modern methods (Berrill, 1950).
Although the homology of epicardia and coelomic cavities in cephalochordates and vertebrates is not definitively established, the derivation from the archenteron and the further development (especially in vertebrates) as an epithelial lining of inner organs (including heart and intestine) support the hypothesis of homology (Groepler, 2016; Romer and Parsons, 1986). Berrill (1950) tentatively suggested this hypothesis. We therefore coded the character state as 1 for outgroup species. In Appendicularia the so-called procardial sacs are not separated from the pericardium and therefore not homologous to the epicardia (own series of sections). Information on character distribution is found in Berrill (1950), and Huus (1956), see also Fig. 5A & B. For Molgulidae we follow Huus (1956) in homologizing epicardia and kidney.

17. Shape of epicardium in adult: (0) unpaired; (1) paired, separated sacs. Information on character distribution is found in Berrill (1950), and Groepler (2016).

18. Heart beat reversal: (0) absent; (1) present. In all tunicates the heart regularly shows a heartbeat reversal (Bone et al., 1997; Fenaux, 1998; Kriebel, 1967).

19. Endocarp: (0) absent; (1) present. Endocarps are projections of the atrial wall into the atrial cavity. They are usually found on the parietal wall but may also be present on the visceral side. Endocarps contain a spongy tissue richly supplied with lacunae and blood cells (Kott, 1985). Endocarps are also called parietal vesicles (Berrill, 1950). *D. grossularia* possesses endocarps (Fig. 5C, contra Rocha et al., 2012). When detailed anatomical descriptions were available, but endocarps were not described, we coded the character state as 0, e.g., for *P. corrugata* (Millar, 1966; Rocha et al., 2012) and *K. borealis* (Millar, 1966; Van Name, 1945). Further information on character distribution is found in Berrill (1950), Kott (1985), Rocha et al. (2012), and Van Name (1945).

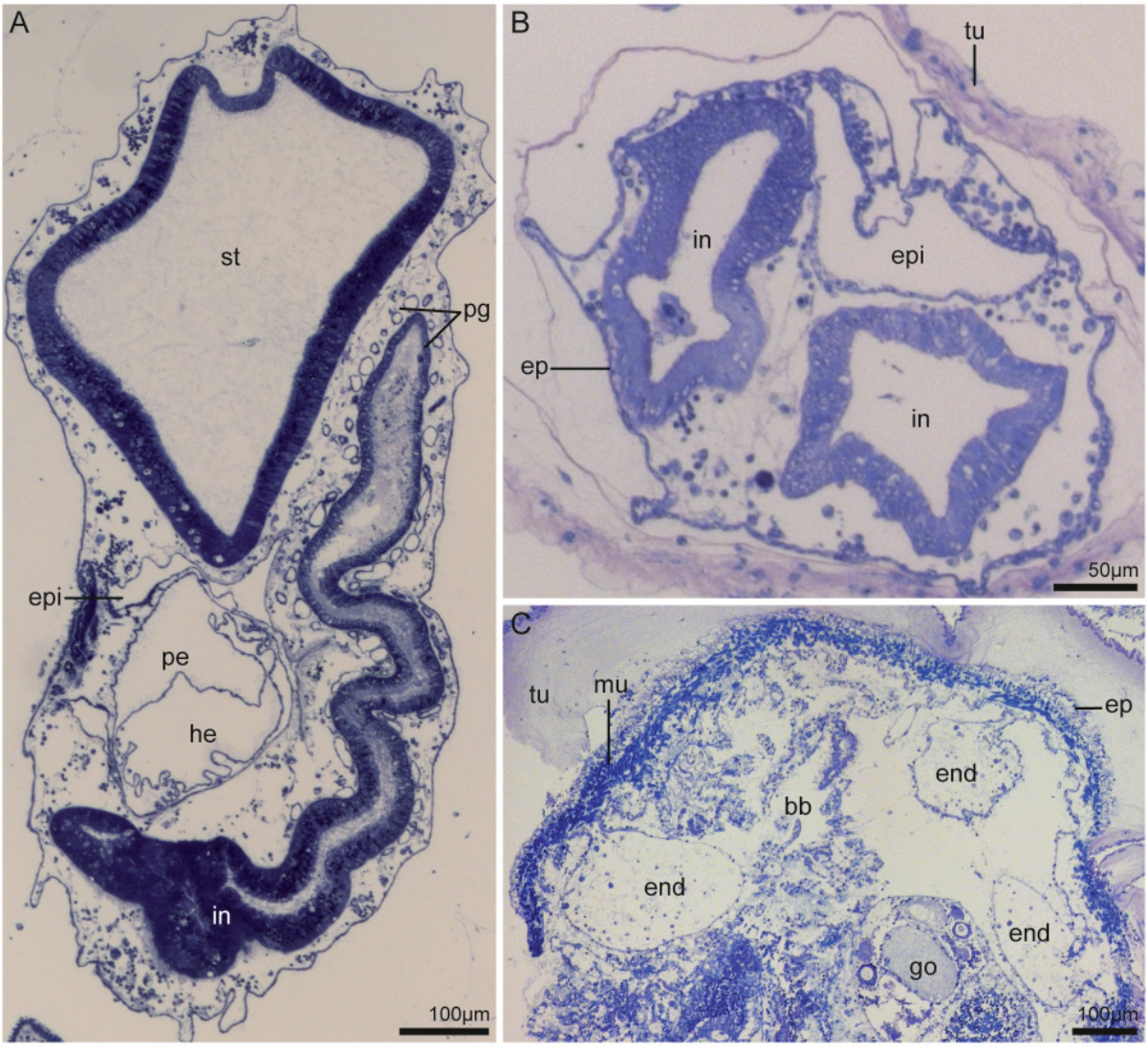

Figure 5. Light micrographs of semithin cross sections through the abdomens of two aplousobranch species, and cross section through one stolidobranch ascidian, stained with toluidine blue. **A:** Section through *Clavelina lepadiformis*, dorsal to the top, left to the right. The epicardium (epi) is positioned in close proximity to the pericardium (pe). It is bordered by an epithelium. **B:** Cross section through *Aplidium turbinatum*, ventral to the top, right to the right. The epicardium is conspicuously large. **C:** Cross section through *Dendrodoa grossularia*, dorsal to the top, right to the right. Endocarps (end) are visible as projections from the body wall into the atrium. ep: epidermis, go: gonad, he: heart, in: intestine, mu: musculature, pg: pyloric gland, st: stomach, tu: tunic.

20. Light organs: (0) absent; (1) present. In Pyrosomatida paired organs with conspicuously large cells that contain symbiotic bacteria with the ability to produce light, are found lateral to the mouth openings (e.g., Mackie and Bone, 1978; Neumann, 1956). Bioluminescence is also known from some salp and appendicularian species without comparable organs (Bone, 1998).

21. Notochord in adults: (0) absent; (1) present. Ontogenetically, in most tunicates the notochord is reduced after metamorphosis. However, in Appendicularia the notochord persists in the adult stage (Lohmann, 1956). In the outgroup species, the cephalochordates and the agnathans, the notochord is present during the complete life-cycle.

22. Notochord in larvae: (0) absent; (1) present. In Salpida and Pyrosomatida and few ascidian species tadpole larvae are not developed (Huus, 1956; Ihle, 1956). Larvae of all other investigated tunicate species as well as larvae of outgroup species possess notochords.

23. Length of notochord (if present): (0) not extending to the anterior end of the body; (1) extending along the entire body to its most anterior tip. In cephalochordates the notochord extends along the whole body. In tunicates and lampreys the notochord does not extend into the anteriormost part of the body (Romer and Parsons, 1986; Ruppert, 1997a).

Asexual reproduction

24. Coloniality: (0) absent; (1) present.

25. Sexually mature form colonial: (0) absent: sexually propagating chain of animals break up; (1) present: sexual forms remain entirely colonial. In members of Salpida and Doliolida the blastozooids become solitary during later development. On the other hand species of Pyrosomatida and the colonial ascidians stay within the colony during the entire development (Huus, 1956; Ihle, 1956).

26. Connection of zooids within colonies: (0) zooids completely embedded in a common tunic; (1) zooids connected via stolons. In *D. violacea* zooids are embedded in a common tunic that however does not surround the complete zooid, but is restricted to the basal part of the animals, their abdomen while the apical parts of the zooids (their thorax) remain separated (Berrill, 1948). We coded the character state for *D. violacea* as 1.

27. Metagenesis: (0) absent; (1) present. Metagenesis is the obligate alteration between asexual and sexual reproductive modes in consecutive generations. Colonial species are coded as metagenesis being present, if the presence of an oozooid (i.e., an individual that does not develop gonads but reproduces only asexually) as the founder of a colony is mentioned in the literature (Berrill, 1950; Brien and Brien-Gavage, 1927; Deviney, 1934; Gutierrez and Brown, 2017; Kott, 1990; Nakauchi, 1982).

28. Polymorphic generations: (0) absent; (1) present. Consecutive generations in a metagenetic life cycle can display drastically different morphologies or can be morphologically highly similar or even indistinguishable (except of course in respect to the presence of gonads).

29. Type of budding: (0) epicardial; (1) mesenchymatic; (2) palleal; (3) complex stolo prolifer. Different modes of budding have been discussed at length in the tunicate literature. Following different authors (Groepler, 2016; Huus, 1956; Nakauchi, 1982), we distinguish four general types of budding: epicardial budding (epicardia as the main source of the growing bud tissue), mesenchymatic (mesenchymatic cells are the main source of the growing bud tissue), palleal (peribranchial wall is the main source of the growing bud tissue), and budding via a complex stolo prolifer (the stolo prolifer contains at least: gonadal strand, pericardial strand,

peribranchial strands, entodermal strand, neuronal strand, and of course ectoderm). In the colonial stolidobranch ascidians *B. schlosseri*, *S. brakenhielmi* mesenchymatic and palleal budding are described (Gutierrez and Brown, 2017), and for *K. borealis* Berrill (1950, p. 175) describes palleal budding, whereas Van Name (1945, p. 234) describes stolons. Here we coded the character as a polymorphic character (1 & 2) for *B. schlosseri*, *S. brakenhielmi*, and *K. borealis*, as both types of budding seem to be present in the three species.

30. Type of epicardial budding: (0) strobilation; (1) pyloric (esophageal and entero-epicardial). Strobilation or transverse fission means that the thoracic region is absorbed, a series of constrictions divide the posterior part into several regions from which the buds develop. In *D. stylifera* buds are already developed in the larvae. According to Berrill (1935), the larval budding of members of *Distaplia* evolved as a heterochronic shift. The main source of tissue in the larval bud is the epicardium. In addition, the author states that larval and adult budding in *Distaplia* are essentially the same. In both cases, Berrill (1935) mentions the "constriction" of the epidermis. Investigated members of Didemnidae show an exceptional mode of budding – pyloric budding. Through epicardial budding a new thorax and abdomen are formed. While the new thorax connects with the old abdomen, the new abdomen connects with the old thorax (Berrill, 1935).

31. Type of strobilation: (0) abdominal; (1) postabdominal. Members of Polyclinidae possess a tripartite body and strobilation is located in the postabdomen. In the other investigated aplousobranch species that develop buds through strobilation, budding occurs in the abdomen.

32. Type of mesenchymatic budding: (0) septal; (1) vascular. In septal budding the septum in the stolon is the major source of cells for the development of buds (Berrill, 1935; Groepler, 2016; Huus, 1956; Nakauchi, 1982). Stolons, however, are also involved in other forms of budding as well (see characters 26 and 29). In vascular budding, hemocytes are the major source of tissue for the developing buds (Groepler, 2016; Nakauchi, 1982).

Branchial basket

33. Shape of branchial basket wall: (0) unfolded; (1) folded. In some ascidians the wall of the branchial basket is folded with clearly demarcated folds extending into the lumen of the branchial basket. Stolidobranchiata is named after this character, yet, the branchial baskets of the smaller colonial stolidobranch species and *P. corrugata* are not folded (e.g., Berrill, 1950; Drasche, 1884; Van Name, 1945). In *D. grossularia* at least one fold is present (Hartmeyer, 1923).

34. Arrangements of stigmata in one side of the body: (0) one stigma; (1) three rows; (2) four rows; (3) more than four rows. The number of rows of stigmata in the branchial basket of adult individuals is considered here. Note that the orientation of rows in ascidians is perpendicular to the anterior-posterior axis. Consequently, a stigma in cephalochordates and lampreys

corresponds to a row of stigmata in tunicates (see also character 36), so we coded the character state for the outgroup species as 3. Information on character distribution is found in Berrill (1950), Ihle (1956), Kott (1985, 1990, 2001), Lohmann (1914), and Van Name (1945).

35. Shape of stigmata: (0) straight; (1) lunate or spiral; (2) round or ovoid; (3) expanded. Most tunicate species and outgroup species possess straight stigmata. Information on character distribution is found in Berrill (1950), Lohmann (1956), and Van Name (1945). In Salpida the branchial wall is almost completely missing resulting in a single pair of largely expanded openings, which we consider as the stigma and code as 3.

36. Orientation of stigmata in adults: (0) longitudinal (anterior to posterior); (1) transversal (ventral to dorsal). This character is only applicable for straight stigmata. The longitudinal axis of a single stigma is considered here. While in the examined ascidian species stigmata are oriented longitudinally, in Doliolida and Pyrosomatida, and in the outgroup species stigmata

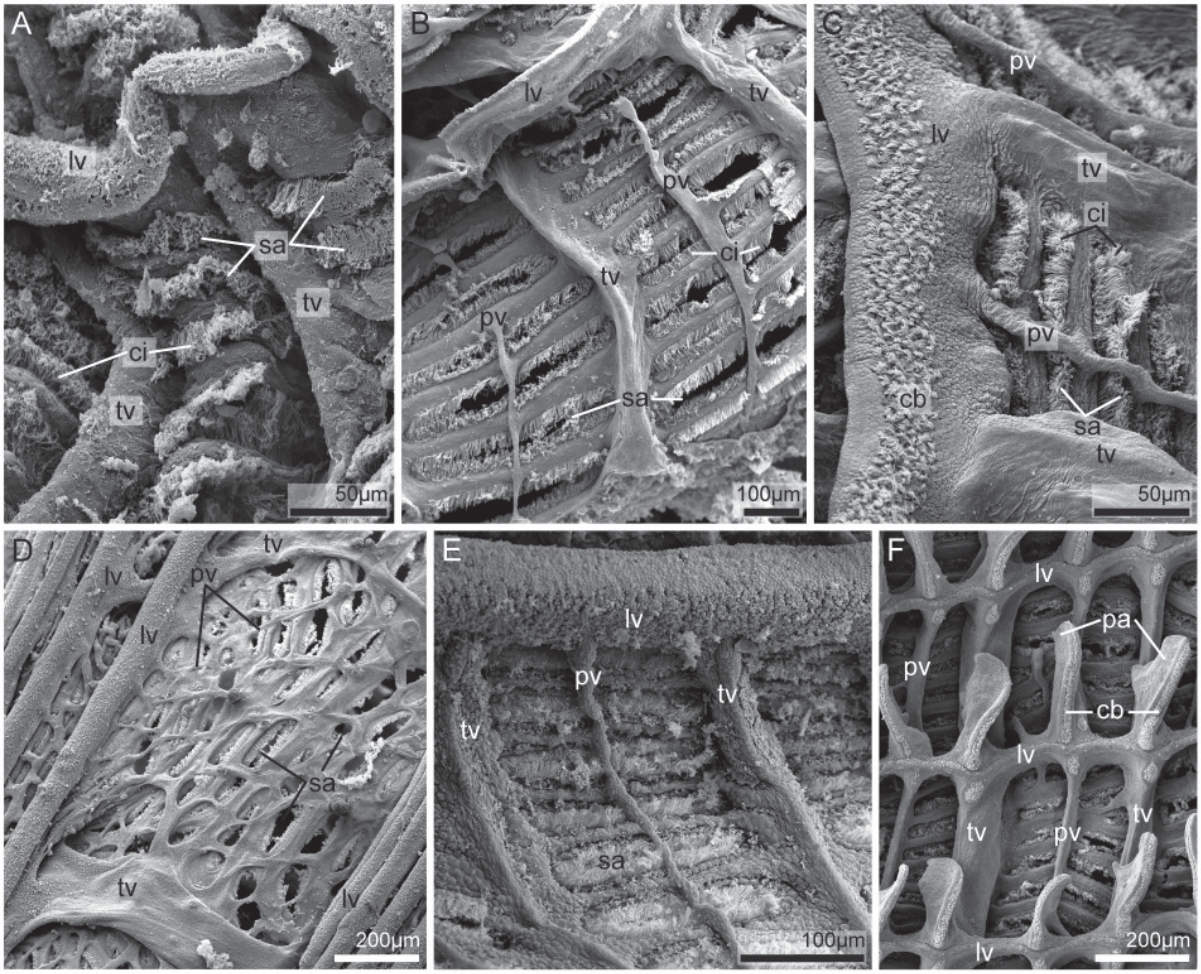

Figure 6. Scanning electron micrographs of parastigmatic blood vessels (pv) in different ascidian species. **A:** The branchial basket of *Botryllus schlosseri* lacks parastigmatic blood vessels. **B:** In the branchial basket of *Kükenthalia borealis* parastigmatic blood vessels cross stigmata (sa). **C:** Parastigmatic blood vessels of *Styela plicata*. Longitudinal blood vessels (lv) are equipped with ciliary bands (cb). **D:** Several parastigmatic blood vessels emanate from longitudinal blood vessels, crossing the stigmata of *Molgula citrina*. **E:** Parastigmatic blood vessels of *Microcosmus claudicans.* **F:** In the branchial basket of *Ciona intestinalis* parastigmatic and transverse blood vessels (tv) alternate. ci: cilia.

are transversal in orientation (see also comment for character 34).

37. Parastigmatic blood vessels: (0) absent; (1) present. These blood vessels are intermediate transverse vessels that cross the stigmata but do not interrupt them (Kott, 1985). Information on character distribution is found in Van Name (1945), see also Fig. 6.

38. Internal longitudinal blood vessels: (0) absent; (1) present. Longitudinal blood vessels are vessels that protrude visibly into the lumen of the branchial basket (Kott, 1985 (Fig. 3); Monniot and Monniot, 1972 (see Fig. 1)). The term is equivalent to the term "internal longitudinal vessels" of Van Name (1945). Longitudinal blood vessels are present in all investigated pyrosome, phlebobranch and stolidobranch species, and in *D. violacea* (Fig. 7).

39. Internal longitudinal blood vessel on papillae: (0) no; (1) yes. In some species longitudinal vessels are situated on papillae (Fig.7A-F).

40. Ciliated internal longitudinal blood vessels: (0) no; (1) yes. Cilia on the internal longitudinal blood vessels project into the lumen of the branchial basket (Fig. 7A-H).

41. Arrangement of cilia on internal longitudinal blood vessels: (0) continuous row of cilia; (1) cilia in individual tufts. In the ascidian species where cilia on internal longitudinal blood vessels are present (character 40: (1)) these cilia are arranged in a continuous row. In *P. atlanticum* cilia are arranged in individual tufts (Fig. 7A-H).

42. Branchial basket with papillae: (0) absent; (1) present. Branchial papillae often project into the lumen of the branchial basket above the level of the internal longitudinal vessels, as spoon or sickle-shaped, free-standing papillae (Kott, 1985). They are present in all members belonging to Phlebobranchiata and in *P. atlanticum* (Fig. 7A), *D. violacea*, and members of the genus *Polyclinum* (Berrill, 1950; Groepler, 2016; Van Name, 1945).

43. Papillae at intersections of transverse and longitudinal vessels: (0) no; (1) yes. From longitudinal vessels papillae bulge into the branchial basket at the intersections of transverse and longitudinal vessels (Fig. 7C-F).

44. Junctions of longitudinal and transverse vessels with cilia: (0) no; (1) yes. Ciliated junctions of these longitudinal and transverse vessels are present in all investigated phlebobranch species (Fig. 7B-F) and *D. violacea*.

45. Dorsal organ: (0) absent; (1) present. The dorsal organ is a fold of the branchial wall along the mid-dorsal line of the branchial basket that usually is curved in transverse section (Kott, 1985). We chose to use this term in order to indicate the correspondence of structures situated in the dorsal midline of the branchial basket, which in traditional taxonomic treaties are labeled as dorsal lamina, dorsal languets, dorsal groove etc. A dorsal organ is present in most tunicate

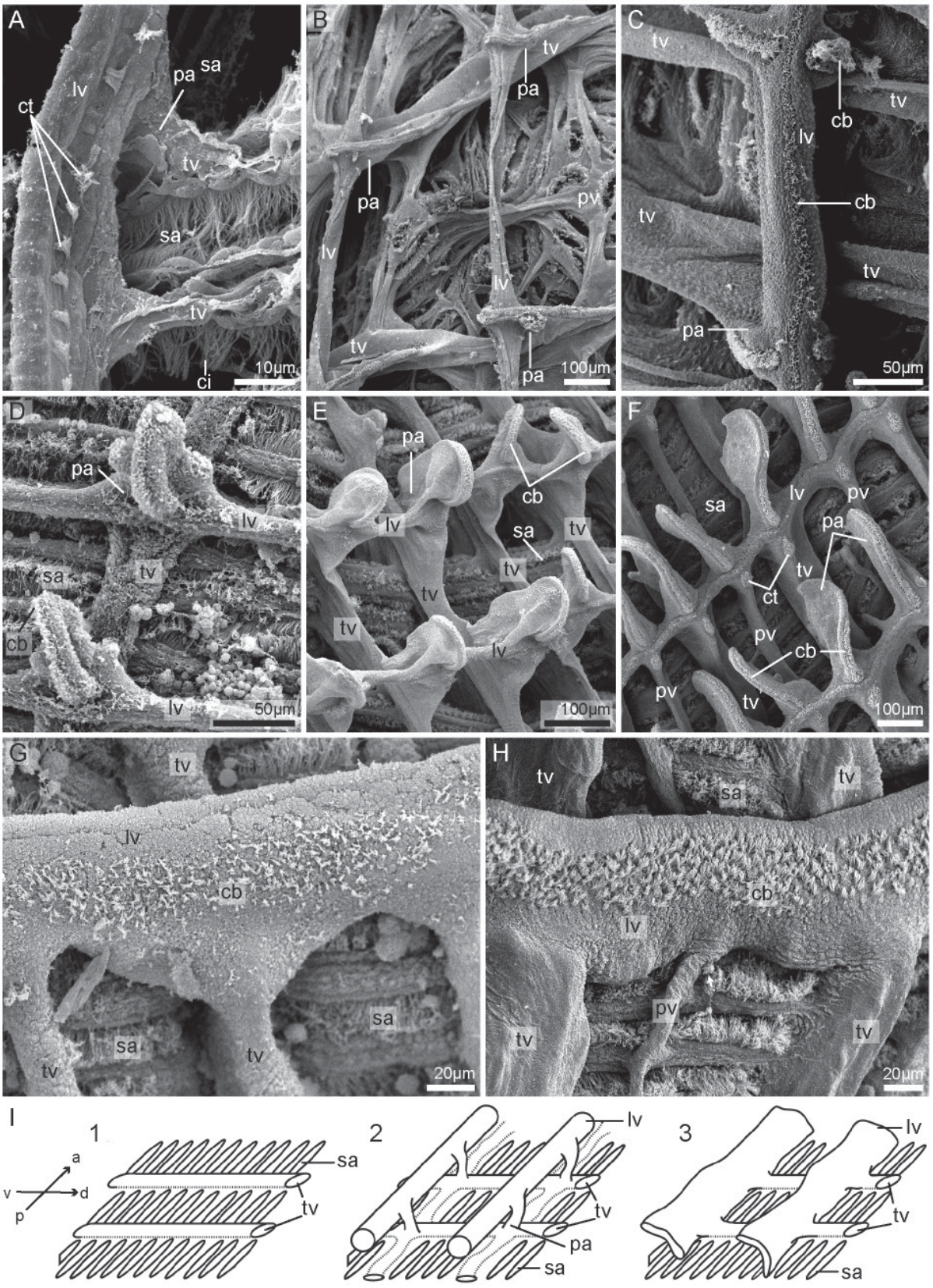

Figure 7. Scanning electron micrographs of longitudinal blood vessels (lv) in the branchial basket of different tunicate species. **A:** Longitudinal blood vessel in the branchial basket of *Pyrosoma atlanticum*. Longitudinal blood vessels settle on papillae (pa) and bear several individual ciliary tufts (ct). **B-F:** Longitudinal and transverse blood vessels of phlebobranch ascidians. Cilia settle on junctions of transverse and longitudinal vessels in form of ciliary bands or ciliary tufts. **B:** In *Corella parallelogramma* longitudinal vessels also settle on papillae. **C:** Longitudinal blood vessels

in *Ascidiella scabra* are situated on papillae and possess ciliary bands that also proceed longitudinally (cb). **D:** In *Ascidia virginea* longitudinal blood vessels that settle on papillae and possess longitudinal ciliary bands are present. **E:** In the branchial basket of *Phallusia nigra* longitudinal vessels are situated on papillae. Ciliary bands run along the longitudinal vessels. **F:** In *Ciona intestinalis* longitudinal blood vessels settle on papillae. Along with longitudinal vessels ciliary bands proceed. At each intersection of longitudinal and transverse blood vessels (tv) an individual ciliary tuft is visible. **G:** Longitudinal blood vessels of *Halocynthia roretzi* are not situated on papillae. They overlap into the cavity of the branchial basket and bear a wide ciliary band. **H:** In *Styela plicata* papillae in the branchial basket are missing. A broad ciliary band runs along with the longitudinal blood vessel. **I:** Schematic drawings of the arrangement of longitudinal and transverse blood vessels in tunicates. **1**: Solely transverse blood vessels are developed. **2**: Longitudinal blood vessels are present, these settle on papillae. **3**: Longitudinal vessels settle on transverse vessels, not on papillae. They project into the lumen of the branchial basket. ci: cilia, sa: stigma.

species, except Doliolida (Deibel and Paffenhöfer, 1988). The dorsal organ in *Branchiostoma* is usually called “epipharyngeal groove” (Franz, 1927; Ruppert, 1997b). It corresponds to the dorsal ridge in lampreys (Mallat, 1979).

46. Dorsal organ consisting of languets: (0) no; (1) yes. Languets are finger- or tongue-like projections into the lumen of the branchial basket. Information on character distribution is found in Berrill (1950), Kott (1985), and Van Name (1945), see also Fig. 8.

47. Number of languet equals number of transverse vessels: (0) no; (1) yes. In most investigated aplousobranch and phlebobranch species the number of languets of the dorsal lamina equaled the number of transverse vessels (Fig. 8B, C, F & H). In a few other species the number of transverse vessels is higher than the number of languets (Fig. 8A & G).

48. Dorsal organ with a membrane: (0) no; (1) yes. In *P. atlanticum*, investigated phlebobranch species and most investigated stolidobranch species a membrane is developed in the dorsal organ that projects into the lumen of the branchial basket and connects the languets (see character 47) (Fig. 8A & G-J).

49. Membrane in the dorsal organ smooth edged or plain: (0) no; (1) yes. See Fig. 8H-J.

50. Dorsal organ with multiple transverse ciliary bands: (0) no; (1) yes. See Fig. 8A-H. We consider the cilia of the gill bar in Salpida homologous to ciliary bands traversing the dorsal organ in ascidians (Fig. 9A). Mallat’s description (1979) shows that this character is absent in lampreys.

51. Dorsal organ as ciliated groove: (0) no; (1) yes. See Fig. 9B-D.

52. Shape of peripharyngeal band: (0) flat ciliated epithelium; (1) ciliated groove. The peripharyngeal band (synonym: pericoronal band (Burighel et al., 2003) limits the branchial basket to the anterior. The shape differs in tunicates. In some species it is present as a groove

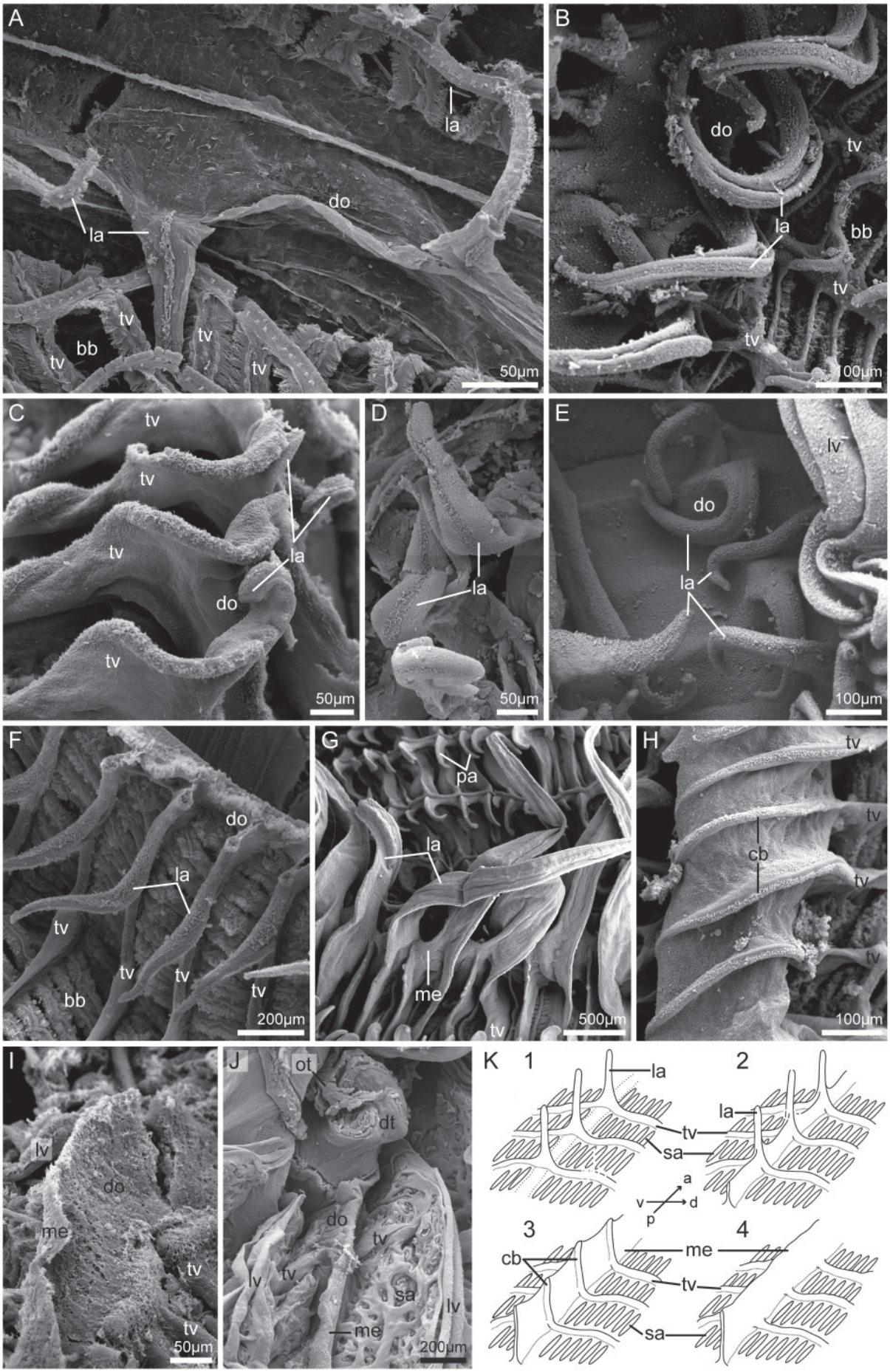
A
la
do
la
tv
bb
tv
tv
tv
50µm
B
do
tv
la
bb
tv
tv
100µm
C
tv
tv
tv
la
do
tv
50µm
D
la
50µm
E
lv
do
la
100µm
F
do
la
tv
tv
tv
bb
tv
200µm
G
pa
la
me
tv
500µm
H
tv
tv
cb
tv
tv
100µm
I
lv
do
me
tv
tv
50µm
J
ot
dt
do
tv
lv
tv
sa
lv
me
200µm
K
1
la
tv
sa
2
la
a
v
d
p
3
cb
4
me
tv
sa

Figure 8

Figure 8. Scanning electron micrographs of the dorsal organs (do) in the branchial basket (bb) of diverse tunicate species. **A:** Dorsal organ with languets (la) in the branchial basket of *Pyrosoma atlanticum*. The number of transverse blood vessels (tv) is higher than the number of languets. **B:** In *Rhodosoma callense* the dorsal organ is equipped with languets, numbers of languets and transverse blood vessels equal. **C:** Languets of the dorsal organ in *Clavelina lepadiformis* are transversally broadened. Numbers of languets correspond to numbers of transverse blood vessels. **D:** In *Herdmania momus* languets settle on the dorsal organ. The number of transverse blood vessels is higher than the number of languets. **E:** In *Halocynthia roretzi* languets at the dorsal organ are present but the number of languets is not identical to the number of transverse blood vessels. **F:** Dorsal organ with languets in *Sycozoa sigillinoides*. Numbers of transverse blood vessels and languets are equal. **G:** In *Ciona intestinalis* every second transverse blood vessels runs into a languet of the dorsal organ, others end blindly. At the base of the languets a membrane (me) is developed connecting the languets. **H:** The membrane of the dorsal organ in *Phallusia nigra* completely covers the languets. They are visible as protruding ciliary bands (cb). The number of languets equals the number of transverse blood vessels. **I:** In *Botryllus schlosseri* the dorsal organ is visible as a smoothly edged membrane without individual languets. **J:** The dorsal organ in *Molgula manhattensis* forms a plain membrane without detectable languets. **K:** Schematic drawings of the different forms of the dorsal organ in tunicates. **1**: Transverse blood vessels form languets that are not connected by a membrane at their base. **2**: A longitudinal membrane connects languets. **3**: A longitudinal membrane completely covers languets. Languets are detectable as ciliary protrusions. **4**: The dorsal organ is smoothly edged or plain without ciliary protrusions. Languets are not present. dt: dorsal tubercle, lv: longitudinal blood vessel, ot: oral tentacle, pa: papillae, sa: stigma.

(Fig. 10A & B) in others it is flat (Fig. 10C & D). The peripharyngeal band corresponds to the pseudobranchial groove in Petromyzontidae.

53. Peripharyngeal band with conspicuous dorsal curvature: (0) no; (1) yes. In some species the peripharyngeal band describes a sharp bend in its dorsal course (Fig. 10C; Fig. 13 E, Fig. 14C).

54. Papillae in prebranchial area: (0) absent; (1) present. Here, we observed the area between the ring of oral tentacles and the peripharyngeal band. Information on character distribution is found in Millar (1966; p. 60), and Gill et al. (2003), see also Fig. 10A.

Excretory and digestive structures

55. Excretory structure: (0) absent; (1) present (see also character 56). In Doliolida, Godeaux et al. (1998) speculate that the pyloric gland might be an excretory organ. We coded the pyloric gland as homologous across Tunicata with a different (main) function and coded this character state as 0 for Doliolida.

56. Type of excretory structure: (0) kidney; (1) renal vesicles or nephrocytes. On the right side of the body Molgulidae possess a compact organ that accumulates excretory products and is called kidney. In all other tunicate species that possess excretory structures these are developed as renal vesicles or nephrocytes. We do not consider kidneys in Cephalochordata and Petromyzontidae as homologous to kidneys or nephrocytes in tunicates and coded the character state as not applicable.

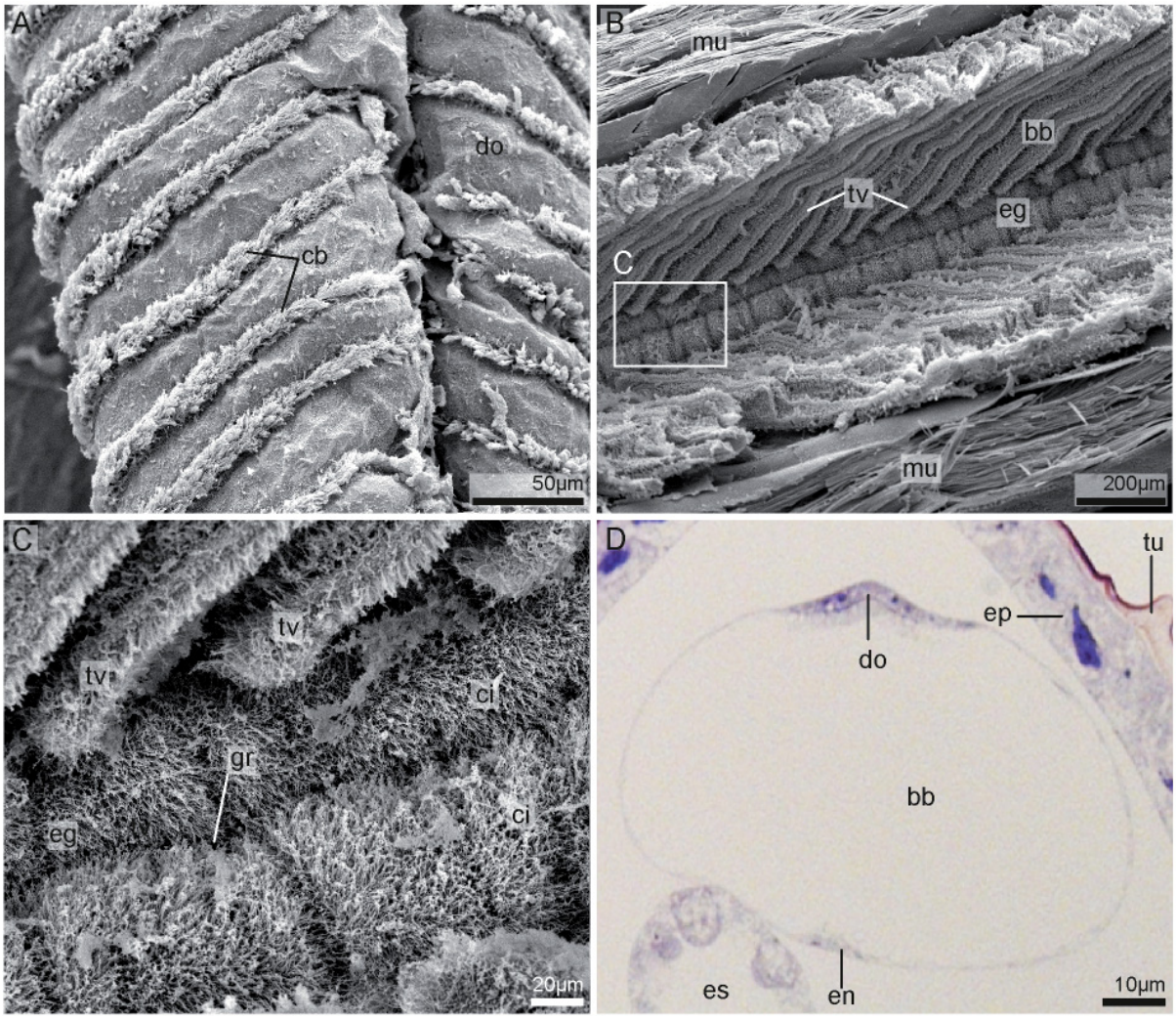

Figure 9. Scanning electron micrographs of the dorsal organs (do) and cilia (ci) in two different tunicate species and the cephalochordate species *Branchiostoma lanceolatum*. **A:** Dorsal organ with evenly distributed ciliary bands (cb) in *Salpa fusiformis*. **B & C:** In *Branchiostoma lanceolatum* the dorsal organ is called epipharyngeal groove (eg). Two ciliated membranes border the ciliated groove (gr). Area marked with a white rectangle is shown in higher magnification in **C**. **D:** Light micrograph of a semithin cross section through *Oikopleura dioica* stained with toluidine blue, dorsal to the top, right to the right. The dorsal organ is visible as a ciliated groove. bb: branchial basket, en: endostyle, ep: epidermis, es: esophagus, mu: musculature, tu: tunic, tv: transverse blood vessel.

57. Stomach folded or plicated: (0) no; (1) yes. This character considers glandular swellings or folds of the stomach wall. The stomach in Salpida is not clearly demarcated from the remainder of the intestine. There are however, a number of caeca that are traditionally considered to open into the area corresponding to the stomach in other tunicates (Ihle, 1956). The exact number of these caeca differs among species and also between generations. Fenaux (1998) depicts a specimen of the appendicularian *Megalocercus abyssorum* Chun, 1887 as representative for the genus and describes the stomach in the general diagnosis of the genus as being without any folds.

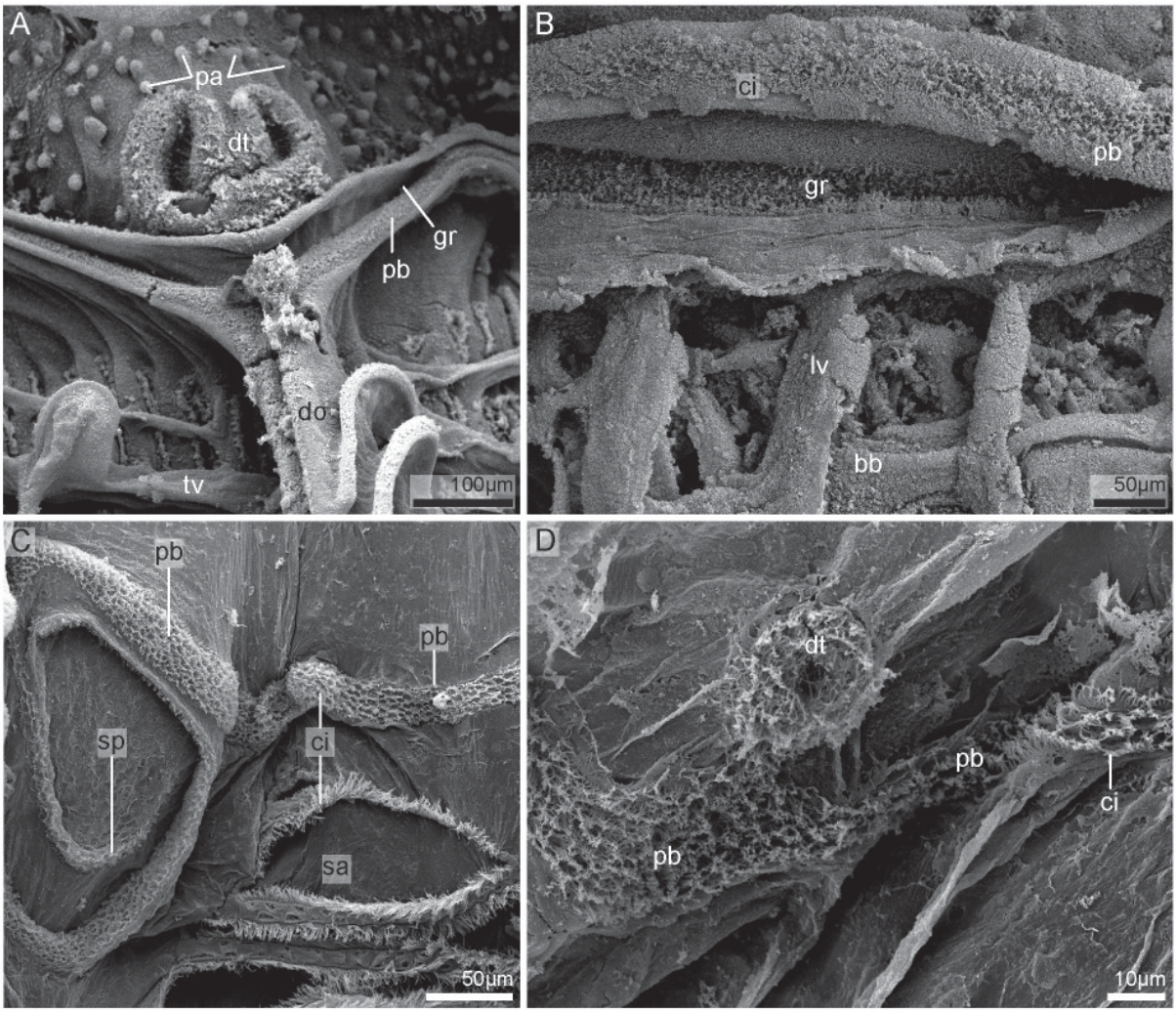

Figure 10. Scanning electron micrographs of the peripharyngeal band (pb) and prebranchial area of four different tunicate species. **A:** In *Phallusia nigra* several papillae (pa) are situated in the prebranchial area. The peripharyngeal band is developed as a ciliated groove (gr). The opening of the dorsal tubercle (dt) is u-shaped. **B:** The peripharyngeal band in *Herdmania momus* is visible as ciliated groove. **C:** The peripharyngeal band in *Doliolum nationalis* is a flat ciliated epithelium that has a conspicuous curvature on its dorsal side, the dorsal spiral (sp). **D:** *Pyrosoma atlanticum* possesses a flat ciliated peripharyngeal band. The opening of the dorsal tubercle is a simple ciliated funnel. bb: branchial basket, ci: cilia, do: dorsal organ, lv: longitudinal blood vessel, sa: stigma, tv: transverse blood vessel.

58. Hepatic gland: (0) absent; (1) present. A hepatic gland (Van Name, 1945) or liver (Kott, 1985) consists of irregular outgrowths on the ventral side of the stomach. In cross sections of the stomach these outgrowths appear branched or more complex compared to the simple regular folds in some other species (Fig. 11). Hepatic glands are developed in some stolidobranch ascidian species (Huus, 1956). We homologize the "hepatic gland" with the "stomach caecum" (see character 59) and regard it as a more complex, more obviously glandular form of this organ.

59. Stomach caecum: (0) absent; (1) present. A stomach caecum is a simple, blindly ending diverticulum protruding from the stomach into the gut loop (Kott, 1985). We homologize the hepatic gland of Molgulidae and Pyuridae with the (often single) stomach caecum. Accordingly, we score stomach caeca as present in Salpida (Ihle, 1956), and most Stolidobranchiata. Some authors called the "stomach caecum" "pyloric caecum" or "hepatic caecum" (Kott, 1985).

60. Pyloric gland: (0) absent; (1) present. The pyloric gland consists of tubules that encircle the ascending limp of the gut loop. Tubules join into a single duct, which opens into the distal end of the stomach (Kott, 1985). The pyloric gland is developed in all investigated tunicate species. In the outgroup species it is not developed (Huus, 1956). Synonym: gastro-intestinal gland (Kott, 1985).

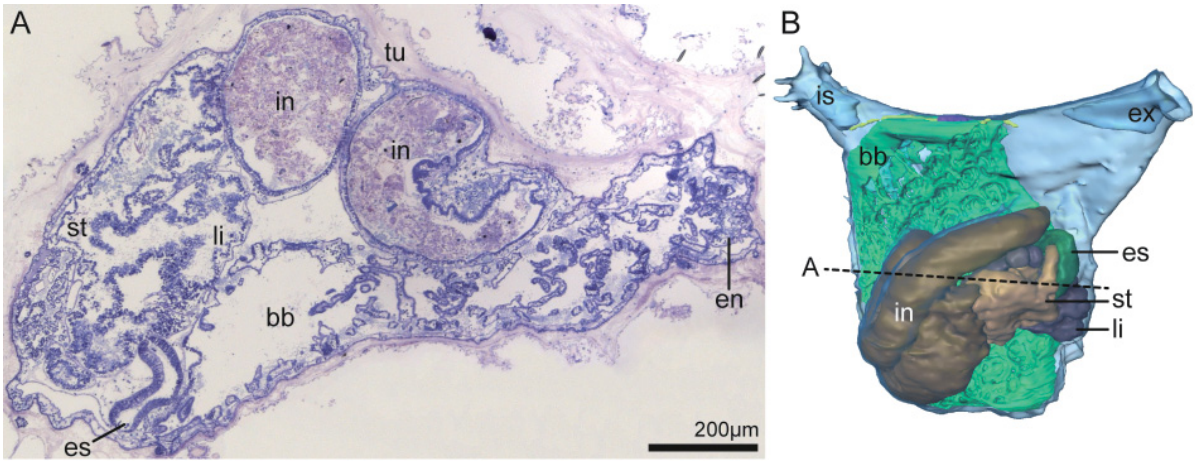

Figure 11. Hepatic gland or liver (li) in *Molgula manhattensis*. **A:** Light micrograph of a semithin cross section through the branchial basket and digestive tract stained with toluidine blue, ventral to the right, left to the top. Several outgrowths on the ventral side of the stomach (st) are visible that constitute the liver. **B:** 3D reconstruction of the internal anatomy, view from left side, anterior to the top. The section plane of **A** is indicated by a dotted back line. The liver is shown in dark purple and visible as several outgrowths of the stomach. bb: branchial basket, en: endostyle, es: esophagus, ex: excurrent siphon, in: intestine, is: incurrent siphon, tu: tunic.

61. Shape of gastrointestinal tract: (0) straight; (1) u-shaped. In tunicate species the gastrointestinal tract is curved or u-shaped, while in the investigated outgroup species the gastrointestinal tract is straight.

62. Position of gastrointestinal tract in relation to branchial basket: (0) mostly posterior; (1) lateral.

63. Position of lateral gastrointestinal tract: (0) on left side; (1) on right side. While in most ascidians with lateral gastrointestinal tracts the latter are situated on the left side of the body, gastrointestinal tracts are situated on the right side of the body in members of Corellidae.

64. Position of rectum in species with a mostly posterior gastrointestinal tracts (character 62: 0): (0) dorsomedian; (1) ventromedian.

Atrium

65. Atrial cavity: (0) absent; (1) present. Gill slits of the branchial basket open into the atrium that in turn is connected with exterior via the excurrent opening. An atrium is present in most tunicate species and in Cephalochordates (Huus, 1956). In Appendicularia gill slits open directly to the exterior, an atrium is absent. In ammocoete larvae gills open individually to the exterior (despite the occurrence in cross sections - see Goodrich (1909) who depicts a longitudinal section). The same situation is observed for adult specimens. Therefore, we coded this character state as 0 for Petromyzontidae.

66. Origin of atrial cavity: (0) ventral; (1) dorsal. The atrium in tunicate species develops (in most cases) as a dorsal invagination of the ectoderm, while in cephalochordates two ventral folds extend and fuse to form the atrium (Franz, 1927; Huus, 1956; Stokes and Holland, 1995).

67. Shape of ontogenetic rudiment of atrial opening: (0) paired; (1) unpaired. Paired atrial cavities fuse later during ontogeny on the dorsal side. In Salpida, Stolidobranchiata, and Cephalochordata the ontogenetic rudiment of the atrial opening is unpaired. Information on character distribution is found in Huus (1956) and Ihle (1956).

68. Position of unpaired rudiment of atrial opening: (0) ventral; (1) dorsal. Rudiments of the atrial opening in tunicates with unpaired rudiments are present on the dorsal side, while in Cephalochordates these rudiments are located on the ventral side (Huus, 1956; Ihle, 1956; Stokes and Holland, 1995).

Sexual reproduction

69. Hermaphroditism: (0) absent; (1) present. With the exception of *O. dioica* and *S. sigillinoides* most examined tunicate species are hermaphroditic. Cephalochordata and Petromyzontidae are diecious.

70. Type (position) of gonads: (0) enterogon; (1) pleurogon. This character is traditionally used in ascidian taxonomy. “Enterogon” gonads are positioned on the visceral side in proximity to the intestinal tract as, e.g., in Phlebobranchiata and Aplousobranchiata. We homologize the position of gonads in Thaliacea and Appendicularia with the enterogon type. Lampreys are coded as enterogon (0) here, because lamprey gonads are unpaired and closely associated with the intestine (Ihle, 1971). In species coded as 1, pleurogon gonads are located on the parietal side as in stolidobranch ascidians. In *Branchiostoma* gonads are positioned on the parietal side of the branchial region (see e.g., Franz, 1927), and are coded 1 accordingly here.

71. Position of gonads in relation to branchial basket: (0) lateral; (1) posterior. In Appendicularia, Thaliacea, *C. intestinalis*, Aplousobranchiata, and Petromyzontidae gonads are positioned posterior to the branchial basket. In most Phlebobranchiata, Stolidobranchiata, and Cephalochordata gonads are positioned lateral to the branchial basket.

72. Occurrence of gonads: (0) unpaired; (1) paired. In most tunicate species and in lampreys gonads are unpaired. Information on character distribution is found in Berrill (1950), Drasche (1884), Rocha et al. (2012), and Van Name (1945).

73. Site of fertilization: (0) external; (1) internal. Tunicate species with internal fertilization also breed their developing embryos. Information on character distribution is found in Berrill (1950), Groepler (2016), Mukai et al. (1983), Rocha et al. (2012), and Van Name (1945).

74. Site of breeding: (0) atrial (= peribranchial) cavity; (1) brood chambers. Species with internal fertilization either breed the embryos in the atrial cavity or in specialized brood chambers. Information on character distribution is found in Berrill (1950), Groepler (2016), Kott (1990, 1992), Manni et al. (2007), and Van Name (1945).

75. Site of brood chamber: (0) outgrowth of peribranchial cavity; (1) common tunic. Information on character distribution is found in Van Name (1945).

76. Location of peribranchial brood chamber: (0) left side; (1) dorsal side. Brood chambers that are outgrowths of the peripharyngeal wall are either positioned on the left side of the body (in *K. borealis*) or on the dorsal side of the body (in *D. stylifera* and *S. sigillinoides*) (Van Name, 1945).

77. Chordate type larva: (0) absent; (1) present. Salpida, Pyrosomatida, *M. retortiformis*, and *P. corrugata* do not develop through a tailed larval stage. In all other investigated species a chordate type larva is present (Ihle, 1956; Millar, 1954; Van Name, 1945).

78. Larval tunic: (0) absent; (1) present. All tunicate larvae (tadpole larvae) possess a larval tunic. Larvae of outgroup species do not possess a larval tunic.

79. Orientation of larval tail in relation to larval trunk: (0) vertical; (1) horizontal. In vertical oriented larval tails, the fluke is oriented along the dorsoventral axis of the body as in most fishes. The power is generated by lateral undulatory movements. In the horizontal orientation the fluke is oriented laterally, like in whales and dolphins. The forward thrust is generated via dorsoventral undulations. Information on character distribution is found in Huus (1956).

80. Larval eye: (0) absent; (1) present. Information on character distribution is found in Berrill (1950), Groepler (2016), Huus (1956), Kott (1990, 1992), Lacalli (1996), Lamb et al. (2007), Millar (1971), and Van Name (1945).

81. Larval statocyte: (0) absent; (1) present. Statocytes are sensory cells situated in the larval sensory vesicle. Statocytes contain a dark, pigmented otolith (or statolith) and are involved in gravitropic perception. They are present in larvae of Appendicularia, Doliolida, Phlebobranchiata, Stolidobranchiata, and Aplousobranchiata (Huus, 1956; Millar, 1971).

82. Larval photolith: (0) absent; (1) present. The photolith combines the light sensitive larval eye and the gravity receptive statocyte in a single organ. Photoliths are only described for examined colonial styelids (Berrill, 1950; Garstang, 1928; Sorrentino et al., 2000).

83. Larval ampullae: (0) absent; (1) present. Ampullae are epidermal outgrowths that usually form a ring surrounding the anterior trunk region. Ampullae are present in most examined stolidobranch larvae, in Didemnidae and Polyclinidae (Berrill, 1950; Kott, 1985, 1990, 1992, 2001; Van Name, 1945).

84. Larval adhesive papillae (more than one): (0) absent; (1) present. These epidermal papillae are present in most tunicate larvae at the anterior trunk region to facilitate the attachment to the substrate before metamorphosis. Adhesive papillae are absent in Appendicularia, Doliolida, Molgulidae, and larvae of the outgroup species (Huus, 1956).

85. Orientation of larval papillae: (0) triradial; (1) sagittal. Usually, three adhesive papillae are present in ascidian tadpole larvae. These are either positioned anteriorly at three corners of a triangle: two dorsolaterally and one medioventrally. This arrangement is called triradial. Alternatively, all papillae are positioned in a single vertical plane, mid-sagittally. Information on character distribution is found in Berrill (1950), Grave (1926), Groepler (2016), Huus (1956), and Van Name (1945).

Serotonin-like immunoreactivity (serotonin-lir)

86. Serotonin-lir in the brain of adult specimens: (0) absent; (1) present. Serotonin-lir in the brain has only been detected in investigated outgroup species (Barreiro-Iglesias et al., 2009; Baumgarten et al., 1973; Candiani et al., 2001; Holland and Holland, 1993; Sakharov and Salimova, 1980), Salpida, Doliolida (Braun and Stach, 2018b), and *O. fusiformis* (Stach, 2005).

87. Serotonin-lir in the peripharyngeal band: (0) absent; (1) present. Serotonin-lir in the peripharyngeal band is described for all Thaliacea, all examined ascidian species and lampreys (Barreiro-Iglesias et al., 2009; Braun and Stach, 2016, 2018b; Sakharov and Salimova, 1980; Fig. 12A, B, G, K & O; Fig. 13B, F & L).

88. Serotonin-lir in the endostyle: (0) absent; (1) present. In Pyrosomatida and ascidians serotonin-lir cells are located in the endostyle (Braun and Stach, 2016, 2018b; Fig. 12C, H, L & P; Fig. 13C, G &L).

89. Serotonin-lir in the retropharyngeal band: (0) absent; (1) present. Information on character distribution is found in Braun and Stach (2016, 2018b), see also Fig. 13B, E & N.

90. Serotonin-lir in the esophagus: (0) absent; (1) present. Serotonin-lir cells are present in the esophagus of Thaliacea and ascidians (Braun and Stach, 2016, 2018b; Fig. 12D, I, M & R; Fig. 13D, H & M).

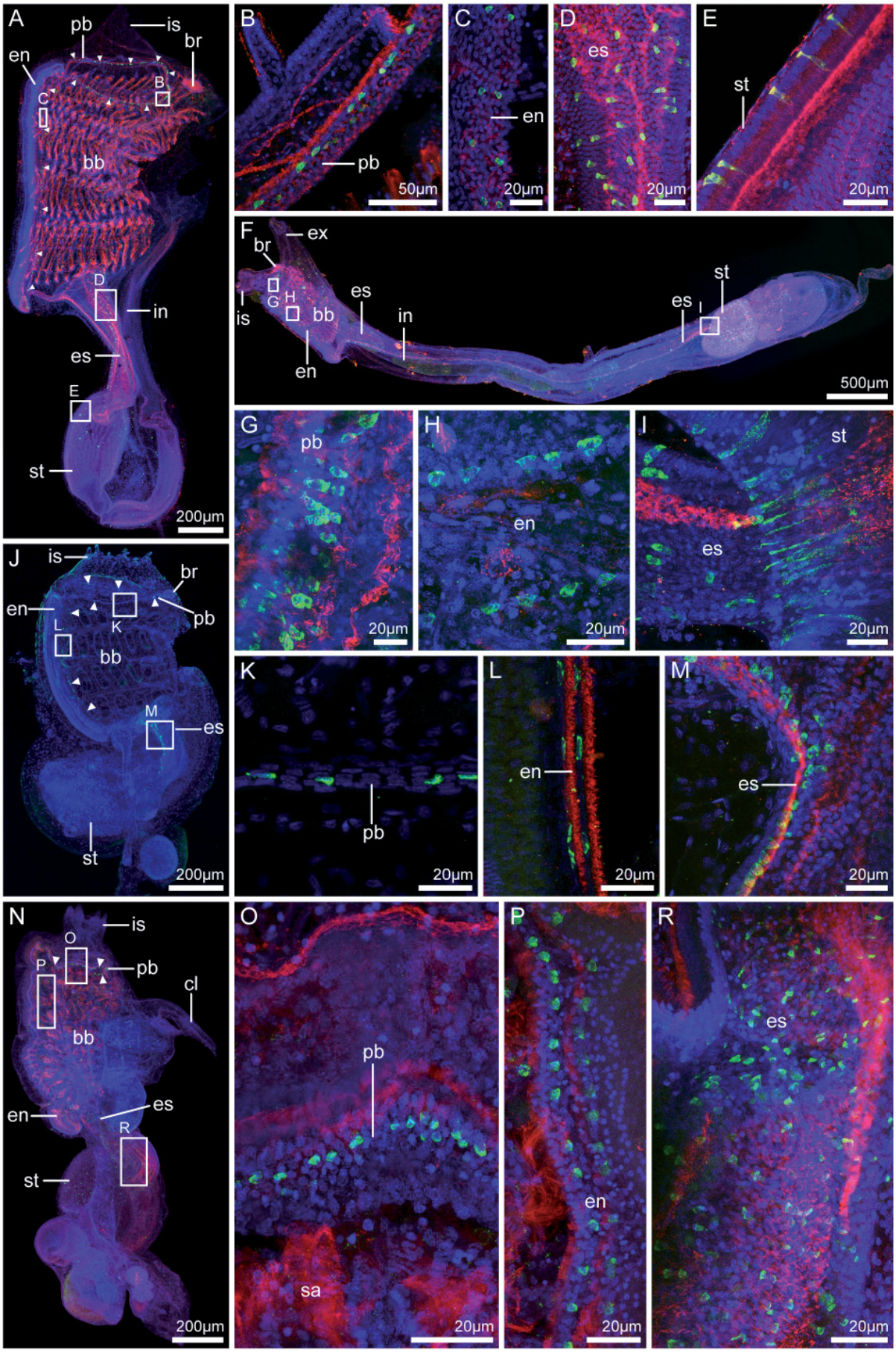
A
pb
is
br
en
B
C
bb
D
in
es
E
st
200µm
B
pb
50µm
C
en
20µm
D
es
20µm
E
st
20µm
F
ex
br
G
H
is
bb
es
in
en
es
st
500µm
G
pb
20µm
H
en
20µm
I
st
es
20µm
J
is
br
en
K
pb
L
bb
M
es
st
200µm
K
pb
20µm
L
en
20µm
M
es
20µm
N
is
O
P
pb
cl
bb
en
es
R
st
200µm
O
pb
sa
20µm
P
en
20µm
R
es
20µm

Figure 12

Figure 12. Z-projections of confocal laser scanning micrographs of immunohistochemical stainings with antibodies against serotonin (green) and tyrosinated-α-tubulin (red), and with DAPI and Hoechst (blue) in four different aplousobranch species **A-E**: Localization of serotonin-like immunoreactivity (serotonin-lir) in *Distaplia stylifera*, anterior to the top, dorsal to the right. Areas with immunopositive cells are marked with white rectangles, higher magnifications of these areas shown in **B-E**. **A:** Lateral view of an entire animal. **B:** Higher magnification of the peripharyngeal band (pb). **C:** Detail of serotonin-lir in the endostyle (en). **D:** Serotonin-lir cells are present as more or less spherical cells and bottle-shaped cells in the esophagus (es). **E**: Elongated serotonin-lir cells are situated in the epithelium of the stomach (st). **F-I**: Serotonin-lir in *Eudistoma obscuratum*, dorsal to the top, anterior to the left. **F:** Lateral view on a complete zooid. White rectangles mark areas that are shown in higher magnification in **G-I**. **G:** Serotonin-lir in the peripharyngeal band. **H:** Localization of serotonin-lir in the endostyle. **I:** Transition zone of esophagus and stomach is characterized by diverse elongated serotonin-lir cells. **J-M:** Distribution of serotonin-lir cells in *Lissoclinum verrilli*, view from left side, anterior to the top. Regions marked with white rectangles are shown in higher magnification in **K-M**. **K:** Detail of the peripharyngeal band. **L:** Higher magnification of the endostyle. **M:** In the esophagus few rows of serotonin-lir cells are situated. **N-R:** Serotonin-lir in *Polyclinum constellatum*, view from left side, anterior to the top, dorsal to the right. White rectangles indicate regions of which higher magnifications are shown in **O-R**. **O:** Serotonin-lir cells in the peripharyngeal band. **P:** In the endostyle two parallel rows of serotonin-lir cells are visible. **R:** Detail of serotonin-lir in the esophagus. bb: branchial basket, br: brain, cl: cloacal languet, ex: excurrent siphon, in: intestine, is: incurrent siphon.

91. Serotonin-lir in the gastrointestinal tract: (0) absent; (1) present. Serotonin-lir cells are located in the gastrointestinal tract of *T. democratica*, ascidians, and species belonging to the outgroup (Barreiro-Iglesias et al., 2009; Braun and Stach, 2016, 2018b; Candiani et al., 2001; Sakharov and Salimova, 1980; Fig. 12E, F, I, J & N; Fig. 13A, B, E, I-K, N).

Nervous system

92. Adult cerebral eye(s): (0) absent; (1) present. Cerebral eyes are closely associated with the brain, i.e., cerebral eyes are organs continuous at the tissue level with the brain enclosed in the same extracellular matrix (Braun and Stach, 2017; Cohen, 1963; Lacalli et al., 1994; Lacalli and Holland, 1998).

93. Type of photoreceptor cells in adult cerebral eyes: (0) rhabdomeric; (1) ciliary. In the animal kingdom two different types of photoreceptor cells are described according to the origin of the membranes that store the light-sensitive photopigments. If the membrane originates in the apical cell membrane and therefore forms microvilli the corresponding photoreceptor cells are classified as rhabdomeric. If this membrane originates from a ciliary membrane, the photoreceptor cell is classified as ciliary (e.g., Eakin, 1979; Salvini-Plawen, 1982). Photoreceptor cells in *T. democratica* are classified as rhabdomeric (Braun and Stach, 2017). In cerebral eyes of Cephalochordata and Petromyzontidae ciliary photoreceptor cells are described (Cohen, 1963; Lacalli, 1996).

94. Adult cerebral eye with lens: (0) no; (1) yes. Lenses are transparent structures that refract light to bundle it (Jonasova and Kozmik, 2008). Lenses in adult cerebral eyes are present in members of Petromyzontidae (Slingsby et al., 2013).

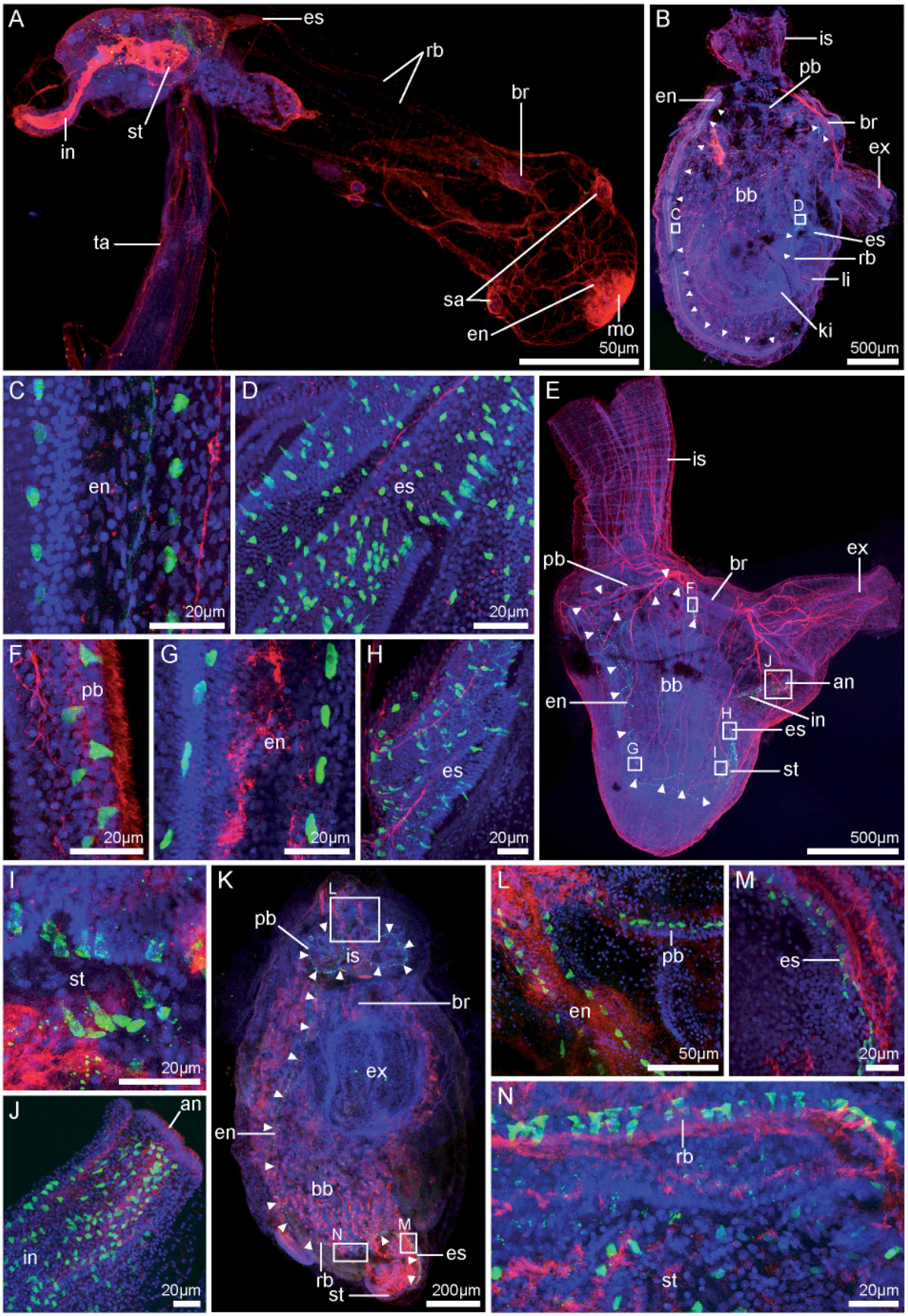

Figure 13. Z-projections of confocal laser scanning micrographs of immunohistochemical stainings with antibodies against serotonin (green) and tyrosinated-α-tubulin (red), and with DAPI and Hoechst (blue) in four different tunicate species. **A:** In the appendicularian *Fritillaria borealis* serotonin-lir is not detectable. **B-N**: Serotonin-like immunoreactivity in three different stolidobranch ascidian species.

B-D: Localization of serotonin-lir cells in *Molgula manhattensis*, anterior to the top, dorsal to the right. Areas with positively labeled cells are marked with white rectangles, higher magnifications of these areas shown in **C & D**. **B:** Lateral view on one complete individual. Exclusively in the dorsal part of the peripharyngeal band (pb) serotonin-lir cells are detectable. **C:** Higher magnification of serotonin-lir cells in the endostyle (en). **D:** Detail of serotonin-lir in the esophagus (es). Approximately spherical and elongated serotonin-lir cells are visible. **E-J**: Serotonin-lir in *Styela clava*, dorsal to the right, anterior to the top. **E:** Lateral view on an entire animal. Note that the peripharyngeal band continuously possesses serotonin-lir cells and on the dorsal side the peripharyngeal band conspicuously curves (character 53). White rectangles mark areas that are shown in higher magnification in **F-J**. **F-J:** Details of the localization of serotonin-lir cells in the peripharyngeal band (**F**), the endostyle (**G**), the esophagus (**H**), the stomach (st, **I**) and the intestine (in, **J**). **K-N:** Distribution of serotonin-lir cells in *Symplegma brakenhielmi*, anterior view, ventral to the left. Regions marked with white rectangles are shown in higher magnification in **L-N**. **L:** Serotonin-lir at the transition of peripharyngeal band and endostyle. **M:** Detail of serotonin-lir cells in the esophagus. **N:** Elongated serotonin-lir cells are located in the retropharyngeal band (rb). In the stomach approximately spherical serotonin-lir cells are detectable. an: anus, bb: branchial basket, br: brain, ex: excurrent siphon, is: incurrent siphon, ki: kidney, li: liver, mo: mouth, sa: stigma, ta: tail.

95. Shape of adult brain: (0) ovoid, pear-shaped; (1) elongated. We considered brains with a relation of length to breadth of at least 1.5 as elongated and brains with a relation of length and breadth of approximately 1 as ovoid. Information on character distribution is found in Braun and Stach (2018a), Nieuwenhuys (1977), and Wicht and Lacalli (2005).

96. Brain divided into cortex and neuropil: (0) no; (1) yes. In all examined tunicate species the brain is divided into a superficial layer where somata of neurons are concentrated and a central neuropil that almost exclusively contains nerve fibers. In the outgroup species the brain is not divided into cortex and neuropil (Braun and Stach, 2018a; Nieuwenhuys, 1977; Wicht and Lacalli, 2005).

97. Neural gland: (0) absent; (1) present. The neural gland is a glandular structure closely associated with the brain in tunicates; together they form the neural complex (see e.g., Burighel and Cloney, 1997; Huus, 1956). A neural gland is present in nearly all investigated species, except thaliacean species (Braun and Stach, 2018a). Based on the similar position of Hatschek's pit and groove as well as the presence of gonadotropin hormones and the indication that gonadotropin releasing hormones are found in neural fibers close to Hatschek's pit, we code Hatschek's pit in Cephalochordata as homologous to the neural gland and dorsal tubercle in tunicates (Stach, 1996; Gorbman, 1999; Roch et al., 2014). For Petromyzontidae we homologize the neural gland with the adenohypophysis, based on similarities of development, position, and function (Gorbman, 1995, 1999; Kah et al., 2007; Romer and Parsons, 1986).

98. Position of neural gland compared to brain: (0) not ventral; (1) ventral. Information on character distribution is largely from Braun and Stach (2018a). Hatschek's pit in Cephalochordates and the adenohypophysis in Petromyzontidae are also positioned on the

ventral side of the brain (see character 97). Terakado (2010) described a ventral position of the neural gland in *H. roretzi*. A dissection of animals of this species revealed that the neural gland is positioned dorsal from the brain slightly shifted to the right so we coded the position as 1 for the species.

99. Position of the not ventrally positioned neural gland (see character 98): (0) dorsomedian; (1) right. Information on character distribution is found in Braun and Stach (2018a).

100. Dorsal tubercle in adults: (0) absent; (1) present. The neural gland opens through a dorsal tubercle as a ciliated funnel in its most simple shape into the lumen of the branchial basket. The dorsal tubercle can also be present when the neural gland is absent (Salpida, see character 97, Braun and Stach, 2018a). We homologized Hatschek's pit in Cephalochordata with the neural gland in tunicates (see character 98) and the ciliated opening of Hatschek's pit with the dorsal tubercle in tunicates. Therefore, all investigated species possess a dorsal tubercle, except from Petromyzontidae, where a homologous structure is missing in adults.

101. Shape of dorsal tubercle: (0) simple; (1) more complex. The dorsal tubercle in some species is a simple ciliated funnel (Fig. 14A); in others it is of a more complex shape, usually a u-, c- or heart-shaped structure (Fig. 14B-F). Information on character distribution is found in Braun and Stach (2018a).

102. Opening of the dorsal tubercle pedestal-like elevated: (0) no; (1) yes. The opening of the dorsal tubercle can be in the same plane as the wall of the branchial basket or can be elevated pedestal-like above the wall of the branchial basket extending into the lumen of the branchial basket (Fig. 14C-F).

103. Dorsal strand: (0) absent; (1) present. The dorsal strand is an extension of the neural gland extending along the roof of the branchial basket to the posterior. It is a tube-like structure, with an epithelial layer surrounding a narrow central lumen (Burighel and Cloney, 1997). Information on character distribution is found in Braun and Stach (2018a).

104. Dorsal strand ends in close proximity to the brain: (0) no; (1) yes. In some species the dorsal strand extends all the way to the gonads, in others it ends blindly close to the brain. Information on character distribution is found in Braun and Stach (2018a).

105. Caudal ganglion in adults: (0) absent; (1) present. The caudal ganglion is a concentration of nerve cell bodies, resulting in a local swelling of the neural tube in the anterior part of the locomotory tail. In adults it is only present in Appendicularia (Lohmann, 1956).

106. Ventral visceral nerve: (0) absent; (1) present. Ventral visceral nerves are nerves that project from the midline of the brain from its ventral side posteriorly (Manni and Pennati, 2016). Information on character distribution is found in Braun and Stach (2018a).

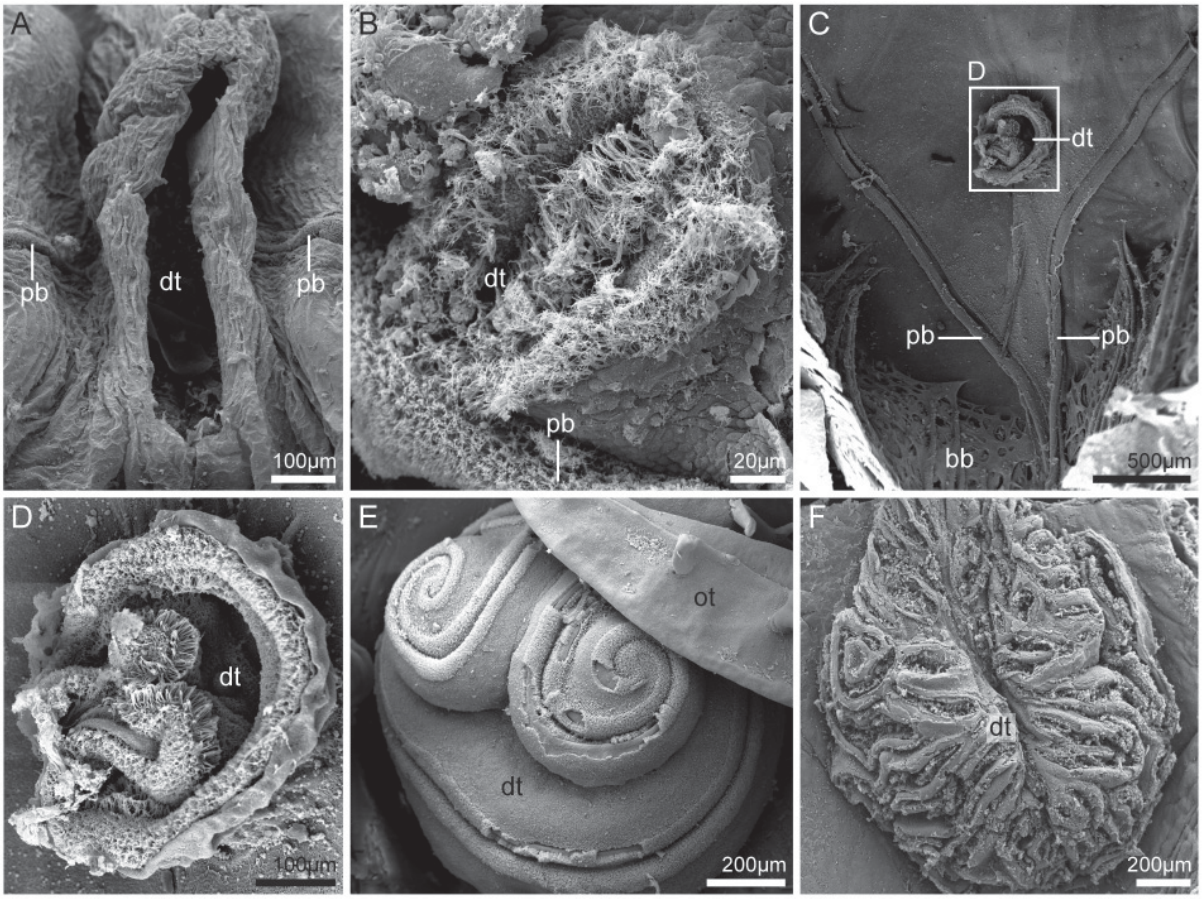

Figure 14. Scanning electron micrographs of the dorsal tubercle (dt) in five different tunicate species. **A:** In *Salpa fusiformis* the dorsal tubercle is shaped as a simple ciliated funnel. **B:** The dorsal tubercle of *Diazona violacea* is u-shaped. **C & D:** In *Molgula citrina* the dorsal tubercle is c-shaped. The peripharyngeal band (pb) possesses a conspicuous dorsal curvature (character 53). The opening of the dorsal tubercle is pedestal-like elevated in excess of the wall of the branchial basket (bb). **E:** *Halocynthia roretzi* possesses a pedestal-like elevated dorsal tubercle with an involute ciliated opening. **F:** In *Herdmania momus* the dorsal tubercle is pedestal-like elevated and possesses several ciliated openings into the branchial basket. ot: oral tentacle.

107. Number of ventral visceral nerves (see character 106): (0) 1; (1) 2; (2) 4. In most tunicate species the ventral nerve is developed as a single unpaired nerve, but in *B. schlosseri* and *P. constellatum* a pair of ventral visceral nerves is present. Specimens of *D. stylifera* even possess four ventral visceral nerves (Braun and Stach, 2018a).

108. Dorsal strand plexus: (0) absent; (1) present. In association with the dorsal strand the ventral visceral nerve can be present as a richly anastomosing plexus. It is then termed dorsal strand plexus (see Braun and Stach, 2018a; Mackie 1995). The dorsal strand plexus contains neurons in all stages of differentiation, therefore being a possible region where neurogenesis takes place in adults (Mackie, 1995).

109. Brain appendages: (0) absent; (1) present. Brain appendages are blindly ending outgrowths of the brain cortex that are usually bilaterally symmetrical on the ventral side of the brain (Braun and Stach, 2017). These appendages are only present in examined specimens belonging to Salpida (Braun and Stach, 2017, 2018a).

110. Number of anterior nerves per side: (0) one; (1) two; (2) three; (3) four; (4) six. Anterior nerves exit the brain on the anterior side and mainly extend anteriorly toward the muscles of the oral sphincter, the oral tentacles, and the peripharyngeal band. They are present in all tunicate species. The homology to anterior nerves in outgroup species is ambiguous, so we coded the character state for these species as ?. In Salpida this character is coded as polymorphic, because of the different character states in the brains and nerves of the blastozooid and oozooid stage (Braun and Stach, 2018a).

111. Number of posterior nerves per side: (0) one; (1) two; (2) three; (3) four. Posterior nerves branch off the brain on the posterior side and mainly extend toward the muscles of the excurrent siphon and lateral body wall. They are present in all tunicate species. The homology to posterior nerves in outgroup species is ambiguous, so we coded the character state for these species as ?. In Salpida this character is coded as polymorphic, because of the different character states in the brains and nerves of the blastozooid and oozooid stage (Braun and Stach, 2018a).

112. Lateral nerves: (0) absent (1) present. Lateral nerves leave the brain laterally and project toward the branchial basket, digestive tract, and the lateral muscles of the body wall (Braun and Stach, 2018a).

113. Number of lateral nerves per side: (0) one; (1) two; (2) three; (3) four; (4) six; (5) more than six. The homology to lateral nerves of outgroup species is ambiguous, so we coded the character state for these species as ?. In Salpida this character is coded as polymorphic, because of the different character states in the brains and nerves of the blastozooid and oozooid stage (Braun and Stach, 2018a).

114. Unpaired anterior nerve projecting toward dorsal tubercle: (0) absent; (1) present. An exceptional unpaired anterior nerve that projects toward the dorsal tubercle is only present in species of Doliolida (Braun and Stach, 2018a; Neumann, 1956).

115. Statocyte in adult brain: (0) absent; (1) present. Statocytes are sensory cells situated in the sensory vesicle in the brain. A brain that is equipped with a statocyte is present in species of Appendicularia (Lohmann, 1956).

116. Conspicuous fiber tracts in adult brains: (0) absent; (1) present. Here we consider conspicuous fiber tracts detectable with the help of immunohistological stainings as investigated in the studies of Braun and Stach (2017, 2018a). Information on Cephalochordata and Petromyzontidae can be found in Barreiro-Iglesias et al. (2009), Lacalli (1996), and Nieuwenhuys (1977).

Discussion

The phylogenetic position of ascidians assured the group a place "back in the limelight" (Pourquié, 2001), just like more than a hundred years earlier, when the affinities between ascidians, cephalochordates, and craniates were discovered by the young Russian zoologist Alexander Kowalevsky in St. Petersburg (Kowalevsky, 1866). The renewed interest at the onset of the 21st century, similar to the interest generated by Kowalevsky, was fueled by studies of the larval stages of ascidians that more obviously than studies of the adults revealed correspondences to the more fish-like chordates. Ascidians, however, while constituting the majority of Tunicata, represent only a fraction of the life history strategies found within Tunicata. Moreover, molecular phylogenetic analyses consistently found "Ascidiacea" not monophyletic and cladistic analyses of phenotypic data of Tunicata are almost completely lacking.

Molecular analyses over the last decades included an increasing number of taxa (Delsuc et al., 2006; Govindarajan et al., 2011; Stach and Turbeville, 2002; Swalla et al., 2000; Tsagkogeorga et al., 2009), concentrated on the usage of slowly evolving genes (Tsagkogeorga et al., 2010), or applied "phylogenomic" methods (Delsuc et al., 2018; Kocot et al., 2018) to resolve phylogenetic interrelationships between higher tunicate taxa (see review in Giribet, 2018). While these studies seemingly approach a more stable framework regarding some contentious points of tunicate phylogeny, it has been pointed out that phylogenetic analysis of tunicate DNA-sequences is difficult due to generally increased mutation rates (Tsagkogeorga et al., 2010) and that phylogenetic information might not be as solid as suggested by statistic support values in published phylogenies (Stach, 2014). Phenotypic data analyzed according to a consistent phylogenetic method can be seen as a way of scrutinizing molecular phylogenies as an additional source of phylogenetic information (Wägele, 2001). Phenotypic data are necessary to suggest hypotheses of character transformation and the reconstruction of ground patterns (Hennig, 1982). Moreover, phenotypic data cannot be dismissed according to a foundational principle of science, the requirement of total evidence (Fitzhugh, 2006; Kluge, 1998).

Moreno and Rocha (2008) have published the first detailed analysis of phenotypic data (47 characters in 41 genera as terminal taxa), traditionally considered in tunicate taxonomy for a higher taxonomic group of Tunicata, Aplousobranchiata. In their study they focused on characters already published in the literature, emphasizing characters associated with coloniality. This had the unfortunate effect that colonial taxa from Phlebobranchiata clustered as sister taxa to the colonial Aplousobranchiata. Colonial Stolidobranchiata, however, were not included in the analysis, rendering Phlebobranchiata polyphyletic, without testing the influence of characters associated with coloniality. Another study, utilizing phenotypic data in a cladistic analysis was published by Stach and Turbeville (2002) and analyzed merely

24 characters for 19 higher tunicate taxa (traditionally given the rank of "family"). This study found the higher taxa Tunicata, Thaliacea, Phlebobranchiata, Aplousobranchiata, and Stolidobranchiata monophyletic, but otherwise showed no resolution between these taxa. A third study of phenotypic data investigated the phylogenetic signal in characters relating to secondary mechanoreceptor cells in Tunicata (Rigon et al., 2013). This analysis recovered major ascidian taxa as monophyletic taxa (Phlebobranchiata, Aplousobranchiata, Stolidobranchiata) but found no support for Thaliacea or "Ascidiacea". "Ascidiacea" was recovered polyphyletic due to thaliacean taxa as well as appendicularians being nested among ascidians. Interestingly, the appendicularian *Oikopleura dioica* was sister taxon to the two aplousobranch ascidian species in this study. Older treatments of detailed tunicate taxonomy did not apply cladistic rigor and often the taxonomic groupings or evolutionary interpretations are not easy to deduce (see below).

The current analysis of 116 phenotypic characters in a consistent cladistic approach therefore can serve as an independent source of evidence for analyses based on molecular data but also for taxonomic groupings not based on cladistic argumentation. The strict consensus tree of the parsimony analysis of the equally weighed character matrix is highly resolved and suggests several groupings in accordance with previous hypotheses but also some unexpected sister group relationships. We will point out the hypotheses briefly here and discuss them in more detail separately below. Tunicata is monophyletic with a high Bremer support as well as with high statistical support. On the higher taxonomic levels within Tunicata, the position of Appendicularia as the sister taxon to the remaining Tunicata has been found in several molecular phylogenetic analyses before (e.g., Delsuc et al., 2018; Kocot et al., 2018; Swalla et al., 2000; Wada 1998) and has been discussed based on morphological data as well (Ax, 2001; Wada, 1998; see detailed discussion below). The support for this positioning of Appendicularia is low. Unexpectedly, Thaliacea, which is a well-supported monophyletic taxon as suggested by molecular data (e.g., Delsuc et al., 2018; Govindarajan et al., 2011; Kocot et al., 2018; Stach and Turbeville, 2002) but also according to morphological considerations (Ax, 2001; Brien, 1948; Stach and Turbeville, 2002), has not been found monophyletic in our more extensive phenotypic analysis. Instead it forms a paraphyletic group with the relationship between Salpida and Doliolida unresolved, and the pyrosome *Pyrosoma atlanticum* forming the sister taxon to monophyletic Ascidiacea. None of the nodes separating the respective thaliacean taxa from Ascidiacea is strongly supported. Ascidiacea, on the other hand, which has been regarded by most modern studies as an obsolete taxon name for a paraphyletic group united by symplesiomorphic sessility of adults (Delsuc et al., 2018; Govindarajan et al., 2011; Kocot et al., 2018; Tsagkogeorga et al., 2009; Wada, 1998), is strongly supported, with high Bremer support index and statistical measures as a monophyletic taxon in our analysis. At an intermediate level we find Stolidobranchiata monophyletic with strong support. Aplousobranchiata, while monophyletic, is only weakly supported. "Phlebobranchiata", on the other hand, is paraphyletic in respect to Stolidobranchiata. Also, *Diazona violacea,* which

traditionally has been included within “Phlebobranchiata” (e.g., Millar, 1970), clustered as the sister taxon to Aplousobranchiata supporting a hypothesis proposed recently based on mitochondrial protein coding genes (Shenkar et al., 2016; see discussion below). At a lower taxonomic level, “Ascidiidae” is paraphyletic with respect to Stolidobranchiata. Within Stolidobranchiata, a monophylum consisting of Pyuridae and Molgulidae is nested within “Styelidae” rendering “Styelidae” paraphyletic. Within Aplousobranchiata, Polyclinidae and Didemnidae are both monophyletic and form a monophyletic sister group contrary to previous studies (Moreno and Rocha, 2008; Tsagkogeorga et al., 2009). In their study, focusing on the phylogenetic relationships of aplousobranch taxa, Moreno and Rocha (2008) found Polyclinidae paraphyletic and Didemnidae nested within paraphyletic “Holozoidae”. “Holozoidae” is also recovered not monophyletic in the present analysis. We did not test the monophyly of Clavelinidae or Polycitoridae.

Monophyly of Ascidiacea

Traditionally, Ascidiacea is one of three major taxa within Tunicata, often given the rank “Class” (e.g., Kott, 1985; Lützen, 1967; Millar, 1966; Shenkar and Swalla, 2011; Van Name, 1945). “The class Ascidiacea comprises those tunicates which have sessile adults.” (Millar, 1966, p. 5).

The monophyly of Ascidiacea was challenged by several molecular phylogenies, positioning Thaliacea within Ascidiacea (e.g., Govindarajan et al., 2011; Stach and Turbeville, 2002; Tsagkogeorgia et al., 2009). Delsuc and coworkers (2018), and Kocot and coworkers (2018) even suggest abandoning the name “Ascidiacea”. However, the phenotypic data from the present study support a monophyly of Ascidiacea with three unambiguous apomorphies: sessile adults (character 1), oral tentacles (character 7), and longitudinal orientation of stigmata in adults (character 36). While sessility clearly evolved several times independently, if one considers all animal taxa, there is no reason to suggest that sessility within Tunicata evolved more than once. In fact, even in the hypotheses based mainly on molecular data, where Thaliacea (e.g., Govindarajan et al., 2011; Kocot et al., 2018) or Thaliacea and Appendicularia (Stach and Turbeville, 2002; Zeng and Swalla, 2005; Zeng et al., 2006) rendered “Ascidiacea” paraphyletic, authors usually assumed that the characteristic ascidian biphasic life history with a tadpole-like larva and a sessile adult stage evolved once at the base of Tunicata and was subsequently lost in the stem lineage of Appendicularia and Thaliacea, respectively. The presence of oral tentacles as an apomorphic character that evolved in the stem lineage of a monophyletic Ascidiacea is also not without problems. The velar tentacles of cephalochordates and agnathan craniates are similarly placed, equipped with sensory cells (Rigon et al., 2008) and we consider them homologous to the oral tentacles of ascidians. Therefore, this character is an autapomorphy for a potentially monophyletic Ascidiacea, but it is homoplastic in comparison to the chordate outgroup taxa considered in the current analysis.

Also, the orientation of the stigmata in adults is liable to evolutionary change as can be seen by the transverse arrangement of the longitudinal stigmata in the pyurid ascidian *Boltenia* spp. or by the spiral stigmata found in corellid ascidians. Interestingly, the combination of these three characters in our matrix has enough informational weight to render Ascidiacea monophyletic in a weighting scheme of 3:1 in favor of the morphological data in a combined matrix, where the molecular positions outnumber the morphological characters by roughly a factor of 20:1. In conclusion, we did find considerable support for a monophyletic Ascidiacea in our purely phenotypic characters, but because each of the apomorphic characters is liable to homoplasy, we suspect that additional evidence is needed to settle this question. Nevertheless, abandoning the name Ascidiacea at the current state of phylogenetic knowledge seems premature.

Within Ascidiacea our phenotypic data do not support the monophyly of Enterogona, which is considered a higher taxon comprised of monophyletic Phlebobranchiata and monophyletic Aplousobranchiata (e.g., Kott, 1985; Perrier, 1898; Plough, 1978). Instead, in our analysis Stolidobranchiata groups within Phlebobranchiata, thereby rendering both "Phlebobranchiata" and "Enterogona" paraphyletic. Nonetheless, Stolidobranchiata and Aplousobranchiata were recovered monophyletic in the present analysis, as has been supported in most molecular phylogenetic analysis (e.g., Delsuc et al., 2018; Kocot et al., 2018; Tsagkogeorga et al., 2009).

One of the main model organisms for research on molecular aspects of chordate development (see e.g., Lemaire, 2011), the ascidian *Ciona intestinalis*, has traditionally been included in the taxon Phlebobranchiata (e.g., Millar, 1966; Plough, 1978). This assessment was based on shared morphological similarities, mainly in the branchial basket, such as the presence of papillae on the internal longitudinal blood vessels projecting into the branchial sac. The affinity of Cionidae to Phlebobranchiata is also recovered in molecular phylogenetic analyses (Delsuc et al., 2018; Kocot et al., 2018; Stach and Turbeville, 2002; Tsagkogeorga et al., 2009). Kott (1990), on the other hand, pointed out that other morphological characteristics, such as the role of the epicardia in wound repair, could be seen as evidence for a closer relationship of Cionidae to the colonial aplousobranchs. Our present phenotypic analysis does not support a closer relationship of Cionidae to Aplousobranchiata; rather our analysis recovers Phlebobranchiata paraphyletic with the traditional phlebobranch taxa Perophoridae and Diazonidae more closely related to Aplousobranchiata than is Cionidae. Like aplousobranch taxa, species in Perophoridae and Diazonidae are colonial and it should be noted that there is recent molecular evidence that Diazonidae belong to Aplousobranchiata (Shenkar et al., 2016) contrary to the traditional taxonomic inclusion of Diazonidae in Phlebobranchiata (e.g., Lützen, 1967; Millar, 1970; Van Name, 1945). The present study grouped Diazonidae as a sister taxon to a monophyletic Aplousobranchiata although the statistical support is low. In this analysis, morphological arguments to support a sister group relationship between Diazonidae and Aplousobranchiata as apomorphic characters are the division of the body (character 2) and coloniality due to asexual epicardial budding (character 29).

Position of "Thaliacea"

One of the most surprising outcomes of the present study is the paraphyly of "Thaliacea". The monophyly of Thaliacea is traditionally thought to be strongly supported (e.g., Govindarajan et al., 2011; see also review in Piette and Lemaire, 2015). A number of life history traits and phenotypic characters are usually interpreted as synapomorphies of thaliacean species. These characters are e.g., the obligate alteration between sexual and asexual reproduction in consecutive generations (Neumann, 1956). In Doliolida and Salpida this metagenetic life cycle is accompanied with a distinct polymorphy of the successive generations. In addition, the position of the excurrent and incurrent openings at opposite ends of the animals is a common character to all thaliaceans (reviewed in Bone, 1998). This latter trait is especially convincing as a synapomorphy, as the intestine at the same time is u-shaped. A u-shaped gut is quite common in sessile animals, but rarely found in planktonic animals (Cohen et al., 2003; Williams, 1996). Therefore the combination of a u-shaped gut with incurrent and excurrent siphons at opposite ends of the body together with a holoplanktonic lifestyle had been taken as evidence that the planktonic Thaliacea were derived from sessile ascidian-like ancestors (Stach and Turbeville, 2002). Our analysis turns this evolutionary interpretation upside down. According to our analysis, the ancestral life history strategy in Tunicata was planktonic and the sessility of Ascidiacea was a later phenomenon evolved within Tunicata. Interestingly, it might be pointed out here, that paleontologists interpret fossils from the early Cambrian relegated to the taxon Vetulicolia as early planktonic chordates with some as yet unclear affinity to present day thaliaceans (Gee, 2001; García-Bellido et al., 2014; Lacalli, 2002c; Li et al., 2018). Our analysis of morphological data can therefore be seen as being in broad agreement with the general appearance of taxa in the fossil record. Note however, that the paraphyletic positions of Pyrosomatida as sister taxon to Ascidiacea has weak statistical support and that the relationship of Doliolida and Salpida is unresolved. While Salpida and Doliolida with high statistical support constitute monophyletic groups we did not test the monophyly of Pyrosomatidae. In the present analysis a group consisting of Pyrosomatidae and Ascidiacea is supported by characters 25, 38, and 88: sexually mature form colonial – colonial forms throughout entire development, internal longitudinal blood vessels, and serotonin-lir in endostyle. This implies that coloniality of the sexually mature form evolved in the stem lineage of Ascidiacea plus the thaliacean taxa and is therefore homologous in phlebobranch ascidians, aplousobranch ascidians, pyrosomes, doliolids, and salps but evolved independently in the colonial styelid species within Stolidobranchiata. The metagenetic alteration between a sexual and asexual generation is also present in colonial ascidians. Here, however, the metagenesis is not obvious, because the generations are not only anatomically identical — save the presence of gonads — but are usually present in the same colony. The sexually produced larva, the founding individual of a colony, can be understood as an oozooid, the asexual generation. This founding individual, like the oozooid generation in salps, doliolids, and pyrosomes, does not develop gonads but reproduces exclusively by the formation of buds (Berrill, 1935; Deviney,

1934; Lauzon et al., 2002; Nakauchi, 1982). An evolutionary scenario, where a pyrosome-like ancestor settled and evolved into a colonial aplousobranch-like ascidian might be envisioned recalling that a benthic pyrosome was described by Monniot and Monniot in 1966. However, the species description is highly suspicious, as it was based on a single colonial specimen from a dredge tow and it has been argued (Van Soest, 1981), that it might have entered the net on its way to the surface rather than being a benthic species and may actually be classified as *P. atlanticum*.

Position of Appendicularia

The phylogenetic position of Appendicularia has been controversially debated by previous investigators for a long time (Garstang, 1928; Herdman 1891; Ihle, 1913; Stach and Turbeville, 2002, 2005; Wada, 1998; Zeng et al. 2006). On the one hand, appendicularians show a simple morphology of the branchial basket, direct development, and short generation times that is probably retained from the last common ancestor of tunicates. On the other hand, the elaborated filter-feeding house and the torsion of the tail indicate that some characters are highly derived (e.g., Ihle, 1913). In 1928 Garstang hypothesized that Appendicularia are paedomorphic doliolids, and suggested that pelagic tunicates are derived from a sessile ascidian-like ancestor. At first, molecular phylogenetic analyses also produced contradictory results regarding the phylogenetic position of Appendicularia. Some earlier molecular studies (Swalla et al., 2000; Wada, 1998) found Appendicularia sister taxon to the rest of Tunicata. Although this hypothesis had already been suggested based on considerations of the evolution of morphological characters (see above), it contradicted ideas of Appendicularia as a taxon evolved through neoteny. In fact, appendicularians had been textbook examples for neoteny, based on the rapid development and it was precisely this argumentation that led to the christening of the taxon with its alternative name – Larvacea (Herdman, 1891; Garstang, 1928; Lacalli, 2005; Stach et al. 2008; see reviews in: Gee, 1996; Ruppert, 1997a). The fact that appendicularians resembled ascidian larvae and the observation that their intestine followed a u-shaped course seemed to support the neoteny-hypothesis, because u-shaped guts in planktonic organisms were interpreted as characters inherited from a sessile ancestor (Williams, 1996). These characteristics were more easily reconciled with the hypothesis based on a combination of molecular and morphological data that Appendicularia and Aplousobranchiata form sister groups (Stach and Turbeville, 2002). In addition to the aforementioned arguments, this hypothesis was supported by the observation that appendicularians and aplousobranch larvae shared the common derived character of a rotation of the swimming tail through 90 degrees to the left (Stach et al., 2008). Interestingly, this trait found in larval aplousobranch ascidians is also found in perophorid phlebobranch ascidians and had always been interpreted there as a homoplastic trait (Berrill, 1950). The third hypothesis based on molecular data suggested that Appendicularia and Stolidobranchiata form sister groups (Zeng et al., 2006). However, it found no further support in molecular studies and no morphological synapomorphies had been

suggested, though the position of the neural gland on the right side of the brain as in many stolidobranch ascidians or the absence of eyes as found in some molgulid ascidians might have been considered as such. All of these studies used 18S rDNA sequences, a molecule that might be limited in its power to resolve tunicate phylogenetic relationships (Tsagkogeorga et al., 2010; Wada, 1998). Recent advances in molecular phylogenetic analyses in respect of taxon sampling as well as number of genes included found unanimous support for a sister group relationship of Appendicularia to the remaining Tunicata (Delsuc et al., 2018; Kocot et al., 2018), however taxon sampling in these studies remains limited. Given the caveats discussed above, we were therefore surprised that the phenotypic data of the present study supported the hypothesis heavily favored in molecular analyses that Appendicularia is sister group to the remaining tunicate taxa. In this hypothesis, appendicularians possess several morphological features that are interpreted as plesiomorphic characters inherited from a free-living, fish-like ancestor. Among these characters is the presence of the notochord in adults, the absence of an atrial cavity, and in general the free-swimming lifestyle. While our data support the latest consensus of molecular data in respect of a sister group relationship of Appendicularia to the remaining Tunicata, apomorphic similarities to different ascidian groups (see above) require additional hypotheses of evolutionary origins and are therefore necessarily interpreted as homoplasies.

Combined analysis of morphological and molecular data

The combined analysis based on morphological and molecular data (aligned 18S rDNA sequences kindly provided by Dr. Delsuc, Université de Montpellier) conforms to the phylogeny based only on morphological data in the position of Appendicularia as sister group to the remaining tunicate groups (Fig. 2). Monophyletic Stolidobranchiata are sister taxon to paraphyletic "Phlebobranchiata", monophyletic Thaliacea and the aplousobranch *Clavelina lepadiformis*. *C. lepadiformis* and Thaliacea form a clade to the exclusion of "Phlebobranchiata". The phlebobranch Perophoridae seem to be closer related to a clade consisting of *C. lepadiformis* and Thaliacea than to other phlebobranch species, rendering "Phlebobranchiata" paraphyletic. Comparing the tunicate phylogeny based on combined morphological and molecular data from the present study with the ones recently published based on phylogenomic methodology (Kocot et al., 2018; Delsuc et al., 2018) reveals many similarities and identical branching of major tunicate taxa. With 32 species as terminal taxa our combined analysis covers a somewhat larger disparity of tunicate taxa compared to the 17 (Delsuc et al., 2018) and 18 (Kocot et al., 2018) tunicate species in previous studies. Nevertheless, there is only minor disagreement between the phylogenomic studies and the result from our combined analysis concerning the phylogenetic positions of Aplousobranchiata, Thaliacea, and Phlebobranchiata. In the present combined study, the aplousobranch *C. lepadiformis* is sister taxon to Thaliacea similar to the molecular phylogenomic studies that found Aplousobranchiata grouping within paraphyletic "Phlebobranchiata" (Delsuc et al., 2018; some analyses in Kocot et al., 2018).

It differs from results under some analysis parameters in the study of Kocot et al. (2018), where Aplousobranchiata was the sister group of a monophyletic Phlebobranchiata. Despite the differences in analysis methods (e.g., we use parsimony as optimizing criterion whereas the phylogenomic studies used model based optimizing criteria), taxon sampling, and the known elevated and heterogeneous substitution rates (Tsagkogeorga et al., 2010), the studies therefore show general agreement.

Does this observation imply that the morphological data have no or little influence on the outcome of the phylogenetic analysis of the combined data? This indeed seems to be the case in our combined data set, but we were interested in the contribution of the morphological data to the overall phylogenetic signal. With 2121 positions in the alignment of the 18S rDNA sequences outnumbered the 116 phenotypic characters by roughly 20:1. The paraphyly of Ascidiacea, supported in the molecular partition of the data gave way to a monophyletic Ascidiacea supported by the morphological partition at a weighting scheme of 3:1. Similarly, the monophyly of Thaliacea, supported in the molecular partition of the data gave way to a paraphyletic Thaliacea supported by the morphological partition at a weighting scheme of 3:1. Both observations indicate that the phylogenetic signal is considerably higher in the morphological data.

Discussion of individual character transformations

Phylogenetic relationships are one main focus of interest and a prerequisite in evolutionary considerations. The tracing of changing morphologies through evolutionary time and the origin of diverse morphologies is another focus in evolutionary research. Even when character transformations are mapped on a sequence-based phylogenetic hypothesis the primary homology hypothesis (sensu Pinna, 1991) is the key component. Here, we evaluated the contribution of selected morphological characters to the formulation of phylogenetic hypotheses. In the following paragraphs we discuss the resulting hypotheses of character transformations at nodes of interest.

Clearly the taxon with the highest support in our morphological analysis is Tunicata itself. It is not only supported by a Bremer support index of 10 and statistical support of 100% (jackknife and bootstrap values), the monophyly is also supported by seven uncontroverted apomorphic characters under acctran optimization. These are: tunic (13), heart beat reversal (18), pyloric gland (60), shape of gastrointestinal tract – u-shaped (61), larval tunic (78), larval statocyte (81), brain divided into cortex and neuropil (96). Hermaphroditism (character 69) is another apomorphic character evolved in the stem lineage of Tunicata. It is, however, not uncontroverted, because *Oikopleura dioica* and *Sycozoa sigillinoides*, are diecious species. While several of these characters (13, 18, 60, 61) have been hypothesized before

to have evolved in the stem lineage of Tunicata (reviewed in Huus, 1956; Stach, 2008) our character matrix suggests additional apomorphic changes not considered before. Moreover, the resulting phylogenetic hypotheses of subordinate tunicate taxa require some additional considerations. The evolution of the ability to secrete cellulose, probably acquired via lateral gene transfer from a bacterium (Nakashima et al., 2004; Sagane et al., 2010), had traditionally been associated with the origin of sessility. With planktonic appendicularians as the sister taxon to the remaining Tunicata and, in our morphological analysis, the planktonic salps and doliolids, and planktonic pyrosomes as consecutively branching taxa, the correlation between the evolution of cellulose secretion and sessility becomes obsolete. However, the ability to secrete an outer, protective tunic containing cellulose, may have occurred in the early life history stages. The character state in adults of the last common ancestor of Tunicata is not entirely obvious, because adult appendicularians feature a highly complicated secretion of the tunic that is based on the complexity and development of the filter-feeding houses (Flood and Deibel, 1998; Körner, 1952). In addition, a duplication of cellulose synthase genes occurred in the stem lineage of appendicularians (Hosp et al., 2012; Sagane et al., 2010). Both facts show that the secretion of the tunic in Appendicularia is highly derived.

Besides the phylogenetic interrelationships of higher tunicate taxa, our analysis of phenotypic characters finds support for several other monophyletic taxa that are traditionally recognized in tunicate taxonomy. E.g., the monophyly of Botryllinae is supported by the presence of a larval photolith, a sensory organ that combines a gravity sensor and a light receptive organ; Molgulidae is characterized by the storage kidney as an apomorphic character, and Didemnidae by their peculiar mode of asexual reproduction via pyloric budding and the rearing of sexually produced larvae within brood chambers in the common tunic. A tabulated summary of uncontroverted apomorphies supporting nodes in the strict consensus of our most parsimonious cladograms (Fig. 1) is listed in Table 2.

The monophyly of Ascidiacea, the paraphyly of the planktonic “Thaliacea”, and the sister group relationship of Appendicularia to the remaining Tunicata suggests that the early evolutionary history of Tunicata took place in the plankton. Appendicularians adapted to the planktonic environment by exploiting the extracorporal tunic evolving it into the most complex external filtering device in combination with an extraordinarily fast life cycle. Thaliaceans are likewise characterized by fast developmental rates, but different from appendicularians possess an asexual period during their life cycles that leads to the formation of a colony. Clonal reproduction has been interpreted as an adaptation to the spotty and unpredictable supply with nutrients in the plankton (e.g., reviewed in Hughes, 1989; Jackson and Coates, 1986) and can be found in diverse groups of animals such as cladoceran crustaceans, hydrozoans or siphonapterans (Boero et al., 1992; Decaestecker et al., 2009; Zakson-Aiken et al., 1996). Sessility, on the other hand, is also often correlated with coloniality, e.g., in the case of kamptozoans, bryozoans, or anthozoans (Schuchert, 1993; Wood, 2015; see also review in Blackstone and

Jasker, 2003). In the present phylogenetic hypothesis the last common ancestor of Ascidiacea is reconstructed as a colonial species. This correlates well with the simple morphology of the branchial basket in Aplousobranchiata. Traditionally, Aplousobranchiata comprise only colonial species and the simplicity of their branchial basket has been interpreted by most authors as primitive within ascidians (Lahille, 1890; Stach, 2009). The evolutionary transition from a planktonic colonial form (as present in Thaliacea, Doliolida and Pyrosomatida) to a sessile colonial form would remain difficult to understand and requires the parallel evolution of coloniality in Botryllinae within Stolidobranchiata. A repeated evolution of coloniality has also been concluded by mapping of this character on different phylogenetic hypotheses based on molecular data (Swalla et al., 2000; Wada et al., 1998; Zeng et al., 2006). Our discussion of the evolutionary interpretations should highlight that there is currently no support for a conflict-free phylogenetic hypothesis. Maybe this is unavoidable in a taxon that shows such a degree of disparity (Berrill, 1950; Kott, 1985, 1990, 1992, 2001; Lemaire, 2011; Shenkar and Swalla, 2011) and with such a long evolutionary history (Chen et al., 2003; Shu et al., 2001).

While we compiled conceptualized phenotypical characters into the biggest data matrix available on tunicate morphology and analyzed it in a consistent cladistic framework, we do not suggest that this is the final solution of tunicate phylogeny, but a first step to use the potential phylogenetic information present in phenotypic characters to elucidate the interrelationships of this diverse marine taxon.

Acknowledgements

We are grateful for access to the tunicate collection and to the Leica SPE CLSM granted by Priv.-Doz. Dr. Carsten Lüter (Museum für Naturkunde Berlin). Financial support by the Deutsche Forschungsgemeinschaft (DFG) and the Elsa-Neumann-Stipendium des Landes Berlin is gratefully acknowledged. We are thankful to the invaluable help of Woody Lee and Scott Jones from the Smithsonian Marine Station in Fort Pierce, Florida, in securing specimens of *Fritillaria borealis*. We are also indebted to Prof. Valerie Paul and Prof. Mary Rice for generously providing access to the facilities of the Smithsonian Marine Station.

References

Ax, P. 2001. Das System der Metazoa: ein Lehrbuch der phylogenetischen Systematik. Spektrum Akademischer Verlag GmbH, Heidelberg, Berlin.

Barreiro-Iglesias, A., Cornide-Petronio, M. E., Anadón, R., Rodicio, M. C. 2009. Serotonin and GABA are colocalized in restricted groups of neurons in the larval sea lamprey brain: insights into the early evolution of neurotransmitter colocalization in vertebrates. J. Anat. 215, 435-443.

Baumgarten, H. G., Björklund, A., Lachenmayer, L., Nobin, A., Rosengren, E. 1973. Evidence for the existence of serotonin-, dopamine-, and noradrenaline-containing neurons in the gut of *Lampetra fluviatilis*. Z. Zellforsch. Mik. Ana. 141, 33-54.

Berrill, N. J. 1935. Studies in tunicate development. Part IV - Asexual reproduction. Philos. Trans. R. Soc. Lond. B - Biological Sciences 225, 327-379.

Berrill, N.J. 1948. The development, morphology and budding of the ascidian *Diazona*. J. Mar. Biol. Assoc. UK, 27(2), 389-399.

Berrill, N. J. 1950. The Tunicata – With an account of the British species. The Ray Society, London, UK.

Braun, K., Stach, T. 2016. Comparative study of serotonin-like immunoreactivity in the branchial basket, digestive tract, and nervous system in tunicates. Zoomorphology 135, 351-366.

Braun, K., Stach, T. 2017. Structure and ultrastructure of eyes and brains of *Thalia democratica* (Thaliacea, Tunicata, Chordata). J. Morphol. 278, 1421-1437.

Braun, K., Stach, T. 2018a. Morphology and evolution of the central nervous system in adult tunicates. J. Zool. Syst. Evol. Res. 00, 1-22.

Braun, K., Stach, T. 2018b. Distribution and evolution of serotonin-like immunoreactive cells in Thaliacea (Tunicata). Zoomorphology 137(4), 565-578.

Brien, P. 1948. Embranchement des Tuniciers. In: Grasse, P. P. (Ed.) Morphologie et reproduction. Traité de Zoologie, Paris.

Brien, P., Brien-Gavage, E. 1927. Bourgeonnement de *Clavelina lepadiformis* Müller. Rec. Inst. Zool. Torley-Rousseau 1, 31–81.

Blackstone, N. W., Jasker, B. D. 2003. Phylogenetic considerations of clonality, coloniality, and mode of germline development in animals. J. Exp. Zool. Part B: Molecular and Developmental Evolution 297B, 35-47.

Boero, F., Bouillon, J., Piraino, S. 1992. On the origins and evolution of hydromedusan life cycles (Cnidaria, Hydrozoa). In: R. Dallai (Ed.) Sex Origian and Evolution, Vol. 6, Selected Symposia and Monographs U.Z.I., Mucchi, Modena, Italy, pp. 59–68.

Bone, Q. 1998. The biology of pelagic tunicates. Oxford University Press, Oxford, New York, Tokyo.

Bone, Q., Braconnot, J.-C., Carré, C. 1997. On the heart and circulation in doliolods (Tunicata: Thaliacea). Scientia Marina, 61(2), pp. 189-194.

Burighel, P., Cloney, R. A. 1997. Urochordata: Ascidiacea. In: Harrison, F. W., Ruppert, E. E. (Eds.), Microscopic anatomy of invertebrates. Hemichordata, Chaetognatha, and the invertebrate chordates. Willey-Liss, Incorporation, New York, Chichester, Weinheim, Brisbane, Singapore, Toronto, pp. 221-347.

Burighel, P., Lane, N. J., Fabio, G., Stefano, T., Zaniolo, G., Carnevali, M. D. C., Manni, L. 2003. Novel, secondary sensory cell organ in ascidians: in search of the ancestor of the vertebrate lateral line. J. Comp. Neurol. 461, 236-249.

Candiani, S., Augello, A., Oliveri, D., Passalacqua, M., Pennati, R., De Bernardi, F., Pestarino, M. 2001. Immunocytochemical localization of serotonin in embryos, larvae and adults of the lancelet, *Branchiostoma flordiae*. Histochem. J. 33, 413-420.

Chamisso, A.v. 1819. De animalibus quibusdam e classe vermium Linnaeana in circumnavigatione terrae auspicante Comite N. Romanzoff duce Ottone de Kotzebue annis 1815. 1816. 1817. 1818. peracta observatis. Fasciculus primus. De Salpa. Dümmler Verlag, Berlin.

Chen, J.-Y., Huang, D.-Y., Peng, Q.-Q., Chi, H.-M., Wang, X.-Q., Feng, M. 2003. The first tunicate from the early Cambrian of South China. Proc. Natl. Acad. Sci. USA 100, 8314-8318.

Cohen, A. I. 1963. Vertebrate retinal cells and their organization. Biol. Rev. 38, 427-459.

Cohen, B. L., Holmer, L. E., Lüter, C. 2003. The brachiopod fold: a neglected body plan hypothesis. Palaeontology 46, 59-65.

Cuvier, G. 1840. Animal Kingdom: arranged according to its organization, forming the basis for a natural history of animals, and introduction to comparative anatomy. Holborn Hill, London.

Decaestecker, E., De Meester, L., Mergeay, J. 2009. Cyclical Parthenogenesis in *Daphnia*: Sexual versus asexual reproduction. In: Schön, I., Martens, K., Dijk, P. (Eds.), Lost Sex: The Evolutionary Biology of Parthenogenesis. Springer Netherlands, Dordrecht, pp. 295-316.

Deibel, D., Paffenhöfer, G. A. 1988. Cinematographic analysis of the feeding mechanism of the pelagic tunicate *Doliolum nationalis*. Bull Mar Sci 43.

Delsuc, F., Brinkmann, H., Chourrout, D., Philippe, H. 2006. Tunicates and not cephalochordates are the closest living relatives of vertebrates. Nature 439, 965-968.

Delsuc, F., Philippe, H., Tsagkogeorga, G., Simion, P., Tilak, M.-K., Turon, X., López-Legentil, S., Piette, J., Lemaire, P., Douzery, E. J. P. 2018. A phylogenomic framework and timescale for comparative studies of tunicates. BMC Biol. 16, 39.

Deviney, E. M. 1934. The behavior of isolated pieces of ascidian (*Perophora viridis*) stolon as compared with ordinary budding. J. Elisha Mitchell Sci. Soc. 49, 185-224.

Drasche, R.v. 1884. Über einige neue und weniger gekannte aussereuropäische einfache Ascidien. Denkschr. Kais. Akad. Wiss. 48: 369-387.

Eakin, R. M. 1979. Evolutionary significance of photoreceptors: in retrospect. Am. Zool. 19, 647-653.

Fenaux, R. 1998. Anatomy and functional morphology of the Appendicularia. In: Bone, Q. (Ed.) The biology of pelagic tunicates. Oxford University Press, Oxford, New York, Tokyo, pp. 25-34.

Fitzhugh, K. 2006. The ‘requirement of total evidence’ and its role in phylogenetic systematics. Biol. Philo. 21, 309-351.

Flood, P. R., Deibel, D. 1998. The appendicularian house. In: Bone, Q. (Ed.) The biology of pelagic tunicates. Oxford University Press, Oxford, New York, Tokyo, pp. 105-124.

Franz, V. 1927. Morphologie der Akranier. Z. ges. Anat. 27, 464-692.

García-Bellido, D. C., Lee, M. S. Y., Edgecombe, G. D., Jago, J. B., Gehling, J. G., Paterson, J. R. 2014. A new vetulicolian from Australia and its bearing on the chordate affinities of an enigmatic Cambrian group. BMC Evol. Biol. 14, 214.

Garstang, W. 1928. The morphology of the Tunicata, and its bearings on the phylogeny of the Chordata. Q. J. Microsc. Sci. 72, 51-187.

Gee, H. 1996. Before the backbone. Chapman & Hall, London, Weinheim, New York, Tokyo, Victoria, Madras.

Gee, H. 2001. On being vetulicolian. Nature 414, 407.

Gill, H. S., Renaud, C. B., Chapleau, F., Mayden, R. L., Potter, I. C., Douglas, M. E. 2003. Phylogeny of living parasitic lampreys (Petromyzontiformes) based on morphological data. Copeia 2003, 687-703.

Giribet, G. 2018. Phylogenomics resolves the evolutionary chronicle of our squirting closest relatives. BMC Biol. 16, 49.

Godeaux, J. E. A., Bone, Q., Braconnot, J. C. 1998. Anatomy of Thaliacea. In: Bone, Q. (Ed.) The biology of pelagic tunicates. Oxford University Press, Oxford.

Godeaux, J. 2003. History and revised classification of the order Cyclomyaria (Tunicata, Thaliacea, Doliolida). Bull. Inst. Roy. Sci. Nat. Belgique 73, 191-222.

Goodrich, E.S. 1909. Vertebrata, Craniata I. Cyclostomes and fishes. In: Lankester, E.R. (Ed.), Treatise on Zoology, Part 9. Adam a. Charles Black, London, pp: XVI – 518.

Gorbman, A. 1995. Olfactory origins and evolution of the brain-pituitary endocrine system: facts and speculation. Gen. Comp. Endocrinol. 97, 171-178.

Gorbman, A. 1999. Brain-Hatschek's pit relationships in amphioxus species. Acta Zool. 80, 301-305.

Govindarajan, A. F., Bucklin, A., Madin, L. P. 2011. A molecular phylogeny of the Thaliacea. J. Plankton Res. 33, 843-853.

Grave, C. 1926. *Molgula citrina* (Alder and Hancock). Activities and structure of the free-swimming larva. J. Morphol. 42, 453-471.

Groepler, W. 2016. Die Seescheiden von Helgoland. Westarp Wissenschaften-Verlagsgesellschaft mbH, Hohenwarsleben.

Goloboff, P. A., Farris, J. S., Nixon, K. C. 2008. TNT, a free program for phylogenetic analysis. Cladistics 24, 774-786.

Gutierrez, S., Brown, F. D. 2017. Vascular budding in *Symplegma brakenhielmi* and the evolution of coloniality in styelid ascidians. Dev. Biol. 423, 152-169.

Hartmeyer, R. 1923. Ascidiacea, Part I. The Danish Ingolf-expedition. H. Hagerup, Copenhagen, pp. 1-370.

Hawkins, C. J., Kott, P., Parry, D. L., Swinehart, J. H. 1983. Vanadium content and oxidation state related to ascidan phylogeny. Comp. Biochem. Physiol. 76B, 555-558.

Hennig, W. 1982. Phylogenetische Systematik. Verlag Paul Parey, Berlin, Hamburg.

Herdman, W. A. 1891. A revised classification of the Tunicata, with definitions of the orders, suborders, families, subfamilies, and genera, and analytical keys to the species. Zool. J. Linn. Soc. 23, 558-652.

Hirose, E. 1999. Pigmentation and acid storage in the tunic: protective functions of the tunic cells in the tropical ascidian *Phallusia nigra*. Invertebr. Biol. 118, 414-422.

Hirose, E., Kimura, S., Itoh, T., Nishikawa, J. 1999. Tunic morphology and cellulosic components of pyrosomas, doliolids, and salps (Thaliacea, Urochordata). Biol. Bull. 196, 113-120.

Holland, L. Z. 1992. The phylogenetic significance of tunicate sperm morphology. In: Baccetti, B. (Ed.), 6th International Congress on Spermatology. Raven Press, Siena.

Holland, N. D., Holland, L. Z. 1993. Serotonin-containing cells in the nervous system and other tissues during ontogeny of a lancelet, *Branchiostoma floridae*. Acta Zool. 74, 195-204.

Hosp, J., Sagane, Y., Danks, G., Thompson, E. M. 2012. The evolving proteome of a complex extracellular matrix, the *Oikopleura* house. PLOS ONE 7, e40172.

Huus, J., 1956. Zweite und letzte Unterklasse der Acopa: Ascdiacea = Tethyodeae =Seescheiden. In: Krumbach, T. (Ed.), Handbuch der Zoologie, Fünfter Band, Zweite Hälfte. Walter de Gruyter, Berlin, pp. 545–692.

Hughes, R. N. 1989. Functional biology of clonal animals. Springer Netherlands.

Ihle, J.E.W. 1913. Die Appendicularien. In: Spengel, J.W. (Ed.), Ergebnisse und Fortschritte der Zoologie, Dritter Band. Verlag von Gustav Fischer, Jena, pp. 463-534.

Ihle, J.E.W. 1956. Dritte und letzte Ordnung der Thaliacea: Desmomyaria. In: Krumbach, T. (Ed.), Handbuch der Zoologie, Fünfter Band, Zweite Hälfte. Walter de Gruyter, Berlin, pp. 401–544.

Ihle, J.E.W. 1971. Die Urogenitalorgane. In: Ihle, J.E.W.; van Kampen, P.N.; Nierstrasz, H.F.; Versluys, J. (Eds.),Vergleichende Anatomie der Wirbeltiere. Springer, Berlin, Heidelberg, pp. 708-787.

Jackson, J.B.C., Coates, A. G. 1986. Life cycles and evolution of clonal (modular) animals. Philos. Trans. R. Soc. Lond. B, Biological Sciences 313, 7-22.

Jonasova, K., Kozmik, Z. 2008. Eye evolution: Lens and cornea as an upgrade of animal visual system. Semin. Cell Dev. Biol. 19, 71-81.

Kah, O., Lethimonier, C., Somoza, G., Guilgur, L. G., Vaillant, C., Lareyre, J. J. 2007. GnRH and GnRH receptors in metazoa: A historical, comparative, and evolutive perspective. Gen. Comp. Endocrin. 153, 346-364.

Karnovsky, M.J. 1965. A formaldehyde-glutaraldehyde fixative of high osmolality for use in electron microscopy. J. Cell Biol. 27, 137A.

Kluge, A. G. 1998. Total evidence or taxonomic congruence: cladistics or consensus classification. Cladistics 14, 151-158.

Kocot, K. M., Tassia, M. G., Halanych, K. M., Swalla, B. J. 2018. Phylogenomics offers resolution of major tunicate relationships. Mol. Phylogenet. Evol. 121, 166-173.

Körner, W. F. 1952. Untersuchungen über die Gehäusebildung bei Appendicularien (*Oikopleura dioica* Fol). Z. Morph. Ökol. Tiere 41, 1-53.

Kott, P. 1985. The Australian Ascidacea. Part 1, Phlebobranchia and Stolidobranchia. Mem. Queensl. Mus. 23, 1-440.

Kott, P. 1990. The Australian Ascidacea. Part 2, Aplousobranchia (1). Mem. Queensl. Mus. 29, 1-266.

Kott, P. 1992. The Australian Ascidacea. Part 3, Aplousobranchia (2). Mem. Queensl. Mus. 32, 375-620.

Kott, P. 2001. The Australian Ascidacea. Part 4, Aplousobranchia (3), Didemnidae. Mem. Queensl. Mus. 47, 1-410.

Kowalevsky, A. 1866. Entwickelungsgeschichte der einfachen Ascidien. Mem. Acad. Imp. Sci. Sa.-Pétersbourgh VIIe Série, 1-19, 13 plates.

Kriebel, M. E. 1967. Conduction velocity and intracellular action potentials of the tunicate heart. J. Gen. Physiol. 50, 2097-2107.

Lacalli, T. C. 1996. Frontal eye circuitry, rostral sensory pathways and brain organization in amphioxus larvae: evidence from 3D reconstructions. Philos. Trans. R. Soc. Lond. B 351, 243-263.

Lacalli, T. C. 2002a. The dorsal compartment locomotory control system in amphioxus larvae. J. Morphol. 252, 227-237.

Lacalli, T. C. 2002b. Sensory pathways in amphioxus larvae I. Constituent fibres of the rostral and anterodorsal nerves, their targets and evolutionary significance. Acta Zool. 83, 149-166.

Lacalli, T. C. 2002c. Vetulicolians - are they deuterostomes? chordates? Bioessays 24, 208-211.

Lacalli, T. C. 2005. Protochordate body plan and the evolutionary role of larvae: old controversies resolved? Can. J. Zool. 83, 216-224.

Lacalli, T. C., Holland, L. Z. 1998. The developing dorsal ganglion of the salp *Thalia democratica*, and the nature of the ancestral chordate brain. Philos. Trans. R. Soc. Lond. B 353, 1943-1967.

Lacalli, T. C., Holland, N. D., West, J. E. 1994. Landmarks in the anterior central nervous system of amphioxus larvae. Philos. Trans. R. Soc. Lond. B 344, 165-185.

Lahille, F. 1890. Recherches sur les tuniciers des côtes de France. Imprimerie Lagarde et Sebille, Tulouse.

Lamb, T. D., Collin, S. P., Pugh, E. N. 2007. Evolution of the vertebrate eye: opsins, photoreceptors, retina and eye cup. Nat. Rev. Neurosci. 8, 960-976.

Lambert, G., Lambert, C. C. 1987. Spicule formation in the solitary ascidian, *Herdmania momus*. J. Morphol. 192, 145-159.

Lauzon, R. J., Ishizuka, K. J., Weissman, I. L. 2002. Cyclical generation and degeneration of organs in a colonial urochordate involves crosstalk between old and new: A model for development and regeneration. Dev. Biol. 249, 333-348.

Lemaire, P. 2011. Evolutionary crossroads in developmental biology: the tunicates. Development 138, 2143-2152.

Lemaire, P., Piette, J. 2015. Tunicates: exploring the sea shores and roaming the open ocean. A tribute to Thomas Huxley. Open Biology 5.

Li, Y., Williams, M., Gabbott, S. E., Chen, A., Cong, P., Hou, X. 2018. The enigmatic metazoan *Yuyuanozoon magnificissimi* from the early Cambrian Chengjiang Biota, Yunnan Province, South China. J. Paleont., 1-11.

Lohmann, H. 1914. Die Appendicularien der Valdivia-Expedition, Verh. Deut. Zool. Gesell. 24: 157-192.

Lohmann, H. 1956. Erste Klasse der Tunicaten. Appendiculariae. In: Krumbach, T. (Ed.) Handbuch der Zoologie. Walter de Gruyter & Co., Berlin, pp. 15-202.

Lützen, J.G. 1967. Sækdyr (Tunicata). Danm. Fauna, 75: 267.

Mackie, G. O. 1995. On the visceral nervous system of *Ciona*. J. Mar. Biol. Assoc. U.K. 75, 141-151.

Mackie, G. O., Bone, Q. 1978. Luminescence and associated effector activity in Pyrosoma (Tunicata: Pyrosomida). Philos. Trans. R. Soc. Lond. B 202, 483-495.

Maddison, W. P., Maddison, D. R. 2018. Mesquite: A modular system for evolutionary analysis. Retrieved from http://mesquiteproject.org

Mallat, J. 1979. Surface morphology and functions of pharyngeal structures in the larval lamprey *Petromyzon marinus*. J. Morphol. 162, 249-274.

Manni, L., Pennati, R. 2016. Tunicata. In: Schmidt-Rhaesa, A., Harzsch, S., Purschke, G. (Eds.), Structure and evolution of invertebrate nervous systems. Oxford University Press, Oxford, UK, pp. 699–718.

Manni, L., Zaniolo, G., Cima, F., Burighel, P., Ballarin, L. 2007. *Botryllus schlosseri*: A model ascidian for the study of asexual reproduction. Dev. Dynam. 236, 335-352.

Millar, R. H. 1954. The breeding and development of the ascidian *Pelonaia corrugata* Forbes and Goodsir. J. Mar. Biol. Assoc. UK 33, 681-687.

Millar, R.H. 1966. Ascidiacea. Mem. Nat. Mus Victoria 27: 357–384.

Millar, R. H. 1970. British ascidians, Tunicata: Ascidiacea: keys and notes for the identification of the species. Academic Press, London.

Millar, R. H. 1971. The Biology of Ascidians. In: Russell, F. S., Yonge, M. (Eds.), Adv. Mar. Biol., Academic Press, pp. 1-100.

Monniot, C., Monniot, F. 1966. A benthic pyrosoma, *Pyrosoma benthica* n. sp. Fr. Acad. Sci. 263: 368–370.

Monniot, C., Monniot, F. 1972. Clé mondiale des genres d'ascidies. Arch. Zool. Exp. Gener. 113, 311-367.

Monniot, F., Monniot, C. 2001. Ascidians from the tropical western Pacific. Editions scientifiques du Muséum, Paris, France.

Moreno, T. R., Rocha, R. M. 2008. Phylogeny of the Aplousobranchia (Tunicata: Ascidiacea). Rev. Bras. Zool. 25, 269-298.

Mukai, H., Koyama, H., Watanabe, H. 1983. Studies on the reproduction of thee species of *Perophora* (Ascidiacea). Biol. Bull. 164, 251-266.

Nakashima, K., Yamada, L., Satou, Y., Azuma, J.-i., Satoh, N. 2004. The evolutionary origin of animal cellulose synthase. Dev. Genes Evol. 214, 81-88.

Nakauchi, M. 1982. Asexual development of ascidians: its biological significance, diversity, and morphogenesis. Am. Zool., 753-763.

Neumann, G. 1956. Zweite Klasse der Tunicata. Acopa = Caducichordata. In: Krumbach, T. (Ed.), Handbuch der Zoologie, Fünfter Band, Zweite Hälfte. Walter de Gruyter, Berlin, pp. 203-400.

Nieuwenhuys, R. 1977. The brain of the lamprey in a comparative perspective. Ann. New York Acad. Sci. 299, 97-145.

Perrier, J.O. 1898. Note sur la classification des Tuniciers. CR Acad Sci Paris 126: 1758–1762.

Piette, J., Lemaire, P. 2015. Thaliaceans, the neglected pelagic relatives of ascidians: a developmental and evolutionary enigma. Q. Rev. Biol. 90, 117-145.

Pietschmann, V. 1962. Acrania. In: Kükenthal, W., Krumbach, T. (Eds.), Handbuch der Zoologie. Walter de Gruyter, Berlin, pp. 3-124.

Pinna, M. C. C. 1991. Concepts and tests of homology in the cladistic paradigm. Cladistics 7, 367-394.

Plough, H.H. 1978. Sea squirts of the Atlantic Continental Shelf from Maine to Texas. Johns Hopkins University Press, Baltimore, Maryland.

Pourquié, O. 2001. A macho way to make muscles. Nature 409, 679-680.

Rigon, F., Stach, T., Caicci, F., Gasparini, F., Burighel, P., Manni, L. 2013. Evolutionary diversification of secondary mechanoreceptor cells in Tunicata. BMC Evol. Biol. 13, 112.

Roch, G. J., Tello, J. A., Sherwood, N. M. 2014. At the transition from invertebrates to vertebrates, a novel GnRH-Like peptide emerges in amphioxus. Mol. Biol. Evol. 31, 765-778.

Rocha, R. M. d., Zanata, T. B., Moreno, T. R. 2012. Keys for the identification of families and genera of Atlantic shallow water ascidians. Biota Neotropica 12, 269-303.

Romer, A. S., Parsons, T. S. 1986. The vertebrate body. Saunders College Publishing, Philadelphia.

Ruppert, E. E. 1997a. Introduction: microscopic anatomy of the notochord, heterochrony, and chordate evolution. In: Harrison, F. W., Ruppert, E. E. (Eds.), Microscopic Anatomy of Invertebrates. Hemichordata, Chaetognatha, and the invertebrate chordates. Willey-Liss, Incorporation, New York, Chichester, Weinheim, Brisbane, Singapore, Toronto, pp. 1-13.

Ruppert, E. E. 1997b. Cephalochordata (Acrania). In: Harrison, F. W., Ruppert, E. E. (Eds.), Microscopic anatomy of invertebrates. Hemichordata, Chaetognatha, and the invertebrate chordates. Wiley-Liss, New York, Chichester, Weinheim, Brisbane, Singapore, Toronto, pp. 349-504.

Sagane, Y., Zech, K., Bouquet, J.-M., Schmid, M., Bal, U., Thompson, E. M. 2010. Functional specialization of cellulose synthase genes of prokaryotic origin in chordate larvaceans. Development 137, 1483-1492.

Sakharov, D. A., Salimova, N. B. 1980. Serotonin neurons in the peripheral nervous system of the larval lamprey, *Lampetra planeri*. A histochemical, microspectrofluorimetric and ultrastructural study. Zool. Jahrb. Allg. Zool. 84, 231-239.

Sakharov, D. A., Salimova, N. 1982. Serotonin-containing cells in the ascidian endostyle. Cell. Mol. Life Sci. 38, 802-803.

Salvini-Plawen, L.V. 1982. On the polyphyletic origin of photoreceptors. In: Westfall, J.A. (Ed.), Visual cells in evolution, Raven Press, New York, pp. 137–154.

Schuchert, P. 1993. Phylogenetic analysis of the Cnidaria. J. Zool. Syst. Evol. Res. 31, 161-173.

Shenkar, N., Koplovitz, G., Dray, L., Gissi, C., Huchon, D. 2016. Back to solitude: Solving the phylogenetic position of the Diazonidae using molecular and developmental characters. Mol. Phylogenet. Evol. 100, 51-56.

Shenkar, N., Swalla, B. J. 2011. Global diversity of Ascidiacea. PLOS ONE 6, e20657.

Shu, D., Chen, L., Han, J., Zhang, X. 2001. An Early Cambrian tunicate from China. Nature 411, 472 - 473.

Slingsby, C., Wistow, G. J., Clark, A. R. 2013. Evolution of crystallins for a role in the vertebrate eye lens. Protein Sci. 22, 367-380.

Sorrentino, M., Manni, L., Lane, N. J., Burighel, P. 2000. Evolution of cerebral vesicles and their sensory organs in an ascidian larva. Acta Zool. 81, 243-258.

Stach, T. 1996. On the preoral pit of the larval amphioxus (*Branchiostoma lanceolatum*). Ann. Sci. Nat. Zool., Paris 17, 129-134.

Stach, T. 2005. Comparison of the serotonergic nervous system among Tunicata: implications for its evolution within Chordata. Organisms, Diversity and Evolution 5, 15-24.

Stach, T. 2008. Chordate phylogeny and evolution: a not so simple three-taxon problem. J. Zool. 276, 117-141.

Stach, T. 2009. Anatomy of the trunk mesoderm in tunicates: homology considerations and phylogenetic interpretation. Zoomorphology 128, 97-109.

Stach, T. 2014. Deuterorstome phylogeny - a morphological perspective. In: Wägele, W. (Ed.) Deep Metazoan Phylogeny: The backbone of the tree of life. De Gruyter, Berlin, pp. 425-457.

Stach, T., Turbeville, J. M. 2002. Phylogeny of Tunicata inferred from molecular and morphological characters. Mol. Phylogen. Evol. 25, 408-428.

Stach, T., Turbeville, J. M. 2005. The role of appendicularians in chordate evolution - a phylogenetic analysis of molecular and morphological characters, with remarks on 'neoteny-scenarios'. In: Gorsky, G., Youngbluth, M.J., Deibel, D. (Eds.), Responses of marine ecosystems to global change. Ecological impact of appendicularians. Contemporary Publishing International, Paris, pp. 9-26.

Stach, T., Winter, J., Bouquet, J.-M., Chourrout, D., Schnabel, R. 2008. Embryology of a planktonic tunicate reveals traces of sessility. Proceed. Nat. Acad. Sci. 105, 7229-7234.

Stokes, M. D., Holland, N. D. 1995. Embryos and larvae of a lancelet, *Branchiostoma floridae*, from hatching through metamorphosis: growth in the laboratory and external morphology. Acta Zool. 76, 105-120.

Swalla, B. J., Cameron, C. B., Corley, L. S., Garey, J. R. 2000. Urochordates are monophyletic within the deuterostomes. Syst. Biol. 49, 52-64.

Swofford, D. L. 2003. PAUP*. Phylogenetic Analysis Using Parsimony (*and Other Methods). Sinauer Associates, Sunderland, Massachusetts.

Terakado, K. 2010. Generation of prolactin-like neurons in the dorsal strand of ascidians. Zool. Sci. 27, 581-588.

Tsagkogeorga, G., Turon, X., Galtier, N., Douzery, E., Delsuc, F. 2010. Accelerated evolutionary rate of housekeeping genes in tunicates. J. Mol. Evol. 71, 153-167.

Tsagkogeorga, G., Turon, X., Hopcroft, R., Tilak, M., Feldstein, T., Shenkar, N., Loya, Y., Huchon, D., Douzery, E., Delsuc, F. 2009. An updated 18S rRNA phylogeny of tunicates based on mixture and secondary structure models. BMC Evol. Biol. 9, 187.

Van Name, W. G. 1945. The north and south american ascidians. Bull. Am. Mus. Nat. Hist. 84, 1-475, 431 plates.

Van Soest, R. W. M. 1981. A monograph of the order Pyrosomatida (Tunicata, Thaliacea). J. Plankton Res. 3, 603-631.

Wada, H. 1998. Evolutionary history of free-swimming and sessile lifestyles in urochordates as deduced from 18S rDNA molecular phylogeny. Mol. Biol. Evol. 15, 1189-1194.

Wägele, J.-W. 2001. Grundlagen der Phylogenetischen Systematik. Verlag Dr. Friedrich Pfeil, München.

Wicht, H., Lacalli, T. C. 2005. The nervous system of amphioxus: structure, development, and evolutionary significance. Can. J. Zool. 83, 122-150.

Williams, J. B. 1996. Sessile lifestyle and origin of chordates. N. Z. J. Zool. 23, 111-133.

Wood, T. S. 2015. Chapter 16 - Phyla Ectoprocta and Entoprocta (Bryozoans). In: Thorp, J. H., Rogers, D. C. (Eds.), Thorp and Covich's Freshwater Invertebrates (Fourth Edition). Academic Press, Boston, pp. 327-345.

Zakson-Aiken, M., Gregory, L. M., Shoop, W. L. 1996. Reproductive strategies of the cat flea (Siphonaptera: Pulicidae): parthenogenesis and autogeny? J. Med. Entomol. 33, 395-397.

Zeng, L., Jacobs, M. W., Swalla, B. J. 2006. Coloniality has evolved once in stolidobranch ascidians. Integr. Comp. Biol. 46, 255-268.

Zeng, L., Swalla, B. J. 2005. Molecular phylogeny of the protochordates: chordate evolution. Can. J. Zool. 83, 24-33.

8.2 Supplementary material

Supplementary Table 1: Complete morphological data matrix containing 116 phenotypic characters for 49 tunicate and 5 outgroup species.

Supplementary Table 2: Data matrix used for the combined analysis of morphological and 18S rDNA sequence data. The matrix consists of 32 taxa and 2121 characters.

9 Discussion

Tunicata is a key taxon for studying chordate and vertebrate (=craniate) evolution. This was emphasized by several large-scale molecular phylogenetic analyses which showed that the diverse tunicates — not the more "fish-like" Cephalochordata — probably are the closest living relatives to Craniota (e.g., Delsuc et al. 2006, Edgecombe et al. 2011, Dunn et al. 2014). All the way up from deep sea-dwelling slime eels to the high capacity human brain, the vertebrate central nervous system (CNS) represents a highly elaborated organ system. Although the anatomy of most adult tunicates, i.e. ascidians and the morphology of their CNS are considered to resemble a "simple" invertebrate anatomy and neuroarchitecture, investigating the tunicate CNS might offer new insights into the evolution of this organ system in chordates.

The overall aim of my morphological study was to test homology hypotheses and to discover corresponding structures and character transformations, especially in the understudied salps and adult ascidians. Morphological data are needed as an independent source of a phylogenetic signal, as phylogenies based on molecular sequence alone underlie problems resulting from increased mutation rates in several tunicate species (Wada 1998, Tsagkogeorga et. al 2010). In the present study, new phenotypic characters were coded that have not been studied in a phylogenetic framework before. Diverse methods were applied to collect new morphological data: high-resolution TEM, SEM, and CLSM, light microscopy and virtual 3d reconstructions. As a result, the so far largest data matrix of tunicate phenotypic characters was established that contains 116 characters of 49 tunicate and 5 outgroup species. This matrix covers representatives of 19 tunicate clades that are traditionally assigned "family" rank and comprises members of all major tunicate taxa ("Thaliacea", Appendicularia, "Phlebobranchiata", Aplousobranchiata, and Stolidobranchiata). Thus, it is possible to draw conclusions on the general anatomy and neuroarchitecture of the last common ancestor of Tunicata and to trace evolutionary changes within this diverse taxon. In the following, I will focus on the main findings of the present study and summarily discuss them.

9.1 Serotonin-like immunoreactivity in tunicates

The biogenic amine 5-hydroxytryptamine, which is more commonly known as serotonin, functions as a tissue hormone and neurotransmitter and was detected in many species throughout the animal kingdom (Hay-Schmidt 2000, Schmidt-Rhaesa et al. 2015). Serotonin-like immunoreactivity (serotonin-lir) in tunicates was studied only in some species, and usually in single selected organs (see below). With the present study, data on distribution patterns of serotonin-lir are complemented for various tunicate species, and whole-mount images of distribution patterns are added. While in Salpida, Doliolida, and in one appendicularian species the presence of serotonin-lir cells has been previously demonstrated in the CNS (Stach 2005,

Pennati et al. 2012, Valero-Gracia et al. 2016, chapter **2**, chapter **3**), various studies failed to locate serotonin-lir cells in the brain of adult ascidians, pyrosomes, and most appendicularians (Pennati et al. 2001, Stach 2005, Tiozzo et al. 2009, Valero-Gracia et al. 2016, chapter **2**, chapter **3,** chapter **6**). In the current study serotonin-lir was for the first time also found to be located along the ciliary bands of the branchial basket, i.e. in the peripharyngeal band, the endostyle, and the retropharyngeal band, of ascidians and pyrosomes, where it forms a specific band-like pattern. Serotonin-lir cells are additionally situated in the esophagus of "Thaliacea" and Ascidiacea, but only in Ascidiacea and Salpida serotonin-lir is present in the digestive tracts (Fig. **6**). In three additional species of Appendicularia serotonin-lir was not detectable (Stach 2005, chapter **2**, chapter **6**).

9.1.1 Serotonin-lir cell types

Comparative analysis of serotonin-lir cells in Tunicata reveals that three different types of serotonin-lir cells are present and can be distinguished based on their morphology: elongated serotonin-lir cells (hereafter just called elongated cells), approximately spherical serotonin-lir cells (hereafter called spherical cells), and serotonin-lir neurons. With the exception of Appendicularia, most species investigated possess at least two types of serotonin-lir cells – elongated and spherical cells. Elongated cells are mainly detectable in the esophagus and digestive tract of these animals. Studies of similar cells in cephalochordates (Candiani et al. 2001) and from different vertebrate species (Chiba 1998, Trandaburu and Trandaburu 2007) identified these cells as enterochromaffin cells that are involved in the regulation of feeding. Thus, the elongated cells in tunicates may potentially serve a similar function with serotonin acting as tissue hormone.

Spherical cells were mainly located in the branchial basket, and also — though less in number — in the esophagus and stomach. Serotonin-lir cells with a similar morphology were located in protostomes (e.g., Willows et al. 1997) and deuterostomes (Naruse et al. 2005, Barreiro-Iglesias et al. 2009). It was deduced from functional studies that these cells control ciliary beating (Wada et al. 1997, Doran et al. 2004, König et al. 2009) and mucus secretion (McKenzie et al. 1998). The location of spherical cells in the ciliary bands of the branchial basket, and the esophagus and stomach — that also contain many cilia — may indicate a similar involvement of these cells in the regulation of ciliary beating in tunicates. The endostyle contains many cilia as well, but one of its main functions is to produce the mucus net that covers the branchial basket and traps food particles (MacGinitie 1939). Therefore, the spherical cells situated in the endostyle of tunicates may additionally control mucus secretion.

Serotonin-lir neurons are only detectable in Doliolida, Salpida, the appendicularian species *Oikopleura fusiformis* and most ascidian larvae (Stach 2005, Valero-Gracia et al. 2016, chapter **2**, chapter **3**). The presence of serotonin as a CNS neurotransmitter is widespread among Metazoa. Studies on the major function of serotonin-lir neurons in protostome species

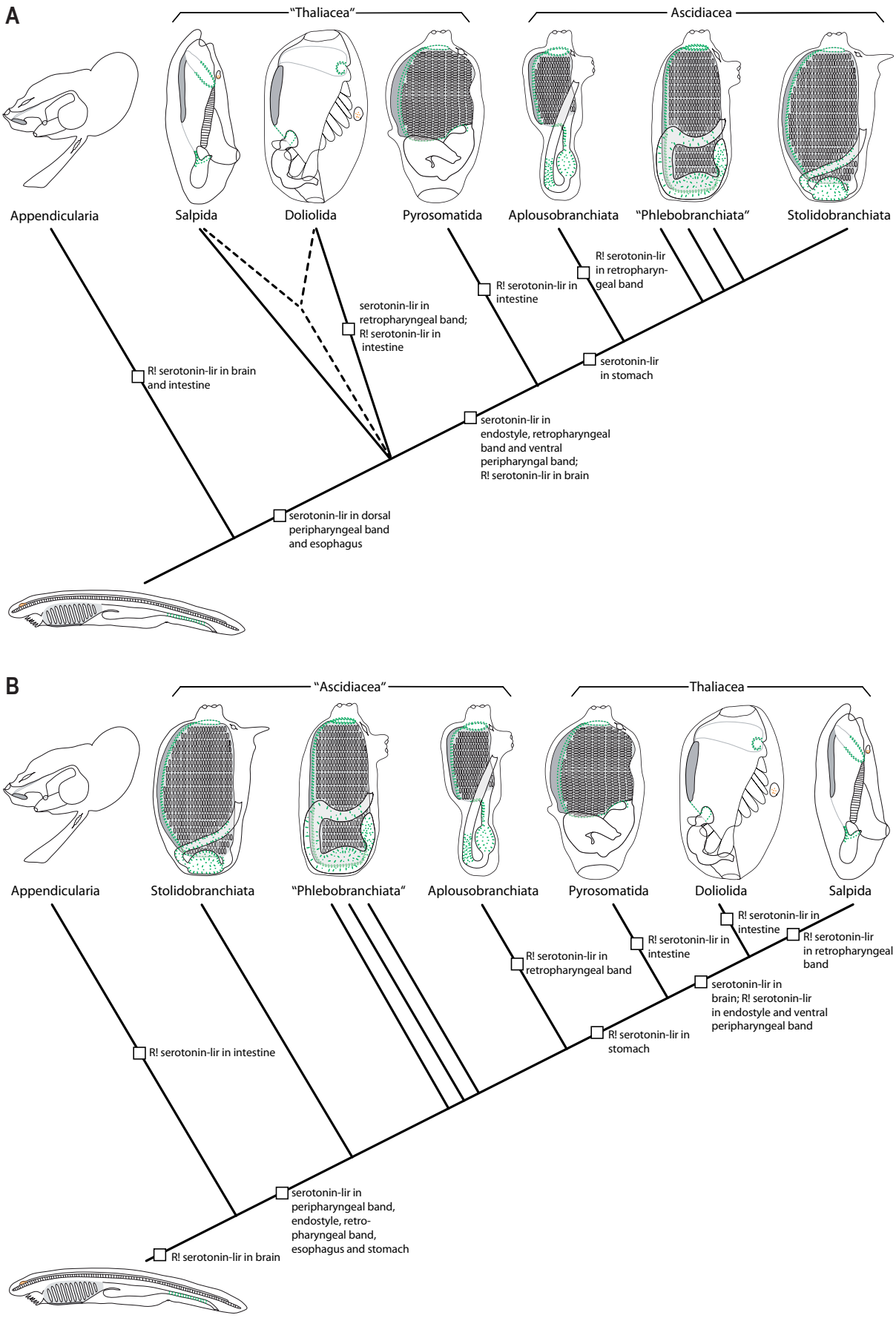

Figure 6: Schematic representations of distribution patterns of serotonin-lir cells plotted on the simplified phylogeny based on morphological data (**A;** see chapter **6**) and combined morphological

and molecular data (**B**; see chapter **6**). The outgroup is represented by Cephalochordata, distribution of serotonin-lir cells is inferred from Candiani et al. (2001) and Holland and Holland (1993). Serotonin-lir neurons are shown in orange, serotonin-lir cells in non-neural tissue are illustrated in green. R! indicates reductions of serotonin-lir cells in certain tissues. When two different evolutionary scenarios were equally parsimonious the one with less homoplasy assumptions was favored.

(Nusbaum and Kristan 1986, Hardaker et al. 2001, Lewis et al. 2011) and vertebrates (e.g., Harris-Warrick and Cohen 1985) demonstrate that these neurons mainly initiate motor activity. In the morphology-based tunicate phylogeny**,** the lack of serotonin-lir neurons in adult ascidians and pyrosomes represents a synapomorphy of the two taxa. Accordingly, a reduction of these neurons must have occured in their stem lineage (chapter **6,** see also Fig. **6A**). This reduction event could be plausibly explained by the sessile lifestyle of postmetamorphic ascidians and the loss of active motility in pyrosomes. Muscles of Pyrosomatida are nearly completely reduced and the colony moves through the water utilizing the jet propulsion of the common colonial opening created only by cilia (Bone 1998). In phylogenetic analyses based on molecular sequence data (Tsagkogeorga et al. 2009, Govindarajan et al. 2011, Delsuc et al. 2018, Kocot et al. 2018) and in my combined analysis of morphological and molecular data (chapter **6)**, the thaliacean taxa form a monophylum that evolved from a sessile ascidian ancestor. Regarding this hypothesis, serotonin-lir neurons in adults must have been regained in the stem lineage of Salpida and Doliolida, probably resulting from the more active lifestyle present in both groups (see also Fig. **6B**).

9.1.2 One species, different distribution patterns

Thaliaceans are characterized by a metagenetic lifecycle, with subsequent morphologically distinct generations – the asexual oozooid and the sexual blastozooid (Delage and Hérouard 1898). More than a century ago, it was already shown that the anatomy of the brain in thaliacean species differs considerably between the consecutive generations (Göppert 1893, Metcalf 1898); yet erroneous and fragmentary descriptions of serotonin-lir extracted in the literature (Stach 2005, Pennati et al. 2012, Valero-Gracia et al. 2016) impeded a detailed insight into this character complex for “Thaliacea”. The present study shows for the first time that — apart from the different brain anatomies — also the respective distribution pattern of serotonin-lir neurons varies between two generations of the same species (see also subchapter **7.2**). As demonstrated by the 3d reconstructed morphologies of the brains of the salp *Thalia democratica* (chapter **4**) and the doliolid *Doliolum nationalis* (chapter **5**), the positions of nerves emanating from the brain considerably differ between oozooid and blastozooid stages. This is consistent with the finding of distinct locations of serotonin-lir neurons in the two consecutive generations (chapter **3**). Besides expanding the knowledge on serotonin-lir in “Thaliacea”, my morphological study also makes an important contribution to the reevaluation of already published hypotheses of serotonin-lir in this tunicate subtaxon.

9.1.3 Serotonin-lir cells in Chordata and evolutionary implications

Comparing the distribution patterns of serotonin-lir cells in tunicates with the ones described in outgroup taxa (Cephalochordata and Craniota) shows that the presence of serotonin-lir neurons is a symplesiomorphic character for Tunicata, Cephalochordata, and Craniota. Two distinct clusters of serotonin-lir neurons are described in larval cephalochordates (Holland and Holland 1993), larval lampreys (Hay-Schmidt 2000) and larval ascidians (Stach 2005). But serotonin-lir was not detected in the endostyle or esophagus of cephalochordates or larval lampreys (Sakharov and Salimova 1980, Holland and Holland 1993, Candiani et al. 2001, Barreiro-Iglesias et al. 2009). For this reason, the presence of serotonin-lir cells in the endostyle and esophagus, as described in the present study for the first time (chapter **2**), should be regarded as evolutionary novelties that evolved within Tunicata. However, depending on which phylogenetic analysis is considered, different time points of the appearance of these two novelties emerge. In the phylogeny of the combined analysis (chapter **6**), serotonin-lir cells in the esophagus as well as in the endostyle evolved in the common stem lineage of "Ascidiacea" and Thaliacea. This hypothesis requires the reduction of serotonin-lir cells in the endostyle in the common stem lineage of Doliolida and Salpida. In contrast, the phylogeny solely based on morphological data, also supports the evolution of serotonin-lir cells in the esophagus in the stem lineage of Ascidiacea and "Thaliacea", but serotonin-lir cells in the endostyle appeared only later in the stem lineage of Pyrosomatida and Ascidiacea (see Fig. **6** for competing hypotheses).

9.1.4 Conclusion

In conclusion, the anatomy of serotonin-lir cells and their distribution patterns in defined tissues of tunicates clearly shows similarities, but also a certain variability between tunicate subtaxa. Therefore, primary homology hypotheses concerning this character complex can be suggested and hence these can be used in a phylogenetic analysis (e.g., Pogue and Mickevich 1990, Wiley and Liebermann 2011, chapter **6**). However, it is clear from the two suggested attempts to reconstruct the evolution of serotonin-lir cells in Tunicata (Fig. **6**) that several homoplasies are necessary to explain the distribution of character states, regardless whether the tunicate phylogeny is inferred solely from morphological or from combined morphological and molecular data (chapter **3**, Fig. **6**).

9.2 The central nervous system of adult tunicates

Most studies on the tunicate CNS were either conducted a long time ago with limited methodological techniques (e.g., Drach 1948, Huus 1956) and/or are limited to certain stages or taxa (e.g., Olsson et al. 1990, Koyama and Kusunoki 1993, Mackie 1995, Burighel et al. 2001). While studies on the nervous system of tunicate model organisms (mainly larvae of *Ciona intestinalis* and *C. robusta*) consistently produce new insights in its composition, development, and functioning (Takamura et al. 2010, Ryan et al. 2018), studies of the adult CNS continue to lag behind (Mackie and Burighel 2005, Manni and Pennati 2016). Especially the CNS of postmetamorphic sessile ascidians and of the planktonic "Thaliacea" has been hitherto neglected, albeit for completely different reasons. The former "tends to be seen as a relatively uninteresting structure" (Mackie and Burighel 2005) that does not seem feature characters of the elaborate vertebrate CNS. The latter is difficult to study as thaliaceans are not easily accessible due to their unpredictable occurrence and their complicated lifecycles (Piette and Lemaire 2015, see review in Manni and Pennati 2016). Therefore, a comparative study with a broad taxon sampling in a rigorous conceptual framework is mandatory in order to elucidate the evolution of the chordate and vertebrate nervous system and to infer the ground pattern of the CNS in tunicates. Although the few existing studies on the adult ascidian CNS indicate considerable morphological variations among different species (Koyama and Kusunoki 1993, Zaniolo et al. 2002, Dahlberg et al. 2009), the ascidian CNS is in general summarized as mainly consisting of a dorsal ganglion (or brain, sensu Richter et al. 2010) divided into a cortex and neuropil. In addition, the ascidian brain is equipped with five main nerves: the paired anterior and posterior nerves and an unpaired ventral visceral nerve. A neural gland is closely associated with this brain, and together, both organs form the neural complex (Burighel and Cloney 1997, Manni and Pennati 2016).

9.2.1 Interspecific variation of neuroarchitecture

In the present study, it was demonstrated that the morphology of the ascidian CNS is species-specific and shows a previously unrecognized interspecific variation in numerous characteristics: the presence, number and position of nerves, the position and extent of the neural gland, the presence of a dorsal strand, and the shape of the dorsal tubercle. When available for a species studied herein, descriptions could be confirmed in their main findings. Further variations at the intraspecific level could be demonstrated to be minor (chapter **5**). Somewhat surprisingly, the neuroanatomy of two relatively closely related species of the taxon Stolidobranchiata, *Molgula manhattensis* and *Botryllus schlosseri,* is substantially different from each other, whereas it can be very similar between more distantly related species which share a similar lifestyle. The latter phenomenon is illustrated, for instance, by the size of the brains, the increased number of nerves, and the shape of the dorsal tubercles in the colonial ascidians like the stolidobranch species *Botryllus schlosseri* and the phlebobranch species *Perophora japonica*.

9.2.2 Evolution of neuronal characters

Some authors suggest homology between the neural gland in tunicates and the circumventricular organ in vertebrates (Ruppert 1990, Deyts et al. 2006, Joly et al. 2007). In contrast, the vast number of authors homologizes the adenohypophysis of vertebrates, Hatschek's pit and groove of cephalochordates and the neural gland of tunicates (Chang et al. 1982, Stach 1996, Burighel et al. 1998, Tsutsui et al. 1998, Gorbman 1999, Kah et al. 2007). In the present study the latter hypothesis was followed (chapter **6**). According to this hypothesis, the presence of a neural gland, gland duct, and dorsal tubercle on the ventral side of the brain was considered as a plesiomorphic condition for tunicates. A shift of the ventral position of the neural gland to the right or dorsal side (as present in Appendicularia and Stolidobranchiata) occurred at least twice independently during tunicate evolution (Fig. **7**). My first idea of a gradual relocation from a ventral position towards a right and then dorsal position of the neural gland within Stolidobranchiata is not supported by a cladistic analysis of morphological data (chapter **6,** Fig. **7A**). Only a single origin is predicted for the evolution of the dorsal strand and the ventral visceral nerve in the tunicate CNS, regardless which of the two presented phylogenetic hypotheses is considered (chapter **6**, Fig. **7**). In the morphology-based phylogeny these two characters originated in the stem lineage of Ascidiacea, while in the combined analysis the ventral visceral nerve and the dorsal strand evolved in the stem lineage of "Ascidiacea" and Thaliacea, to be reduced again in the stem lineage of the latter. This observation is plausible, as in several ascidian species these two characters occur together and compose the dorsal strand plexus. On the other hand, some other ascidian taxa lack one of these two characters (*Aplidium turbinatum* - absent dorsal strand; *Perophora japonica* - absent ventral visceral nerve; see chapter **6**). This indicates that the dorsal strand and the ventral visceral nerve evolved independently.

9.2.3 Special characteristics of thaliacean brains

In my comparative morphological study it was verified that in all examined tunicate species the brain is divided into cortex and neuropil. Just as in the ascidian brain, the discernable division of the thaliacean brain is limited to a cortex and the neuropil. Nevertheless, conspicuous neurite tracts that are detectable with the aid of immunohistological stainings were revealed to be present in all investigated salp species and in the pyrosome *Pyrosoma atlanticum* for the first time. In addition, eyes were solely described in these two taxa (chapter **4**, Göppert 1893, Metcalf 1898, Redikorzew 1905, Neumann 1909) suggesting that neurite tracts in salps and pyrosomes connect optical structures with the main part of the brain. Therefore, the independence of the characters adult eyes and conspicuous neurite tracts has to be questioned. More data regarding the presence of these neurite tracts in other thaliacean species will be necessary to settle this matter.

Eye and brain morphologies in Salpida were found to differ between the sexual and asexual

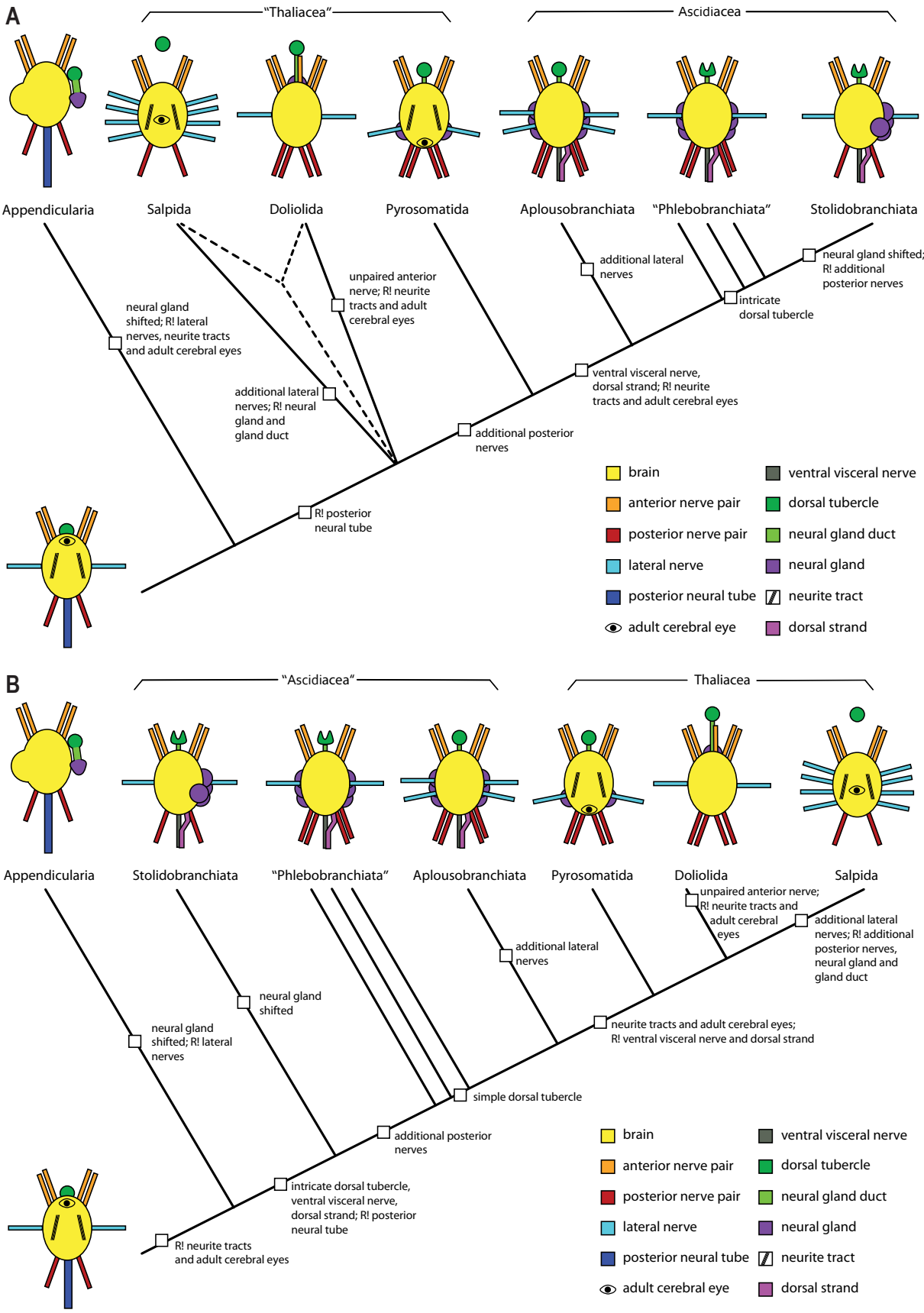

Figure 7: Schematic representations of the neural complex architecture in major tunicate taxa and inferred ancestral state plotted on the simplified phylogeny based on morphological data (**A**) and combined morphological and molecular data (**B**; see also chapter **6** for a better understanding of reconstructed ancestral states). R! indicates reductions of certain characters. When two different

evolutionary scenarios were equally parsimonious the one with less homoplasy assumptions was favored.

generation, the extent and the course of neurite tracts also differ between these two stages within the same salp species (chapter **3** & **4**). Conspicuous neurite tracts detectable with the help of immunohistological stainings are likewise present in the brain of Cephalochordata (Holland and Holland 1993, Lacalli 1996, Candiani et al. 2001) and Petromyzontidae (Nieuwenhuys 1977, Barreiro-Iglesias et al. 2009). Therefore, the presence of these conspicuous neurite tracts can be reconstructed as a plesiomorphic character for "Thaliacea" in the morphology-based phylogeny and might represent a remnant of a more "fish-like" ancestor. However, in this hypothesis it is equally parsimonious to assume that these neurite tracts evolved independently in Pyrosomatida and Salpida (Fig. **7A**). According to the phylogeny based on the combined analysis, the presence of neurite tracts has to be regarded as a homoplasy (Fig **7B**).
Typical features of Salpida are conspicuous motoneurons, additional optical neuropils, brain appendages and a lack of the neural gland and gland duct, although the animals still possess a dorsal tubercle with unknown function. Notably, ultrastructural studies of the dorsal tubercles are still missing (Bone 1998) and there is no definite statement, whether any remnants of the neural gland complex are present in salps.

9.2.4 Tunicate cerebral eyes

Cerebral eyes in tunicates are present in Salpida, Pyrosomatida and most ascidian tadpole larvae. These cerebral eyes are reduced in adult sessile ascidians, allowing for the hypothesis that the possession of eyes is possibly related to the holoplanktonic mode of life. However, eyes are reduced in holoplanktonic Appendicularia and Doliolida as well.
In Salpida eyes do probably not form images, as they feature a wide aperture and relatively few photoreceptor cells; they definitely detect the direction of incident light. The eyes are only composed of photoreceptor cells and shading pigment cells in both salp generations, they are lensless and the membrane that stores photosensitive pigments (opsins) is located on the apical side of the photoreceptor cell, without traces of a cilium, classifying the photoreceptor cells of salps as rhabdomeric (Gorman et al. 1971, chapter **4**). With neurites that are oriented toward the direction of the incoming light, salp eyes belong to the inverse eye type. In most salp species the anatomy of the blastozooid eye is variable at the interspecific level regarding the shape, orientation, and number of eyes and usually possesses multiple simple pigment-cup eyes, while in the oozooid stage a horseshoe-shaped eye is developed, with the opening of the horseshoe pointing anteriorly (chapter **4** and **5**, Göppert 1893, Metcalf 1898, Redikorzew 1905). In the present study different modes of locomotion between the oozooid and blastozooid stage are suggested to be the reason for these unusually different morphologies of the eyes between the two different lifecycle stages. While oozooids have individual control over their movements, blastozooids are aggregated in long chains, with little individual influence on the

direction of movement. Furthermore, a possible explanation why the anatomies of blastozooid eyes are variable among salps might be that the arrangements of blastozooids in the chains differ depending on the species (see Bone 1998). Underwater, light is only perceivable through Snell's window (Lythgoe 1979, Nilsson 1997), so the direction of the incoming light is limited. An aggregated blastozooid has a determined position in a chain which is species-specific and which it cannot change until the chain breaks up. In some species blastozooids are vertically, in some circularly, and in others obliquely horizontally arranged (see Bone 1998). The orientation of the eye which is associated with the position of pigment cells and photoreceptor cells is species-specific and might be correlated with the arrangement of a blastozooid in its chain.
Cephalochordates possess frontal eyes that are positioned in the brain and are composed of photoreceptor cells of the ciliary type (Wicht and Lacalli 2005). These eyes are considered homologous to vertebrate eyes that are also equipped with ciliary photoreceptor cells (Lacalli et al. 1994, Vopalensky et al. 2012). Nevertheless, photoreceptor cells of cephalochordate and vertebrate eyes are obviously not homologous to photoreceptor cells in salps. However, salp eyes show similarities to rhabdomeric photoreceptor cells found in addition to the frontal eyes in cephalochordates, Hesse ocelli and Joseph cells (Lacalli and Stach 2016), but also in enteropneusts (Braun et al. 2015), and echinoids (Ullrich-Lüter et al. 2011). However, the complex rhabdomeric eye with additional neuropils and neurite tracts has to be considered a derived trait within tunicates. As the knowledge on the ultrastructure of pyrosome eyes is only partial and incomplete (Bone 1998), the question whether the special rhabdomeric eyes of salps are an apomorphic trait of this taxon, or evolved more than once within the "Thaliacea" remains unresolved.

9.2.5 Special characteristics of appendicularian brains

As most — especially molecular — phylogenies favor the hypothesis of appendicularians being sister to the rest of tunicates (Govindarajan 2011, Delsuc et al. 2018, Kocot et al. 2018, chapter **6**), studying their nervous system might be particularly promising from a phylogenetic point of view. Among tunicates, Appendicularia have the smallest brains, with only about 70-100 neurons (Olsson 1990, chapter **5**). However, the CNS of the species studied (*Oikopleura dioica*) is more complex than one would expect. Appendicularians possess a larval statolith as an integrated part of the brain, which is still present in adults and most likely constitutes an apomorphy of the taxon. The posterior neural tube is a plesiomorphic trait inherited from the last common chordate ancestor. Also the presence of the neural gland appears to be a plesiomorphic character based on an outgroup comparison, although this organ is greatly reduced with only few cells left. Still, a neural gland duct and dorsal tubercle are developed. Surprisingly, the appendicularian brain lacks neurite tracts, additional neuropils or cerebral eyes as found in the more complex pyrosome and salp brains. Assuming that these characters are linked to a planktonic lifestyle, the presumed traces of a more "fish-like" mode of life in the CNS of appendicularians are at least non-obvious.

9.2.6 Conclusions

The distribution of character states in the two discussed phylogenetic hypotheses (see simplified schematic drawings in Fig. **7** and chapter **6)** indicates a notable degree of homoplasy in several of the neuronal characters studied. The amount of homoplasies suggests, for instance, that the recent anatomies of the neural complexes in different tunicate taxa are probably correlated with life-history strategies. Therefore, some character transformations are linked to certain life styles rather than retained from a common ancestor. Among others, this applies also to the presence and number of lateral nerves (see discussion above for colonial ascidian species). In species without lateral nerves, posterior or anterior nerves adopt the innervation of targeted areas.

All in all, this study improves the availability of detailed neuroanatomical descriptions of adults of 18 tunicate species. Based on the extended data basis, it was possible to trace some neuronal character transformations, and to form primary homology hypotheses of distinct phenotypic neuronal characters (chapter **6**).

9.3 Phylogeny of Tunicata

Within the last two decades molecular techniques made significant progress, enabling researchers to easily and cheaply perform DNA-sequencing and thereby obtain more data on animal genomes in increasingly shorter time periods. In 2006, a large-scale molecular phylogenetic analysis suggested for the first time that the enigmatic Tunicata are closest living relatives to the well-known Craniota (Delsuc et al. 2006) supporting an older hypothesis derived from a cladistic analysis of enigmatic fossils (Jefferies 1986). Since then, several molecular phylogenetic analyses were performed that all supported this idea (e.g., Dunn et al. 2008, 2014, Stach et al. 2010, Edgecombe et al. 2011, Philippe et al. 2011, Delsuc et al. 2018, Kocot et al. 2018). With Tunicata suddenly occupying a phylogenetic key position to understand chordate and vertebrate evolution, attention of many scientists was drawn to the yet unresolved tunicate relationships. This resulted in several molecular phylogenetic analyses that consistently pointed out that the sea-squirts, Ascidiacea, might be a paraphyletic assemblage from which thaliaceans emerged (e.g., Swalla et al. 2000, Tsagkogeorga et al. 2009, Govindarajan et al. 2011). On the other hand, these studies disagreed on the interrelationships of major tunicate taxa (Zeng et al. 2006, Tsagkogeorga et al. 2009, Govindarajan et al. 2011, Delsuc et al. 2018). Although these molecular analyses seemed to provide a solid basis to resolve the relationships of major tunicate clades, some authors pointed out that increased mutation rates impede a phylogenetic analysis of tunicate DNA-sequences (Wada 1998, Tsagkogeorga et al. 2010) and that statistical support values in these published analyses might be unreliable (Stach 2014). For this reason, it is advisable to perform additional phylogenetic analyses with independent non-sequence data to evaluate the potential influence of mutation rates on the resulting phylogenetic hypothesis. An analysis of morphological data might serve as such an additional and independent source

(Wägele 2001). Furthermore, a cladistic analysis of morphological data offers the opportunity to reconstruct character transformations and ground patterns (Hennig 1982).

However, only few studies have hitherto attempted to use a comparative morphological approach to resolve tunicate phylogeny and these studies are limited to selected taxa (Moreno and Rocha 2008) or to selected character complexes (Hawkins et al. 1983, Holland 1992, Rigon et al. 2013). A first study combining 18S rDNA sequences with morphological data was presented by Stach and Turbeville (2002). Yet, including a total of 24 phenotypic characters only, the resolution of interrelationships between major taxa was weak, but potential character transformations were nonetheless deduced from the distribution pattern of phenotypic characters.

The present study substantially increases the amount of analyzed data to 116 phenotypic characters for 49 tunicate species and 5 outgroup taxa (chapter **6**). Two phylogenies were inferred resulting from a parsimony analysis either based solely on morphological data or on a combined data set of 18S rDNA-sequences (kindly provided by Dr. Frédéric Delsuc, Université de Montpellier) and phenotypic characters (chapter **6**). With this setup, the phylogenetic signal hidden in the morphological data could be tested by using different weighting schemes in additional analyses of morphological and molecular data and thereby the contribution of morphological data toward the resulting phylogenetic hypothesis could be evaluated. Herein, I will focus on major findings of the analysis that is solely based on morphological data and highlight the impact of these data on the resolution of tunicate interrelationships.

The morphological phylogenetic analysis resulted in a well resolved strict consensus tree and recovered monophyletic Tunicata with high statistical support (branching pattern shown in Fig. **6A**). Appendicularia forms the sister taxon to all other tunicate taxa which is coherent with the findings of many previous molecular analyses (e.g., Wada 1998, Govindarajan et al. 2011, Delsuc et al. 2018, Kocot et al. 2018). In contrast to these former molecular studies, “Thaliacea” is found paraphyletic with *Pyrosoma atlanticum* more closely related to monophyletic Ascidiacea than to the remaining thaliacean groups Salpida and Doliolida. Moreover, Ascidiacea is found to be monophyletic challenging the previous hypotheses based on molecular data that assume Ascidiacea to be paraphyletic (Delsuc et al. 2018, Kocot et al. 2018). From the three major ascidian taxa (Stolidobranchiata, “Phlebobranchiata”, and Aplousobranchiata), only Stolidobranchiata and Aplousobranchiata were found to be monophyletic in the morphology-based analysis. “Phlebobranchiata” is paraphyletic with Stolidobranchiata nested within “Phlebobranchiata”.

9.3.1 Basal position of Appendicularia

Two competing phylogenetic positions of the taxon Appendicularia are discussed in the tunicate literature. On the one hand, some researchers argue that Appendicularia derived from a sessile ascidian-like ancestor (Ihle 1913, Garstang 1928, Stach and Turbeville 2002). Their seemingly

"simple" morphology is explained by neoteny, as adult appendicularians closely resemble the morphology of an ascidian tadpole larva. Beyond this, the u-shaped appendicularian gut seems to support this hypothesis, because u-shaped intestines are typical of sessile animals and might have been inherited from a sessile ancestor (Williams 1996). On the other hand, the simple morphology of the appendicularian branchial basket, the direct development, and the short generation time are interpreted as being inherited from a free-living, fish-like last common ancestor of tunicates. In this scenario, Appendicularia is advocated as sister taxon to all other tunicate taxa (Wada 1998, Swalla et al. 2000, Zeng et al. 2006, Delsuc et al. 2018, Kocot et al. 2018) — a hypothesis that also finds support in my morphological, and combined analysis. Additional phenotypic characters inferred from the cladistic analysis that additionally support the hypothesis of basal Appendicularia are the presence of the notochord in adults, the absence of an atrial cavity, and in general the free-swimming lifestyle as plesiomorphic characters inherited from the last common ancestor of Chordata.

Notably, there are some phenotypic characters appendicularians share with some ascidian taxa that appear to be more derived rather than inherited from the last common ancestor of tunicates. For instance, the horizontal orientation of the larval tail is also present in Aplousobranchiata and Perophoridae, the reduction of serotonin-lir cells in the brain also occurred in ascidians, the position of the neural gland at the right side of the brain which is likewise present in some stolidobranch species, and lacking eyes in all appendicularian developmental stages as in some molgulid species (Herdman 1891, Garstang 1928, Stach and Turbeville 2002, Stach et al. 2008).

9.3.2 Monophyletic Ascidiacea

Most recent molecular phylogenetic studies position the pelagic thaliaceans within paraphyletic Ascidiacea (e.g., Stach and Turbeville 2002, Tsagkogeorga et al. 2009, Govindarajan et al. 2011). In contrast, Ascidiacea are found to be monophyletic in my morphology-based analysis with three supportive apomorphies: (1) sessile adults, (2) presence of oral tentacles, and (3) longitudinal orientation of stigmata in adults. Although these apomorphies are homoplastic (sessility obviously evolved more than once in animal taxa, velar tentacles are likewise present in cephalochordates and vertebrates, and some ascidians have transversely oriented or spiral stigmata), morphological support for the taxon is high. This is evident from the combined analysis of molecular and morphological data at different weighting schemes. With 2005 18S rDNA-sequence data outnumbering 116 morphological data, Ascidiacea in the combined analysis still emerges as monophyletic, when phenotypic characters are upweighted by a factor of three (see discussion below).

In our analysis (chapter **6**) Stolidobranchiata is placed within paraphyletic "Phlebobranchiata". Therefore, the present phylogenetic hypothesis does not support the monophyly of "Enterogona", a traditionally recognized taxon comprising the monophyletic taxa "Phlebobranchiata" and

Aplousobranchiata (e.g., Perrier 1898, Plough 1978, Kott 1985). Likewise, the monophyly of some lower ascidian taxonomic units was tested, traditionally given the rank "family". The stolidobranch taxon Molgulidae, the phlebobranch taxa Corellidae and Perophoridae, and the aplousobranch taxa Didemnidae and Polyclinidae were recovered monophyletic. On the other hand, the stolidobranch groups "Pyuridae" and "Styelidae", and the phlebobranch group "Ascidiidae" are paraphyletic, while the aplousobranch group "Holozoidae" is even polyphyletic. The monophyly of Diazonidae — traditionally belonging to "Phlebobranchiata" (e.g., Van Name 1945, Lützen 1967) — and of the stolidobranch groups Clavelinidae and Polycitoridae was not tested, as they were covered by only one representative species in the analysis. In traditional taxonomy, *Ciona intestinalis* — one of the main chordate model organisms — is regarded as a member of "Phlebobranchiata", due to morphological characteristics of the branchial basket (Millar 1966, Plough 1978). First doubts regarding the phylogenetic position of Cionidae were put forward by Kott (1990) because of the shared morphology of epicardia and body division with Aplousobranchiata. In the present morphological analysis, no support for the latter hypothesis is found. Instead, "Phlebobranchiata" is paraphyletic and Cionidae is deeply nested in a group of phlebobranch ascidians more closely related to Stolidobranchiata. In this analysis the traditional phlebobranch clade Diazonidae is sister to Aplousobranchiata. Interestingly, also some molecular analyses favor the inclusion of Diazonidae within Aplousobranchiata (Shenkar et al. 2016). Although the statistical support of this node is low, the presence of body division and epicardial budding supports a sister group relationship of Diazonidae and Aplousobranchiata in our morphological analysis (chapter **6**).

9.3.3 Paraphyletic "Thaliacea"

The monophyly of the pelagic thaliaceans — pyrosomes, salps and doliolids — is not only considered in traditional morphological taxonomy (reviewed in Bone 1998) but has been also recovered in modern molecular phylogenetic analyses (reviewed in Lemaire and Piette 2015). In line with monophyletic thaliaceans, the traditional hypothesis assumed the detachment of a colonial, ascidian-like ancestor subsequently evolving into the planktonic thaliaceans (Garstang 1928).

The present phylogeny solely based on morphological data rendered "Thaliacea" paraphyletic turning the idea of Garstang (1928) upside down. Within "Thaliacea" the taxa Salpida and Doliolida are monophyletic with high statistical support; the monophyly of Pyrosomatida could not be tested as only a single representative species was included.

Characters that are usually seen as synapomorphies of all thaliacean groups are, e.g., the position of the excurrent and incurrent openings at opposite ends of the animals and the obligate alternation between sexual and asexual reproduction in consecutive generations (Metcalf 1918, Garstang 1928). The result of the morphological analysis indicates that a metagenetic life-history strategy is a plesiomorphic condition shared by "Thaliacea" and

Ascidiacea, meaning that coloniality is homologous in phlebobranch and aplousobranch ascidians, pyrosomes, doliolids, and salps. Coloniality in Botryllinae, on the other hand, must have evolved independently. It is noteworthy that the position of Pyrosomatida as sister taxon to Ascidiacea has weak statistical support, and that the relation between Doliolida and Salpida is unresolved, although a sister group relationship between Doliolida and Salpida is supported in the bootstrap analysis with a bootstrap value of 83%. The group consisting of Pyrosomatida and Ascidiacea is supported by three apomorphies: the sexually mature form is colonial, the presence of longitudinal blood vessels, and the location of serotonin-lir cells in the endostyle — the latter representing a conflict-free apomorphy. A reasonable hypothesis for the evolution of sessile ascidians from an ancestor with a planktonic lifestyle might be a scenario where a colony of a pyrosome-like ancestor settled and evolved into colonial ascidians. This is essentially a reversal of the scenario proposed by Monniot and Monniot (1966, see discussion below).

9.3.4 Phylogenetic signal in morphological data

In order to evaluate the phylogenetic signal present in morphological data, a combined analysis of morphological and molecular 18S rDNA-sequence data was performed. Different weighting schemes were tested, to gauge the contribution of morphological data to the resulting hypothesis that indeed was found to have an enormous impact on the outcome of the phylogenetic analysis. The number of positions in the 18S rDNA alignment outnumbered the amount of phenotypic characters approximately by 20:1. Paraphyletic ascidians and monophyletic thaliaceans supported the molecular partition while monophyletic Ascidiacea and paraphyletic “Thaliacea” supported the morphological partition. At a weighting scheme of 3:1 the molecular data were in an inferior position regarding the morphological data, so that monophyletic Ascidiacea and paraphyletic “Thaliacea” were reconstructed in this analysis.

18S rDNA sequence data were kindly provided by Dr. Frédéric Delsuc and a resulting phylogeny only based on these molecular data has already been published by Tsagkogeorga et al. (2009). Herein, a sister group relation of monophyletic Stolidobranchiata and monophyletic Appendicularia is opposed by an unresolved grouping of paraphyletic phlebobranchs, monophyletic aplousobranchs and monophyletic thaliaceans. A combination of these data with morphological data resulted in a better resolution of the interrelationships of tunicate taxa and even changed the phylogenetic position of Appendicularia and Stolidobranchiata (chapter **6**). The combined phylogeny with equally weighted characters reconstructed monophyletic Appendicularia as basal taxon and sister taxon to the rest of Tunicata, monophyletic thaliaceans, and paraphyletic ascidians, a result that is identical to the phylogenetic hypotheses based only on molecular data in published studies. Recently, two phylogenomic studies on tunicate evolution and phylogeny were published (Delsuc et al. 2018, Kocot et al. 2018, see Fig. **4B** in chapter **1**). Comparison with the results from my combined analysis reveals only a minor disagreement in

the position of Aplousobranchiata. In the current phylogeny Aplousobranchiata is sister taxon to “Thaliacea”, whereas it mostly groups within “Phlebobranchiata” in the aforementioned phylogenomic studies. Besides, in one consensus tree in the analysis of Kocot and coworkers (2018) aplousobranchs and phlebobranchs form monophyletic sister taxa.

9.3.5 Character transformations and evolutionary implications

One of the most fascinating outcomes of evolutionary research is not the establishment of a new phylogenetic hypothesis for a taxon, but rather the tracing of characters and the uncovering of how individual characters transformed morphologies within the investigated clade. Characters that bear phylogenetic information should be scorable in a data matrix (Kitching et al. 1998). Because two taxonomic units usually have distinct morphologies, transformational homology is the general case (Scholtz 2005), which complicates the detection of homologies. Therefore, a cladistic analysis of morphological data in a conceptual framework offers the opportunity to reveal character transformations and to evaluate primary homology hypotheses (sensu Pinna 1991). In the present analysis, a number of – in part newly hypothesized – apomorphies can be identified for the taxon Tunicata: a tunic, a pyloric gland, heart beat reversal, a u-shaped gastrointestinal tract, a larval tunic, a larval statocyte, and a brain that is divided into cortex and neuropil. In the following, selected characters will be discussed in more detail.

According to my morphology-based study, a sessile lifestyle originated in the stem-lineage of Ascidiacea, while Tunicata derived from a planktonic ancestor. With Appendicularia as sister group to the remaining tunicate taxa, our data support the hypothesis that the last common ancestor of tunicates was free-swimming with a rather “fish-like” appearance (chapter **6**). Therefore, morphological data imply that sessility, as present in adult ascidians, is a derived character within Tunicata. Pyrosomatida are the presumed sister taxon of Ascidiacea. It is reasonable to assume that a colony of pyrosomes settled and evolved into colonial ascidians. A benthic pyrosome was described Monniot and Monniot (1966) but this species description is doubtful, because it was pointed out that the collected single colony might have entered the net on its way toward the water surface and that the species should be classified as *Pyrosoma atlanticum* (Van Soest 1981). On the other hand, a free-swimming ancestor might have settled utilizing a stalk to adhere to the sea ground resembling the present-day colonial aplousobranch *Sycozoa.* Some authors proposed an ancestor similar to the aplousobranch *Distaplia*, because of a similar mode of budding (Uljanin 1884, Brien 1928). However, the conclusion of a free-swimming pyrosome-like ancestor of Ascidiacea invokes some inconsistencies that are difficult to reconcile with some phenotypic characters and formerly accepted hypotheses. One of these characters is the u-shaped gut present in all tunicates (reviewed in Huus 1956). This character is typical of sessile animals throughout the animal kingdom, while planktonic animals usually have a straight gut (Williams 1996, Cohen et al. 2003). If tunicates derived from a planktonic ancestor, the evolution of a u-shaped gut occurred in the stem-lineage

of Tunicata and was present in a planktonic ancestor. This scenario remains difficult to understand. On the other hand, Appendicularia are considered one of the prime examples for neoteny, due to the acceleration of their development and early onset of sexual maturity (Garstang 1928, see reviews in: Gee 1996, Lacalli 2005, Stach et al. 2008). The outcome of the present study suggests a basal position of Appendicularia within Tunicata. That indicates that a tadpole-like larva is plesiomorphic for Tunicata and evolved in the stem-lineage of Chordata. According to this hypothesis, a tadpole larva equipped with a statocyte evolved in the stem-lineage of Tunicata. The reduction of the tadpole larva in Salpida and Pyrosomatida then has to be regarded as homoplastic, because some doliolids retain a tadpole stage (e.g., reviews in Godeaux 1998, Piette and Lemaire 2015).

The results from my morphological study agree with molecular phylogenetic analyses in indicating that coloniality evolved at least twice within Tunicata (Wada et al. 1992, Swalla et al. 2000, Zeng et al. 2006): first, in the common stem-lineage of "Thaliacea" and Ascidiacea and second in the stem-lineage of Botryllinae. However, this also means that coloniality in "Thaliacea", colonial phlebobranchs, and Aplousobranchiata is homologous. This coincides with the idea that Aplousobranchiata, with their simple morphology of the branchial basket, are a basally diverging group within Ascidiacea (Lahille 1890, Stach 2009).

9.4 Concluding remarks

This study significantly improves the availability of comparative data on serotonin-lir, neuroanatomy, and general morphology for many tunicate species by using modern morphological methods. The neural complexes of 18 tunicate species representing the five major tunicate taxa were comparatively examined, whereby also different ontogenetic stages like the morphologically different generations of the metagenetic Salpida and Doliolida were taken into account. As presented in here, morphological data are collected in a conceptual framework and are now accessible for 49 tunicate species. For a broad taxon and character sampling, new phylogenetically informative characters were compiled including phenotypic characters traditionally used in tunicate taxonomy, and complemented with data already available in the scientific literature. The established character matrix contains primary homology hypotheses for 116 phenotypic characters for 49 tunicate species and five outgroup species (see chapter **6**) — the largest data matrix published in tunicate literature so far.

A cladistic analysis of this comprehensive morphological dataset yielded a new phylogenetic hypothesis of internal relationships of Tunicata. Character transformations were uncovered based on the new phylogeny and homology hypotheses were tested. As some questions could not be answered and many more questions were raised by the outcome of the present study, the phylogenies presented are not suggested to be the final version of the tunicate phylogeny, but show that morphological data clearly can contribute phylogenetic information and therefore should not be neglected in studies on the evolution of Tunicata.

10 Abbreviations

CLSM: confocal laser scanning microscopy

CNS: central nervous system

prc: photoreceptor cell

pigc: pigment cell

SEM: scanning electron microscopy

serotonin-lir: serotonin-like immunoreactivity

serotonin-lir cell: serotonin-like immunoreactive cell

TEM: transmission electron microscopy

11 References

Alldredge, A. (2005). The contribution of discarded appendicularian houses to the flux of particulate organic carbon from oceanic surface waters. In: G. Gorsky, M. J. Youngbluth, D. Deibel (eds.), Response of marine ecosystems to global change: Ecological impact of appendicularians. Paris: Archives contemporaines, pp. 315-332.

Ärnbäck, A. (1923). Northern and Arctic invertebrates in the collection of the Swedish State Museum (Riksmuseum). IX Tunicata. 2. Botryllidae: Reproductive organs of *Metrocarpa* (n. gen.) *leachi* Savigny and *Botryllus schlosseri* Pallas. Stockholm: Kungliga Svenska Vetenskaps-akademiens Handlingar, 63(9), 25.

Ax, P. (2001). Das System der Metazoa III: Ein Lehrbuch der phylogenetischen Systematik. Heidelberg: Spektrum Akademischer Verlag.

Balfour, F. M. (1881). A treatise on comparative embryology. Vol. 2, London: Macmillan.

Barreiro-Iglesias, A., Aldegunde, M., Anadón, R., & Rodicio, M. C. (2009). Extensive presence of serotonergic cells and fibers in the peripheral nervous system of lampreys. The Journal of Comparative Neurology, 512(4), 478-499.

Barrington, E. J. W., & Thorpe, A. (1965). An autoradiographic study of the binding of iodine 125 in the endostyle and pharynx of the ascidian, *Ciona intestinalis* L. General and Comparative Endocrinology, 5(3), 373-385.

Berrill, N. J. (1936). II - Studies in Tunicate development. Part V - The evolution and classification of Ascidians. Philosophical Transactions of the Royal Society of London. Series B, Biological Sciences, 226(530), 43-70.

Berrill, N. J. (1947). The development and growth of *Ciona*. Journal of the Marine Biological Association of the United Kingdom, 26(4), 616-625.

Berrill, N. J. (1950). The Tunicata – with an account of the British species. London: The Ray Society.

Biggs, D. C. (1977). Respiration and ammonium excretion by open ocean gelatinous zooplankton. Limnology and Oceanography, 22(1), 108-117.

Bone, Q. (1998). The biology of pelagic tunicates. Oxford, New York, Tokyo: Oxford University Press.

Braun, K., Kaul-Strehlow, S., Ullrich-Lüter, E., & Stach, T. (2015). Structure and ultrastructure of eyes of tornaria larvae of *Glossobalanus marginatus*. Organisms Diversity & Evolution, 15(2), 423-428.

Brenneis, G., Ungerer, P., & Scholtz, G. (2008). The chelifores of sea spiders (Arthropoda, Pycnogonida) are the appendages of the deutocerebral segment. Evolution & Development, 10(6), 717-724.

Brien, P. (1928). Contribution à l'étude de l'embryogénèse et de la blastogénèse des salpes. Recueil de l'Institut Zoologique Torley-Rousseau, 2, 6-98.

Brien, P. (1948). Embranchement des Tuniciers. In: P. P. Grasse (ed.), Morphologie et reproduction. Paris: Traité de Zoologie.

Brooks, W. K. (1893). The genus Salpa. Memoirs from the Biological Laboratory of the Johns Hopkins University II. Baltimore: The Johns Hopkins Press.

Burighel, P., & Cloney, R. (1997). Urochordata: Ascidiacea. In: F. W. Harrison, E. E. Ruppert (eds.), Microscopic Anatomy in Invertebrates, Vol. 15, Hemichordata, Chaetognatha, and the invertebrate chordates. New York: Wiley-Liss.

Burighel, P., Lane, N. J., Zaniolo, G., & Manni, L. (1998). Neurogenic role of the neural gland in the development of the ascidian, *Botryllus schlosseri* (Tunicata, Urochordata). Journal of Comparative Neurology, 394(2), 230-241.

Burighel, P., Sorrentino, M., Zaniolo, G., Thorndyke, M. C., & Manni, L. (2001). The peripheral nervous system of an ascidian, *Botryllus schlosseri*, as revealed by cholinesterase activity. Invertebrate Biology, 120(2), 185-198.

Caicci, F., Zaniolo, G., Burighel, P., Degasperi, V., Gasparini, F., & Manni, L. (2010). Differentiation of papillae and rostral sensory neurons in the larva of the ascidian *Botryllus schlosseri* (Tunicata). Journal of Comparative Neurology, 518(4), 547-566.

Cameron, C. B., Garey, J. R., & Swalla, B. J. (2000). Evolution of the chordate body plan: New insights from phylogenetic analyses of deuterostome phyla. Proceedings of the National Academy of Sciences of the United States of America, 97(9), 4469-4474.

Candiani, S., Augello, A., Oliveri, D., Passalacqua, M., Pennati, R., De Bernardi, F., & Pestarino, M. (2001). Immunocytochemical localization of serotonin in embryos, larvae and adults of the lancelet, *Branchiostoma floridae*. The Histochemical Journal, 33(7), 413-420.

Cañestro, C., Bassham, S., & Postlethwait, J. (2005). Development of the central nervous system in the larvacean *Oikopleura dioica* and the evolution of the chordate brain. Developmental Biology, 285(2), 298-315.

Chamisso, A. V. (1819). De animalibus quibusdam e classe Vermium Linnaeana in circumnavigatione terrae. Fasciculus primus. De Salpa. Berlin:Dümmler.

Chang, C. Y., Chu, Y., & Chen, D. (1982). Immunocytochemical demonstrations of luteinizing hormone (LH) in Hatschek's pit of amphioxus (*Branchiostoma belcheri* Gray). Kexue Tongbao, 27, 1233-1234.

Chen, J. Y., Huang, D. Y., Peng, Q. Q., Chi, H. M., Wang, X. Q., & Feng, M. (2003). The first tunicate from the Early Cambrian of South China. Proceedings of the National Academy of Sciences of the United States of America, 100(14), 8314-8318.

Chiba, A. (1998). Ontogeny of serotonin-immunoreactive cells in the gut epithelium of the cloudy dogfish, *Scyliorhinus torazame*, with reference to coexistence of serotonin and neuropeptide Y. General and Comparative Endocrinology, 111(3), 290-298.

Cohen, B. L., Holmer, L. E., & Lüter, C. (2003). The brachiopod fold: A neglected body plan hypothesis. Palaeontology, 46(1), 59-65.

Cuvier, G. (1840). Animal Kingdom: Arranged according to its organization, forming the basis for a natural history of animals, and introduction to comparative anatomy. London: Holborn Hill.

Dahlberg, C., Auger, H., Dupont, S., Saakura, Y., Thorndyke, M. C., & Joly, J.-S. (2009). Refining the *Ciona intestinalis* model of central nervous system regeneration. PLoS One, 4(2), e4458-e4458.

Delage, Y., & Hérouard, E. (1898). Les procordés. In: Schleicher Frères (eds.), Traité de Zoologie Concrète, T.8. Paris: Masson.

Delsuc, F., Brinkmann, H., Chourrout, D., & Philippe, H. (2006). Tunicates and not cephalochordates are the closest living relatives of vertebrates. Nature, 439(7079), 965-968.

Delsuc, F., Philippe, H., Tsagkogeorga, G., Simion, P., Tilak, M.-K., Turon, X., López-Legentil, S., Piette, J., Lemaire, P., Douzery, E. J. P. (2018). A phylogenomic framework and timescale for comparative studies of tunicates. BMC Biology, 16(1), 39.

Delsuc, F., Tsagkogeorga, G., Lartillot, N., & Philippe, H. (2008). Additional molecular support for the new chordate phylogeny. Genesis, 46, 592-604.

Deyts, C., Casane, D., Vernier, P., Bourrat, F., & Joly, J. S. (2006). Morphological and gene expression similarities suggest that the ascidian neural gland may be osmoregulatory and homologous to vertebrate peri-ventricular organs. European Journal of Neuroscience, 24(8), 2299-2308.

Dilly, N. (1964). Studies on the receptors in the cerebral vesicle of the ascidian tadpole, 2. The ocellus. Quarterly Journal of Microscopical Science, s3-105(69), 13-20.

Doran, S. A., Koss, R., Tran, C. H., Christopher, K. J., Gallin, W. J., & Goldberg, J. I. (2004). Effect of serotonin on ciliary beating and intracellular calcium concentration in identified populations of embryonic ciliary cells. Journal of Experimental Biology, 207(8), 1415-1429.

Drach, P. (1948). Embranchement des Céphalochordés. In: P. P. Grassé (ed.), Traité de zoologie, vol. 11. Paris: Masson & Cic, pp. 931-1037.

Dunn, A. D. (1974). Ultrastructural autoradiography and cytochemistry of the iodine-binding cells in the ascidian endostyle. Journal of Experimental Zoology, 188(1), 103-123.

Dunn, C. W., Giribet, G., Edgecombe, G. D., & Hejnol, A. (2014). Animal phylogeny and its evolutionary implications. Annual Review of Ecology, Evolution, and Systematics, 45(1), 371-395.

Dunn, C. W., Hejnol, A., Matus, D. Q., Pang, K., Browne, W. E., Smith, S. A., Seaver, E., Rouse, G. W., Obst, M., Edgecombe, G. D., Sorensen, M. V., Haddock, S. H. D., Schmidt-Rhaesa, A., Okusu, A., Kristensen, R. M., Wheeler, W. C., Martindale, M. Q., & Giribet, G. (2008). Broad phylogenomic sampling improves resolution of the animal tree of life. Nature, 452(7188), 745-749.

Eakin, R. M., & Kuda, A. (1970). Ultrastructure of sensory receptors in ascidian tadpoles. Zeitschrift für Zellforschung und Mikroskopische Anatomie, 112(3), 287-312.

Edgecombe, G. D., Giribet, G., Dunn, C. W., Hejnol, A., Kristensen, R. M., Neves, R. C., Rouse, G. W., Worsaae, K., & Sørensen, M. V. (2011). Higher-level metazoan relationships: Recent progress and remaining questions. Organisms Diversity & Evolution, 11(2), 151-172.

Fenaux, R. (1998). Anatomy and functional morphology of the Appendicularia. In: Q. Bone (ed.), The biology of pelagic tunicates. Oxford, New York, Tokyo: Oxford University Press, pp. 25-34.

Fritzsch, B., Sonntag, R., Dubuc, R., Ohta, Y., & Grillner, S. (1990). Organization of the six motor nuclei innervating the ocular muscles in lamprey. The Journal of Comparative Neurology, 294(4), 491-506.

Garstang, W. (1928). The morphology of the Tunicata, and its bearings on the phylogeny of the Chordata. Quarterly Journal of Microscopical Science, s2-72(285), 51-187.

Gee, H. (1996). Before the backbone. London, Weinheim, New York, Tokyo, Victoria, Madras: Chapman & Hall.

Georges, D. (1985). Presence of cells resembling serotonergic elements in four species of tunicates. Cell and Tissue Research, 242(2), 341-348.

Gilland, E., & Baker, R. (2005). Evolutionary patterns of cranial nerve efferent nuclei in vertebrates. Brain, Behavior and Evolution, 66(4), 234-254.

Gilland, E., & Baker, R. (2005). Evolutionary patterns of cranial nerve efferent nuclei in vertebrates. Brain, Behavior and Evolution, 66(4), 234-254.

Godeaux, J. (1998). The relationships and systematics of the Thaliacea, with keys for identification. In: Q. Bone (ed.), The biology of pelagic tunicates. Oxford, New York, Tokyo: Oxford University Press, pp. 273–294.

Godeaux, J. (2003). History and revised classification of the order Cyclomyaria (Tunicata, Thaliacea, Doliolida). Bulletin of the Royal Belgian Institute of Natural Sciences - Biology, 73, 191–222.

Godeaux, J. E. A., Bone, Q., & Braconnot, J. C. (1998). Anatomy of Thaliacea. In: Q. Bone (ed.), The biology of pelagic tunicates. Oxford, New York, Tokyo: Oxford University Press, pp. 1-24.

Göppert, E. (1893). Untersuchungen über das Sehorgan der Salpen. In: C. Gegenbaur (ed.), Morphologisches Jahrbuch – Eine Zeitschrift für Anatomie und Entwicklungsgeschichte, Band 19, Heft 3. Leipzig: Verlag von Wilhelm Engelmann, pp. 250-294.

Gorbman, A. (1999). Brain – Hatschek's pit relationships in amphioxus species. Acta Zoologica, 80(4), 301-305.

Gorman, A. L. F., McReynolds, J.S., & Barnes S.N. (1971). Photoreceptors in primitive chordates: Fine structure, hyperpolarizing receptor potentials, and evolution. Science, 172(3987), 1052-1054.

Govindarajan, A. F., Bucklin, A., & Madin, L. P. (2011). A molecular phylogeny of the Thaliacea. Journal of Plankton Research, 33(6), 843-853.

Groppelli, S., Pennati, R., Scarì, G., Sotgia, C., & De Bernardi, F. (2003). Observations on the settlement of *Phallusia mammillata* larvae: Effects of different lithological substrata. Italian Journal of Zoology, 70(4), 321-326.

Hardaker, L. A., Singer, E., Kerr, R., Zhou, G., & Schafer, W. R. (2001). Serotonin modulates locomotory behavior and coordinates egg-laying and movement in *Caenorhabditis elegans*. Journal of Neurobiology, 49(4), 303-313.

Harris-Warrick, R. M., & Cohen, A. H. (1985) Serotonin modulates the central pattern generator for locomotion in the isolated lamprey spinal cord. Journal of Experimental Biology, 116, 27-46.

Hawkins, C. J., Kott, P., Parry, D. L., Swinehart, J. H. (1983). Vanadium content and oxidation state related to ascidan phylogeny. Comparative Biochemistry and Physiology, 76B, 555-558.

Hay-Schmidt, A. (2000). The evolution of the serotonergic nervous system. Proceedings of the Royal Society of London B: Biological Sciences, 267(1448), 1071-1079.

Hennig, W. (1982). Phylogenetische Systematik. Berlin, Hamburg: Verlag Paul Parey.

Herdman, W. A. (1891). A revised classification of the Tunicata, with definitions of the orders, suborders, families, subfamilies, and genera, and analytical keys to the species. Zoological Journal of the Linnean Society, 23, 558-652.

Holland, L. Z. (1992). The phylogenetic significance of tunicate sperm morphology. In: B. Baccetti (ed.), 6th International Congress on Spermatology. Siena: Raven Press.

Holland, N. D., & Holland, L. Z. (1993). Serotonin-containing cells in the nervous system and other tissues during ontogeny of a lancelet, *Branchiostoma floridae*. Acta Zoologica, 74(3), 195-204.

Holmberg, K. (1982). The ciliated brain duct of *Oikopleura dioica* (Tunicata, Appendicularia). Acta Zoologica, 63(2), 101-109.

Holmberg, K. (1984). A transmission electron microscopic investigation of the sensory vesicle in the brain of *Oikopleura dioica* (Appendicularia). Zoomorphology, 104(5), 298-303.

Huus, J. (1956). Zweite und letzte Unterklasse der Acopa: Ascidiacea = Tethyoideae = Seescheiden. In: T. Krumbach (ed.), Handbuch der Zoologie. Berlin: Walter de Gruyter & Co, pp. 545-692.

Huxley, T. H. (1851). Remarks upon the Appendicularia and *Doliolum*, two genera of the Tunicata. Philosophical Transactions of the Royal Society of London, 141, 595-605.

Huxley, T. H. (1860). XVI. On the anatomy and development of *Pyrosoma*. Transactions of the Linnean Society of London, 23(1), 193-250.

Ihle, J.E.W. (1913). Die Appendicularien. In: J.W. Spengel (ed.), Ergebnisse und Fortschritte der Zoologie, Dritter Band. Jena: Verlag von Gustav Fischer, pp. 463-534.

Ihle, J. E. W. (1956). Dritte und letzte Ordnung der Thaliacea: Desmomyaria. In: T. Krumbach (ed.), Handbuch der Zoologie, Fünfter Band, Zweite Hälfte. Berlin: Walter de Gruyter, pp. 401–544.

Imai, J. H., & Meinertzhagen, I. A. (2007). Neurons of the ascidian larval nervous system in *Ciona intestinalis*: I. Central nervous system. Journal of Comparative Neurology, 501(3), 316-334.

Jacobson, C.-O. (1962). Cell migration in the neural plate and the process of neurulation in the axolotl larva. Zoologiska Bidrag Fran Uppsala, 35, 433-449.

Jefferies, R. P. S. (1986). The ancestry of the vertebrates. London: Cambridge University Press.

Joly, J.-S., Osório, J., Alunni, A., Auger, H., Kano, S., & Rétaux, S. (2007). Windows of the brain: Towards a developmental biology of circumventricular and other neurohemal organs. Seminars in Cell & Developmental Biology, 18(4), 512-524.

Jørgensen, C. B. (1952). On the relation between water transport and food requirements in some marine filter feeding invertebrates. The Biological Bulletin, 103(3), 356-363.

Kah, O., Lethimonier, C., Somoza, G., Guilgur, L. G., Vaillant, C., & Lareyre, J. J. (2007). GnRH and GnRH receptors in metazoa: A historical, comparative, and evolutive perspective. General and Comparative Endocrinology, 153(1), 346-364.

Katz, M. J. (1983). Comparative anatomy of the tunicate tadpole, *Ciona intestinalis*. The Biological Bulletin, 164(1), 1-27.

Kimura, S., Ohshima, C., Hirose, E., Nishikawa, J., & Itoh, T. (2001). Cellulose in the house of the appendicularian *Oikopleura rufescens*. Protoplasma, 216(1), 71.

Kitching, I. J., Forey, P. L., Williams, D., & Humphries, C. (1998). Cladistics: The theory and practice of parsimony analysis. Oxford, New York, Tokyo: Oxford University Press.

Kocot, K. M., Tassia, M. G., Halanych, K. M., & Swalla, B. J. (2018). Phylogenomics offers resolution of major tunicate relationships. Molecular Phylogenetics and Evolution, 121, 166-173.

König, P., Krain, B., Krasteva, G., & Kummer, W. (2009). Serotonin increases cilia-driven particle transport via an acetylcholine-independent pathway in the mouse trachea. PLoS One, 4(3), e4938.

Körner, W. F. (1952). Untersuchungen über die Gehäusebildung bei Appendicularien (*Oikopleura dioica* Fol). Zeitschrift für Morphologie und Ökologie der Tiere, 41(1), 1-53.

Kott, P. (1985). The Australian Ascidiacea. Part 1, Phlebobranchia and Stolidobranchia. Memoirs of the Queensland Museum, 23. Brisbane: Queensland Museum.

Kott, P. (1990). The Australian Ascidiacea. Part 2, Aplousobranchia (1). Memoirs of the Queensland Museum, 29. Brisbane: Queensland Museum.

Kowalevsky, A. (1866). Entwicklungsgeschichte der einfachen Ascidien. Mémoires de l'Académie Impériale des Sciences de St. Pétersbourg VIIe Série, Tome X (15), pp. 1-19.

Koyama, H. (2002). The dorsal strand of *Polyandrocarpa misakiensis* (Protochordata: Ascidiacea): A light and electron microscopic study. Acta Zoologica, 83(3), 231-243.

Koyama, H., & Kusunoki, T. (1993). Organization of the cerebral ganglion of the colonial ascidian *Polyandrocarpa misakiensis*. The Journal of Comparative Neurology, 338(4), 549-559.

Krieger, J., Sombke, A., Seefluth, F., Kenning, M., Hansson, B. S., & Harzsch, S. (2012). Comparative brain architecture of the European shore crab *Carcinus maenas* (Brachyura) and the common hermit crab *Pagurus bernhardus* (Anomura) with notes on other marine hermit crabs. Cell and Tissue Research, 348, 47-69.

Krohn A (1846) Observations sur la génération et le développement des Biphores (Salpa). Annales des Sciences naturelles. Troisième série Zoologie 6, 110–132.

Kusakabe, T., & Tsuda, M. (2007). Photoreceptive systems in ascidians. Photochemistry and Photobiology, 83(2), 248-252.

Lacalli, T. C. (1996). Frontal eye circuitry, rostral sensory pathways and brain organization in amphioxus larvae: Evidence from 3D reconstructions. Philosophical Transactions of the Royal Society of London. Series B: Biological Sciences, 351(1337), 243-263.

Lacalli, T. C. (1999). Tunicate tails, stolons, and the origin of the vertebrate trunk. Biological Reviews, 74(2), 177-198.

Lacalli, T. C. (2005). Protochordate body plan and the evolutionary role of larvae: Old controversies resolved? Canadian Journal of Zoology, 83, 216-224.

Lacalli, T. C., & Holland, L. Z. (1998). The developing dorsal ganglion of the salp *Thalia democratica*, and the nature of the ancestral chordate brain. Philosophical Transactions of the Royal Society of London B: Biological Sciences, 353(1378), 1943-1967.

Lacalli, T. C., Holland, N. D., & West, J. E. (1994). Landmarks in the anterior central nervous system of amphioxus larvae. Philosophical Transactions of the Royal Society of London. Series B: Biological Sciences, 344(1308), 165-185.

Lacalli, T. C., Stach, T. (2016). Acrania (Cephalochordata). In: A. Schmidt-Rhaesa, S. Harzsch, G. Purschke (eds.), Structure & evolution of invertebrate nervous systems. Oxford, New York, Tokyo: Oxford University Press, pp. 719-728.

Lahille, M. F. (1886). Sur la classification des Tuniciers. Comptes rendus de l'Académie des sciences Paris, 102, 1573-1575.

Lahille, M. F. (1890). Recherches sur les tuniciers des côtes de France. Tulouse: Imprimerie Lagarde et Sebille.

Lamarck, J. B. (1816). Histoire naturelle des animaux sans vertèbres, Tome III, Les Tuniciers. Paris: Verdier, pp. 80-130.

Lambert, G. (2005). Ecology and natural history of the protochordates. Canadian Journal of Zoology, 83(1), 34-50.

Lemaire, P., & Piette, J. (2015). Tunicates: Exploring the sea shores and roaming the open ocean. A tribute to Thomas Huxley. Open Biology, 5(6).

Lewis, S. L., Lyons, D. E., Meekins, T. L., & Newcomb, J. M. (2011). Serotonin influences locomotion in the nudibranch mollusc *Melibe leonina*. The Biological Bulletin, 220(3), 155–160.

Linnaeus, C. (1758). Systema naturæ per regna tria naturæ, secundum classes, ordines, genera, species, cum characteribus, differentiis, synonymis, locis. Tomus I, 10, Holmiæ, Laurentii Salvii 1-4, 1-824.

Loesel, R. (2011). Neurophylogeny: Retracing early metazoan brain evolution. In P. Pontarotti (ed.), Evolutionary Biology – Concepts, Biodiversity, Macroevolution and Genome Evolution. Berlin, Heidelberg: Springer Berlin Heidelberg, pp. 169-191.

Lützen, J.G. (1967). Sækdyr (Tunicata). Danmarks Fauna, 75.

Lythgoe, J. N. (1979). The ecology of vision. Oxford: Clarendon Press.

MacGinitie, G. E. (1939). The method of feeding of tunicates. The Biological Bulletin, 77(3), 443-447.

Mackie, G. O. (1995). On the 'visceral nervous system' of *Ciona*. Journal of the Marine Biological Association of the United Kingdom, 75(1), 141-151.

Mackie, G. O., & Burighel, P. (2005). The nervous system in adult tunicates: Current research directions. Canadian Journal of Zoology, 83, 151-183.

Madin, L. P. (1995). Sensory ecology of salps (Tunicata, Thaliacea): More questions than answers. Marine and Freshwater, Behaviour and Physiology, 26(2-4), 175-195.

Manni, L., Lane, N. J., Sorrentino, M., Zaniolo, G., & Burighel, P. (1999). Mechanism of neurogenesis during the embryonic development of a tunicate. Journal of Comparative Neurology, 412(3), 527-541.

Manni, L., & Pennati, R. (2016). Tunicata. In: A. Schmidt-Rhaesa, S. Harzsch, G. Purschke (eds.) Structure and evolution of invertebrate nervous systems. Oxford, New York, Tokyo: Oxford University Press, pp. 699–718.

Masterman, A.T. (1898). On the Diplochorda. 1. The structure of Actinotrocha. 2. The structure of Cephalodiscus. Quarterly Journal of Microscopical Science, 40, 281–366.

Mayer, G., Whitington, P. M., Sunnucks, P., & Pflüger, H.-J. (2010). A revision of brain composition in Onychophora (velvet worms) suggests that the tritocerebrum evolved in arthropods. BMC Evolutionary Biology, 10(1), 1-9.

McKenzie, J. D., Caunce, M., Hetherington, M., & Winlow, W. (1998). Serotonergic innervation of the foot of the pond snail *Lymnaea stagnalis* (L.). Journal of Neurocytology, 27(6), 459-470.

Metcalf, M. M. (1898). The eyes and subneural gland of salpa. Memoirs from the Biological Laboratory of the Johns Hopkins University II. Baltimore: The Johns Hopkins Press, pp. 305-371.

Metcalf, M. M. (1918) The Salpidae: A taxonomic study. Bulletin - United States National Museum, 100, 1–193.

Millar, R.H. (1966). Ascidiacea. Memoirs of the National Museum of Victoria, 27, 357–384.

Millar, R. H. (1971). The Biology of Ascidians. In: F. S. Russell, M. Yonge (eds.), Advances in Marine Biology, Volume 9. London, Oxford, Boston, New York und San Diego: Academic Press, pp. 1-100.

Minot, C. S. (1897). Cephalic homologies. A contribution to the determination of the ancestry of vertebrates. The American Naturalist, 31(371), 927-943.

Miyazaki, I. (1938). On fouling organisms in the oyster Farm. Nippon Suisan Gakkaishi, 6(5), 223-232.

Monniot, C. (1969). Les Molgulidae des Mers Européennes. Memoires du Museum National d'Histoire Naturelle, 60, 171-272.

Monniot, C., & Monniot, F. (1966). A benthic pyrosoma, *Pyrosoma benthica* n. sp. French Academy of Science, 263, 368–370.

Monniot, C., & Monniot, F. (1990). Revision of the class Sorberacea (benthic tunicates) with descriptions of seven new species. Zoological Journal of the Linnean Society, 99(3), 239-290.

Moreno, T. R., & Rocha, R. M. (2008). Phylogeny of the Aplousobranchia (Tunicata: Ascidiacea). Revista Brasileira de Zoologia, 25(2), 269-298.

Naruse, H., Gomi, T., Kimura, A., Adriaensen, D., & Timmermans, J.-P. (2005). Structure of the respiratory tract of the red-bellied newt *Cynops pyrrhogaster*, with reference to serotonin-positive neuroepithelial endocrine cells. Anatomical Science International, 80(2), 97-104.

Neumann, G. (1909). Die Pyrosomen. Dr. H. G. Bronn's Klassen und Ordnungen des Thier-Reichs, wissenschaftlich dargestellt in Wort und Bild, Band 3, Supplement 2, Abteilung 2.

Neumann, G. (1956). Erste Unterklasse der Acopa. Thaliaceae. In T. Krumbach (ed.), Handbuch der Zoologie. Berlin: Walter de Gruyter, pp. 203-323.

Nicol, D., & Meinertzhagen, I. A. (1988). Development of the central nervous system of the larva of the ascidian, *Ciona intestinalis* L.: II. Neural plate morphogenesis and cell lineages during neurulation. Developmental Biology, 130(2), 737-766.

Nieuwenhuys, R. (1977). The brain of the lamprey in a comparative perspective. Annals of the New York Academy of Sciences, 299(1), 97-145.

Nieuwenhuys, R., Smeets, W. J. A. J., Wicht, H., Donkelaar, H. J., Meek, J., Nicholson, C., Dubbeldam, J. L., van Dongen, P. A. M., & Voogd, J. (2014). The central nervous system of vertebrates. Berlin, Heidelberg: Springer Berlin Heidelberg.

Nilsson, D.-E. (1997). Eye design, vision and invisibility in planktonic invertebrates. Abingdon: Taylor & Francis.

Nozaki, M., & Gorbman, A. (1992). The question of functional homology of Hatschek's pit of amphioxus (*Branchiostoma belcheri*) and the vertebrate adenohypophysis. Zoological Science, 9(2), 387-395.

Nusbaum, M. P., & Kristan, W. B. (1986). Swim initiation in the leech by serotonin-containing interneurones, cells 21 and 61. Journal of Experimental Biology, 122, 277–302.

Okuyama, M., Saito, Y., Ogawa, M., Takeuchi, A., Jing, Z., Naganuma, T., & Hirose, E. (2002). Morphological studies on the bathyal ascidian, *Megalodicopia hians* Oka 1918 (Octacnemidae, Phlebobranchia), with remarks on feeding and tunic morphology. Zoological Science, 19(10), 1181-1189.

Olsson, R. (1975). Primitive coronet cells in the brain of *Oikopleura* (Appendicularia, Tunicata). Acta Zoologica, 56(2), 155-161.

Olsson, R., Holmberg, K., & Lilliemarck, Y. (1990). Fine structure of the brain and brain nerves of *Oikopleura dioica* (Urochordata, Appendicularia). Zoomorphology, 110, 1-7.

Onuma, T. A., Isobe, M., & Nishida, H. (2017). Internal and external morphology of adults of the appendicularian, *Oikopleura dioica*: An SEM study. Cell and Tissue Research, 367(2), 213-227.

Orton, J. H. (1913). The ciliary mechanisms on the gill and the mode of feeding in amphioxus, ascidians, and *Solenomya togata*. Journal of the Marine Biological Association of the United Kingdom, 10(1), 19-49.

Osugi, T., Sasakura, Y., & Satake, H. (2017). The nervous system of the adult ascidian *Ciona intestinalis* Type A (*Ciona robusta*): Insights from transgenic animal models. PLoS One, 12(6), e0180227.

Pennati, R., Groppelli, S., Sotgia, C., Candiani, S., Pestarino, M., & De Bernardi, F. (2001). Serotonin localization in *Phallusia mammillata* larvae and effects of 5-HT antagonists during larval development. Development, Growth & Differentiation, 43(6), 647-656.

Pennati, R., Dell'Anna, A., Zega, G., & De Bernardi, F. (2012). Immunohistochemical study of the nervous system of the tunicate *Thalia democratica* (Forsskal, 1775). European Journal of Histochemistry, 56(16), 96-101.

Perrier, E. (1898). Note sur la Classification des Tuniciers. Comptes rendus de l'Académie des sciences Paris, 126, 1758-1762.

Philippe, H., Brinkmann, H., Copley, R. R., Moroz, L. L., Nakano, H., Poustka, A. J., Wallberg, A., Peterson, K. J., & Telford, M. J. (2011). Acoelomorph flatworms are deuterostomes related to *Xenoturbella*. Nature, 470, 255-258.

Piette, J., & Lemaire, P. (2015). Thaliaceans, the neglected pelagic relatives of ascidians: A developmental and evolutionary enigma. The Quarterly Review of Biology, 90(2), 117-145.

Pinna, M. C. C. (1991). Concepts and tests of homology in the cladistic paradigm. Cladistics, 7(4), 367-394.

Plough, H. H. (1978). Sea squirts of the Atlantic Continental Shelf from Maine to Texas. Baltimore: Johns Hopkins University Press.

Pogue, M. G., & Mickevich, M. F. (1990). Character definitions and character state delineation: The bete noire of phylogenetic inference. Cladistics, 6(4), 319-361.

Quiroga, S. Y., Carolina Bonilla, E., Marcela Bolaños, D., Carbayo, F., Litvaitis, M. K., & Brown, F. D. (2015). Evolution of flatworm central nervous systems: Insights from polyclads. Genetics and Molecular Biology, 38, 233-248.

Quoy, J. R. C., & Gaimard, P. (1834). Voyage de Découvertes de l'Astrolabe, exécuté par Ordre du Roi pendant les Années 1826-1829, sous le Commandement de J. Dumont d'Urville. Zoologie, 3, 599-602.

Redikorzew, W. (1905). Über das Sehorgan der Salpen. Gegenbaurs Morphologisches Jahrbuch, 34, 204-239.

Richter, S., Loesel, R., Purschke, G., Schmidt-Rhaesa, A., Scholtz, G., Stach, T., Vogt, L., Wanninger, A., Brenneis, G., Döring, C., Faller, S., Fritsch, M., Grobe, P., Heuer, C. M., Kaul, S., Møller, O. S., Müller, C. H. G., Rieger, V., Rothe, B. H., Stegner, M. E. J., & Harzsch, S. (2010). Invertebrate neurophylogeny: Suggested terms and definitions for a neuroanatomical glossary. Frontiers in Zoology, 7(1), 29.

Rigon, F., Stach, T., Caicci, F., Gasparini, F., Burighel, P., & Manni, L. (2013). Evolutionary diversification of secondary mechanoreceptor cells in Tunicata. BMC Evolutionary Biology, 13(1), 112.

Rinehart, K. L., Holt, T. G., Fregeau, N. L., Stroh, J. G., Keifer, P. A., Sun, F., Li, L. H., & Martin, D. G. (1990). Ecteinascidins 729, 743, 745, 759A, 759B, and 770: Potent antitumor agents from the Caribbean tunicate *Ecteinascidia turbinata*. The Journal of Organic Chemistry, 55(15), 4512-4515.

Robison, B. H., Reisenbichler, K. R., & Sherlock, R. E. (2005). Giant larvacean houses: Rapid carbon transport to the deep sea floor. Science, 308(5728), 1609-1611.

Rocha, R. M., Zanata, T. B., & Moreno, T. R. (2012). Keys for the identification of families and genera of Atlantic shallow water ascidians. Biota Neotropica, 12, 269-303.

Rodriguez, L. F., & Ibarra-Obando, S. E. (2008). Cover and colonization of commercial oyster (*Crassostrea gigas*) shells by fouling organisms in San Quintin Bay, Mexico. Journal of Shellfish Research, 27(2), 337-343.

Ruppert, E. E. (1990). Structure, ultrastructure, and function of the neural gland complex of *Ascidia interrupta* (Chordata, Ascidiacea): Clarification of hypotheses regarding the evolution of the vertebrate anterior pituitary. Acta Zoologica, 71, 135-149.

Ryan, K., Lu, Z., & Meinertzhagen, I. A. (2018). The peripheral nervous system of the ascidian tadpole larva: Types of neurons and their synaptic networks. Journal of Comparative Neurology, 526(4), 583-608.

Sakharov, D. A., & Salimova, N. B. (1980). Serotonin neurons in the peripheral nervous system of the larval lamprey, *Lampetra planeri*. A histochemical, microspectrofluorimetric and ultrastructural study. Zoologische Jahrbücher für allgemeine Zoologie und Pysiologie der Tiere, 84, 231-239.

Sakharov, D. A., & Salimova, N. B. (1982). Serotonin-containing cells in the ascidian endostyle. Experientia, 38(7), 802-803.

Schmidt, C. (1845). Zur vergleichenden Physiologie der wirbellosen Thiere. Justus Liebig´s Annalen der Chemie, 54, 284-330.

Schmidt-Rhaesa, A., Harzsch, S., & Purschke, G. (2015). Structure and evolution of invertebrate nervous systems. Oxford, New York, Tokyo: Oxford University Press.

Schoenwolf, G. C., & Smith, J. L. (1990). Mechanisms of neurulation: Traditional viewpoint and recent advances. Development, 109(2), 243-270.

Scholtz, G. (2005). Homology and ontogeny: Pattern and process in comparative developmental biology. Theory in Biosciences, 124(2), 121-143.

Seeliger, O. (1885). Die Entwicklungsgeschichte der socialen Ascidien. Jenaische Zeitschrift für Naturwissenschaften, 18, 45-120.

Sereno, P. C. (2007). Logical basis for morphological characters in phylogenetics. Cladistics, 23(6), 565-587.

Shenkar, N., Koplovitz, G., Dray, L., Gissi, C., & Huchon, D. (2016). Back to solitude: Solving the phylogenetic position of the Diazonidae using molecular and developmental characters. Molecular Phylogenetics and Evolution, 100, 51-56.

Shu, D. G., Conway Morris, S., Zhang, Z. F., & Han, J. (2001). Primitive deuterostomes from the Chengjiang Lagerstätte (Lower Cambrian, China). Nature, 414, 472-473.

Søviknes, A. M., Chourrout, D., & Glover, J. C. (2007). Development of the caudal nerve cord, motoneurons, and muscle innervation in the appendicularian urochordate *Oikopleura dioica*. Journal of Comparative Neurology, 503(2), 224-243.

Stach, T. (1996). On the preoral pit of the larval amphioxus (*Branchiostoma lanceolatum*). Annales des sciences naturelles, Zoologie, Paris, 17, 129–134.

Stach, T. (2005). Comparison of the serotonergic nervous system among Tunicata: Implications for its evolution within Chordata. Organisms Diversity & Evolution, 5, 15-24.

Stach, T. (2007). Ontogeny of the appendicularian *Oikopleura dioica* (Tunicata, Chordata) reveals characters similar to ascidian larvae with sessile adults. Zoomorphology, 126(3), 203-214.

Stach, T. (2008). Chordate phylogeny and evolution: A not so simple three-taxon problem. Journal of Zoology, 276(2), 117-141.

Stach, T. (2009). Anatomy of the trunk mesoderm in tunicates: Homology considerations and phylogenetic interpretation. Zoomorphology, 128(1), 97-109.

Stach, T. (2014). Deuterostome phylogeny - a morphological perspective. In: J.W. Wägele, T. Bartolomaeus (eds.), Deep Metazoan Phylogeny: The Backbone of the Tree of Life. Berlin: De Gruyter, pp. 425-457.

Stach, T., Braband, A., & Podsiadlowski, L. (2010). Erosion of phylogenetic signal in tunicate mitochondrial genomes on different levels of analysis. Molecular Phylogenetics and Evolution, 55(3), 860-870.

Stach, T., & Turbeville, J. M. (2002). Phylogeny of Tunicata inferred from molecular and morphological characters. Molecular Phylogenetics and Evolution, 25(3), 408-428.

Stach, T., Winter, J., Bouquet, J.-M., Chourrout, D., & Schnabel, R. (2008). Embryology of a planktonic tunicate reveals traces of sessility. Proceedings of the National Academy of Sciences, 105(20), 7229-7234.

Swalla, B. J., Cameron, C. B., Corley, L. S., & Garey, J. R. (2000). Urochordates are monophyletic within the deuterostomes. Systematic Biology, 49(1), 52-64.

Swalla, B. J., & Smith, A. B. (2008). Deciphering deuterostome phylogeny: Molecular, morphological and palaeontological perspectives. Philosophical Transactions of the Royal Society of London B: Biological Sciences, 363(1496), 1557-1568.

Takamura, K. (1998). Nervous network in larvae of the ascidian *Ciona intestinalis*. Development Genes and Evolution, 208(1), 1-8.

Takamura, K., Minamida, N., & Okabe, S. (2010). Neural map of the larval central nervous system in the ascidian *Ciona intestinalis*. Zoological Science, 27, 191-203.

Tiozzo, S., Murray, M., Degnan, B. M., & De Tomaso, A. W. (2009). Development of the neuromuscular system during asexual propagation in an invertebrate chordate. Developmental Dynamics, 238(8), 2081-2094.

Torrence, S. A., & Cloney, R. A. (1982). Nervous system of ascidian larvae: Caudal primary sensory neurons. Zoomorphology, 99(2), 103-115.

Trandaburu, T., & Trandaburu, I. (2007). Serotonin (5-hydroxytryptamine, 5-HT) immunoreactive endocrine and neural elements in the chromaffin enteropancreatic system of amphibians and reptiles. Acta Histochemica, 109(3), 237-247.

Tsagkogeorga, G., Turon, X., Galtier, N., Douzery, E. J. P., & Delsuc, F. (2010). Accelerated evolutionary rate of housekeeping genes in tunicates. Journal of Molecular Evolution, 71(2), 153-167.

Tsagkogeorga, G., Turon, X., Hopcroft, R. R., Tilak, M.-G., Feldstein, T., Shenkar, N., Loya, Y., Huchon, D., Douzery, E. J. P., & Delsuc, F. (2009). An updated 18S rRNA phylogeny of tunicates based on mixture and secondary structure models. BMC Evolutionary Biology, 9, 187.

Tsutsui, H., Yamamoto, N., Ito, H., & Oka, Y. (1998). GnRH-immunoreactive neuronal system in the presumptive ancestral chordate, *Ciona intestinalis* (ascidian). General and Comparative Endocrinology, 112(3), 426-432.

Uljanin, B. N. (1884). Die Arten des Gattung *Doliolum* in Golfe von Neapel und den angrenzen den Meeresabschnitten. Leipzig: Verlag von Wilhelm Engelmann.

Ullrich-Lüter, E. M., Dupont, S., Arboleda, E., Hausen, H., & Arnone, M. I. (2011). Unique system of photoreceptors in sea urchin tube feet. Proceedings of the National Academy of Sciences, 108(20), 8367-8372.

Ussow, M. (1876). Beiträge zur Kenntnis der Organisation der Tunicaten. Mémoires de la Société Imperiale des naturalistes de Moscou, 18, 1-54.

Valero-Gracia, A., Marino, R., Crocetta, F., Nittoli, V., Tiozzo, S., & Sordino, P. (2016). Comparative localization of serotonin-like immunoreactive cells in Thaliacea informs tunicate phylogeny. Frontiers in Zoology, 13(1), 45.

Van Name, W. G. (1945). The north and south American ascidians. Bulletin of the American Museum of Natural History, 84, 1-476.

Van Soest, R. W. M. (1981). A monograph of the order Pyrosomatida (Tunicata, Thaliacea). Journal of Plankton Research, 3, 603-631.

Van Soest, R.W.M. (1998) The cladistic biogeography of salps and pyrosomas. In: Q. Bone (ed.), The biology of pelagic tunicates. Oxford, New York, Tokyo: Oxford University Press, pp. 231–249.

van Straaten, H. W. M., Hekking, J. W. M., Wiertz-Hoessels, E. J. L. M., Thors, F., & Drukker, J. (1988). Effect of the notochord on the differentiation of a floor plate area in the neural tube of the chick embryo. Anatomy and Embryology, 177(4), 317-324.

Vopalensky, P., Pergner, J., Liegertova, M., Benito-Gutierrez, E., Arendt, D., & Kozmik, Z. (2012). Molecular analysis of the amphioxus frontal eye unravels the evolutionary origin of the retina and pigment cells of the vertebrate eye. Proceedings of the National Academy of Sciences, 109, 15383-15388.

Wada, H. (1998). Evolutionary history of free-swimming and sessile lifestyles in urochordates as deduced from 18S rDNA molecular phylogeny. Molecular Biology and Evolution, 15(9), 1189-1194.

Wada, H., Makabe, K. W., Nakauchi, M., & Satoh, N. (1992). Phylogenetic relationships between solitary and colonial ascidians, as inferred from the sequence of the central region of their respective 18S rDNAs. The Biological Bulletin, 183(3), 448-455.

Wada, Y., Mogami, Y., & Baba, S. (1997). Modification of ciliary beating in sea urchin larvae induced by neurotransmitters: Beat-plane rotation and control of frequency fluctuation. Journal of Experimental Biology, 200(1), 9-18.

Wägele, J.-W. (2001). Grundlagen der Phylogenetischen Systematik. München: Verlag Dr. Friedrich Pfeil.

Wicht, H., & Lacalli, T. C. (2005). The nervous system of amphioxus: Structure, development, and evolutionary significance. Canadian Journal of Zoology, 83(1), 122-150.

Wiley, E. O., & Lieberman, B. S. (2011). Phylogenetics: Theory and practice of phylogenetic systematics. Hoboken: Wiley.

Williams, J. B. (1996). Sessile lifestyle and origin of chordates. New Zealand Journal of Zoology, 23(2), 111-133.

Willows, A. O., Pavlova, G. A., & Phillips, N. E. (1997). Modulation of ciliary beat frequency by neuropeptides from identified molluscan neurons. Journal of Experimental Biology, 200(10), 1433-1439.

WoRMS Editorial Board (2018). World Register of Marine Species. Available from http://www.marinespecies.org at VLIZ. Accessed 2018-08-02.

Wright, G. M., & Youson, J. H. (1976). Transformation of the endostyle of the anadromous sea lamprey, *Petromyzon marinus* L., during metamorphosis: I. Light microscopy and autoradiography with 125I. General and Comparative Endocrinology, 30(3), 243-257.

Zaniolo, G., Lane, N. J., Burighel, P., & Manni, L. (2002). Development of the motor nervous system in ascidians. Journal of Comparative Neurology, 443(2), 124-135.

Zeng, L., Jacobs, M. W., & Swalla, B. J. (2006). Coloniality has evolved once in stolidobranch ascidians. Integrative and Comparative Biology, 46(3), 255-268.

12 Acknowledgements

I am deeply grateful to Priv.-Doz. Dr. Thomas Stach for his permanent support over the past decade, the fruitful discussions, and his patience in teaching me so much about our common passion which is the evolution of such fantastic animals like tunicates. I am thankful to the "AG Elektronenmikroskopie", particularly to Gabriele Drescher and Peer Martin for assisting in the lab.

I am indebted to Prof. Gerhard Scholtz for taking-over the chair of my Committee. Furthermore, I am thankful for the warm welcome in his group and for providing access to the lab facilities and to the office. I am much obliged to every one of the "AG Vergleichende Zoologie" (former and recent members) for discussing scientific and non-scientific issues, especially to my roommates and fellow PhD candidates: Kristin Jütz, Katja Kienbaum, Franziska Meusel, and Juliane Vehof. Juliane read and ameliorated sections of this work. I am grateful to Dr. Georg Brenneis for introducing me into the field of immunohistology, for the common trouble-shooting when staining experiments did not work — even if it was all just "Schlonz" — and for reading and commenting on former versions of the discussion part.

I am also indebted to Prof. Lucia Manni and Prof. John Nyakatura for agreeing to review this work.

I am much obliged to Priv.-Doz. Dr. Carsten Lüter for generously providing access to the collection of marine invertebrates and to the CLSM in the Museum für Naturkunde Berlin. Dr. Esther Ullrich-Lüter and Dr. Nina Furchheim are thanked for the support in operating the CLSM and for picking me up several times at the museum's door. Nina also had the patience to read and comment on parts of former versions of this work.

I learned a lot at the Smithsonian Marine Station in Fort Pierce, Florida. Sincere thanks are given to everybody I got to know there, especially to Prof. Valerie Paul and Prof. Mary Rice for granting access to lab facilities, to Woody Lee and Scott Jones for the invaluable help in collecting marine plankton from the Gulf stream, to Sherry Reed for cordially welcoming me, for helping me with non-scientific problems, and for borrowing her bike so that I was able to collect additional plankton samples, and to Dr. Michael Boyle for his advice and the shared fascination for marine plankton. This time was unique!

The effort of Prof. Hans-Joachim Pflüger and Heike Wolfenberg in teaching me the method to backfill selected nerves and in helping me to test different protocols for antibody stainings is highly appreciated. I am also thankful to Dr. Stefano Tiozzo for the expert collection and fixation of some salp specimens.

I am grateful for the financial support granted by the Elsa-Neumann-Stipendium des Landes Berlin and the Deutscher Akademischer Austauschdienst (German Academic Exchange

Service). As an expert in bureaucratic affairs, Dorothea Haselow helped a lot in overcoming some obstacles and gave invaluable advice.

My friends Dr. Fanny Weitz, Dr. Jürgen Strassert and Dr. Isaak Unger critically read parts of the present work and several times exhilarated me at the end of a tough working day. My best friend Yvonne Petersen keeps on looking after me. Thanks to the four of you for enlightening my days.

I am deeply thankful for the support and encouragement given by my family. I still do not know much about botany, but I will always keep on telling you interesting stuff about animals. During the last decade, I was additionally supported by another family; the support of the Deutsch family is highly appreciated. Last but not least, I am deeply grateful to my boyfriend Florian Deutsch for his unconditional support and belief in me.